Advanced Waterflooding of North Sea Chalk Reservoirs

Hao, Jiasheng

Publication date:
2020

Document Version
Publisher's PDF, also known as Version of record

Advanced Waterflooding of North Sea Chalk Reservoirs

Jiasheng Hao

Ph.D. Thesis

February 2020

The Danish Hydrocarbon Research and Technology Centre
Center for Energy Resources Engineering
Department of Chemical and Biochemical Engineering
The Technical University of Denmark
2800-Kgs. Lyngby, Denmark

Centre for Oil and Gas - DTU
The Danish Hydrocarbon Research and Technology Centre

Center for Energy Resources Engineering
CERE

Preface

This thesis is submitted as partial fulfillment of the requirement for Ph.D. degree at the Technical University of Denmark (DTU). The work was done at the Centre for Oil and Gas-DTU and the Center for Energy Resources Engineering at the Department of Chemical and Bio-chemical Engineering. The project was carried out from February 2017 to February 2020, under the supervision of Dr. Alexander Shapiro and Dr. Karen L. Feilberg.

First of all, I would like to sincerely thank my principle supervisor, Alexander Shapiro, for his tremendous support throughout my Ph.D. study, it has been a very fruitful journey. I would also like to thank my co-supervisor Karen L. Feilberg for the constructive scientific discussions and suggestions. Special thanks to Sidsel M. Nielsen, thank you for choosing me for this Ph.D. project, and your trust on me in the first year of my study.

Secondly, I am grateful for all the support from our laboratory technicians, Tran Thoung Dang, Duc Thuong Vu, Zacarias Tecle, Annette Eva Jensen and Jesper Arvedlund Hollensen, the work could never go as smoothly without your help. I also want to say thank you to Amalia Yunita Halim and Sian Jones, your help at the beginning of my Ph.D. made it a lot easier for me to get started.

During my Ph.D. study, I had the opportunity to visit Saskatchewan Research Council (SRC) at Regina, Canada. Many thanks to Petro Nakutnyy for warmly hosting me as a visiting researcher. Thanks to Danie Subido and Peng Luo for your great help in the laboratory.

I also want to thank all my fellow Ph.D. students and friends that make this journey colorful. Especially, Teeratorn Kadeethum and Moein Jahanbani Veshareh, thank you for your accompany during this special journey, all the jokes, laughter, food, fishing… will be a life-long memory. Maiya Medetbekova and Maria Bonto, thank you for sharing the same office with me and creating an efficient working environment.

Thanks to my families, especially my mother. Your support from thousands of miles away is like a lighthouse in the dark, keep reminding me where I am from and where is the destiny. I will never give up because of you.

Sincerely,
Jiasheng Hao
Kgs. Lyngby, Denmark, February 2020

This dissertation is dedicated to my family and all the people who helped me through the course of this study.

Summary

Advanced, or smart waterflooding is a term denoting directed alteration of the ionic composition of the injected brine to achieve a better oil recovery. While the subject has been extensively researched during the past decades, the acting mechanisms of advanced waterflooding are not fully clarified, especially, for carbonate reservoirs. The purpose of this project is to summarize current research progress, further investigate promising mechanisms and explore previously uncovered aspects, especially, under the conditions of North Sea reservoirs.

The first part of the study is an updated and comprehensive literature review of smart waterflooding in carbonate reservoirs. The potential recovery mechanisms were classified into two groups: static and dynamic. The term “static mechanisms” refers to those that could happen without flow. Wettability alteration, double layer expansion, surface ion exchange, surface complexation, etc. belong to this group. On the other hand, the term “dynamic mechanisms” refers to those that occur during the flow, like fines relocation, flow diversion, emulsification, etc.. The numerous experimental works were categorized and the key information was extracted to identify the status of current research.

The second part of the project focuses on the kinetics of calcite dissolution and Ca-Mg exchange on chalk surfaces. These processes have been proposed by several researchers as the potential causes of additional recovery. The kinetics of such processes is essential to evaluate their significance in flow-through scenarios. Experimental works were carried out with commercial calcite powder and powders made from Stevns Klint outcrop and North Sea reservoir chalk. It was found that the dissolution of all three materials is similar. The equilibrium time is in the order of seconds and the equilibrium concentration is a few milligrams per liter. This means in the flooding experiments, calcite dissolution can only affect the inlet of the core, even after tens or hundreds of porous volume injected (PVI). Considering the amount of PVIs involved in common flooding experiments, it does not seem to be able to cause large additional recovery.

On the other hand, Ca-Mg exchange showed slow kinetics. The process kept going throughout the two weeks experimental period and did not stop at the end of the experiments. A two-layer model was proposed to describe the process and it fitted well with experimental data. The predicted exchange capacity of the calcite/chalk surfaces is in the order of 10^{-5} mol/m^2/layer. These facts indicate that Ca-Mg exchange has only little impact on laboratory experiments. However, on the reservoir scale, where the range of time is much larger, it may be of more importance.

The third part of the thesis investigates the effect of flow diversion during smart waterflooding. Core flooding experiments were performed on sandstone and chalk reservoir cores. Based on the CT scanning images, homogeneous and heterogeneous cores were selected for both types of rock. It was found that the flow diversion mechanism can occur in both sandstone and chalk cores. However, the plugging agents that trigger this mechanism are different. The emulsions and precipitated fines worked in chalk, and most probably clay particles affected the recovery in the sandstone. The additional recovery was consistently observed from heterogeneous cores, which suggests that heterogeneity could amplify the effect of flow diversion. A simplified multi-layer model was employed to simulate the experiments. It was able to match well with experimental data, supporting the above-mentioned mechanisms.

The last part of the project studies the effect of chalk compaction on oil recovery. Core flooding experiments with simultaneous measurement of core length were conducted with Stevns Klint outcrop and North Sea reservoir cores. Again, heterogeneous and homogeneous cores were selected based on their

CT scanning images. The displacement of oil by water caused slight compaction in both types of rocks. This is consistent with the existing theory of water weakening of chalk. Subsequent injection of low salinity brines did not lead, neither to further compaction nor to additional recovery. Significant compaction caused by increasing of overburden pressure resulted in small additional recoveries in both heterogeneous and homogeneous outcrop cores and a considerable (compared to a homogeneous core) additional recovery from the heterogeneous reservoir core. A characteristic calculation showed that the additional production was correlated to the heterogeneity of the cores. The flow diversion mechanism was discussed in this context.

Overall, the current project shows that static mechanisms are not enough to explain the diverse experimental observations. Dynamic mechanisms that are related to the flow need further investigation.

Dansk Resumé

Avanceret eller ”Smart waterflooding” er et udtryk, der betegner brugen af saltvand med en modificeret ionisk sammensætning for at opnå en højere udvindingsgrad af olie. På trods af, at der har været forsket i emnet de sidste årtier, er der især for karbonat reservoirer stadig uklarhed omkring de mekanismer, der optræder i avanceret waterflooding. Formålet med dette projekt er, at opsummere de seneste fremskridt i forskningen, at undersøge yderligere lovende mekanismer og at udforske emner, der især under de forhold, der gør sig gældende i reservoirerne i Nordsøen, endnu ikke er blevet afdækket.

Første del af studiet var et opdateret og fyldestgørende litteraturstudie af ”Smart waterflooding” i karbonat reservoirer. De potentielle udvindingsmekanismer var klassificeret i to grupper: statiske og dynamiske. Begrebet ”statiske mekanismer” henviser til de mekanismer, der sker uden gennemstrømning (flow) så som modifikation af fugtpræference (wettability), dobbeltlags udvidelse (double layer expansion), overflade ionbytning (surface ion exchange), overflade kompleksdannelse (surface complexation) osv. som alle tilhører denne gruppe. Begrebet ”dynamiske mekanismer” henviser til de mekanismer, der forekommer under strømning, såsom relokering af finkornet materiale (fines relocation), strømningsafledning (flow diversion), emulgering osv. Det omfattende eksperimentelle arbejde er kategoriseret, og de vigtigste informationer fra den nuværende forskning er blevet identificeret.

Anden del af studiet fokuserede på kinetikken ved opløsning af kalcit og på udveksling mellem Ca og Mg på kalkoverfladerne. Disse processer har af flere forskere været foreslået som potentiel årsag til øget udvinding og forståelsen af disse processers kinetik er derfor essentielt for at kunne evaluere deres indflydelse på gennemstrømmende (flow-through) scenarier. De eksperimentelle forsøg blev udført med kommercielt kalcit pulver og pulver lavet af kalk fra Stevns Klint og fra Nordsø reservoiret. Det viste sig, at opløsningen af alle tre materialer lignede hinanden. Tiden indtil ligevægt er i størrelsen sekunder og ligevægts-koncentrationen er et par milligram per liter. Dette betyder, at i ”flooding”-eksperimenterne kan kalcit-opløsningen kun påvirke ende fladen af kernen, selv efter injektion af ti eller hundrede porøsitets-volumener (PVI). Dette tyder på, at med de mængder af PVI, der er involveret i de almindelige ”flooding” eksperimenter, vil denne effekt ikke kunne resultere i en øget udvinding.

På den anden side viste udveksling mellem Ca og Mg langsom kinetik. Processen fortsatte hele forsøgsperioden på to uger og stoppede ikke, da eksperimenterne sluttede. En to-lags model var foreslået til at beskrive processen og den var i overensstemmelse med de eksperimentelle data. Den forventede udvekslingskapacitet af kalcit/kalk overfladerne er i størrelsen 10^{-5} mol/m^2/lag. Disse fakta indikerer, at Ca-Mg udveksling kun har en lille påvirkning på laboratorieeksperimenter. Dog, på reservoir skala, hvor tidsintervallet er større, kan det have større betydning.

Tredje del af studiet undersøgte effekten af strømningsafledningen under ”Smart waterflooding”. Kerne ”flooding” eksperimenter er udført på sandsten og kalk reservoir kerner og hvor både homogene og heterogene kerner er udvalgt baseret på CT scannings-billeder. Eksperimenter viste, at strømningsafledningen (flow diversion) sker både i sandsten og kalk kerne, dog er de blokerende elementer (plugging agents), der udløser denne mekanisme, forskellige. I kalken blokerede emulsioner og udfældet finkornet materiale, mens det i sandsten højst sandsynligt var ler-partikler, som påvirkede udvindingsgraden. Øget udvinding blev konsekvent observeret fra de heterogene kerner, hvilket tyder på, at heterogenitet kan forstærke effekten af strømningsafledningen. En simplificeret multilags-model blev anvendt for at simulere eksperimenterne. Modellen var i overensstemmelse med de eksperimentelle data og understøttede derved teorien om de førnævnte mekanismer.

Sidste del af projektet undersøgte kalkens kompakteringseffekt på oliens udvindingsgrad. Kerne "flooding" eksperimenter med sideløbende målinger af kernens længde, er udført på kerner fra Stevns Klint og fra Nordsø reservoiret. Igen var både heterogene og homogene kerner udvalgt baseret på CT scannings-billeder. Vands fortrængning af olie forårsagede en mindre kompaktering i begge typer af bjergart. Dette er i overensstemmelse med den eksisterende teori om vands svækkelse af kalk. Efterfølgende injektion af saltvand med lavt saltindhold ledte ikke til hverken yderligere kompaktering eller yderligere udvinding. Betydelige kompaktering forårsaget af en stigning i det omkringliggende tryk, resulterede i en begrænset mængde ekstra udvundet olie i både de heterogene og homogene Stevns Klint kerner og en betydelig (sammenlignet med en homogen kerne) ekstra indvinding fra de heterogene reservoir kerner. En karakteristisk udregning viste, at den ekstra produktion hang sammen med heterogeniteten af kernerne. Effekten af strømningsafledningen (flow diversion) blev diskuteret i denne sammenhæng.

Samlet set viser det aktuelle projekt, at statiske mekanismer ikke er nok til at beskrive de forskellige eksperimentelle observationer. Dynamiske mekanismer, som er relateret til strømningen, kræver yderligere undersøgelse.

Table of Contents

Chapter 1. Introduction

1.1 Why smart waterflooding in the North Sea chalk reservoirs?

The discovery and production of the Danish North Sea oil can be dated back to the early 1970s. The primary depletion of the reservoirs lasted until the 1980s, then water injection projects were launched one after another from the late 1980s (The Danish Hydrocarbon Research and Technology Centre, 2019). Nowadays the reservoirs are at the late stage of development and the production has a high water cut. Thus, an effective EOR method should be applied to those reservoirs.

The North Sea chalk reservoirs are characterized as high porosity, low permeability (0-10 mD) and are naturally fractured (Fabricius, 2007; Agarwal et al., 1997; Agarwal et al., 2009). Such properties eliminate the possibility of some mature recovery technologies such as polymer and surfactant flooding: the injectivity would severely decline and the high retention of the injected chemicals would not allow them to travel far from the injectors.

Alternatively, modification of the ionic composition of the injection brine and utilization of the reactive nature of carbonate surfaces may be an option. This recovery method is commonly referred to as smart waterflooding (Hao et al., 2019). Various chemical and physicochemical processes can happen during flooding, which may consequently change the characteristics of the displacement process and produce additional oil (Yutkin et al., 2016). In recent years, numerous studies have attempted to reveal the mechanisms of such processes, however, the conclusion is still far from definite.

1.2 Overview of the current stage of smart waterflooding: sandstone and chalk

Smart waterflooding as a method to enhance oil recovery has been studied for over two decades. The first dedicated research for it as an enhanced oil recovery (EOR) method was made for sandstone rocks: injection of low salinity brines resulted in additional recovery (Tang & Morrow, 1999). Many studies attributed the additional recovery to the clay content in the rock (Jackson et al., 2016). Upon injection of low salinity brines, clay particles may be detached from the rock surface and enter the flow. Further capture of the particles by pore throats may lead to a diverted flow of water into the inswept zones and produce additional oil. On the other hand, the surfaces of clay particles are active, oil can adsorb on them through chemical or physical bonds. Injection of low salinity brine may alter the surface properties of clay particles. As a result, oil detaches from clay and joins the flow, eventually being produced from the core or the reservoir.

It was not until recently that the research was extended to carbonate rocks, where the problem became more complicated, and the opinions from researchers were more diverse. For carbonate rocks, the term ‘smart waterflooding’ is more often used (Hao et al., 2019). This is because, apart from reducing the salinity of the injection water, adding salts that contain magnesium, calcium, sulfate or other ions has also been extensively studied. Removing particular ionic components from the brine was attempted as well. Behind the various approaches to modify the ionic composition of injection water lays the lack of understanding of the fundamental mechanisms governing the additional recovery. Many mechanisms involving surface electrostatic interactions, chemical processes, and flow dynamics have been discussed. Along with the increasing diversity of the proposed potential mechanisms, the complexity to evaluate the significance of the individual phenomena in separation from other mechanisms is also problematic. The

numerous experimental observations are sometimes inconsistent, and, in rare cases, contradictory. Apparently, there are some gaps to fill up and some relationships that worth further investigation.

1.3 Previously uncovered problems in the research

One of the widely discussed potential mechanisms is the wettability alteration of the rock surface under flooding the cores with magnesium-containing brines. The magnesium ions in the brine can substitute the calcium ions from carbonaceous rock, which releases the initially adsorbed carboxylic components from the surface (Zhang, Tweheyo, & Austad, 2007). This mechanism is extensively researched to understand its optimum working conditions and significance for enhanced oil recovery. However, one of the fundamental questions about this mechanism has not been studied to the full extent: how fast is the ion exchange process and how much ions can be exchanged during a reasonable experimental time? The answer to this question is crucial to quantitatively evaluate the importance of this process of improving oil recovery.

An important factor that is rarely mentioned in the literature is the physical structure of the cores that were used in the experiments, namely, heterogeneity/homogeneity of the cores. A lot of effort has been put on the research of chemical or physicochemical processes during smart waterflooding, which is, indeed, important to reveal the acting mechanisms. However, one should not neglect the crucial role of heterogeneity of the core itself, as it may create very different flow characteristics even under similar experimental conditions (Halim, et al., 2015; Mohammadkhani et al., 2019). The proposed physicochemical mechanisms, such as emulsification and fines relocation, may be combined with the flow characteristics induced by heterogeneity and result in a more effective hybrid recovery process. Such a hypothesis needs further investigation.

The relationship between smart waterflooding and water weakening of chalk is another uncovered topic (Hao & Shapiro, 2019). The link between them has not been explicitly studied but it appears to be strong. Some common mechanisms, such as calcite dissolution and adsorption of divalent ions, etc., were proposed in the literature of smart waterflooding and chalk weakening. Meanwhile, studies have shown that compaction of the reservoir could facilitate oil production by adding additional pressure support (Chin & Thomas, 1999). Hence, the link becomes obvious: smart waterflooding results in weaker chalk, weakened chalk then gets compacted by overburden pressure, more oil can potentially be produced due to compaction.

1.4 Objectives of this Ph.D. project

Based on the current status of the research progress, this project is dedicated to further explore the promising mechanisms and to shed light on the currently being overlooked factors. The objectives of the study are:

1. To analyze the published research outcomes and to categorize the proposed potential mechanisms of smart waterflooding. To identify the most promising possible mechanisms, as well as gaps under the current scope of research.
2. To investigate the kinetics of calcite/chalk dissolution and Ca-Mg ion exchange on the calcite/chalk surfaces.
3. To evaluate the impact of calcite dissolution and Ca-Mg ion exchange during the flooding process. To analyze their potential contribution to oil recovery by comparison with literature data.

4. To identify potential mechanisms for additional oil production associated with heterogeneity and evaluate their significance.
5. To study the relationship between smart waterflooding and chalk compaction.
6. To investigate the contribution of chalk compaction on oil recovery.

1.5 Thesis outline

The thesis contains six chapters. The first two chapters present the motivation of the project and an updated literature review, respectively. The next four chapters contain the experimental and modeling work, as well as the derived conclusions. A brief overview of each chapter is given below.

Chapter 1 introduces the motivation and general background of the project, as well as the research goals and organization of the thesis.

Chapter 2 is based on a published paper that addresses the first research objective. In this chapter, the proposed potential mechanisms in the literature are grouped into two major categories: static and dynamic. The term “static mechanisms’’ refers to those that could occur without the flow, such as surface ion exchange and wettability alteration, etc.. The term “dynamic mechanisms’’ corresponds to the ones that take place with the flow, such as fines migration and flow diversion, etc. The literature review clarifies the future directions of the research: more fundamental experimental analysis is needed to examine the chemical processes; dynamic mechanisms may also play an important role, they should not be overlooked.

Chapter 3 presents the investigation of the kinetics of calcite dissolution and Ca-Mg ion exchange on the calcite surface. This chapter addresses the second and third research objectives. Static experiments were performed with a commercial calcite powder and the powders produced from Stevns Klint outcrop chalk and North Sea reservoir chalk. A two-layer model was proposed to approximate experimental results. The model was also coupled with the transport equations to match with literature data. The fast equilibration of calcite dissolution makes it unlikely to be the cause of the reported additional recovery. The slow kinetics of Ca-Mg ion exchange cannot explain the experimental observations, either. However, its effect may be more significant on the reservoir scale.

Chapter 4 contains the study of flow diversion in homogeneous and heterogeneous cores, addressing the fourth research objectives. The core flooding experiments were performed with specially selected chalk and sandstone cores, with different levels of heterogeneity. Similar flooding procedures were applied to each type of rock. The additional production was consistently observed from heterogeneous cores. Meanwhile, indications of a flow diversion process were observed (an increase of pressure drop, production of emulsions and fines). A simplified multi-layer model that represents the flow diversion mechanism was able to reproduce the experimental data. Heterogeneity, combined with the flow diversion mechanism, appeared to be a reasonable explanation of the observations.

Chapter 5 presents the study of the effect of chalk compaction on oil recovery, addressing the fifth and sixth research objectives. The core flooding experiments were performed with Stevens Klint outcrop and North Sea reservoir chalk cores. Each type of rock was represented by a homogeneous and a heterogeneous sample. The lengths of the cores were monitored by a linear variable differential transformer (LVDT) during the flooding and compaction. The natural water weakening of chalk turned out to be insignificant in the experiments, the compaction occurred only during the secondary flooding process. Forced compaction by increasing overburden pressure resulted in additional recovery from the

cores. The additional recovery was larger in the heterogeneous cores than the homogeneous ones. Characteristic analysis of the production suggests that the additional recovery could be related to the heterogeneity of the cores.

1.6 List of research papers and conference contribution

Published article:

Hao, J., Mohammadkhani, S., Shahverdi, H., Esfahany, M., & Shapiro, A. (2019). Mechanisms of smart waterflooding in carbonate oil reservoirs – A review. *Journal of Petroleum Science and Engineering, 179*(January), 276-291. (Chapter 1)

Conference contributions:

Hao, J., Mohammadkhani, S., Louise Feilberg, K. and Shapiro, A. (2019). Smart Waterflooding of Homogeneous and Heterogeneous Cores from Carbonaceous Reservoir. *81st EAGE Conference and Exhibition 2019.* London, UK. (Poster)

Hao, J., and Shapiro, A. (2019). Effect of Compaction on Oil Recovery Under Low Salinity Flooding in Homogeneous and Heterogeneous Chalk. *SPE Annual Technical Conference and Exhibition 2019.* Calgary, Canada. (Oral presentation) (Chapter 5)

Submitted articles:

Hao, J., Feilberg, K. L. and Shapiro, A., Kinetics and Calcite Dissolution and Ca-Mg Ion Exchange on the Surfaces of North Sea Chalk powders. Submitted to *Energy & Fuels.* (Chapter 3)

Hao, J., Nakutnyy, P. and Shapiro A., Effect of Flow Diversion on Oil Recovery Under Smart Waterflooding in Homogeneous and Heterogeneous Chalk and Sandstone. Submitted to the *Journal of Petroleum Science and Engineering*. (Chapter 4)

References

Agarwal, B., Hermansen, H., Sylte, J., & Thomas, L. (2009). Reservoir characterization of Ekofisk field: a giant fractured chalk reservoir in the Norwegian north sea-history match. *SPE Reprint Series*(December), 534-543.

Agarwal, B., Thomas, L., Sylte, J., & O'Meara, D. (1997). Reservoir characterization of Ekofisk field: A giant, fractured chalk reservoir in the Norwegian North Sea - upscaling. *Proceedings - SPE Annual Technical Conference and Exhibition, Sigma*, 311-321.

Chin, L., & Thomas, L. (1999). Fully Coupled Analysis of Improved Oil Recovery by Reservoir Compaction. *SPE Annual Technical Conference and Exhibition.* Houston, Texas, USA.

Fabricius, I. (2007). Chalk: Composition, diagenesis and physical properties. *Bulletin of the Geological Society of Denmark, 55*, 97-128.

Hao, J., & Shapiro, A. (2019). Effect of Compaction on Oil Recovery Under Low Salinity Flooding in Homogeneous and Heterogeneous Chalk. *SPE Annual Technical Conference and Exhibition.*

Hao, J., Mohammadkhani, S., Shahverdi, H., Esfahany, M., & Shapiro, A. (2019). Mechanisms of smart waterflooding in carbonate oil reservoirs - A review. *Journal of Petroleum Science and Engineering, 179*(January), 276-291.

Jackson, M., Vinogradov, J., Hamon, G., & Chamerois, M. (2016). Evidence, mechanisms and improved understanding of controlled salinity waterflooding part 1: Sandstones. *Fuel, 185*, 772-793.

Mohammadkhani, S., Shahverdi, H., Marie Nielsen, S., Nasr Esfahany, M., & Shapiro, A. (2019). Bicarbonate flooding of homogeneous and heterogeneous cores from a carbonaceous petroleum reservoir. *Journal of Petroleum Science and Engineering, 178*(March), 251-261.

Tang, G.-Q., & Morrow, N. (1999). Influence of brine composition and fines migration on crude oil/brine/rock interactions and oil recovery. *Journal of Petroleum Science and Engineering, 24*(1), 99-111.

The Danish Hydrocarbon Research and Technology Centre. (2019, October 29). Retrieved from https://www.oilgas.dtu.dk/english/about-us/denmarks-oil

Yunita Halim, A., Marie Nielsen, S., Eliasson Lantz, A., Sander Suicmez, V., Lindeloff, N., & Shapiro, A. (2015). Investigation of spore forming bacterial flooding for enhanced oil recovery in a North Sea chalk Reservoir. *Journal of Petroleum Science and Engineering, 133*, 444-454.

Yutkin, M., Mishra, H., Patzek, T., Lee, J., & Radke, C. (2016). Bulk and Surface Aqueous Speciation of Calcite: Implications for Low-Salinity Waterflooding of Carbonate Reservoirs. *SPE Kingdom of Saudi Arabia Annual Technical Symposium and Exhibition.* Dammam, Saudi Arabia.

Zhang, P., Tweheyo, M., & Austad, T. (2007). Wettability alteration and improved oil recovery by spontaneous imbibition of seawater into chalk: Impact of the potential determining ions Ca2+, Mg2+, and SO4 2-. *Colloids and Surfaces A: Physicochemical and Engineering Aspects, 301*(1-3), 199-208.

Chapter 2. Recent Advances of Smart Waterflooding in Carbonate Rocks

This chapter has been published as an journal article: Hao, J., Mohammadkhani, S., Shahverdi, H., Esfahany, M., & Shapiro, A. (2019). Mechanisms of smart waterflooding in carbonate oil reservoirs - A review. *Journal of Petroleum Science and Engineering, 179*(January), 276-291.

Abstract

The goal of the present paper is to provide a comprehensive review of the literature describing the physical and chemical mechanisms for enhanced oil recovery under smart waterflooding in carbonate reservoirs. Advanced, or smart waterflooding is a term denoting directed alteration of the ionic composition of the injected brine in order to achieve a better oil recovery, in particular, the low salinity flooding. While injection of a low salinity brine in sandstones is well described, the acting mechanisms of advanced waterflooding are not fully clarified, and only few reservoir-scale tests have been carried out. Demonstration and comparison of the different phenomena explaining the effect of smart waterflooding are the goals of the present review. Unlike the previous such reviews, we do not only concentrate on the phenomena occurring on the rock-brine-oil interfaces, but also address dynamic phenomena caused by flow, like fluid diversion and emulsification. The paper comprises an up-to-date information, classification and guidance and, consequently, is intended to serve advancing the research in the area of smart waterflooding in carbonates.

Keywords: Engineered water injection; smart waterflooding; low salinity; carbonates; physical and chemical mechanisms of recovery; improved oil recovery

2.1 Introduction

Smart waterflooding in carbonate rocks has recently drawn an increasing attention. For sandstone rocks smart water flooding is often identified with the low salinity flooding (Bartels et al., 2019; Afekare and Radonjic, 2017; Sohal et al., 2016). However, in carbonates the approaches to smart waterflooding may be more diverse. In this work, the term 'smart waterflooding' is used to denote production of additional oil by injection of a specially prepared brine, which has a different ionic composition from the formation water or previously injected brine. Although injection of low salinity water is applicable also in carbonates (Derkani et al., 2018), addition or removal of particular salts containing calcium, magnesium, sulfate and other ions may also be an option.

Compared to other methods applicable to enhancement in oil recovery from carbonates, water is easy to inject and is usually relatively inexpensive, although desalination and getting fresh water may be a challenge in some places (Yousef et al., 2011). Injection of low salinity brine for oil recovery was applied long ago (Goolsby and Anderson, 1964; Hallenbeck et al., 1991) and was recognized as a method for enhanced oil recovery for at least fifty years (Bernard G.G., 1967). Active development of this recovery method started by revealing the acting mechanism of low salinity waterflooding in sandstones (Tang and Morrow, 1999). This form of smart waterflooding has been successfully applied in sandstone reservoirs (Aghaeifar et al., 2015; Alvarado et al., 2014; Austad et al., 2010; Jackson et al., 2016; Kuznetsov et al., 2015; Mahani et al., 2015; Morrow and Buckley, 2011; RezaeiDoust et al., 2011; Rotondi et al., 2014; Shehata and Nasr El-Din, 2015; Suman et al., 2014; Zeinijahromi et al., 2015), followed by development

of desalination technologies (Ayirala and Yousef, 2016). However, application of smart waterflooding for development of carbonate reservoirs has so far been limited to separate pilot tests (Rassenfoss, 2016; Yousef et al., 2012a).

A possible reason for limited application of smart waterflooding in carbonates is thatthe involved physico-chemical mechanisms are not fully clarified yet. The literature suggests different recovery mechanisms, and the experimental data look sometimes controversial. Absence of clarity about the working mechanisms results in impossibility of formulating the operating conditions for successful application of smart waterflooding in carbonates, contrary to sandstones, where the LoSal™ technology was successfully implemented by BP (Lager et al., 2008b).

Recently, several review papers have discussed smart waterflooding from different angles (Jackson et al., 2016; Afekare and Radonjic, 2017; Ayirala and Yousef, 2016; Bartels et al., 2019; Derkani et al., 2018; Sheng, 2014; Sohal et al., 2016). They have put a great effort on explaining the chemical and physical processes, laboratory and field tests, as well as required working conditions for low salinity flooding. Extensive work has been put on comparing and grouping the reported experimental observations and finding the links and inconsistencies between similar studies. Analysis of the working mechanisms for low salinity flooding has also been carried out, especially, regarding solid-liquid and liquid-liquid interface interactions (Derkani et al., 2018). The disucssion has also been extended to a more fundamental level, of the interaction between the different length and time scales under low salinity flooding (Bartels et al., 2019). Still, some mechanisms have remained uncovered by the current reviews, or described only with regard to low salinity flooding. Some researchers applied surfactants and polymers assisted smart water and low salinity brines to improve oil recovery (Alagic et al., 2011; Gupta et al., 2011; Karimi et al., 2016; Shaddel and Tabatabae-Nejad, 2015; Shaker Shiran and Skauge, 2013; Standnes and Austad, 2000a, 2000b; Sun et al., 2014). This is outside the scope of the present review.

The present review paper aims at providing a complete overview over the oil recovery mechanisms under smart waterflooding in carbonate rocks, and experimental evidence supporting or contradicting these mechanisms. We have tried to classify the chemical and physical phenomena explaining positive effects of smart waterflooding. Such classification may only be approximate and relative, since (as realized by many authors) experimental behavior of the rock-fluid system and additional oil production are the results of multiple mechanisms acting simultaneously. We have approximately divided the phenomena observed in a oil-brine-rock system into *static* and *dynamic* phenomena.

The static phenomena may in principle be observed and studied in the experiments where no flow is required. Such phenomena like wettability alteration or compaction are static. It may happen, however, that the static mechanisms manifest itself differently in the flow-through experiments (like selective compaction may result in flow diversion).

On the contrary, *dynamic phenomena* require appearance of the flow. A characteristic example is flow diversion due to plugging of high-permeable areas. There are many phenomena that are on the border between static and dynamic, like formation of emulsions. We have included them into the dynamic phenomena, since in most cases they require liquid movement (snap-off, vibrations) in order to develop to a significant extent.

Most of the literature is related to the static mechanisms, investigating chemical and physico-chemical transformations occurring on the oil-rock, water-rock or water-oil interfaces, as reflected in the previous reviews (Mahani et al., 2015; Sohal et al., 2016; Derkani et al., 2018). We have tried, on the other hand, to keep the discussion more balanced, overviewing also mechanisms that have not been addressed as extensively. In sandstones, it is a combination of the static and dynamic mechanisms (surface chemistry

and release of fines) that has resulted in successful application of the low salinity flooding. A similar combination is probably required to successfully apply waterflooding in carbonate rocks.

The paper is organized as follows. Section 2 discusses the static mechanisms relevant to smart waterflooding. Section 2.1 covers phenomena related to wettability alteration, like surface ion exchange, surface charge alteration, mineral dissolution or precipitation. Other static mechanisms, like modification of the oil-brine interface, viscosity reduction and rock compaction, are reviewed in section 2.2. Section 3 discusses dynamic mechanisms, like those related to general flow dynamics, heterogeneity, production of fines and emulsions. The paper ends with the general discussion.

2.2 Static mechanisms

In this section, the static phenomena that can appear without any flow through porous media are presented. Wettability alteration, surface ion exchange, change of the surface charge, rock dissolution, interfacial tension and oil viscosity reduction, as well as rock compaction, fall into this category.

2.2.1 Wettability related mechanisms

2.2.1.1 Wettability alteration

Wettability alteration is usually not a separate mechanism, but an effect produced by other microscale mechanisms, such as surface ion exchange, surface charge change, double layer expansion, mineral dissolution. However, some authors refer to wettability alteration without explaining, or giving multiple explanations of, how it appears. In order to cover such cases, we present a review accounting wettability alteration as a separate phenomenon. Particular microscale mechanisms that may lead to wettability alteration are considered further in the review.

Measurement of wettability

In petroleum applications, there are several non-equivalent ways to quantify wettability. The wettability of a solid surface can be specified by measuring the contact angle of an oil drop on the surface (Dandekar, 2013). On the other hand, wettability of a porous medium, namely the rock, can be described by Amott-Harvey, USBM, or similar indices. Another method, based on the difference of sulfate and thiocyanate adsorption, was introduced lately to measure the wettability of chalk (Strand et al., 2006). The authors claim that it is faster than the Amott-Harvey method and provides similar results for chalk. The methods based on the electrical resistivity and NMR spectroscopy have also been applied (Katika et al., 2018).

Effect of oil composition

The acid and base number of oil may have an impact on the initial chalk wettability, which dictates the effectiveness of wettability alteration by smart water flooding. It was pointed out that oil wet surfaces are not preferable for wettability alteration if an oil does not contain substantial amount of acidic components (Austad and Standnes, 2003).

The acid number (AN) is the major parameter that determines rock wettability (Zhang and Austad, 2005). Usually, the carbonate rock surface is positively charged. This facilitates adsorption of the negatively charged carboxylic groups, whose amount is indicated by the AN. Therefore, the higher the AN, the more oil-wet the rock can be (Standnes and Austad 2000). Austad and Standnes (2003) studied the impact of AN on wettability of Stevns Klint chalk by imbibition experiments. It was shown that oil recovery

substantially decreased with increased AN. The difference in recovery was as large as 30% for the AN varying from 0.08 to 0.70.

On the other hand, the base number (BN) plays a minor role on rock wettability. Puntervold *et al.*(2007) performed a series of imbibition experiments with the oils having a constant AN (0.5 mg KOH/g), but a wide range of BN (0.178-2.08 mg KOH/g). The final recovery varied within only 10%, which is much less significant than the variation obtained by changing the AN.

Beside AN/BN, other details of the oil composition, such as fraction of heavy components (resins, asphaltenes) and viscosity also have impact on smart water flooding. Zahid *et al.* (2010) carried out core flooding experiments with crude oils from Latin America, North Sea and Middle East, which have a wide range of asphaltene content. The additional recovery by injecting modified seawater varied between 1.2% to 4.5% for different oils.

Effect of potential determining ions

It has been reported by many researchers that certain ions in a brine may promote wettability alteration of the rock surface. Rezaei Gomari and Hamouda (2006) performed contact angle measurements to investigate the effect of NaCl, $MgCl_2$ and Na_2SO_4 on wettability alteration. Contact angles of fatty acid drops on calcite surface were measured in different brine environments. It was observed that the $MgCl_2$ and Na_2SO_4 solutions changed wettability more effectively than the NaCl solution. Alshakhs and Kovscek, 2016, also studied the impact of Mg^{2+} and SO_4^{2-} ions on the contact angle. The measurements were performed on an Iceland spar crystal chip at ambient conditions. It was observed that the contact angle was reduced from 95.7 to 55.4 degrees when the aqueous phase varied from seawater to a $MgSO_4$ rich brine.

In agreement with the above observations, (Rashid et al., 2015) found that Mg^{2+} alone could change wettability of the rock surface, and presence of SO_4^{2-} could enhance wettability alteration. Karimi *et al.*(2016) observed also that wettability alteration is more pronounced when both Mg^{2+} and SO_4^{2-} are present. Similar observations regarding the effect of Mg^{2+} and SO_4^{2-} on the contact angle were reported by Karoussi and Hamouda, (2007). However, in contradiction with these observations, Gupta *et al.* (2011) found that SO_4^{2-} and Ca^{2+} ions play a more important role than Mg^{2+} ions. This was established by the contact angle measurements at 90 °C with a model oil consisting of n-decane with 0.15%wt cyclohexanepentaonic acid.

In surprising contradiction with the above results, Lashkarbolooki *et al.* (2017) reported that distilled water altered the wettability of a carbonate reservoir rock from strongly oil-wet to strongly water-wet, while high concentrations of NaCl, $CaCl_2$, $MgCl_2$ solutions did not significantly change the contact angle. Meanwhile, KCl was found to be able to alter the wettability to strongly water-wet. A capability of the different salts to alter wettability was reported to be: KCl > DIW > NaCl > $MgCl_2$ > $CaCl_2$.

Effect of low salinity brine

Injection of low salinity brine may also make the chalk more water-wet. However, the reported results of contact angle measurements with low salinity brines are rather controversial. Yousef *et al.* (2012) performed such measurements under reservoir conditions and pointed out that diluted seawater makes the reservoir rock more water-wet. Mahani *et al.* (2015) also observed lower contact angles for seawater and diluted seawater than for the formation water. However, Mohsenzadeh *et al.* (2016) did not observe a significant change in contact angles by low salinity brines.

Patil *et al.* (2008) measured the Amott-Harvey indices of the cores flooded by a low salinity brine. The cores became more water-wet after flooding. It was concluded that mechanisms involved in low salinity water injection (LSWI) resemble those engaged in alkaline flooding.

Al-Shalabi *et al.* (2014) investigated the main mechanisms behind LSWI on oil recovery from carbonates through history matching of the results of the core flooding experiments. The experimental data used in this study were reported by Mohanty and Chandrasekhar, (2013). Wettability alteration was shown to be the main mechanism of the LSWI. Incremental oil recovery was found to be mainly controlled by the relative permeability for oil, rather than for water. A difference between the experimental and modeling outputs was attributed to heterogeneity of the core samples.

Sheng *et al.* (2010) compared the effect of wettability alteration under different oil-water interfacial tensions, in both fractured and non-fractured dolomite reservoir cores. Input data were obtained from the experiments of Hirasaki and Zhang (2004). It was concluded from the simulation that wettability alteration played an effective role only when IFT was high, which was more important at the early stages of the experiments.

Zaeri et al. (2018a, 2018b) carried out Amott (imbibition) tests with the reservoir oils and the carbonate rock materials from Iranian petroleum reservoirs. It was showed that there is an optimum degree of dilution corresponding to a maximum recovery. The recovery under imbibition of the 20 times diluted brine was found to be higher than under imbibition of the distilled water. These results were confirmed by measurements of the contact angles. It was also found that a higher permeability promotes the recovery by the low salinity brine. The authors explained this effect by interplay between viscous and capillary forces.

Salinity gradients

Shehata *et al.* (2014) injected brines with different ionic strength into limestone cores at 195°F. The main conclusion of their work was that a sudden change in salinity is more important than salinity itself. Mobility of the oil drops under varying salinity in the surrounded brine may be caused by the effect called diffusiophoresis (Prieve and Roman, 1987). A double layer around a drop in the surrounding concentration gradient may be non-uniform, which creates a moving force.

Zaeri et al. (2018b) showed that recovery by imbibition of the low salinity water increases much if the rock contains initially a certain (but not-so-large) amount of the saline connate water. Increasing the initial water saturation to a certain value improves the oil recovery, but any further increase has a negative impact. As discussed by Zaeri et al. (2018a), existence of initial water saturation may facilitate ion transport between the rock surface and the brine leading to the rock wettability alteration. Another explanation might be, though, that the formed salinity gradients cause diffusiophoresis of the oil drops and their joining of the infinite oil cluster. This mechanism needs further study.

Effect of temperature

It was reported by various researchers that temperature affects wettability alteration. Schembre *et al.* (2006) measured the Amott wettability indices for sandstone and carbonate cores. It was shown that increased temperature can change the rock wettability from intermediate and low water-wet to strongly water-wet. Hamouda and Rezaei Gomari (2006) reported also that increased temperature could make calcite surface more water-wet. Contact angle measurements confirmed these observations: contact angle decreased with increased temperature, indicating a more water-wet surface (Karoussi and Hamouda, 2007). A positive effect of high temperature was also reported by Zaeri et al. (2018a, 2018b).

However, there is a different possibility. Anhydrate dissolution by low salinity flooding may supply Ca^{2+} and SO_4^{2-} to the injection brine in-situ, which are among the key ions to trigger wettability alteration (Austad et al., 2015; Strand et al., 2017). If the solubility of anhydrate in a particular brine decreases with increased temperature, the amount of Ca^{2+} and SO_4^{2-} supplied by anhydrate dissolution may also decrease. This makes high temperatures unfavorable for wettability alteration.

Discussion

It can be seen from the above review that the observations of wettability alteration mechanism are not always consistent. Most studies used the contact angle as an indicator of wettability. However, some important information, such as surface roughness of the solid substrate and the time scale of the measurements, was rarely reported. These factors could largely affect the measurements. The contact angle is not only related to the brine composition, but also to the oil composition and rock mineralogy (Buckley et al. 1998). Hence, the results reported by different researchers, who applied different materials in their experiments, may not be directly comparable.

Another factor that is worth discussing is an optimal state of wettability for oil production. While most published results imply that a more water-wet rock is preferred for oil production, Skauge and Ottesen (2002) pointed out that an intermediate-wet state is most efficient. They summarized waterflooding results from 30 fields from the North Sea area and plotted residual oil saturation against Amott-Harvey index. The lowest residual oil saturation was found when the index was around zero (which indicates intermediate-wet rock). A possible explanation is that the magnitude of capillary pressure is minimized at the intermediate-wet state, which helps mobilizing small oil drops in the pore space by flooding (the Jamin effect). Another explanation is that intermediate wettability reduces the snap-off and entrapment of the residual oil. This has been observed in micro-CT experiments and numerical simulations performed on the capillary networks (Høiland et al., 2007).

Importance of the wettability change has also been questioned. The study of Katika *et al.* (2018) indicates that enhanced recovery due to wettability change was unlikely in that case since the NMR measurement did not show any wettability alteration under smart water flooding. Other factors, like pore collapse and fines precipitation, might be more important in this case.

Wettability, after all, is a macroscopic property of the two liquids on the solid substrate. The wettability alteration may be caused by the different physical phenomena. It may be that these phenomena, but not wettability itself, that result in better recovery. When studying wettability, one tends to focus on one or two parameters or microscopic mechanisms, often leaving other parameters uncontrolled. This could be a reason why wettability still remains mysterious after so many years of research. In the following sections, we present a number of particular chemical/physical wettability modifying mechanisms that may potentially increase the recovery.

2.2.1.2 Surface ion exchange

Surface ion exchange is often believed to be the main mechanism for improved oil recovery by smart waterflooding. It acts via detachment of polar components of oil from the surface; changing the surface charge; expanding the double layer; and, finally, altering the wettability of the rock surface. In this part, we discuss experimental studies based on this mechanism.

Description and evidence of the mechanism

The mechanism of multi-ion exchange was first proposed by Zhang *et al.* (2007) based on a series of imbibition experiments and chromatography wettability tests (Zhang et al., 2006; Zhang and Austad, 2006). It was suggested that adsorption of negatively charged ion SO_4^{2-} onto positively charged chalk

surface reduces the total charge of the surface. Then, positively charged Ca^{2+} and Mg^{2+} ions could gain access to the surface.

Ca^{2+} may react with the adsorbed carboxylic groups and release them from the rock surface by replacing surface-carboxylate bonds. The carboxylic groups belong to organic acids presented in the oil. When the bonds are broken, the oil is detached from the surface and may be further produced. If the attached carboxylic groups belong to a layer of heavy hydrocarbons adsorbed on the surface, their detachment may result in a more water-wet surface.

Unlike Ca^{2+} functioning at any temperature, Mg^{2+} comes into play at high temperatures: Mg^{2+} may displace a Ca-carboxylate complex from the surface. Eqs (1) and (2) demonstrate this reaction (Zhang et al. 2007):

$$2CaCO_3 + Mg^{2+} = CaMg(CO_3)_2 + Ca^{2+} \quad (1)$$

$$Ca^{2+} + R - COOH \rightarrow Oil\ recovery \quad (2)$$

Interplay between the potential determining ions (PDI), e.g. Ca^{2+}, Mg^{2+} and SO_4^{2-}, is an important factor for this recovery mechanism. Numerous experiments were performed to verify the roles of these ions, in order to maximize performance of the waterflooding under particular conditions. Often, the ion exchange was not directly observed; instead, additional oil recovery from imbibition and core flooding experiments using the PDI containing brines was regarded as an indicator for the process.

First, it was noticed that a higher SO_4^{2-} concentration is beneficial for oil production. Zhang and Austad (2006) performed spontaneous imbibition experiments with an outcrop chalk at various temperatures. The concentration of SO_4^{2-} in the imbibing brine varied between 0 and 4 times of its concentration in seawater, while the Ca^{2+} concentration was kept constant, equal to concentration in seawater. It was observed that oil recovery increased substantially with increasing SO_4^{2-} concentration. Similar observations was made by Strand *et al.* (2006a), where a significant increase in oil recovery was achieved by three-times increasing the SO_4^{2-} concentration in the imbibing seawater. Puntervold *et al.* (2015) reported a 10% additional recovery in the imbibition experiments by spiking 3-4 times SO_4^{2-} concentration in the NaCl depleted seawater.

Core flooding experiments with Stevns Klint chalk confirmed the effectiveness of SO_4^{2-} (Zahid et al., 2010). A slight yet definite (3-5%) additional oil recovery was obtained by injecting seawater or seawater with a three times increased SO_4^{2-} concentration in both secondary and tertiary modes. However, this effect was not observed for a reservoir rock (see the discussion below).

The effect of Ca^{2+} and Mg^{2+} was also studied in the imbibition experiments (Zhang et al., 2007, 2006; Zhang and Austad, 2006). The oil recovery increased consistently with the increase of the Ca^{2+} concentration, while the SO_4^{2-} concentration was kept constant in the imbibing brine. In addition, when Mg^{2+} or Ca^{2+} were added into the imbibing brine, which was initially free of them, the oil recovery increased significantly.

Co-existence of Mg^{2+} and SO_4^{2-} was found to be crucial for this mechanism. Karoussi and Hamouda (2007) reported increased oil recovery from the Stevns Klint chalk by imbibition experiments with the brines containing Mg^{2+} and SO_4^{2-}. Similar results were observed with limestone cores by Karimi *et al.* (2016). It was found that injection of the Mg^{2+} and SO_4^{2-} containing brine may result in higher imbibition, and that the brines containing both Mg^{2+} and SO_4^{2-} are more efficient than only the Mg^{2+} containing brine.

However, despite the numerous evidences of the beneficial effects of PDIs, negative results were also reported. After secondary recovery by injecting single component brines (NaCl, $MgCl_2$, Na_2SO_4, $MgSO_4$, $CaCl_2$), Gandomkar and Rahimpour (2015) did not observe any additional oil recovery by seawater or formation water injection into reservoir limestone cores.

In some cases, the smart water effect was observed even if PDIs were selectively removed or displaced. Gupta *et al.* (2011) obtained additional oil recovery by applying the SO_4^{2-} depleted seawater. Adding borate and phosphate into such a brine increased further the oil recovery.

Temperature dependence

The ion exchange process discussed above appears to be temperature dependent. Since the mechanism involves exchange of the Ca^{2+} ion from a rock by the Mg^{2+} from a brine, this may detected by measurements of the ion concentrations in the effluent in the course of the flooding experiments.

The exchange becomes more effective at higher temperatures (Zhang et al., 2007). The Ca^{2+} concentrations in the effluent at different temperatures were analyzed in that work. There was no detectable increase of Ca^{2+} concentration at 23°C and 70°C, while the increase of about 20% and 40-50% was observed at 100°C and 130°C, correspondingly. The temperature of 70°C was found to be the lowest threshold for the Ca-Mg exchange to take place (Austad, 2013).

The affinity of Ca^{2+}, Mg^{2+}, and SO_4^{2-} toward the limestone surface was evaluated for a range of temperatures, from the room temperature to 130°C. It was observed that Mg^{2+} adsorbed stronger at higher temperatures. Similar results were obtained for a chalk surface (Strand et al., 2008). The observations were explained by the level of hydration of Mg^{2+} and SO_4^{2-}. At low temperatures SO_4^{2-} and Mg^{2+} are strongly hydrated. If the temperature rises above 100°C, the degree of hydration decreases, so that Mg^{2+} and SO_4^{2-} are easier to adsorb on the chalk surface.

The effect of the temperature dependence of the ion exchange process on oil recovery was studied by the imbibition and core flooding experiments (Zhang et al., 2007; Zhang and Austad, 2006). A substantial increase of oil recovery was observed upon increasing temperature from 40 to 70, 100 and 130 ^{o}C in the imbibition experiments with the PDI containing brines. The same tendency was also observed when the brines containing only single PDI were injected (in the brines containing $MgCl_2$ or Na_2SO_4). Fathi *et al.* (2011) observed a significant increase of oil recovery with the increase of temperature by injecting a seawater depleted by NaCl, but spiked with 4 times of SO_4^{2-} or Ca^{2+} concentration.

However, the impact of temperature is less significant in the core flooding experiments. Zahid *et al.* (2012b) observed increase of oil recovery by injection of seawater into the Stevns Klint and North Sea chalk plugs. The additional recovery ranged from 1.1% at 40 °C to 4.4% at 120 °C, which is a rather small increase compared to the imbibition experiments.

Effect of rock type

In many experiments described above, the outcrop chalk from Stevns Klint was used as an analog for North Sea reservoir chalk. However, regarding the mechanism of surface ion exchange, it may not be representative for the reservoir rocks. The researchers reported different reaction, under similar experimental conditions, of the outcrop and reservoir chalk on smart waterflooding, as well as from the outcrops of a different origin. Zhang *et al.* (2007) pointed out that the ion exchange mechanism is difficult to be extended to limestone reservoir rock, since the reactivity of biogenic chalk is much higher than of the recrystallized limestone.

Romanuka *et al.* (2012) performed a series of imbibition experiments with the Stevns Klint chalk, limestone cores, and dolomite cores. Only the Stevns Klint chalk exhibited higher recovery with the increased sulfate concentration, while for other cores additional recovery was obtained by injection of a low salinity brine. The authors speculated that, apart from chemical composition of the rock, other properties (e.g. structure of the pore space) may affect the recovery. Similar observations regarding sulfate were reported by Zahid *et al.* (2012): injection of seawater with a high SO_4^{2-} content resulted in a substantial additional recovery from the Stevns Klint chalk, while no response was observed for a North Sea reservoir chalk.

The effect of low salinity flooding was also different depending on a particular rock. A number of researchers reported successful application of the low salinity flooding in the Middle East limestone reservoir rock (Mohsenzadeh et al., 2016; Yousef et al., 2012b, 2011, 2010; Zhang and Sarma, 2012). However, no additional recovery was obtained when flooding an Aalborg outcrop core (Zahid et al., 2012b). Austad *et al.* (2012) pointed out that anhydrite must be present in the rock matrix in order to obtain the low salinity effect. Dissolution of anhydrite by injection of low salinity brine could produce SO_4^{2-} and Ca^{2+} in situ, which facilitates surface ion exchange. They performed core flooding experiments with limestone cores from the aqueous zone of a reservoir. A small amount of additional recovery (1% to 5% OOIP) was obtained by low salinity flooding, in association with anhydrite dissolution. Shehata *et al.* (2014) performed corefloods on Indiana limestone core samples. No additional oil was produced after injection of the diluted seawater, while presence of potential determining ions resulted in additional production, similar to the Stevns Klint core flooding. Finally, Alameri *et al.* (2014) described flooding experiments in a Middle East rock, where both low salinity and PDIs produced additional effect. In general, the results presented in the different works look controversial and cannot be interpreted as an evidence in favor or against a single production mechanism.

Behavior of the dolomite rock regarding smart waterflooding was also examined. Mahani *et al.* (2015) carried out the contact angle and the Zeta potential measurements with a dolomite outcrop and a limestone reservoir rock from Middle East. When exposed to diluted seawater, the contact angle on the dolomite surface exhibited an insignificant change compared to the limestone. The dolomite exhibited also a higher zeta potential for all the tested brines (e.g. formation water, seawater, 25 times diluted seawater), which is not favorable for desorption of hydrocarbons. This conclusion was strengthened by Gachuz-muro and Sohrabi (2017). Core flooding experiments were performed with a dolomite core plug, and no additional recovery was observed under injection of seawater or diluted seawater.

Discussion

It is evident from the numerous reported observations that the surface ion exchange is one of the mechanisms behind smart waterflooding, or, at least, accompanying it. However, in order to benefit from such a mechanism, some conditions should be met. For some rocks, temperature should be higher than a certain threshold value to maximize the extend of the reaction, so that the effect becomes significant enough to produce residual oil. From the aspect of chemical kinetics in general, the extent of a reaction is always related to the concentrations of the reactants. Hence, it can be speculated that the threshold value of the temperature should be dependent on the composition of the brine. However, this has not been verified yet.

As discussed above, the mechanism is not universal, and depends on the rock lithology. A general trend is that the biogenic outcrop chalk, which has undergone less re-crystallization process than dolomite and limestone, is more responsive to the surface ion exchange. Other types of carbonate rock are more inert toward this mechanism. The different ions may behave differently in the different rocks, even with very close mineralogies. As remarked by Romanuka *et al.* (2012), other properties of the rock may also be

important. In other words, surface ion exchange may not be the sole mechanism responsible for additional recovery under smart waterflooding.

2.2.1.3 Surface charge alteration

Basic concepts

The surfaces of solids are usually charged. For example in the case of positive charge, a layer of negative charges is accumulated in the solution at some distance from the surface. Additional positive and negative layers may also appear. This distribution of the ions is efficiently described by a double layer, characterized by thickness and potential difference (the so-called zeta-potential). If another surface is introduced in a vicinity of solid, it may be repelled, with the repulsive force characterized by a value of disjoining pressure. In particular, an oil surface near a solid in a brine environment may be considered. A larger thickness of the double layer, a higher disjoining pressure, or a negative value of the zeta-potential means that the oil is repelled from the solid surface and becomes easier to produce.

Hirasaki (1991) proposed a model of surface forces between water, oil and mineral surface, which includes electrostatic, van der Waals, and structural components. According to the model, a thin water film is present between the oil and mineral surfaces. The total effect of the forces acting in this system is expressed as a disjoining pressure isotherm. Its integral gives the specific interaction potential isotherm which can be used to determine stability of the water film at a three phase contact region. A higher disjoining pressure indicates the stable water film and vice versa.

The disjoining pressure is affected by the surface potential and thickness of the electrical double layer (EDL) (Hiorth et al., 2010). If the charges of both oil and the mineral surfaces are of the same sign, the water film will be stable, and the surface will be water-wet. Otherwise the water film will collapse and the surface will become oil-wet. On the other hand, the thicker the EDL, the higher the electrostatic force, hence the higher the disjoining pressure, and vice versa.

Distribution of the charges near the solid surface may be evaluated on the basis of the DLVO model (Derjaguin and Landau, 1941; Elimelech et al., 1998; Verwey and Overbeek, 1948). This theory describes repulsive or attractive forces between charged surfaces or colloidal particles in an electrolyte solution. Figure 1 shows a characteristic distribution of the electrostatic potential and the DLVO force between a negatively charged particle and a negatively charged infinite plane in an electrolyte solution.

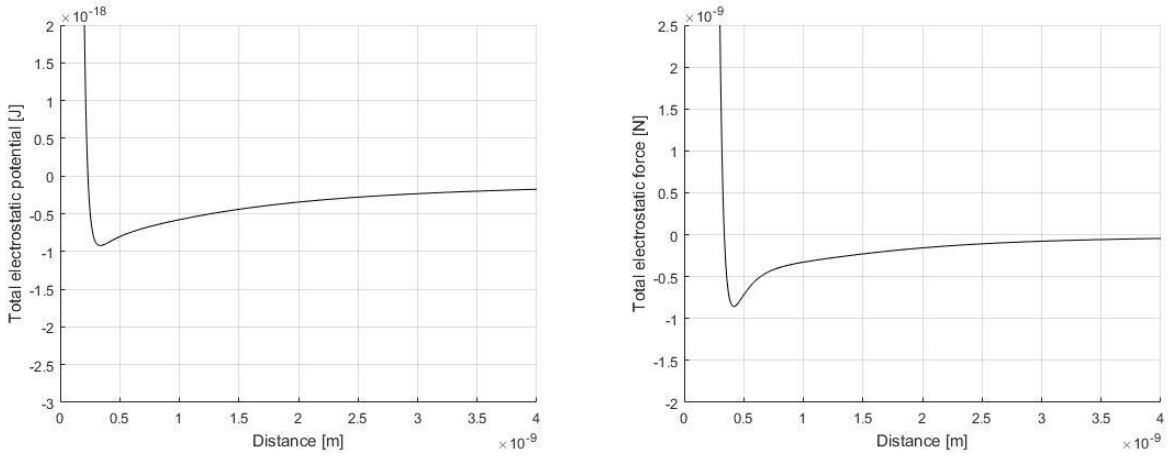

(a) (b)

Figure 1. DLVO forces (a) energy potential between a particle and a surface as a function of distance; (b) force between the particle and surface as a function of distance.

Alshakhs and Kovscek (2016) demonstrated application of the DLVO in order to evaluate the effect of divalent ions in carbonates. In this study, zeta potential data were used to predict contact angles and disjoining pressures by the DLVO theory. Close agreement between the experimental and the simulation results was reported.

Zeta potential

The oil may be attached to the surface of a rock by carboxylic groups belonging to the heavy oil components. Since the carboxylic groups are negatively charged, a negative value of zeta potential on mineral surface is preferred to reduce adsorption of oil. This value means that negative ions from the solution accumulate near the positively charged surface, repelling the oil.

Several factors may increase negative charge of the mineral surface. It was reported that injection of diluted seawater resulted in a more negative zeta potential of carbonate rock than of seawater and formation water, which produces the change in surface charge and increases oil recovery (Mahani et al., 2015; Yousef et al., 2012b). Increase in temperature from 40 to 60 °C leaded to a more negative surface charge (Yousef et al., 2012b). It was also reported by Zhang and Austad, 2006, that a higher SO_4^{2-}/ Ca^{2+} ratio lowers the zeta potential, corresponding to increase of the oil recovery under water imbibition.

Karoussi and Hamouda (2007) calculated disjoining pressure for several calcite-oil-water systems with the aqueous phase being distilled water, 0.1M Na_2SO_4, or 0.1M $MgCl_2$ solution. A significant increase of disjoining pressure was observed for the 0.1M $MgCl_2$ solution. The imbibition experiments also showed increased recovery when applying this solution. Alshakhs and Kovscek (2016) calculated the disjoining pressure between the oil and rock surfaces in brine environments for various brine compositions. The most stable water film was found when applying the diluted $MgSO_4$ brine.

Mahani *et al.* (2015) measured both zeta potentials and contact angles with limestone and dolomite samples. It was reported that under application of a low salinity brine the zeta potential of the limestone becomes more negative. This is consistent with the results of contact angle measurements, which showed that the limestone surface is less oil-wet when exposed to a low salinity brine. But low salinity has much less effect on dolomite. Due to different values of the zeta potential, the adhesion forces between oil and dolomite are stronger. This was confirmed in the contact angle measurements. It was concluded that the change of surface charge was the primary mechanism in low salinity water flooding.

Effect of non-potential determining ions

Fathi *et al.* (2010, 2011) observed that not only compositions of the active ions Ca^{2+}, Mg^{2+}, and SO_4^2, but also an amount of the non-active salt, NaCl, is important in oil recovery from carbonates. If the ionic double layer near a positively charged calcite surface contains less amount of a non-active salt, such as NaCl, access of sulfate to the calcite surface increases. In this way, sulfate, which is the key ion to change wettability of a rock surface, can act more efficiently in the absence of non-active ions.

Although it is mentioned in some works that monovalent ions like Na^+ and Cl^- are among the non-active ions, this may be not that definite. Depletion of seawater from NaCl causes significant reduction in salinity, which may produce additional effects. Alameri *et al.* (2014) removed NaCl from the injection water and concluded that oil recovery increased by 8%. A proposed explanation was expansion of the electrical double layer, which can be a sign of the low salinity effect, but not of the inactivity of the removed ions.

Effect of pH

One of the important parameters affecting electrostatic interactions between the three phases: oil, brine and carbonate surface, is pH (Sohal et al., 2016). Calcite is normally charged positively at neutral pH. However, it can become negatively charged at higher values of pH (Hirasaki and Zhang, 2004). In particular, application of alkali changes positive surface charge of the calcite during imbibition by alkaline-surfactant solutions (Hirasaki and Zhang, 2004).

Buckley *et al.* (1989) determined the conditions, under which various crude oils adhere to a solid surface at different pH and ionic strengths of the brine. They reported reduction of the zeta-potential by discreteness effect of dissociated groups at the interface at higher pH.

Somasundaran and Agar (1967) investigated the zero point of charge (ZPC) as a function of pH. The values of ZPC lied within the range of pH from 8 to 9.5. The zeta potential, pH, Ca^{2+} and CO_3^{2-} concentrations in the system were measured periodically. When pH in the solution was more basic, the surface was negatively charged, since negative ions predominated at the interface. For a more acidic pH, the surface was positively charged. It was suggested that Ca^{2+}, HCO_3^{2-}, H^+,OH^- and CO_3^{2-} become the potential-determining ions at the values of pH above 9.

Interaction between the double layer and the surface complexation

Some recent studies involving surface complexation modelling (SCM) indicated relationships between the charge of a double layer and wettability of the minerals. The surface complexation models describe preferential sorption of the ions on the charged surfaces. Song et al. (2017) proposed a SCM based on a generalized double layer model. The SCM model was developed to predict zeta potentials of a synthetic calcite surface in brines containing various potential determining ions (Mg^{2+}, Ca^{2+}, SO_4^{2-} and CO_3^{2-}) under different CO_2 partial pressures. The model was fitted to measured zeta potential data. It was found that synthetic calcite exhibited positive zeta potentials in brines containing Ca^{2+}or Mg^{2+}. The zeta potential can shift from positive to negative when increasing CO_3^{2-} or SO_4^{2-} concentrations at a partial pressure of CO_2 equal to $10^{-3.4}$ atm. However, at a partial pressure of 1 atm the zeta potential did not become negative, even if the brine contained 0.1M CO_3^{2-} or SO_4^{2-}.

Another study by Erzuah et al. (2017) explained how the surface charge affects wettability of calcite by hydrocarbon adhesion. The authors constructed a surface complexation model with the PHREEQ-C software, in order to estimate the wettability of quartz, kaolinite and calcite. Validity of the model was confirmed by the wettability estimation by the floatation method. It was concluded that the surface charge of a mineral has a dominant effect on the oil adhesion, rather than the properties of the brine/oil interface. For a positively charged mineral, like calcite, the carboxylic acid components in the oil are more effective, than its basic counterparts, in changing wettability of the mineral through adhesion.

Yutkin et al. (2016) studied the calcite/brine bulk kinetics and equilibria, as well as the calcite/brine surface equilibria with an ion comlexation model. It was pointed out that the double layer expansion is not possible unless the ionic strength is lower than 0.1 M. The rock dissolution cannot be a LSW mechanism because of the rapid rock/brine equilibration (carbonate could rapidly equilibrate with a brine in a short distance). The fines mobilization cannot occur because there is low clay content and low amounts of loose fines in the carbonate rocks studied by these authors. LSW cannot work as an alkaline flood because all the injected base will be consumed by carbonate dissolution near the wellbore and the pH will substantially decrease. The surface ion exchange remains a possible LSW mechanism, but, according to Yutkin et al., this is still unproven.

Discussion

As discussed in this section, expansion of double layer, higher disjoining pressure, or negative values of zeta potential can be reached at higher pH and lower salinities. This results in detachment of an oil from a solid surface and production of the residual oil. The zeta potential is used as an indicator for variation of the surface charge.

Measurement of zeta potential at different pH and calculation of disjoining pressure are often accompanied with uncertainties, especially, when measured in situ. Generally, there is a correlation between values of zeta potential and recoveries under the imbibition tests. However, this correlation is incomplete. Sometimes, inconsistency between the zeta potential data and the oil recovery is observed (Zhang et al., 2006). In the presence of magnesium, positive zeta potentials were observed; moreover, the potential increased by increasing the solution molarity. However, more oil was produced in the core flooding experiments. Yousef *et al.* (2012) reported that dilution of the injected seawater results in a more negative zeta potential. However, no additional oil was produced.

Hiorth *et al.* (2010) pointed out that alteration of the surface potential alone cannot explain the observed changes in oil recovery caused by changes in the water chemistry and temperature. The same is related to zeta potential: although it seems to be an important factor, it is insufficient for explanation of the recovery enhancement observed under smart waterflooding.

2.2.1.4 Mineral dissolution

Mineral dissolution, including calcite, dolomite and anhydrate, is one of the smart waterflooding mechanisms introduced in the literature. Dissolution of these species results in different effects, but some similarities are observed as well.

Observations of the dissolution

The calcite dissolution in a diluted brine occurs due to the following chemical reactions:

$$CaCO_3 \Leftrightarrow Ca^{2+} + {CO_3}^{2-} \quad (3)$$

$${CO_3}^{2-} + H_2O \Leftrightarrow {HCO_3}^{-} + OH^- \quad (4)$$

Additionally to calcite, dissolution/precipitation of magnesite and sulfate may take place (eqs. 3 and, correspondingly) (Alexeev, 2015):

$$MgCO_3\,(s) + H^+ \Leftrightarrow Mg^{2+} + {HCO_3}^{-} \quad (5)$$

$$CaSO_4\,(s) + H^+ \Leftrightarrow Ca^{2+} + {SO_4}^{2-} \quad (6)$$

These reactions show that the calcite dissolution causes pH alteration (Lager et al., 2008a). Thus, increase in pH and Ca^{2+} concentration in the effluent during oil recovery may indicate that the dissolution happens. Hamouda and Maevskiy (2014) observed increase of the Ca^{2+} concentration in the effluent, which was attributed to the chalk dissolution. They suggested Ca^{2+}/Mg^{2+} ion exchange and rock dissolution to be the main recovery mechanisms. Higher calcium and lower magnesium concentration in the effluent in comparison to the injection fluid was observed when injecting the diluted brines. However, Mahani *et al.* (2015) pointed out that the surface charge variation is a primary mechanism, while rock dissolution is a secondary reason for enhancement of the oil recovery. Additional oil recovery was observed under injection of $CaCO_3$ saturated seawater, where the calcite dissolution was excluded.

Mohammadkhani *et al.* (2018) investigated the effect of connate water salinity and saturation, as well as of the injected brine salinity, by conducting five core floodings on limestone core plugs at the room temperature. It was concluded that de-dolomitization and anhydride precipitation were among the determining mechanisms. The rock dissolution, indicated by increased pH, was only observed at tertiary stage, under injection of very low salinity seawater (< 3000 ppm).

Production mechanisms related to mineral dissolution

The mineral dissolution may facilitate oil production in several ways. Permeability modification is its one benefit. Gachuz-muro and Sohrabi (2017) injected the 50 times diluted seawater into a dolomite core in the tertiary recovery mode. A certain increase in permeability was observed along with a slightly higher oil recovery. The change in permeability was attributed to rock dissolution, which was verified by increase of the calcium and bicarbonate concentrations in the collected effluent.

Hiorth *et al.* (2010) constructed a chemical model to study surface charge and rock dissolution in a pure calcium carbonate rock. Numerous experimental data were used to tune the model. It was found that calcite dissolution matches well with the observed chemical and temperature dependences. It appeared to be a controlling factor for the observed smart water effect. The oil adsorbed on the calcium carbonate surface may be released due to its dissolution. Then surface that has formed after dissolution and oil release becomes water-wet.

Yousef *et al.* (2010, 2012) performed NMR measurements for a Middle East reservoir core before and after low salinity flooding. The results showed improved connectivity between macro- and micropores due to dissolution of the rock material in small pores, which is beneficial to improve sweep efficiency of the water flooding.

Karimi *et al.* (2016) described the rock dissolution in connection with the electric double layer interactions. The calcite dissolution results in an increased pH, which creates a more negatively charged brine/rock interface, which is repelled by a negatively charged brine/oil interface.

Dissolution of anhydrate was suggested to be able to promote wettability alteration by producing Ca^{2+} and SO_4^{2-} in-situ. Then it is related to the multi-ion exchange process and, subsequently, to release of the oil from the surface. This factor is often associated with injection of a low salinity brine (Austad et al., 2012; Chandrasekhar and Mohanty, 2013). Yousef *et al.* (2012) detected anhydrite dissolution by analyzing SO_4^{2-} concentration during low salinity injection. It was pointed out that presence of the anhydrite is a key factor for low salinity injection, since its dissolution could produce in situ the potential deterimining ion SO_4^{2-} (Austad et al., 2015, 2012). Alshakhs and Kovscek (2016) confirmed this mechanism and suggested that mineral dissolution supplied more divalent ions during flooding.

pH alteration may also occur under dissolution of calcite. Increase of pH may have a positive effect on the emulsion formation, as will be discussed in section 3.4. On the other hand, dissolution of calcite may occur mainly in the water filled part of the porous space, increasing mobility of the water compared to oil (although, to the best of our knowledge, the extent of this effect has not been studied).

Dynamics of dissolution

The mineral dissolution or precipitation is a static effect, according to our classification: It appears even if there is no flow. From the practical point of view, however, it is important to find out how this effect will manifest itself when coupled with the flow characteristic of reservoir development or laboratory flooding experiments (Houston et al., 2006). Such a study has been carried out by Alexeev et al., (2015), following and extending previous similar works (as applied to other processes) (Aharonov and Spiegelman, 1997; P.

Bedrikovetsky et al., 2009; P. G. Bedrikovetsky et al., 2009; Lam et al., 2008; Rubin, 1983; Spivey et al., 2004).

By extended numerical simulations it was found that the most important parameter is the ratio of the characteristic time of the dissolution reaction to the flow time. The last time may be chosen, for example, to be a time necessary for injection of one porous volume. If the time ratio is high (the dissolution is slow), then the effect of dissolution is insignificant, almost uniform, and occurs only after many porous volumes injected. As opposite, fast dissolution appears only close to the injection spot, without spreading deeply into the rock. As injection proceeds, porosity in a zone close to the injection spot increases, while the rest of the reservoir (or laboratory core) remains almost intact. In the extreme cases of fast reactions and many porous volumes injected, structures like wormholes may be formed.

Another observed effect is related to non-additivity of the volumes under dissolution. When the rock is dissolved in brine, the total volume usually decreases. The negative volume excess may rather significant, up to 0.8 of the initial rock volume. In dynamics, this results in a slight acceleration of the oil displacement by brine.

2.2.2 Other mechanisms

2.2.2.1 Interfacial tension, reology, and liquid-liquid interactions

Interfacial tension (IFT) measurements for smart waterflooding were conducted by many researchers (Al-Attar et al., 2013; Mahani et al., 2015; Yousef et al., 2012b). In particular, Khaksar Manshad *et al.* (2016) measured IFT of various ionic brines at a high temperature and atmospheric pressure. It was found that the K_2SO_4 solution at 2000 ppm produces the lowest IFT out of all the tested brines. However, in all the studies above, reduction of the IFT was too small to have an impact on oil recovery.

Sheng *et al.* (2010) pointed out that IFT plays a very important role with or without wettability alteration, during the entire process of flooding. On the contrary, Yousef *et al.* (2010, 2011) investigated the impact of salinity and ionic composition of injection water on oil recovery from carbonate reservoir cores. Interfacial tensions between the reservoir live oil and the field connate water, the seawater, and it's different dilutions were measured. The results showed that smart water flooding has an impact on the contact angle rather than IFT. This implies that diluted seawater influences rock/oil/brine rather than oil/brine interactions.

In some cases, even reverse effect of low salinity water on IFT was observed. An increase in IFT with decreasing salinity was reported by Alameri *et al.* (2014), in contradiction with improvement of the oil recovery by the low salinity effect.

Some studies pointed out that qualitative modification of an oil-water interface may be more important than just variation of the interfacial tension (Ayirala et al., 2017a, 2017b; Varadaraj and Brons, 2012). Depending on compositions of the contacting fluids, the interface may be viscous (liquid-like) or elastic (solid-like); the intermediate states are also possible. This effect is known for at least 60 years for oil-brine contacts (Criddle and Meader, 1955). It was attributed to the presence of surface-active compounds in oil, particularly, to asphaltenes (Hasiba and Jessen, 1966; Sheu et al., 1995; Varadaraj and Brons, 2012).

Recently it has been realized that the mentioned studies are important for smart waterflooding. If an oil-brine interface becomes solid-like, oil separates easier from the rock surface. On the contrary, if the interface is liquid-like, separate oil drops are easier to coalesce and to form a continuous flowing oil phase. Thus, in the "ideal brine recipe", the ions increasing the elasticity of the oil-water interface should

concentrate near the rock surface, while the ions making the interface more viscous should stay in the solution. Particularly, presence of sulfates in a brine promotes in some cases hardening of the interface (Ayirala et al., 2017a, 2017b).

2.2.2.2 Oil viscosity reduction

It has been reported that interactions between oil and brine may affect the oil viscosity. This effect may be combined with the effect of a high temperature, usually resulting in the viscosity decrease.

Gachuz-muro *et al.* (2016) examined a crude oil after contact with a sweetened and diluted seawater. It was concluded that the structure of the crude oil varies in contact with the different brines. In another work Gachuz-muro *et al.* (2013) put an oil and a brine in contact, with a volume ratio of 1:4 (20% oil and 80% brine) and measured viscosity of the oil before and after the contact. Normal brine (NW), distilled water (DW), formation water (FW) and a synthetic seawater (SW) corresponding to the Gulf of Mexico seawater were studied. Oil viscosity was reduced for all the tested brines, for the temperatures under 60 °C, while after this point the trend was reversed. It was also observed that viscosity was reduced more if it was initially higher.

Zahid et al. (2012) measured viscosity of a Latin American oil, a Middle East oil, and heptane, after their interaction with seawater under different SO_4^{2-} concentrations, under high temperature and pressure. Emulsification of these oils with a SO_4^{2-} spiked seawater was also studied in this work. It was observed that viscosity was affected for the oils containing heavy components, while emulsification was detected for the oils where such components were not present in significant amounts. The mechanism of viscosity reduction was explained by association or dissociation of the heavy molecules upon variation of ionic components of the brine in contact. Variation of the viscosity could not be explained by emulsification, since it was higher for other oils involved in the study.

2.2.2.3 Compaction

Compaction due to the rock weakening has been considered as one of the mechanisms of additional recovery. To the best of our knowledge, however, only few studies relate compaction to smart waterflooding (Katika et al., 2018). Meanwhile, the connection is obvious, since injection of an incompatible brine might result in chalk weakening. Shrinking of the pore space results in the oil squeezing out of it. Here we provide a short overview of the field observations and recovery mechanisms under reservoir compaction.

Compaction is classified as a static mechanism, since it may be, and usually is, measured in the laboratory experiments not involving liquid flow (saturation of a rock sample by brine with subsequent compression). On the other hand, selective compaction may result in fluid diversion, which is a purely dynamic effect. This is a particular case of contribution of the rock heterogeneity, which will be discussed further.

Field observations

Seafloor subsidence was observed in North Sea chalk reservoirs in 1980s after their development in early 1970s (Boade et al., 1989; Ruddy et al., 1989; Sylte et al., 1999). More than 7.8 meters of seafloor subsidence was detected in the Ekofisk field at the Norwegian sector of the North Sea since its production from 1971. The subsidence was primarily considered to be a result of pressure depletion due to production. However, in 1994, the subsidence did not stop, although water injection was sufficient to stabilize reservoir pressure (Sylte et al., 1999). The North Sea Valhall chalk reservoir also demonstrated significant compaction and subsidence associated with reservoir pressure depletion (Ruddy et al., 1989).

Reservoir compaction and oil recovery

Observations of the reservoir compaction and seafloor subsidence in the North Sea triggered several research projects to study water weakening of chalk and reservoir compaction. Although reservoir compaction may lead to additional operation cost, it was demonstrated to be beneficial for hydrocarbon production (Boade et al., 1989; Ruddy et al., 1989; Sulak et al., 1991). A combination of experimental measurements and modelling tools was employed to study compaction. Ruddy *et al.* (1989) used experimentally determined rock compressibility of Valhall Chalk samples in a reservoir model. It was found that the chalk compaction provided a significant part of hydrocarbon recovery from the Valhall field. A similar procedure was applied to study the Ekofisk field. Sylte *et al.* (1999) measured the relationship between strain and porosity for the Ekofisk chalk. It was then used in a reservoir model to predict production and subsidence. The results showed that water weakening could add a significant amount of energy to the reservoir system, which facilitated oil production.

Reservoir simulations brought similar conclusions. Sulak *et al.*, (1991) developed a modelling procedure to study reservoir compaction as a mechanism for hydrocarbon production in the Ekofisk field. It was concluded that reservoir compaction leads to increased production from the field. Boade *et al.* (1989) simulated compaction of the Ekofisk field by the ANSYS and DYNAFLOW simulators. It was found that waterflooding has a positive effect on compaction and subsidence. Chin and Thomas (1999) coupled a reservoir multiphase flow model with a geomechanical model and concluded that the water weakening effect may result in additional oil recovery, which may make a waterflood project more economically favorable for a water-sensitive reservoir.

Mechanisms of water weakening of chalk

Several studies focused on the mechanisms of the water weakening of chalk. Johnson *et al.* (1986) performed uniaxial and hydrostatic tests on the Ekofisk chalk samples. The results revealed that a dominant mechanism of deformation is rotation and mechanical breakdown of coccolith fragments and other calcium carbonate grains of the chalk matrix. No obvious evidence was found for chemical processes, such as dissolution-reprecipitation of the carbonate material during compaction. Similar conclusions were reported later by Powell and Lovell (1994), who performed the SEM image analysis on North Sea chalk samples before and after compaction. It was concluded that a dominant mechanism is simple grain displacement, which is characterized by rotation and sliding of individual calcite grains. Chemically assisted compaction mechanisms such as pressure dissolution and stylolitization were found to be insignificant for the production-induced compaction in the North Sea chalk.

However, more recent studies pointed out that chemistry of a saturating fluid plays an important role in the water weakening of chalk. By comparison of mechanical properties of the outcrop Lagerdorf chalk samples saturated with water and synthetic oil, Høeg *et al.* (2000) suggested that water-chalk interactions are governed by both capillary forces and chemical or physico-chemical processes.

Activity of water in the pore space may have an effect on mechanical strength of chalk (Risnes et al., 2005). Adsorption of the water molecules (which is a function of water activity) adds pressure on the grains. This pressure acts like a pore pressure and decreases cohesion of the chalk.

Calcite dissolution is another mechanism considered in the literature. Increased calcite solubility results in increased deformation rate (Hellmann et al., 2002). A study by Heggheim et al. (2004) showed 20 to 25% strength reduction for the cores saturated by seawater with an increased sulfate concentration, compared with the cores saturated by formation brine and seawater. The increased sulfate concentration was claimed to precipitate Ca^{2+} in a saturation fluid, which promoted dissolution of calcite. Dissolution of

calcite and precipitation of $CaSO_4$, rather than the capillary forces or water activity, was claimed to be responsible for weakening of the chalk.

A more complex mechanism involving ion adsorption and exchange was reported by Korsnes *et al.* (2008) and Austad *et al.* (2007). When a brine containing Mg^{2+} and SO_4^{2-} is present in the pore space, Mg^{2+} substitutes Ca^{2+} at the grain contacts. SO_4^{2-} acts as a catalyst in this process, by lowering down positive charge of the calcite surface. Hence, accessibility of Mg^{2+} to the surface increases. Different sizes of the Ca^{2+} and Mg^{2+} ions lead to structural changes in the inter-grain regions, which can weaken the chalk.

An effect of temperature on the water weakening of chalk was also studied by some researchers (Austad et al., 2007; Hellmann et al., 2002; Korsnes et al., 2008; Madland et al., 2002, 2006). However, contradictory conclusions were drawn. It was observed by Madland *et al.* (2002) that increased temperature from 20 to 130 degrees resulted, on average, in 20% reduction of yield and cohesion strength for water and glycol saturated chalk. Similarly, Hellmann *et al.* (2002) reported an increased strain with increased temperature during triaxial tests on water saturated chalk. On the contrary, it was reported by Korsnes *et al.* (2008) that hydrostatic yield stress was higher at 130 degrees than 90 degrees for chalk saturated by seawater and distilled water. Austad *et al.* (2007) also reported that water saturated chalk cores become stronger when temperature increases. A similar effect was observed for cores flooded with carbonated water (Madland et al., 2006).

Katika *et al.* (2018) observed that divalent ions contribute to the pore collapse in chalks, by weakening contacts between the grains. Nermoen *et al.* (2018) observed certain softening and weakening of chalk in sulfate rich brines. However, they concluded that neither presence of the certain ions in brine, temperature or aging alone are sufficient in order to predict chalk stiffness and strength. It is a combination of factors that determines elastic behavior of chalk.

Discussion

To the best of our knowledge, there are no studies indicating explicitly a relationship between smart water flooding, chalk compaction and oil recovery. However, there are links between them (Katika et al., 2018, 2015). It was widely reported in smart water projects that potential determining ions, mineral dissolution/precipitation, and temperature could have an impact on the oil recovery. The studies regarding water weakening of chalk involve similar parameters. It is shown that the potential determining ions have an impact on the mechanical properties of chalk. Although the reported effects are controversial, it may still be speculated that the following production mechanism takes place: Smart waterflooding reduces the strength of chalk; the weakened chalk undergoes enhanced compaction, which results in a change of pore structure and a decreased pore volume. Decrease of the pore space helps mobilizing stagnant oil. Verification of this mechanism is a subject for future research.

2.3 Dynamic mechanisms

In this section, mechanisms of smart waterflooding dependent on flow are discussed. These mechanisms include heterogeneity and flow diversion, as well as fines production and emulsion formation.

2.3.1 Flows dynamics and denuded zones

Many experimental works referred above contain results of flooding experiments carried out in a regime of spontaneous imbibition. The imbibition is governed primarily by capillary forces. Hence, no wonder that wettability and properties of the oil-brine-rock interfaces have been reported to determine success of the smart waterflooding.

Meanwhile, the literature indicates a large difference between the results of the spontaneous imbibition experiments and forced displacement (Strand et al., 2008; Zhang et al., 2007). While the role of capillary forces may be significant in laboratory waterflooding experiments, on the large reservoir-scales it may be less important, and viscous forces may prevail over capillarity (Bedrikovetsky, 1993).

The flow dynamics under injection of a different salinity brine and prevailing viscous forces (forced displacement) is generally similar to the dynamics of chemical flooding (Bedrikovetsky, 1993; Zeinijahromi *et al.*, 2011). A commonly used model is based on the classical Buckley-Leverett theory and its extensions (Bedrikovetsky, 1993; Pope, 1980). This theory predicts frontal character of displacement, with a residual oil being slowly produced after arrival of the water displacement front. A typical saturation profile is shown in Figure 2, a) (Alexeev, 2015). It should be noticed that the front of the displacing brine propagates always behind the oil displacement front. The reason is that the displacing brine fills a larger volume than oil, replacing both oil and the formation water.

Assume now that the injected brine contains a salt (or a chemical) affecting the recovery. The corresponding profiles of oil and brine saturations are schematically shown in Figure 2, b), for the case of tertiary injection. Due to the activity of the injected brine component, an additional oil bank is formed. Its production results, eventually, in decrease of the final oil saturation. If the injected chemical gets adsorbed (as most of them do), it travels behind the carrying brine. A zone of the so-called denuded water is formed. As a result, the effect of the injected brine on oil production is postponed. This delay may be even higher if the active component in the injected brine does not act instantaneously, but with a certain delay (reaction time). Then a positive effect of enhanced oil recovery may appear after many porous volumes injected. Additionally, the residual oil mobilized by the active component may travel with a different velocity than the "main" connected oil. This causes an extra delay (Alexeev, 2015). The whole picture of recovery is smeared, to a certain degree, by dispersion caused by heterogeneity of the rock, capillary forces, flow dispersion and reaction kinetics.

If the oil is produced in a regime of continuous secondary flooding, the active component (or the brine with a different salt composition) should appear after additional produced oil, like on the Figure 2. To the best of our knowledge, this has never been reported. Under tertiary recovery, additional oil production may sometimes happen simultaneously with the arrival of the injected additive (Alexeev, 2015).

Dispersion is responsible for mixing of the injected and connate brine, as experimentally studied by Graue *et al.* (2012). By nuclear-tracer imaging of the dynamic water saturation profiles, it has been verified that the mixing zone between the injected and the connate water is of a limited extent, and that, eventually, all the connate water becomes displaced by the injected brine (Graue et al., 2012) .

A system of flow equations describing all the physical mechanisms discussed above may only be solved numerically. Several attempts have been carried out to match available experimental data by solutions of such systems (Alexeev, 2015; Andersen et al., 2012; Eftekhari et al., 2017; Evje et al., 2009; Madland et al., 2011; Qiao et al., 2015). Complexity of the described process results in a relatively large number of adjustment parameters. It has been found that the resulting solutions can be fitted more or less accurately to experimental data, although Alexeev (2015) mentions that the concentration "tails" during long flooding experiments cannot be captured by the model. Fitting to the flooding data is necessary, and the flooding results cannot be predicted based on other experiments. This has been demonstrated by Eftekhari *et al.* (2017) by attempting to predict the flooding results, adjusting the reaction equilibria to data on independently measured zeta potentials. Especially, such a practically important parameter as residual oil saturation after flooding cannot be determined in advance and must be fitted every time to particular experimental data.

Alexeev (2015) and Eftekhari *et al.* (2017) indicated a correlation between the residual oil saturation and amounts of the adsorbed sulfate ions, while (contrary to the expectations) a correlation with concentrations of other potential determining ions is not that clear. This is confirmed by observations of Qiao *et al.* (2015), who account for mineralogy of the rock. In this study, it is shown that the recovery improvement is correlated with the amount of anhydrite, which is considered as a source for sulfate.

Another important observation is presence of the different characteristic time scales in the system, ranging from minutes to months (Alexeev, 2015; Andersen et al., 2012). Short-time transient behavior is better approximated by the rate-driven ion exchange on the surface, while long-time behavior is quasi-steady state on the laboratory scale.

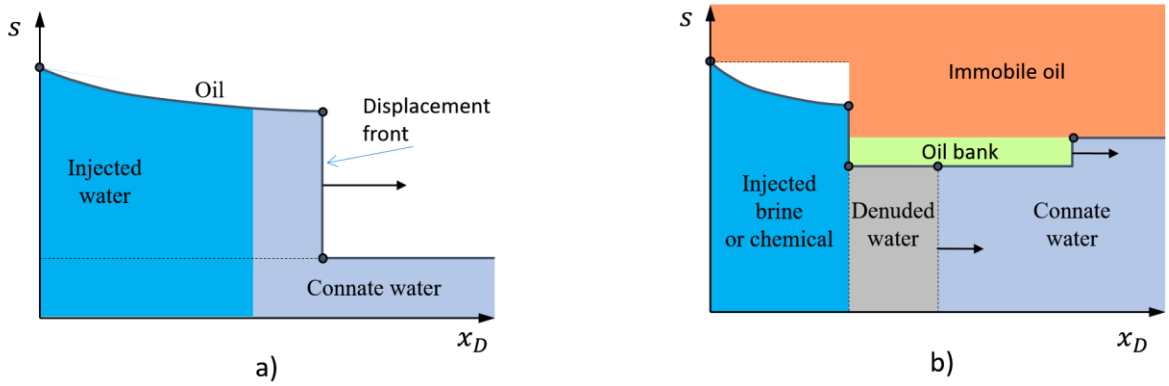

Figure 2. a) Displacement of oil by brine in the Buckley-Leverrett theory; b) Displacement of the oil by a chemical solution in a tertiary mode (after A. Alexeev, 2015)

2.3.2 Heterogeneity and fluid diversion

Although heterogeneity is not a mechanism by itself, it can amplify contributions of other mechanisms, especially, in the form of flow diversion. Petroleum reservoirs are highly heterogeneous at all scales. The pore scale is characterized by diversity in the pore geometries and by mixed wettability. On the formation scale, a reservoir is often represented as a layer-cake structure, containing also fractures and other structural elements. The laboratory core samples are never homogeneous, either, as revealed by the X-ray computer tomography (Figure 3).

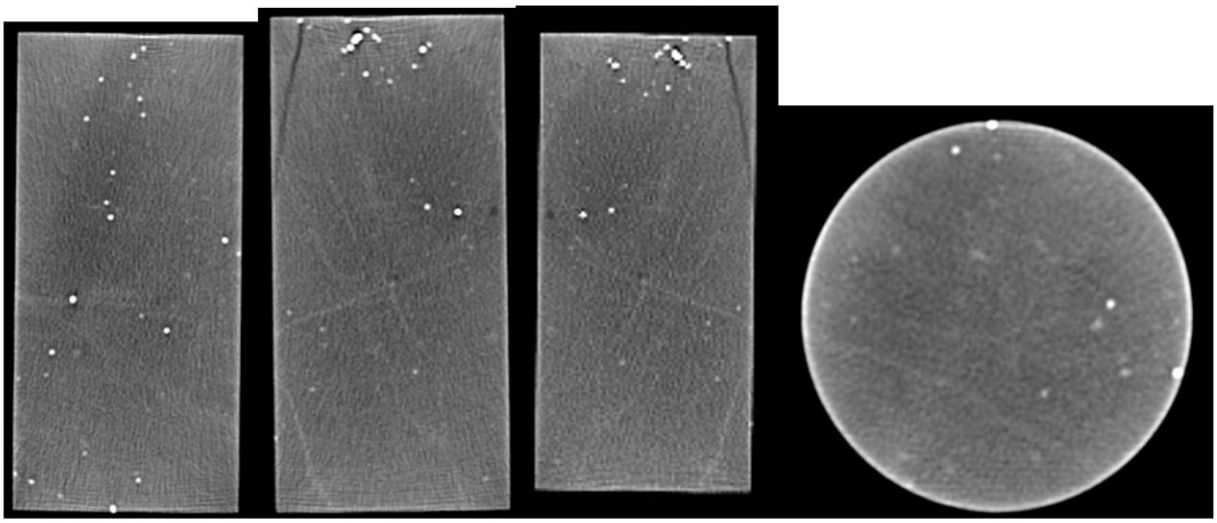

Figure 3. A sample X-ray computer tomography scan of a carbonaceous core sample (limestone from the North Sea).

Impact of heterogeneity on smart waterflooding has not been studied experimentally to a sufficient extent, although it has been recognized and discussed in the literature. Concerning the micro-scale heterogeneity, it was noticed that flooding experiments in a mixed-wet limestone cores are not well repeatable (Loahardjo et al., 2010). The pore geometry and surface structure were claimed to be among responsible factors, resulting in the fact that application of enhanced or desalinated brines leads to qualitatively different results for the different rocks (Romanuka et al., 2012).

The core-scale heterogeneity has been regarded as an important factor for the different methods of enhanced oil recovery (Spildo et al., 2012). It may contribute to the recovery via mobilization and relocation of reservoir fines. This effect was extensively studied for the sandstone rocks (Al-Sarihi et al., 2018; Borazjani et al., 2018; Hussain et al., 2013; Yu et al., 2018). The clay particles contained in the rock may be released, reacting on low salinity of the brine. They travel an insignificant distance and then deposit in narrow capillaries. As a result, permeability in the flooded zones decreases and the injected water is diverted to displace oil from other places. In heterogeneous rocks, this results in more uniform displacement and less bypassed and trapped oil. A set of recovery mechanisms based on re-direction of the injected fluid from the flooded zones has been regarded to as fluid diversion (Spildo et al., 2012). Apart from production of fines, there are other phenomena that may lead to fluid diversion in a carbonaceous rock, such like compaction, precipitation or emulsification. They are addressed elsewhere in the present review.

The work of Zahid et al. (Zahid et al., 2012a, 2012b) compared the recovery under low salinity flooding from a less consolidated Middle East reservoir core, and from a consolidated outcrop core of Aalborg chalk. While the Middle East core reacted on smart waterflooding, the Aalborg chalk core exhibited no additional recovery. This is explained by the rock weakening and fines mobilization in the less consolidated core. It is specially mentioned by Zahid et al. that wettability alteration and surface ion substitution cannot explain observed differences between the two cases. In particular, the surface ion substitution was observed for the Aalborg chalk core, but did not result in additional recovery.

Few simulations reveal the effect of heterogeneity on the macroscale. Attar and Muggeridge (2016) utilized a commercial reservoir simulator in order to study the effect of dispersion on mixing of the

injected and formation water under low salinity flooding in a layer-cake reservoir. The coefficient of transversal dispersion (Lake and Hirasaki, 1981) was found to be the main parameter responsible for the effect. Yuan and Shapiro (2011) performed a simulation of the effect of fines precipitation and mobilization in a layer-cake reservoir, applying an approximate method developed by Zhang et al., 2011. Decrease of permeability in the flooded zones had a significant impact and evens propagation of the water-oil displacement front (Yuan and Shapiro, 2011). Zeinijahromi *et al.* (2011) demonstrated that similar computations may be carried out by application of an option for polymer flooding in a commercial reservoir simulator.

2.3.3 Fines

Formation of the fine particles can occur during smart waterflooding. These particles can appear from mixing of injected and formation water or by releasing the minerals from the rock surface. Production and migration of fines may increase water-wetness of the rock surface. Besides, relocation of fines may block some pore throats, diverting the fluid flow and increasing sweep efficiency, as mentioned in the previous subsection. Additionally, appearance of the fines may facilitate formation of the oil-brine-particle emulsions (so-called Pickering emulsions). This mechanism will be considered in the next section.

Fines may appear both in static and dynamic way. While their precipitation due to incompatibility of the injected and formation brines may be regarded as static, mobilization of the inherent reservoir fines requires flow. A positive effect of the fines on recovery is mainly associated with the flow diversion and may only be investigated under flow conditions. That is why we consider the effect of fines as a dynamic phenomenon.

2.3.3.1 Precipitation from interaction between injected and formation water

Madland *et al.* (2011) pointed out that loss of Mg^{2+} during injection of a Mg^{2+} containing brine is not only due to ion substitution, but also due to precipitation of new minerals. SEM images of the core slices confirmed precipitation of the Mg bearing carbonates and Mg bearing clay-like minerals. Anhydrate precipitation by injection of a SW-like brine was also confirmed. Puntervold and Austad (2008) suggested that mineral precipitation may also occur due to mixing of seawater and produced water, as a general trend. The more seawater is mixed, the more $CaSO_4$ and $SrSO_4$ precipitates.

Chakravarty *et al.* (2015a, 2015b, 2015c) analyzed existing imbibition and flooding experimental data. By extensive thermodynamic computations, it was demonstrated that additional production is observed whenever mixing of the formation brine and injected water under experimental thermodynamic conditions results in precipitation of the $CaSO_4$. It was speculated that precipitation occurs in the form of fines. These fines may later be dissolved again when the brine is produced from the core, where temperature and pressure fall down. Inside the core the fines may facilitate formation of the emulsions and diversion of the flow, as discussed in the next section. Precipitation of such fines from an Mg-rich brine was indirectly detected by the NMR spectroscopy (Katika et al., 2015).

2.3.3.2 Release of the fines from the rock

Detachment and relocation of fines has been considered as one of the primary mechanisms for action of low salinity waterflooding in sandstones (Al-Sarihi et al., 2018; Tang and Morrow, 1999). Injection of low salinity brine results in released clay particles (fines) from the sandstone rock. These fines are relocated by the flow of water and further plug narrow pores on their flow path, resulting in a diverted water flow into non-flooded areas. Zeinijahromi et al. (2011, 2013, 2015) showed a significant effect of

fines migration, with consequent permeability damage, on sweep efficiency during low salinity waterflooding.

Similar effects have been observed for recovery from the chalk rocks, for example, by application of the fresh water injection to the Middle East chalk (Zahid et al., 2012a). Many chalk rocks are not well consolidated and "produce" fines just by touching them. During flooding, fines may promote emulsification, as considered in detail in the next section.

The detachment can be triggered by instability of electric forces induced by variation of ionic strength. DLVO theory was employed to predict stability of fine particles and indicates a decreased stability during low salinity flooding (Schembre et al., 2006). Detachment of fines can also be a result of mineral dissolution. Pu *et al.* (2010) proposed that dissolution of anhydrate cement in sandstone leads to release of dolomite crystals and other embedded minerals. Similar phenomena may be observed in carbonates.

2.3.4 Emulsion formation

Brine and oil can form emulsions, especially, in the presence of solid particles. Although the literature on emulsions is overwhelming, the studies related to waterflooding in carbonates are not multiple.

Formation of emulsions requires usually a certain mechanism of mixing, like stirring or vibrations. Only in rare cases the emulsions form spontaneously. A porous medium works as a "natural emulsifier", mixing the flowing liquids. That is why formation of emulsions is regarded to as a dynamic phenomenon requiring a flow or another mixing mechanism in order to appear.

Emulsions may play an important role in smart waterflooding. The efficient viscosities of emulsions are high; if the emulsion drop sizes are comparable to the pore sizes, the pores may be plugged, and the injected water may be re-directed to the non-flooded zones. Thus, emulsion formation may contribute to fluid diversion.

2.3.4.1 Emulsion formation at the brine-oil contacts

A study of Emadi and Sohrabi (2013) based on application of the micro-models under reservoir conditions revealed that, when a low salinity brine was in contact with certain crude oil, water micro-dispersions were formed in the oil phase near the oil/water interface. Formation and precipitation of the micro-dispersions could only be observed under high magnifications. Presence of a low salinity injected brine, of the high salinity formation water, and of the mixed-wet rock were found to be necessary conditions for emulsification.

Mahzari and Sohrabi (2014) brought different crude oil samples in contact with brines of different salinities. Spontaneous formation of water-in-oil dispersions occurred when salinity of the brine was below 2000 ppm, in agreement with the work of Emadi and Sohrabi (2013).

2.3.4.2 Fines assisted emulsification

Chakravarty *et al.* (2015a, 2015b, 2015c) suggested that mobile fines formed in a pore space during smart water flooding may lead to emulsion formation, which enhances the mobility of the oil phase and therefore increases the displacement efficiency. A mixture of fines, model oil and deionized water was studied in these experiments. Different water insoluble salts, including Li_2CO_3, $CaCO_3$, $MgCO_3$, $CaSO_4$, $SrSO_4$ and $BaSO_4$, formed fines. It was concluded that the fines interact with crude oil in the presence of a low salinity water and produce oil-in-water emulsions. Formation of oil micelles was only possible under presence of polar hydrocarbons in oil. It was also pointed out that light alkanes prefer forming emulsions with light acids, while heavy alkanes require heavier acids. In these studies it was also verified

that fines may appear as a result of incompatibility between injected brine and formation water (as described in the previous section). Formation of such fines promotes in situ emulsification.

Arshad *et al.* (2017) investigated the effect of $CaCO_3$ and $CaSO_4$ fines on emulsification with model (decane and hexane-hexadecane) and North Sea crude oils with deionized water, seawater and formation water. The sonification method was applied to create emulsions. Increase in emulsion formation and better emulsion stability was observed with increasing the amount of fines (Arshad et al., 2017). This study confirmed the results of Chakravarty *et al.* (2015a, 2015b, 2015c) that the distilled water emulsifies better than the seawater when synthetic oils are involved. However, a North Sea crude oil formed equal or larger amounts of emulsions with seawater than with distilled water. In another experimental study Arshad et al., (2018) focused on understanding the role of particle sizes on emulsification. This study involved particles of the sizes between 15 and 90 nm. For the model oils, larger amounts of emulsions with smaller droplet sizes were formed with smaller particles. Decrease of salinity also facilitated formation of emulsions. However, formation of emulsions with a North Sea oil did not show any significant dependence on the particle sizes and brine salinity.

2.3.4.3 Effect of pH on emulsification

Formation of emulsions is often attributed to activity of natural surfactants, like organic acids, on the water-oil interface. The value of pH affects this activity. This value is determined by the composition of an injected brine. Additionally, chemical interactions between rock, initial water and injected brine may cause increase in the pH by cation exchange or mineral dissolution.

Previous studies showed importance of the pH for emulsion formation by in-situ surfactants. Buckley *et al.* (1989) pointed out that dissolution of organic acids, which is dependent on pH, can take place at a water/oil interface. Addition of weak acids and bases to water may lead to well-buffered pH, which is maintained despite of the ionization of polar components of oil at the interface. Hirasaki and Zhang (2004) investigated the effect of alkaline surfactant solutions on carbonate reservoirs during imbibition tests and concluded that moderately high pH obtained from alkali solutions generated natural surfactants from naphthenic acids contained in the crude oil by in situ saponification. Rezaei Gomari and Hamouda (2006) implied that generation of surfactants from residual oil at elevated pH was the main low salinity recovery mechanism. Elevated pH can enhance oil recovery in several ways: generation of surfactant, change in wettability and reduction in IFT (McGuire et al., 2005; Rezaei Gomari and Hamouda, 2006).

Summarizing, formation of emulsions may be facilitated by production of fines and change of the pH of the solution. In situ formation of the emulsions may result in plugging waterflooded zones and diversion of the injected brine to displace oil from un-flooded zones.

2.4 General Discussion and Conclusion

We have overviewed the studies directed onto investigation of the possible chemical and physical mechanisms resulting in additional recovery under smart waterflooding of the carbonate rocks. We have attempted also to classify the works according to the investigated mechanisms. This classification is necessarily imperfect, since many studies consider multiple phenomena occurring simultaneously (which validates their mentioning in the different sections). However, on the positive side, we believe that nearly all the phenomena important for smart waterflooding have been described in the literature; and they have been mentioned in this review. It is unlikely that in the nearest future a totally new and unknown mechanism of recovery for smart waterflooding will be revealed.

A common point of agreement between the different authors is that it is possible, indeed, to increase recovery in carbonates by application of smartly composed and selected brines. However, here the agreement ends. The researchers argue for importance of potential determining ions in the brine (in different combinations: calcium, magnesium, sulfates, bicarbonate, other specific ions). Other works demonstrate efficiency of the low salinity water injection. There are also works claiming success of both specific ions and fresh water; or of neither of them.

The smart waterflooding mechanisms may roughly be divided into static (appearing in equilibrium) and dynamic (related to the flow). A more detailed classification is hardly possible. Many mechanisms work in combination, like expansion of the double layer and formation of the bonds (complexation) on the rock surface; or fines precipitation, emulsion formation and fluid diversion. At present, it is difficult to conclude about relative contributions of the specific mechanisms to gain additional recovery. Most probably, the recovery mechanisms work in combination and/or are differently important for specific carbonaceous rocks. The future experimental research should be designed in such a way that makes it possible to study the different mechanisms separately, confirming their importance or excluding them. An observation that phenomenon A is observed in the recovery process B is not sufficient to assert that A is a reason for B. It should, at least, be checked that A results in success of B in all the cases reported in the literature. In other words, not only positive, but also negative observations should be reported, and Propper's criterion of falsifiability should be verified.

Analysis of the importance of the different mechanisms of smart waterflooding is complicated by the fact that many experimental parameters are not reported or measured. Among the least often reported factors, are: exact timing of the experiment, mineral composition of the rock, homogeneity or heterogeneity of the rock samples, degree of their consolidation, compositions of the oil and effluent, production of fines, emulsification (or not), and other. In many cases, a more comprehensive analysis of experimental conditions, than provided by the authors, is required in order to make a definite conclusion about an actually working recovery mechanism. It is important to extract quantitative information whenever possible (e.g. analysis of the dependence of the residual saturations on the value of capillary number). Characteristic time scales for the different determining processes (e.g. ion adsorption) are also insufficiently studied. As stated by Bartels et al. (2017), analysis of the different processes with regard to the characteristic time and length scales may be a subject for the future research.

Experimental conclusions must be complemented and verified by a proper modeling. At present, models for most of the recovery mechanisms, both static and dynamic, are well established and match experimental results, at least, qualitatively. However, their predictive capability regarding expected recovery is not high. The main parameters, like residual saturations and characteristic times of the process, cannot be estimated in advance, without direct matching the performed flooding experiments. There is no way to evaluate these parameters better than within an order of magnitude, based on independent experiments. On the other hand, any reasonable flow model incorporating a relevant recovery mechanism and using residual saturations and characteristic relaxation times as adjustment parameters will be capable of matching the core flooding data within their accuracy. The models can well capture the recovery physics and chemistry, provided that it is known; however, it is unlikely that they may help discriminating between the different recovery mechanisms. This problem may probably be partly overcome by development of the advanced models involving multiscale analysis and averaging. However, necessary experimental information will still be missing there.

In sum, direct flooding tests are unavoidable at the present level of knowledge, but they should be supplemented by detailed accompanying experimental studies, like measurements of the oil-water-rock interactions or the experiments involving ordinary and micro CT scanning and other ways of non-invasive

flow monitoring. The static mechanisms are probably unable to explain the observed variety of the experimental results, and the recovery mechanisms based on flow dynamics should also be involved. A large body of experimental work has already been carried out and may serve as a basis for further analysis; however, many questions still remain open and require further studies.

References

Afekare, D.A., Radonjic, M., 2017. From Mineral Surfaces and Coreflood Experiments to Reservoir Implementations: Comprehensive Review of Low-Salinity Water Flooding (LSWF). Energy and Fuels 31, 13043–13062. https://doi.org/10.1021/acs.energyfuels.7b02730

Aghaeifar, Z., Strand, S., Austad, T., Puntervold, T., Aksulu, H., Navratil, K., Storås, S., Håmsø, D., 2015. Influence of Formation Water Salinity/Composition on the Low-Salinity Enhanced Oil Recovery Effect in High-Temperature Sandstone Reservoirs. Energy and Fuels 29, 4747–4754. https://doi.org/10.1021/acs.energyfuels.5b01621

Aharonov, E., Spiegelman, M., 1997. Three-dimensional flow and reaction in porous media: Implication for the Earth's mantle and sedimentary basins. Jouranl Geophys. Res. 102, 821–833.

Al-Attar, H.H., Mahmoud, M.Y., Zekri, A.Y., Almehaideb, R., Ghannam, M., 2013. Low-salinity flooding in a selected carbonate reservoir: Experimental approach. J. Pet. Explor. Prod. Technol. 3, 139–149. https://doi.org/10.1007/s13202-013-0052-3

Al-Sarihi, A., Zeinijahromi, A., Genolet, L., Behr, A., Kowollik, P., Bedrikovetsky, P., 2018. Effects of Fines Migration on Residual Oil during Low-Salinity Waterflooding. Energy and Fuels 32, 8296–8309. https://doi.org/10.1021/acs.energyfuels.8b01732

Al-Shalabi, E.W., Sepehrnoori, K., Pope, G., 2014. Mysteries behind the Low Salinity Water Injection Technique. J. Pet. Eng. 2014, 1–11. https://doi.org/10.1155/2014/304312

Alagic, E., Spildo, K., Skauge, A., Solbakken, J., 2011. Effect of crude oil ageing on low salinity and low salinity surfactant flooding. J. Pet. Sci. Eng. 78, 220–227. https://doi.org/10.1016/j.petrol.2011.06.021

Alameri, W., Teklu, T.W., Graves, R.M., Kazemi, H., AlSumaiti, A.M., 2014. Wettability Alteration During Low-Salinity Waterflooding in Carbonate Reservoir Cores, in: SPE Asia Pacific Oil & Gas Conference and Exhibition. Adelaide, Australia. https://doi.org/10.2118/171529-MS

Alexeev, A., 2015. Modeling of Salinity Effects on Waterflooding of Petroleum Reservoirs. Technical University of Denmark.

Alexeev, A., Shapiro, A., Thomsen, K., 2015. Modeling of Dissolution Effects on Waterflooding. Transp. Porous Media 106, 545–562. https://doi.org/10.1007/s11242-014-0413-5

Alshakhs, M.J., Kovscek, A.R., 2016. Understanding the role of brine ionic composition on oil recovery by assessment of wettability from colloidal forces. Adv. Colloid Interface Sci. 233, 126–138. https://doi.org/10.1016/j.cis.2015.08.004

Alvarado, V., Bidhendi, M.M., Garcia-olvera, G., Morin, B., Oakey, J.S., 2014. Interfacial Visco-Elasticity of Crude Oil - Brine : An Alternative EOR Mechanism in Smart Waterflooding. SPE Improv. Oil Recover. Symp. 1–17. https://doi.org/10.2118/169127-MS

Andersen, P., Evje, S., Madland, M. V., Hiorth, A., 2012. A geochemical model for interpretation of chalk core flooding experiments. Chem. Eng. Sci. 84, 218–241. https://doi.org/10.1016/j.ces.2012.08.038

Arshad, M.W., Feilberg, K.L., Shapiro, A., Thomsen, K., 2018. Characterization of Emulsion Formation With Nanoparticles for Enhanced Oil Recovery. SPE Kingdom Saudi Arab. Annu. Tech. Symp. Exhib. 23-26 April. Dammam, Saudi Arab. https://doi.org/https://doi.org/10.2118/192170-MS

Arshad, M.W., Loldrup Fosbøl, P., Shapiro, A., Thomsen, K., 2017. Water-Oil Emulsions with Fines in Smart Water Enhanced Oil Recovery. SPE Kuwait Oil Gas Show Conf. https://doi.org/10.2118/187620-MS

Attar, A., Muggeridge, a H., 2016. Evaluation of Mixing in Low Salinity Waterflooding. SPE EOR Conf. Oil Gas West Asia 21–23. https://doi.org/10.2118/179803-MS

Austad, T., 2013. Water-Based EOR in Carbonates and Sandstones: New Chemical Understanding of the EOR Potential Using "Smart Water," First Edit. ed, Enhanced Oil Recovery Field Case Studies. Elsevier Inc. https://doi.org/10.1016/B978-0-12-386545-8.00013-0

Austad, T., Rezaeidoust, A., Puntervold, T., 2010. Chemical Mechanism of Low Salinity Water Flooding in Sandstone Reservoirs, in: SPE Improved Oil Recovery Symposium. Tulsa, Oklahoma, U.S.A. https://doi.org/10.2118/129767-MS

Austad, T., Shariatpanahi, S.F., Strand, S., Black, C.J.J., Webb, K.J., 2012. Conditions for a low-salinity Enhanced Oil Recovery (EOR) effect in carbonate oil reservoirs. Energy and Fuels 26, 569–575. https://doi.org/10.1021/ef201435g

Austad, T., Shariatpanahi, S.F., Strand, S., Aksulu, H., Puntervold, T., 2015. Low Salinity EOR Effects in Limestone Reservoir Cores Containing Anhydrite: A Discussion of the Chemical Mechanism. Energy and Fuels 29, 6903–6911. https://doi.org/10.1021/acs.energyfuels.5b01099

Austad, T., Standnes, D.C., 2003. Spontaneous imbibition of water into oil-wet carbonates. J. Pet. Sci. Eng. 39, 363–376. https://doi.org/10.1016/S0920-4105(03)00075-5

Austad, T., Strand, S., Madland, M. V., Puntervold, T., Korsnes, R.I., 2007. Seawater in Chalk: An EOR and Compaction Fluid, in: International Petroleum Technology Conference. Dubai, UAE. https://doi.org/10.2118/118431-PA

Ayirala, S.C., Yousef, A.A., 2016. A critical review of water chemistry alteration technologies to develop novel water treatment schemes for smartwater flooding in carbonate reservoirs, in: SPE Symposium on Improved Oil Recovery Conference. Tulsa, Oklahoma, U.S.A. https://doi.org/https://doi.org/10.2118/179564-MS

Ayirala, S.C., Al-Saleh, S.H., Al-Yousef, A.A., 2017a. Microscopic scale interactions of water ions at crude oil/water interface and their impact on oil mobilization in advanced water

flooding. J. Pet. Sci. Eng. 163, 640–649. https://doi.org/10.1016/j.petrol.2017.09.054

Ayirala, S.C., AlYousef, A.A., Li, Z., Xu, Z., 2017b. Water Ion Interactions at Crude Oil-Water Interface: A New Fundamental Understanding on SmartWater Flood, in: SPE Middle East Oil & Gas Show and Conference. Manama, Kingdom of Bahrain. https://doi.org/10.2118/183894-MS

Bartels, W.B., Mahani, H., Berg, S., Hassanizadeh, S.M., 2019. Literature review of low salinity waterflooding from a length and time scale perspective. Fuel 236, 338–353. https://doi.org/10.1016/j.fuel.2018.09.018

Bedrikovetsky, P., Silva, R.M.P., Daher, J.S., Gomes, J.A.T., Amorim, V.C., 2009. Well-data-based prediction of productivity decline due to sulphate scaling. J. Pet. Sci. Eng. 68, 60–70. https://doi.org/10.1016/j.petrol.2009.06.006

Bedrikovetsky, P.G., 1993. Mathematical Theory of Oil and Gas Recovery. Kluwer Pub.

Bedrikovetsky, P.G., Mackay, E.J., Silva, R.M.P., Patricio, F.M.R., Rosário, F.F., 2009. Produced water re-injection with seawater treated by sulphate reduction plant: Injectivity decline, analytical model. J. Pet. Sci. Eng. 68, 19–28. https://doi.org/10.1016/j.petrol.2009.05.015

Bernard G.G., 1967. Effect of Floodwater Slinity on Recovery of Oil from Cores Containing Clays. SPE J. https://doi.org/10.2118/1725-MS

Boade, R.R., Chin, L.Y., Siemers, W.T., 1989. Forecasting of Ekofisk Reservoir Compaction and Subsidence by Numerical Simulation. J. Pet. Technol. 41. https://doi.org/10.2118/17855-pa

Borazjani, S., Behr, A., Genolet, L.C., Kowollik, P., 2018. Fines-Migration-Assisted Waterflooding to Improve Sweep Efficiency Analytical Model, in: SPE International Conference and Exhibition on Formation Damage Control. Lafayette, Louisiana, USA.

Buckley, J.S., Takamura, K., Morrow, N.R., 1989. Influence of Electrical Surface Charges on the Wetting Properties of Crude Oils. SPE Reserv. Eng. 332–340.

Chakravarty, K.H., Fosbøl, P.L., Thomsen, K., 2015a. Interactions of fines with base fractions of oil and its implication in smart water flooding. SPE. https://doi.org/10.2118/173855-MS

Chakravarty, K.H., Fosbøl, P.L., Thomsen, K., 2015b. Fine formation during brine-crude oil-calcite interaction in smart water enhanced oil recovery for Caspian carbonates, in: Society of Petroleum Engineers - SPE Annual Caspian Technical Conference and Exhibition. Baku, Azerbaijan.

Chakravarty, K.H., Fosbøl, P.L., Thomsen, K., 2015c. Significance of fines and their correlation to reported oil recovery, in: Society of Petroleum Engineers - Abu Dhabi International Petroleum Exhibition and Conference. Abu Dhabi, UAE.

Chandrasekhar, S., Mohanty, K.K., 2013. Wettability Alteration with Brine Composition in High Temperature Carbonate Reservoirs. SPE J.

Chin, L.Y., Thomas, L.K., 1999. Fully Coupled Analysis of Improved Oil Recovery by

Reservoir Compaction, in: SPE Annual Technical Conference and Exhibition. Houston, Texas, USA. https://doi.org/10.2118/56753-ms

Criddle, D.W., Meader, A.L., 1955. Viscosity and elasticity of oil surfaces and oil-water interfaces. J. Appl. Phys. 26, 838–842. https://doi.org/10.1063/1.1722104

Dandekar, A.Y., 2013. Petroleum reservoir rock and fluid properties, 2nd ed. CRC Press. https://doi.org/10.1006/jesp.1998.1365

Derjaguin, B., Landau, L., 1941. Theory of the stability of strongly charged lyophobic sols and of the adhesion of strongly charged particles in solutions of electrolytes. Prog. Surf. Sci. 43, 30–59. https://doi.org/10.1016/0079-6816(93)90013-L

Derkani, M.H., Fletcher, A., Abdallah, W., Sauerer, B., Anderson, J., Zhang, Z., 2018. Low Salinity Waterflooding in Carbonate Reservoirs: Review of Interfacial Mechanisms. Colloids and Interfaces 2, 20. https://doi.org/10.3390/colloids2020020

Eftekhari, A.A., Thomsen, K., Stenby, E.H., Nick, H.M., 2017. Thermodynamic Analysis of Chalk-Brine-Oil Interactions. Energy and Fuels 31, 11773–11782. https://doi.org/10.1021/acs.energyfuels.7b02019

Elimelech, M., Gregory, J., Jia, X., Williams, R.., 1998. Particle Deposition and Aggregation Measurement, Modelling and Simulaiton (Colloid & Surface Engineering). Butterworth-Heinemann, Oxford, UK.

Emadi, A., Sohrabi, M., 2013. Visual Investigation of Oil Recovery by LowSalinity Water Injection: Formation of Water Micro-Dispersions and WettabilityAlteration, in: SPE Annual Technical Conference and Exhibition. New Orleans, Louisiana, USA. https://doi.org/10.2118/166435-MS

Erzuah, S., Fjelde, I., Omekeh, A.V., 2017. Wettability Estimation by Surface Complexation Simulations, in: SPE Europec Featured at 79th EAGE Conference and Exhibition. Paris, France. https://doi.org/10.2118/185767-MS

Evje, S., Hiorth, A., Madland, M. V, Korsnes, R.I., 2009. A Mathematical Model Relevant for Weakening of Chalk Reservoirs Due to Chemical Reactions. Networks Heterog. Media 4, 755–788. https://doi.org/10.3934/nhm.2009.4.755

Fathi, S.J., Austad, T., Strand, S., 2011. Water-based enhanced oil recovery (EOR) by "smart water": Optimal ionic composition for EOR in carbonates. Energy and Fuels 25, 5173–5179. https://doi.org/10.1021/ef201019k

Fathi, S.J., Austad, T., Strand, S., 2010. "smart water" as a wettability modifier in chalk: The effect of salinity and ionic composition. Energy and Fuels 24, 2514–2519. https://doi.org/10.1021/ef901304m

Gachuz-muro, H., Sohrabi, M., 2017. Prediction, Control and Validation of Rock Dissolution During Smart Water Injection and Its Impact on Waterflood Performance in Heavy Oil Carbonate Reservoirs, in: International Symposium of the Society of Core Analyst. Vienna, Austria. https://doi.org/CMI1415 [pii]\r10.1111/j.1462-5822.2009.01415.x

Gachuz-muro, H., Watt, H., Sohrabi, M., 2016. Natural Generation of Acidic Water as a Cause

of Dissolution of the Rock During Smart Water Injection in Heavy Oil Carbonate Reservoirs, in: SPE Latin America and Caribbean Heavy Oil Conference. Lima, Peru.

Gachuz-muro, H., Watt, H., Sohrabi, M., 2013. Effects of brine on Crude Oil viscosity at different temperature and brine composition - heavy oil/water interaction, in: EAGE Annual Conference & Exhibition Incorporating. Society of Petroleum Engineers. London, UK. https://doi.org/10.2118/164910-MS

Gandomkar, A., Rahimpour, M.R., 2015. Investigation of Low-Salinity Waterflooding in Secondary and Tertiary Enhanced Oil Recovery in Limestone Reservoirs. Energy and Fuels 29, 7781–7792. https://doi.org/10.1021/acs.energyfuels.5b01236

Goolsby, J.L., Anderson, R.C., 1964. Pilot Water Flooding in a Dolomite Reservoir , The McElroy Field, in: SPE Secondary Recovery Symposium. Wichita Falls, Texas, USA.

Graue, A., Fermi, M.A., Moe, R.W., Baldwin, B.A., Needham, R., 2012. Water Mixing During Waterflood Oil Recovery: The Effect of Initial Water Saturation. SPE J. 17, 43–52. https://doi.org/10.2118/149577-PA

Gupta, R., Smith Jr., P.G., Hu, L., Willingham, T.W., Lo Cascio, M., Shyeh, J.J., Harris, C.R., 2011. Enhanced waterflood for Middle East carbonate cores - Impact of injection water composition, in: SPE Middle East Oil and Gas Show and Conference. Manama, Bahrain. https://doi.org/10.2118/142668-MS

Hallenbeck, L.D., Sylte, J.E., Ebbs, D.J., Thomas, L.K., 1991. Implementation of the Ekofisk Field Waterflood. SPE Form. Eval. 6, 284–290. https://doi.org/10.7860/JCDR/2017/24192.9615

Hamouda, A.A., Maevskiy, E., 2014. Oil recovery mechanism(s) by low salinity brines and their interaction with chalk. Energy and Fuels 28, 6860–6868. https://doi.org/10.1021/ef501688u

Hamouda, A.A., Rezaei Gomari, K.A., 2006. Influence of Temperature on Wettability Alteration of Carbonate Reservoirs, in: SPE/DOE Symposium on Improved Oil Recovery. Tulsa, Oklahoma, U.S.A. https://doi.org/10.1016/j.saa.2014.06.016

Hasiba, H.H., Jessen. F.W, 1966. Film properties of interfance-active compounds adsorbed from crude oils at the oil/water interface. SPE J.

Heggheim, T., Madland, M. V., Risnes, R., Austad, T., 2004. A chemical induced enhanced weakening of chalk by seawater. J. Pet. Sci. Eng. 46, 171–184. https://doi.org/10.1016/j.petrol.2004.12.001

Hellmann, R., Renders, P.J.N., Gratier, J.-P., Guiguet, R., 2002. Experimental Pressure Solution Compaction of Chalk in Aqueous Solutions: Part 1. Deformation Behavior and Chemistry, in: Hellmann, R.S.A.W. (Ed.), Water-Rock Interactions, Ore Deposits, and Environmental Geochemistry: A Tribute to David A. Crerar. The Geochemical Society, pp. 129–152.

Hiorth, A., Cathles, L.M., Madland, M. V., 2010. The Impact of Pore Water Chemistry on Carbonate Surface Charge and Oil Wettability. Transp. Porous Media 85, 1–21. https://doi.org/10.1007/s11242-010-9543-6

Hirasaki, G., Zhang, D.L., 2004. Surface Chemistry of Oil Recovery From Fractured, Oil-Wet,

Carbonate Formations. SPE J. 9, 151–162. https://doi.org/10.2118/88365-PA

Hirasaki, G.J., 1991. Wettability: Fundamentals and Surface Forces. SPE Form. Eval. 6, 217–226. https://doi.org/10.2118/17367-PA

Houston, S.J., Yardley, B.W.D., Leeds, U., Smalley, P.C., Collins, I., 2006. Precipitation and Dissolution of Minerals During Waterflooding of a North Sea Oil Field, in: SPE International Oilfield Scale Symposium. Aberdeen, Scotland, UK.

Hussain, F., Zeinijahromi, A., Bedrikovetsky, P., Badalyan, A., Carageorgos, T., Cinar, Y., 2013. An experimental study of improved oil recovery through fines-assisted waterflooding. J. Pet. Sci. Eng. 109, 187–197. https://doi.org/10.1016/j.petrol.2013.08.031

Høeg, K., Gutierrez, M., Øino, L.E., 2000. The Effect of Fluid Content on the Mechanical Behaviour of Fractures in Chalk. Rock Mech. Rock Eng. 33, 93–117. https://doi.org/10.1007/s006030050037

Høiland, L.K., Spildo, K., Skauge, A., 2007. Fluid flow properties for different classes of intermediate wettability as studied by network modelling. Transp. Porous Media 70, 127–146. https://doi.org/10.1007/s11242-006-9088-x

Jackson, M.D., Vinogradov, J., Hamon, G., Chamerois, M., 2016. Evidence, mechanisms and improved understanding of controlled salinity waterflooding part 1: Sandstones. Fuel 185, 772–793. https://doi.org/10.1016/j.fuel.2016.07.075

Johnson, J.P., Rhett, D.W., Johnsen, Rhett, D.W., Johnson, J.P., Rhett, D.W., 1986. Compaction Behavior of Ekofisk Chalk as a Function of Stress, in: SPE European Petroleum Conference. London, UK. https://doi.org/10.2118/15872-MS

Karimi, M., Al-Maamari, R.S., Ayatollahi, S., Mehranbod, N., 2016. Wettability alteration and oil recovery by spontaneous imbibition of low salinity brine into carbonates: Impact of Mg2+, SO42−and cationic surfactant. J. Pet. Sci. Eng. 147, 560–569. https://doi.org/10.1016/j.petrol.2016.09.015

Karoussi, O., Hamouda, A.A., 2007. Imbibition of sulfate and magnesium ions into carbonate rocks at elevated temperatures and their influence on wettability alteration and oil recovery. Energy and Fuels 21, 2138–2146. https://doi.org/10.1021/ef0605246

Katika, K., Addassi, M., Alam, M.M., Fabricius, I.L., 2015. The effect of divalent ions on the elasticity and pore collapse of chalk evaluated from compressional wave velocity and low-field Nuclear Magnetic Resonance (NMR). J. Pet. Sci. Eng. 136, 88–99. https://doi.org/10.1016/j.petrol.2015.10.036

Katika, K., Alam, M.M., Alexeev, A., Chakravarty, K.H., Fosbøl, P.L., Revil, A., Stenby, E., Xiarchos, I., Yousefi, A., Fabricius, I.L., 2018. Elasticity and electrical resistivity of chalk and greensand during water flooding with selective ions. J. Pet. Sci. Eng. 161, 204–218. https://doi.org/10.1016/j.petrol.2017.11.045

Khaksar Manshad, A., Olad, M., Taghipour, S.A., Nowrouzi, I., Mohammadi, A.H., 2016. Effects of water soluble ions on interfacial tension (IFT) between oil and brine in smart and carbonated smart water injection process in oil reservoirs. J. Mol. Liq. 223, 987–993. https://doi.org/10.1016/j.molliq.2016.08.089

Korsnes, R.I., Madland, M. V., Austad, T., Haver, S., Røsland, G., 2008. The effects of temperature on the water weakening of chalk by seawater. J. Pet. Sci. Eng. 60, 183–193. https://doi.org/10.1016/j.petrol.2007.06.001

Kuznetsov, D., Cotterill, S., Oil, T., Marie, ;, Giddins, A., Blunt, M.J., 2015. SPE-174615-MS Low-Salinity Waterflood Simulation: Mechanistic and Phenomenological Models, in: SPE Enhanced Oil Recovery Conference. Kuala Lumpur, Malaysia. https://doi.org/10.2118/174615-MS

Lager, A., Webb, K.J., Black, C.J.J., Singleton, M., Sorbie, K.S., 2008a. Low Salinity Oil Recovery - An Experimental Investigation. Petrophysics 49, 28–35.

Lager, A., Webb, K.J., Collins, I.R., Richmond, D.M., 2008b. LoSal Enhanced Oil Recovery: Evidence of Enhanced Oil Recovery at the Reservoir Scale, in: SPE Symposium on Improved Oil Recovery Symposium. Tulsa, Oklahoma, U.S.A. https://doi.org/10.2118/113976-MS

Lake, L.W., Hirasaki, G.J., 1981. Taylor â€™ s Dispersion in Stratified Porous Media. SPE J. 459–468.

Lam, E.J., Alvarez, M.N., Galvez, M.E., Alvarez, E.B., 2008. A model for calculating the density of aqueous multicomponent electrolyte solutions. J. Chil. Chem. Soc. 53, 1404–1409. https://doi.org/10.4067/S0717-97072008000100015

Lashkarbolooki, M., Ayatollahi, S., Riazi, M., 2017. Mechanistical study of effect of ions in smart water injection into carbonate oil reservoir. Process Saf. Environ. Prot. 105, 361–372. https://doi.org/10.1016/j.psep.2016.11.022

Loahardjo, N., Xie, X., Morrow, N.R., 2010. Oil recovery by sequential waterflooding of mixed-wet sandstone and limestone. Energy and Fuels 24, 5073–5080. https://doi.org/10.1021/ef100729b

Madland, M.V., Korsnes, R.I., Risnes, R., 2002. Temperature effects in Brazilian , uniaxial and triaxial compressive tests with high porosity chalk, in: SPE Annual Technical Conference and Exhibition. San Antonio, TX, USA. https://doi.org/10.2118/77761-MS

Madland, M. V., Finsnes, A., Alkafadgi, A., Risnes, R., Austad, T., 2006. The influence of CO2gas and carbonate water on the mechanical stability of chalk. J. Pet. Sci. Eng. 51, 149–168. https://doi.org/10.1016/j.petrol.2006.01.002

Madland, M. V., Hiorth, A., Omdal, E., Megawati, M., Hildebrand-Habel, T., Korsnes, R.I., Evje, S., Cathles, L.M., 2011. Chemical Alterations Induced by Rock-Fluid Interactions When Injecting Brines in High Porosity Chalks. Transp. Porous Media 87, 679–702. https://doi.org/10.1007/s11242-010-9708-3

Mahani, H., Keya, A.L., Berg, S., Bartels, W.B., Nasralla, R., Rossen, W.R., 2015. Insights into the mechanism of wettability alteration by low-salinity flooding (LSF) in carbonates. Energy and Fuels 29, 1352–1367. https://doi.org/10.1021/ef5023847

Mahzari, P., Sohrabi, M., 2014. Crude Oil/Brine Interactions and Spontaneous Formation of Micro-Dispersions in Low Salinity Water Injection. SPE Improv. Oil Recover. Symp. https://doi.org/10.2118/169081-MS

McGuire, P.L., Chatham, J.R., Paskvan, F.K., Sommer, D.M., Carini, F.H., 2005. Low Salinity Oil Recovery: An Exciting New EOR Opportunity for Alaska's North Slope, in: SPE Western Regional Meeting. Irvine, CA, U.S.A. https://doi.org/10.2118/93903-MS

Mohammadkhani, S., Shahverdi, H., Esfahany, M.N., 2018. Impact of salinity and connate water on low salinity water injection in secondary and tertiary stages for enhanced oil recovery in carbonate oil reservoirs. J. Geophys. Eng. 15, 1242–1254. https://doi.org/10.1088/1742-2140/aaae84

Mohanty, K.K., Chandrasekhar, S., 2013. Wettability Alteration with Brine Composition in High Temperature Carbonate Reservoirs. SPE Annu. Tech. Conf. Exhib. https://doi.org/10.2118/166280-MS

Mohsenzadeh, A., Pourafshary, P., Al-Wahaibi, Y., 2016. Oil Recovery Enhancement in Carbonate Reservoirs Via Low Saline Water Flooding in Presence of Low Concentration Active Ions; A Case Study, in: SPE EOR Conference at Oil and Gas West Asia. Muscat, Oman. https://doi.org/10.2118/179767-MS

Morrow, N., Buckley, J., 2011. Improved Oil Recovery by Low-Salinity Waterflooding. J. Pet. Technol. 63, 106–112. https://doi.org/10.2118/129421-JPT

Nermoen, A., Korsnes, R.I., Storm, E.V., Stødle, T., Madland, M.V., Fabricius, I.L., 2018. Incorporating electrostatic effects into the effective stress relation - Insights from chalk experiments. Geophysics 83. https://doi.org/10.1190/geo2016-0607.1

Patil, S., Dandekar, A.Y., Patil, S.L., Khataniar, S., 2008. IPTC 12004 Low Salinity Brine Injection for EOR on Alaska North Slope (ANS), in: International Petroleum Technology Conference. Kuala Lumpur. https://doi.org/10.2523/12004-MS

Pope, G.A., 1980. The Application of Fractional Flow Theory to Enhanced Oil Recovery. Soc. Pet. Eng. J. 20, 191–205. https://doi.org/10.2118/7660-PA

Powell, B.N., Lovell, G.L., 1994. Mechanisms of chalk compaction, in: SPE/ISRM Rock Mechanics in Petroleum Engineering Conference. Delft, The Netherlands. https://doi.org/10.2118/28132-MS

Prieve, D.C., Roman, R., 1987. Diffusiophoresis of a rigid sphere through a viscous electrolyte solution. J. Chem. Soc. Faraday Trans. 2 Mol. Chem. Phys. 83, 1287–1306. https://doi.org/10.1039/F29878301287

Pu, H., Xie, X., Yin, P., Morrow, N.R., 2010. Low Salinity Waterflooding and Mineral Dissolution, in: SPE Annual Technical Conference and Exhibition. Florence, Italy. https://doi.org/10.2118/134042-MS

Puntervold, T., Strand, S., Ellouz, R., Austad, T., 2015. Modified seawater as a smart EOR fluid in chalk. J. Pet. Sci. Eng. 133, 440–443. https://doi.org/10.1016/j.petrol.2015.06.034

Puntervold, T., Strand, S., Austad, T., 2007. New method to prepare outcrop chalk cores for wettability and oil recovery studies at low initial water saturation. Energy and Fuels 21, 3425–3430. https://doi.org/10.1021/ef700323c

Puntervold, T., Austad, T., 2008. Injection of seawater and mixtures with produced water into

North Sea chalk formation: Impact of fluid-rock interactions on wettability and scale formation. J. Pet. Sci. Eng. 63, 23–33. https://doi.org/10.1016/j.petrol.2008.07.010

Qiao, C., Johns, R., Li, L., Xu, J., 2015. Modeling Low Salinity Waterflooding in Mineralogically Different Carbonates, in: SPE Annual Technical Conference and Exhibition. Houston, Texas, USA. https://doi.org/10.2118/175018-MS

Rashid, S., Mousapour, M.S., Ayatollahi, S., Vossoughi, M., Beigy, A.H., 2015. Wettability alteration in carbonates during "Smart Waterflood": Underling mechanisms and the effect of individual ions. Colloids Surfaces A Physicochem. Eng. Asp. 487, 142–153. https://doi.org/10.1016/j.colsurfa.2015.09.067

Rassenfoss, S., 2016. Scaling Up Smart Water. J. Pet. Technol. 68, 39–41. https://doi.org/10.2118/0916-0039-JPT

Rezaei Gomari, K.A., Hamouda, A.A., 2006. Effect of fatty acids, water composition and pH on the wettability alteration of calcite surface. J. Pet. Sci. Eng. 50, 140–150. https://doi.org/10.1016/j.petrol.2005.10.007

RezaeiDoust, A., Puntervold, T., Austad, T., 2011. Chemical verification of the EOR mechanism by using low saline/smart water in sandstone. Energy and Fuels 25, 2151–2162. https://doi.org/10.1021/ef200215y

Risnes, R., Madland, M. V., Hole, M., Kwabiah, N.K., 2005. Water weakening of chalk - Mechanical effects of water-glycol mixtures. J. Pet. Sci. Eng. 48, 21–36. https://doi.org/10.1016/j.petrol.2005.04.004

Romanuka, J., Hofman, J., Ligthelm, D.J., Suijkerbuijk, B., Marcelis, F., Oedai, S., Brussee, N., van der Linde, H., Aksulu, H., Austad, T., 2012. Low Salinity EOR in Carbonates, in: SPE Improved Oil Recovery Symposium. Tulsa, Oklahoma, U.S.A. https://doi.org/10.2118/153869-MS

Rotondi, M., Callegaro, C., Masserano, F., Bartosek, M., 2014. Low Salinity Water Injection: eni' s experience, in: Abu Dhabi International Petroleum Exhibition and Conference. Abu Dhabi, UAE. https://doi.org/http://dx.doi.org/10.2118/171794-MS

Rubin, J., 1983. Transport of reacting solutes in porous media: Relation between mathematical nature of problem formulation and chemical nature of reactions. Water Resour. Res. 19, 1231–1252. https://doi.org/10.1029/WR019i005p01231

Ruddy, I., Andersen, M.A., Pattillo, P.D., Bishlawi, M., Foged, N., 1989. Rock Compressibility, Compaction, and Subsidence in a High-Porosity Chalk Reservoir: A Case Study of Valhall Field. J. Pet. Technol. 41, 741–746. https://doi.org/10.2118/18278-PA

Schembre, J.M., Tang, G.Q., Kovscek, A.R., 2006. Wettability alteration and oil recovery by water imbibition at elevated temperatures. J. Pet. Sci. Eng. 52, 131–148. https://doi.org/10.1016/j.petrol.2006.03.017

Shaddel, S., Tabatabae-Nejad, S.A., 2015. Alkali/Surfactant Improved Low-Salinity Waterflooding. Transp. Porous Media 106, 621–642. https://doi.org/10.1007/s11242-014-0417-1

Shaker Shiran, B., Skauge, A., 2013. Enhanced oil recovery (EOR) by combined low salinity water/polymer flooding. Energy and Fuels 27, 1223–1235. https://doi.org/10.1021/ef301538e

Shehata, A.M., Nasr El-Din, H.A., 2015. Spontaneous Imbibition Study: Effect of Connate Water Composition on Low-Salinity Waterflooding in Sandstone Reservoirs, in: SPE Western Regional Meeting. Garden Grove, California, USA. https://doi.org/10.2118/174063-MS

Shehata, A.M., Alotaibi, M.B., Nasr-El-Din, H.A., 2014. Waterflooding in Carbonate Reservoirs: Does the Salinity Matter? SPE Reserv. Eval. Eng. 17, 304–313. https://doi.org/10.2118/170254-PA

Sheng, J., Morel, D., Gauer, P., 2010. Evaluation of the Effect of Wettability Alteration on Oil Recovery in Carbonate Reservoirs Questions, in: AAPG GEO 2010 Middle East Geoscience & Exhibition. Manama, Bahrain.

Sheng, J.J., 2014. Critical review of low-salinity waterflooding. J. Pet. Sci. Eng. 120, 216–224. https://doi.org/10.1016/j.petrol.2014.05.026

Sheu, E.Y., Shields, M.B., Texaco, R., 1995. Asphaltene Surface Activity at Oil / Water Interfaces, in: SPE International Symposium on Oilfield Chemistry. San Antonio, TX, USA.

Skauge, A., Ottesen, B., 2002. A Summary of Experimentally Derived Relative Permeability and Residual Saturation on North Sea Reservoir Cores, in: International Symposium of the Society of Core Analyst. Monterey, California, USA, pp. 1–12.

Sohal, M.A., Thyne, G., Søgaard, E.G., 2016. Review of Recovery Mechanisms of Ionically Modified Waterflood in Carbonate Reservoirs. Energy and Fuels 30, 1904–1914. https://doi.org/10.1021/acs.energyfuels.5b02749

Somasundaran, P., Agar, G.., 1967. The zero point of charge of calcite. J. Colloid Interface Sci. 24, 433–440. https://doi.org/10.1016/0021-9797(67)90241-X

Song, J., Zeng, Y., Wang, L., Duan, X., Puerto, M., Chapman, W.G., Biswal, S.L., Hirasaki, G.J., 2017. Surface complexation modeling of calcite zeta potential measurements in brines with mixed potential determining ions (Ca2+, CO32−, Mg2+, SO42−) for characterizing carbonate wettability. J. Colloid Interface Sci. 506, 169–179. https://doi.org/10.1016/j.jcis.2017.06.096

Spildo, K., Johannessen, A., Skauge, A., 2012. Low Salinity Waterflood at Reduced Capillarity, in: Eighteenth SPE Improved Oil Recovery Symposium. Tulsa, Oklahoma, U.S.A., pp. 1–13. https://doi.org/10.2118/154236-MS

Spivey, J.P., McCain, W.D., North, R., 2004. Estimating density, formation volume factor, compressibility, methane solubility, and viscosity for oilfield brines at temperatures from 0 to 275° C, pressures to 200 MPa, and salinities to 5.7 mole/kg. J. Can. Pet. Technol. 43, 52–61. https://doi.org/10.2118/04-07-05

Standnes, D.C., Austad, T., 2000a. Wettability alteration in chalk 2. Mechanism for wettability alteration from oil-wet to water-wet using surfactants. J. Pet. Sci. Eng. 28, 123–143. https://doi.org/10.1016/S0920-4105(00)00084-X

Standnes, D.C., Austad, T., 2000b. Wettability alteration in chalk 1. Preparation of core material and oil properties. J. Pet. Sci. Eng. 28, 111–121. https://doi.org/10.1016/S0920-4105(00)00083-8

Strand, S., Henningsen, S.C., Puntervold, T., Austad, T., 2017. Favorable Temperature Gradient for Maximum Low-Salinity Enhanced Oil Recovery Effects in Carbonates. Energy and Fuels 31, 4687–4693. https://doi.org/10.1021/acs.energyfuels.6b03019

Strand, S., Høgnesen, E.J., Austad, T., 2006. Wettability alteration of carbonates - Effects of potential determining ions (Ca2+and SO42-) and temperature. Colloids Surfaces A Physicochem. Eng. Asp. 275, 1–10. https://doi.org/10.1016/j.colsurfa.2005.10.061

Strand, S., Standnes, D.C., Austad, T., 2006. New wettability test for chalk based on chromatographic separation of SCN- and SO42-. J. Pet. Sci. Eng. 52, 187–197. https://doi.org/10.1016/j.petrol.2006.03.021

Strand, S., Austad, T., Puntervold, T., Høgnesen, E.J., Olsen, M., Barstad, S.M.F., 2008. "Smart Water" for oil recovery from fractured limestone: A preliminary study. Energy and Fuels 22, 3126–3133. https://doi.org/10.1021/ef800062n

Sulak, R.M., Thomas, L.K., Boade, R.R., 1991. 3D Reservoir Simulation of Ekofisk Compaction Drive (includes associated papers 24317 and 24400). J. Pet. Technol. 43, 1272–1278. https://doi.org/10.2118/19802-PA

Suman, Y.K., Shirif, E., Ibrahim, H., Ala-Ktiwi, A., 2014. Evaluation of Low Saline "Smart Water" Enhanced Oil Recovery in Light Oil Reservoirs. World J. Eng. Technol. 2, 13–22. https://doi.org/10.4236/wjet.2014.21002

Sun, L., Spildo, K., Djurhuus, K., Skauge, A., 2014. Salinity Selection for a Low Salinity Water-Low Salinity Surfactant Process. J. Dispers. Sci. Technol. 35, 551–555. https://doi.org/10.1080/01932691.2013.800456

Sylte, J.E., Thomas, L.K., Rhett, D.W., Bruning, D.D., Nagel, N.B., 1999. Water Induced Compaction in the Ekofisk Field, in: SPE Annual Technical Conference and Exhibition. Houston, Texas, USA. https://doi.org/10.2118/56426-MS

Tang, G.-Q., Morrow, N.R., 1999. Influence of brine composition and fines migration on crude oi/brine/rock interactions and oil recovery. J. Pet. Sci. Eng. 24, 99–111. https://doi.org/10.1016/S0920-4105(99)00034-0

Varadaraj, R., Brons, C., 2012. Molecular origins of crude oil interfacial activity. part 4: Oil-water interface elasticity and crude oil asphaltene films. Energy and Fuels 26, 7164–7169. https://doi.org/10.1021/ef300830f

Verwey.E.J.W, Overbeek.J.T.G, 1948. Theory of the Stability of Luophobic Colloids. Elsevier Amsterdam.

Yousef, A.A., Liu, J.S., Blanchard, G., Al-Saleh, S., Al-Zahrani, T., Al-Zahrani, R., Al-Tammar, H., Al-Mulhim, N., 2012a. Smart Waterflooding: Industry's First Field Test in Carbonate Reservoirs, in: SPE Annual Technical Conference and Exhibition. San Antonio, Texas, USA. https://doi.org/10.2118/159526-MS

Yousef, A.A., Al-Saleh, S., Al-Jawfi, M.S., 2012b. Improved/Enhanced Oil Recovery from Carbonate Reservoirs by Tuning Injection Water Salinity and Ionic Content, in: SPE Improved Oil Recovery Symposium. Tulsa, Oklahoma, U.S.A. https://doi.org/10.2118/154076-MS

Yousef, A.A., Al-Saleh, S., Al-Kaabi, A., Al-Jawfi, M., 2011. Laboratory investigation of the impact of injection-water salinity and ionic content on oil recovery from carbonate reservoirs. SPE Reserv. Eval. Eng. 14, 578–593. https://doi.org/10.2118/137634-PA

Yousef, A.A., Al-Saleh, S., Al-Kaabi, A., Al-Jawfi, M., 2010. Laboratory Investigation of Novel Oil Recovery Method for Carbonate Reservoirs, in: Canadian Unconventional Resources & International Petroleum Conference. Calgary, Canada.

Yu, M., Hussain, F., Arns, J.Y., Bedrikovetsky, P., Genolet, L., Behr, A., Kowollik, P., Arns, C.H., 2018. Imaging analysis of fines migration during water flow with salinity alteration. Adv. Water Resour. 121, 150–161. https://doi.org/10.1016/j.advwatres.2018.08.006

Yuan, H., Shapiro, A.A., 2011. Induced migration of fines during waterflooding in communicating layer-cake reservoirs. J. Pet. Sci. Eng. 78, 618–626. https://doi.org/10.1016/j.petrol.2011.08.003

Yutkin, M.P., Mishra, H., Patzek, T.W., Lee, J., Radke, C.J., 2016. Bulk and Surface Aqueous Speciation of Calcite: Implications for Low-Salinity Waterflooding of Carbonate Reservoirs, in: SPE Kingdom of Saudi Arabia Annual Technical Symposium and Exhibition. Dammam, Saudi Arabia. https://doi.org/10.2118/182829-PA

Zaeri, M.R., Hashemi, R., Shahverdi, H., Sadeghi, M., 2018a. Enhanced oil recovery from carbonate reservoirs by spontaneous imbibition of low salinity water. Pet. Sci. 15, 564–576. https://doi.org/10.1007/s12182-018-0234-1

Zaeri, M.R., Shahverdi, H., Hashemi, R., Mohammadi, M., 2018b. Impact of water saturation and cation concentrations on wettability alteration and oil recovery of carbonate rocks using low-salinity water. J. Pet. Explor. Prod. Technol. 1–12. https://doi.org/10.1007/s13202-018-0552-2

Zahid, A., 2012. Smart Waterflooding in Carbonate Reservoirs. Technical University of Denmark. https://doi.org/10.2118/154508-MS

Zahid, A., Shapiro, A.A., Skauge, A., 2012a. Experimental Studies of Low Salinity Water Flooding Carbonate: A New Promising Approach. SPE EOR Conf. Oil Gas West Asia. https://doi.org/10.2118/155625-MS

Zahid, A., Shapiro, A., Stenby, E.H., Yan, W., 2012b. Managing injected water composition to improve oil recovery: A case study of north sea chalk reservoirs. Energy and Fuels 26, 3407–3415. https://doi.org/10.1021/ef2008979

Zahid, A., Stenby, E.H., Shapiro, A.A., 2010. Improved Oil Recovery in Chalk: Wettability Alteration or Something Else?, in: SPE EUROPEC/EAGE Annual Conference. Barcelona, Spain. https://doi.org/10.2118/131300-MS

Zeinijahromi, A., Machado, F.A., Bedrikovetsky, P.G., 2011. Modified Mathematical Model for Fines Migration in Oil Fields, in: Brasil Offshore Conference and Exhibition. Macea,

Brazil, pp. 14–17. https://doi.org/10.2118/143742-MS

Zeinijahromi, A., Nguyen, T.K.P., Bedrikovetsky, P., 2013. Mathematical model for fines migration assisted waterflooding with induced formation damage, Journal of Society of Petroleum Engineers SPEJ, 18(3) June, 518-533.

Zeinijahromi, A., Ahmetgareev, V., Badalyan, A., Khisamov, R., Bedrikovetsky, P., 2015. Case Study of Low Salinity Water Injection in Zichebashskoe Field. J. Pet. Sci. Res. 4, 16–31. https://doi.org/10.12783/jpsr.2015.0401.03

Zhang, P., Tweheyo, M.T., Austad, T., 2007. Wettability alteration and improved oil recovery by spontaneous imbibition of seawater into chalk: Impact of the potential determining ions Ca2+, Mg2+, and SO42-. Colloids Surfaces A Physicochem. Eng. Asp. 301, 199–208. https://doi.org/10.1016/j.colsurfa.2006.12.058

Zhang, P., Tweheyo, M.T., Austad, T., 2006. Wettability alteration and improved oil recovery in chalk: The effect of calcium in the presence of sulfate. Energy and Fuels 20, 2056–2062. https://doi.org/10.1021/ef0600816

Zhang, P., Austad, T., 2006. Wettability and oil recovery from carbonates: Effects of temperature and potential determining ions. Colloids Surfaces A Physicochem. Eng. Asp. 279, 179–187. https://doi.org/10.1016/j.colsurfa.2006.01.009

Zhang, P., Austad, T., 2005. The Relative Effects of Acid Number and Temperature on Chalk Wettability. SPE Int. Symp. Oilf. Chem. 3–9. https://doi.org/10.2118/92999-MS

Zhang, X., Shapiro, A., Stenby, E.H., 2011. Gravity Effect on Two-Phase Immiscible Flows in Communicating Layered Reservoirs. Transp. Porous Media 92, 767–788. https://doi.org/10.1007/s11242-011-9932-5

Zhang, Y., Sarma, H., 2012. Improving waterflood recovery efficiency in carbonate reservoirs through salinity variations and ionic exchanges: A promising low-cost "smart-waterflood" approach. Abu Dhabi Int. Pet. Exhib. Conf. 2012 - Sustain. Energy Growth People, Responsib. Innov. ADIPEC 2012 3, 2163–2183. https://doi.org/10.2118/161631-MS

Supplementary documents

Summary of engaged mechanisms in Low salinity/smart water injection efforts in the literature

Surface charge change/EDL					
Investigator	**Rock type**	**Oil properties**	**Brine properties**	**Using method**	**Results**
Fathi et al.(Fathi et al. 2011)	Stevns Klint	Base crude oil: μ=20.47 cP Diluted oil(base	Synthetic brine 62000ppm 33390ppm 10010ppm	EDL effect Chromatographic wettability analyses	1-Removing NaCl from SW increase 10% in OR (IOIP) and adding 4 times SO_4^{2-} to this brine increase 5-18% OR (IOIP) afterward at T=70-120°C

		oil+40 vol% n-heptane)	16790ppm 11430ppm 33390ppm		
Alameri et al.(Alameri et al. 2014)	Homogenous low-perm. carbonate	Crude oil °API=32	NaCl, Na_2SO_4, $CaCl_2$, $MgCl_2$	EDL	1-8% incremental oil recovery by removing NaCl from seawater 2-6 and 1.1% incremental oil recovery by 2 and 4 times diluted SW
Mahani et al.(Mahani et al. 2015)	Limestone Dolomite	Crude oil μ=20.75 cP ,ρ= 0.8567 g/cm^3 At 20 °C	NaCl, Na_2SO_4, KCl, $NaHCO_3$, $MgCl_2$, $CaCl_2$ FW:179855ppm SW:43731ppm 25dSW:1751ppm	Zeta potential (ZP)	1-WA was only occurred when ZP of oil and carbonate surface is lower than ZP in FW 2-Surface charge change is the primary mechanism in LSE in carbonates

Wettability alteration

Investigator	Rock type	Oil properties	Brine properties	Using method	Results
Drummond et al.(Drummond et al. 2004)	Mica surface	Crude oil °API=28 and 23.1	HNO_3, NaOH, and $NaNO_3$ adjust salinity	Static contact angle measurement	1-Brine salinity and pH change the wettability 2-Effect of Na^+
Schembre et al.(Schembre et al. 2006)	Diatomite	Crude oil °API=34	14.454 kppm salinity pH=8	Amott method	Rise in temperature from 45 to 230 °C increases IOIP*
Hamouda et al.(Hamouda et al. 2006)	Stevns Klint	Model oil (n-decane)	Water	Contact angle measurement	Rise in temperature from 25 to 80°C change wettability for pre-treated calcite by different acids
Rezaei Gomari et al.(Rezaei Gomari et al. 2006)		Model oil (n-decane)	NaCl, $MgCl_2$, Na_2SO4 (0.5 M)	Contact angle measurement	Effect of Na^+,Mg^{2+} and SO_4^{2-}on the WA at different pH for treated calcite surface
Gupta et al.(Gupta et al. 2008)	Fractured limestone	Field oil model oil**	MgCl, NaCl, Na_2SO_4	Contact angle measurement	Effect of Na^+,Mg^{2+} and SO_4^{2-} by changing the salinity
Patil et al.(Patil et al. 2008)	ANS***	ANS crude oil	1-$NaHCO_3$, Na_2SO_4, NaCl,	Amott-Harvey	1-Decrease brine salinity reduce ROS 20%

		(dead oil)	KCl, $CaCl_2$, $SrCl_2$, $MgCl_2$ TDS=22-5.5kppm 2-ANS lake water	wettability index	2-Effect of aging on EOR
Sheng et al.(Sheng et al. 2010)	Fracture and non-fractured dolomite	Stock tank crude oil °API=27.2 to 28.4	Nacl,KCl,$CaCl_2$ $MgCl_2$, Na_2SO_4	Simulation effort	1-WA has important role when IFT is high and at the earlier time of beginning the experiment 2-Investigating the effect of gravity and diffusion on SI when using surfactant
Yousef et al.(Yousef et al. 2011)	Carbonate cores	Live oil	Connate water(200kppm) SW(57.6kppm) diluted seawater	Contact angle measurement	Twice/10times/20 times diluted SW injection improve 7-8.5/9-10/1-1.6% OOIC****
Alameri et al.(Alameri et al. 2014)	Carbonate	Crude oil °API=32	NaCl, Na_2SO_4, $CaCl_2$, $MgCl_2$	Captive oil-droplet contact angle	By decreasing brine salinity crude-aged cores wettability change from oil-wet to intermediate-wet and cleaned un-aged cores from water-wet to more water-wet
Al-Shalabi et al.(Al-Shalabi et al. 2014)	Carbonate	Field oil °API=40	Field water: 179.726kppm SW: 43.619kppm Diluted SW	History matching of core flood data	1-WA is still the main contribution mechanism in LSWI 2-EOR obtained by LSWI is more controlled by K_{ro} parameters rather than K_{rw} at T=248°F
Shehata et al.(Shehata et al. 2014)	Outcrop limestone	Crude oil °API=27.8	DW, connate water,shallow-aquifer water SW,DSW 54.68,27.34,10.936kppm	Due to observations in ROS reduction	Sudden change in salinity of the injected brine leads to EOR significantly at T=195°F and P_{atm}
Mahani et al.(Mahani et al. 2015)	Limestone Dolomite	Crude oil μ=20.75 cP At 20 °C	NaCl, Na_2SO_4, KCl, $NaHCO_3$, $MgCl_2$, $CaCl_2$ FW:179.855kppm SW:43.731kppm	Contact angle measurement	By replacing FW with SW contact angle reduces 5 to 17 degree

* IOIP = Initial Oil in Place

** 0.15%wt Cyclhexanepentaonic acid to n-decane

*** ANS = Alaska North Slope

****OOIC = Original Oil in Core

Mineral dissolution and pH alteration

Investigator	Rock type	Oil properties	Brine properties	Using method	Results
Hamouda et al.(Hamouda et al. 2014)	Stevns Klint	Synthetic oil (n-decane, 0.005 mol/L steric acid)	SSw(seawater:33388ppm) LSW(different dilution form of SSW: 6678, 3339,2226 and 1336 ppm)	pH measurements Dionex ICS-3000 chromatograph	ΔpH between effluent and inlet increased with increasing brine dilution factor Increase in Ca^{2+} in effluent shows mineral dissolution
Mahani et al.(Mahani et al. 2015)	Limestone Dolomite	Crude oil μ=20.75 cP ,ρ= 0.8567 g/cm^3 At 20 °C	NaCl, Na_2SO_4, KCl, $NaHCO_3$, $MgCl_2$, $CaCl_2$ FW:179855ppm SW:43731ppm	Imbibition tests and pH measurements	ΔpH=0 in LS/25dSWEQ experiments so no mineral dissolution occurred. Mineral dissolution is not a primary mechanism.

IFT reduction

Investigator	Rock type	Oil properties	Brine properties	Using method	Results
Sheng et al.(Sheng et al. 2010)	Fractured non-fractured dolomite	Stock tank crude oil °API=27.2 to 28.4	Formation brine Nacl,KCl,$CaCl_2$ $MgCl_2$, Na_2SO_4	Simulation effort	IFT plays an important role with or without WA and is effective during the entire process
Yousef et al.(Yousef et al. 2010, Yousef et al. 2011)	Carbonate	Live oil	Connate water(200kppm) SW(57.6kppm)	High T/high P pendent drop instrument	Different diluted form of SW has insignificant effect on IFT

			diluted seawater		
Alameri et al.(Alameri et al. 2014)	Heterogeneous low-perm. carbonate	Crude oil °API=32	NaCl, Na_2SO_4 $CaCl_2$, $MgCl_2$	Pendant drop oil-brine IFT measurements	IFT increases as brine salinity decreases
Khaksar Manshad et al.(Khaksar Manshad et al. 2016)	Carbonate	Asmari reservoir of Gachsatan oilfield pH=7.5	NaCl, KCl $MgCl_2$, Na_2SO_4 $MgSO_4$, KI K_2SO_4	Pendant drop method	IFT between oil and different smart water solutions at T=75°C and P=1 atm has been reported. No big chnge was reported.

Fine migration

Investigator	Rock type	Oil properties	Brine properties	Using method	Results
Chakravarty et al.(Chakravarty et al. 2015)	Carbonate fines produced by Li_2CO_3, $CaCO_3$, $MgCO_3$, $CaSO_4$, $SrSO_4$ and $BaSO_4$	Design oil(hexane and hexadecane) Acid number mimic by stearic acid and heptanoic acid	Deionized water	GC analysis of initial and final floating oil	Oil which contains heavier acids form more stable micelles. In oil which contains Steric acid/ Heptanoic acid: 95/50-60% of it was accumulated in micelles respectively

Micro dispersion

Investigator	Rock type	Oil properties	Brine properties	Using method	Results
Emadi et al.(Emadi et al. 2013)	Glass surface	°API=19.1 μ=92.3cP@50°C	NaCl, $CaCl_2$ LS:0.5,2kppm HS:30kppm	High P micro model rig	Formation of droplets of water in oil phase at oil/LS brine interface results in change in oil distribution and ROS reduction
Mahzari et al.(Mahzari et al. 2014)	*	5 different crude oil °API: 31.1 ,22.2, 26.16 ,19.1, 16.7	NaCl, $CaCl_2$ LS:2, 0.5kppm HS:60kppm	ESEM FTIR	1-Formation of water-in-oil dispersions at brine salinity < 2000ppm 2-Crude oil with high asphaltene/resin ratio and at higher T has more tendency to form water micro dispersions

*Mahzari et al. only investigate the effect of oil/brine interactions and did not use any type of rock

Chapter 3. Kinetics of Calcite Dissolution and Ca-Mg Ion Exchange on the Surfaces of North Sea Chalk Powders

This chapter has been submitted as a paper manuscript to *Energy and Fuels*

Abstract

Calcite dissolution and Ca – Mg ion exchange on carbonate rock surface have been proposed as potential mechanisms of smart waterflooding in carbonate reservoirs. However, there is still a lack of fundamental understanding of these reactions to quantitatively evaluate their effects in the reservoir flooding process. Especially, the data on precipitation and dissolution kinetics are insufficient. In this work, the equilibration kinetics of calcite dissolution and Ca – Mg exchange was experimentally studied. The behavior of three powders was compared: pure calcium carbonate, Stevns Klint outcrop chalk, and North Sea reservoir chalk. It was found that the equilibration time for calcite dissolution was in the order of seconds for a given surface area to liquid volume ratio. The existing theory of calcite dissolution could well reproduce our observations. The Ca – Mg exchange showed two-step kinetics: the first step was fast, it dominated the process within the first hour of reaction; the second step was slow, it continued longer than the time of observation (two weeks). Characteristic times for the two steps were extracted by fitting the experimental curves. A two-layer adsorption model was proposed to characterize the kinetic process and successfully matched with experimental data. The findings were further extended to flow through scenarios. By comparing with literature data and surface complexation models (SCM), it was concluded that calcite dissolution alone was unlikely to be able to explain the additional recovery reported in the literature. The Ca – Mg exchange process could dominate the fluid-rock interactions at a high temperature in pure calcium carbonate rocks, while competitive adsorption of cations appeared to control the process at a lower temperature. Different carbonate rocks possess different properties with regard to the ion exchange process.

3.1 Introduction

Smart waterflooding in carbonate reservoirs has been extensively studied in recent years. Various chemical and physical mechanisms have been proposed to explain the observed effects. Several review works have summarized and analyzed the reported observations from different perspectives (Afekare & Radonjic, 2017; Ayirala & Yousef, 2016; Bartels et al., 2019; Derkani, et al., 2018; Sohal, Thyne, & Søgaard, 2016; Hao et al., 2019). Among the proposed mechanisms, the dissolution of calcite mineral and the Ca – Mg ion exchange at the surface of carbonate rocks have been mentioned by several researchers.

Dissolution of carbonate minerals has been thoroughly studied in the field of geochemistry (Plummer, Parkhurst, & Wigley, 2007; Finneran & Morse, 2009; Subhas, et al., 2015; Sulpis et al., 2017). It has also been suggested as a mechanism of smart waterflooding in carbonate rocks (Hamouda & Maevskiy, 2014; Lager et al., 2008). Dissolution of calcium carbonate minerals may trigger various effects that could facilitate the production of oil. Mechanisms such as improved inter-pore connectivity (Yousef et al., 2010), and further, increased permeability (Gachuz-muro & Sohrabi, 2017) were reported in association with the rock dissolution. The dissolution may also affect oil production through alteration of the electric double layer interactions (Karimi et al, 2016). Hiorth, Cathles, & Madland (2010) found a linear relationship between calcite dissolution and oil recovery from imbibition experiments. Nonetheless, the

importance of dissolution for additional recovery was evaluated differently in different works. Whether dissolution is considered as the primary recovery mechanism (Hamouda & Maevskiy, 2014), or the secondary mechanism (Mahani, et al., 2015), it deserves a more careful study to reveal its importance.

The exchange reaction between Mg^{2+} ions in the aqueous solution and the Ca^{2+} ions on the surface of carbonate rocks was also reported as a potential mechanism of smart waterflooding (Zhang, Tweheyo, & Austad, 2006). The ion exchange process may promote detachment of adsorbed polar components from oil (Zhang & Austad, 2006); change the surface potential of the rock, expanding the electrostatic double layer; and, finally, make the surface more water wet (Rezaei Gomari & Hamouda, 2006; Rashid et al, 2015; Alshakhs & Kovscek, 2016).

Waterflooding of a core or a reservoir is a dynamic process. Characteristic times of the chemical or physicochemical processes that occur during waterflooding are crucial parameters to evaluate their effects. Studies of the kinetics of ion exchange in waterflooding have been carried out in numerical simulations (Alexeev, Shapiro, & Thomsen, 2015). This study demonstrated that the ratio between the characteristic times of the convective flow and chemical equilibration (the Damköhler number) is one of the most important parameters for the efficiency of the process.

In this work, we study the kinetics of calcite dissolution and Ca – Mg ion exchange. Analysis of the experimental data makes it possible to extract characteristic equilibration times of the process. Mathematical models are proposed to describe the kinetics of the processes. The results are then coupled with the flow equations to evaluate the flow-through experiments reported in the literature.

The paper is organized as follows: Section 2 introduces the materials and experimental procedures involved in this work; Section 3 describes the experimental results and formulates the kinetic models for dissolution and exchange needed for their evaluation; section 4 presents the modeling of the flow-through and flooding experiments found in the literature, comparing them to our experimental findings; finally, Section 5 formulates the main conclusions of this work.

3.2 Materials and methods

3.2.1 Materials

3.2.1.1 Powder samples

Three types of calcite/chalk materials were applied in this study: pure calcite (calcium carbonate) powder purchased from VWR Chemicals, with a grain diameter less than 30μm; outcrop chalk obtained from Stevns Klint (SK), approximately 60 kilometers south of Copenhagen; and reservoir chalk (RS) obtained from a North Sea chalk reservoir. The powders from natural materials have a grain diameter between 53 and 160μm.

Apart from the commercial calcium carbonate powder, Stevns Klint and reservoir chalk powders were prepared from bulk rock samples. The samples were first subjected to a cleaning procedure by methanol and toluene to remove the initially precipitated salts and organic compounds, in order to expose the chalk surface.

Core samples of Stevns Klint chalk (approx. 7.5 cm in length, 3.8 cm in diameter) were assembled in a classic Hassler type core holder and flooded by methanol and toluene alternatively. The injection rate of the solvents was 0.3 ml/min, the sleeve pressure was 20 bar. At the end of cleaning, the presence of residual salts in the methanol effluent was tested by adding 3-4 drops of 0.03M $AgNO_3$ solution into the last 2-3 ml effluent. The core was considered to be clean if no precipitation was observed.

For cleaning of the reservoir chalk samples, a Soxhlet extraction setup was applied due to highly irregular shapes of the chalk pieces. The chalk samples were first crushed by a mortar and pestle into approximately 3-5mm diameter grains. The crushed grains were then loaded into a Soxhlet setup. Toluene and methanol were used alternatively as extraction solvents. The process was finished after a colorless toluene eluent was obtained after at least 3 days of extraction. Complete removal of salts was detected by testing the methanol eluent with $AgNO_3$, as described above.

The cleaned chalk samples were dried in the oven at 80^{o}C for 2 days. Then the dry samples were ground by mortar and pestle into powders. The sizes of the powder particles were controlled by sieving the powder by two meshes, with the mesh sizes of 63μm and 150μm. The sieved particles were collected into a glass sample bottle and sealed for later use.

Since the characteristic pore diameter of the chalk is 3μm, the ground particles are still porous and consist of smaller elemental grains. The SEM images of the powders confirm this fact (Figure 1).

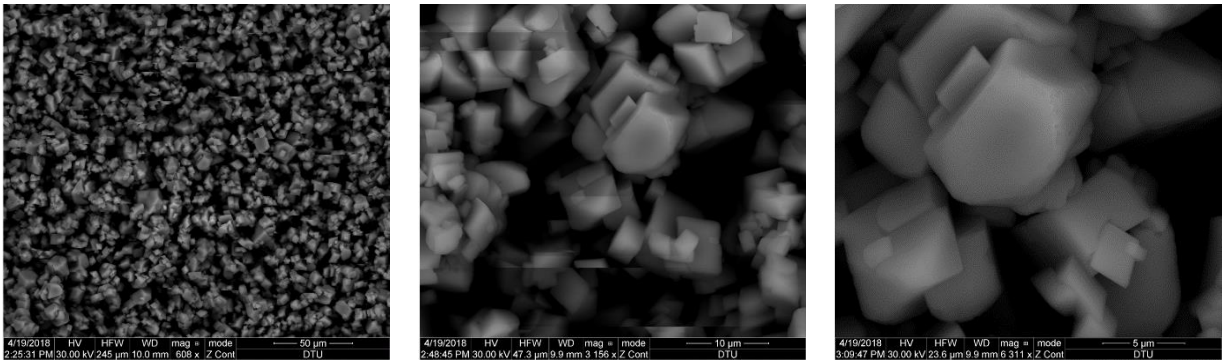

(a) Calcite powder

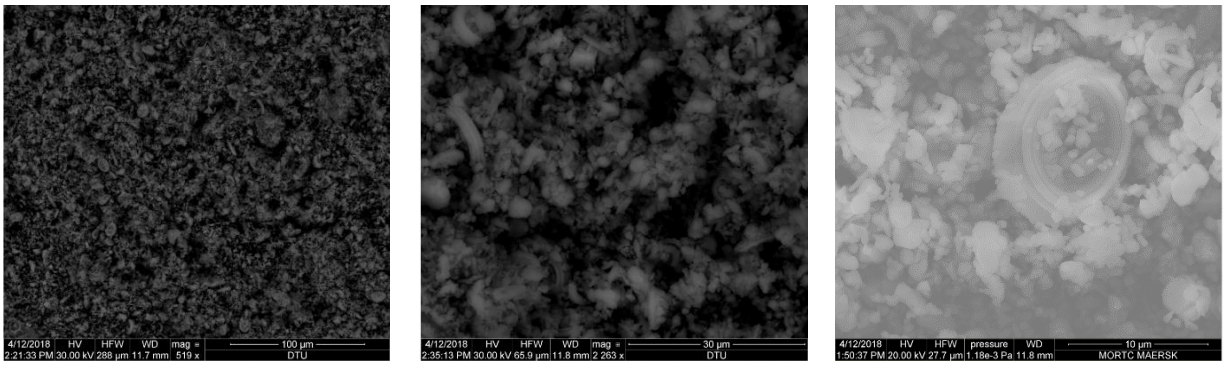

(b) SK powder

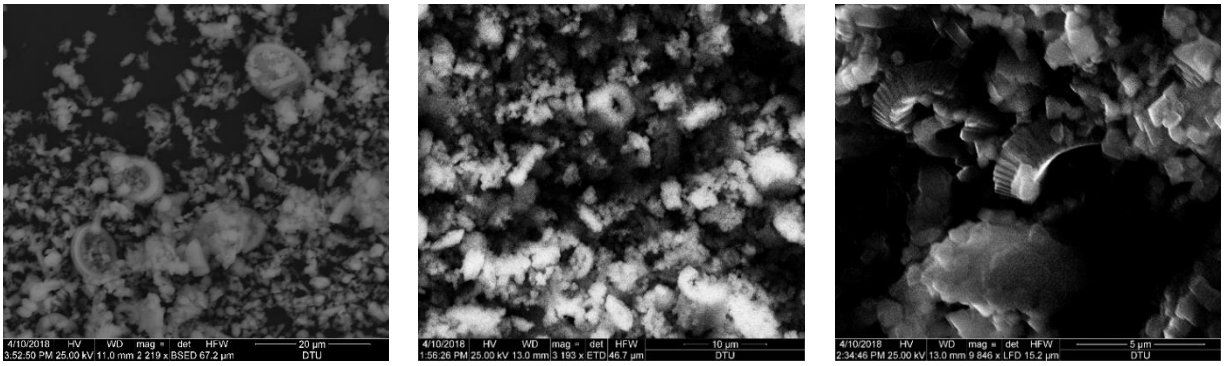

(c) RS powder

Figure 1. The SEM images of (a) calcite powder, (b) Stevns Klint powder, and (c) reservoir sample powder on different scales. It can be seen that the natural rock materials consist of much smaller grains than the selected particle grain size: 63 – 150 μm.

Specific surface areas (SSA) of the powder samples were measured by the multi-point BET method with liquid nitrogen. Each powder was measured twice. The average values for calcite powder, Stevns Klint chalk powder, and reservoir chalk powder are 0.344, 2.214 and 2.661 m^2/g, respectively.

It should be noted that the measured SSA of Stevns Klint chalk is slightly higher than the commonly reported 2 m^2/g. This may be an indication of the appearance of new surfaces of the rock in the grinding procedure. At least, none of the measurements reported the SSA below 2 m^2/g. Since we are targeting at observing the behavior of the original pore surface, it is important to have an order-of-magnitude estimation of the relative amount of the newly exposed surface. In order to obtain this estimate, we apply the following conceptual model of the particles: the particles are spherical and porous; the outer surface of the sphere is considered as newly exposed area due to grinding; and the internal surface area (porosity) of a particle is the original pore surface, as in the intact rock. In this way, the new surface area of a single particle may be calculated as

$$S_{new} = 4(1-\varphi)\pi R^2 \tag{1}$$

Here φ is the porosity of the rock, and R is the radius of the particle.

The original specific surface area can be estimated with Kozeny's equation:

$$S_{old} = \sqrt{c\frac{\varphi^3}{k}} \tag{2}$$

so that the internal surface area of a single particle is equal to $S_{old} \times \frac{4\pi}{3}R^3$. In this equation, k is the permeability of the rock, and c is a dimensionless factor, as derived by Mortensen et al. (1998):

$$c = \left(4\cos\left(\frac{1}{3}arc\cos\left(\varphi\frac{64}{\pi^3}-1\right)+\frac{4}{3}\pi\right)+4\right)^{-1} \tag{3}$$

Applying the measured petrophysical properties of the intact core materials as input, we can obtain the estimated SSA by Kozeny's equation, as shown in Table 1.

Core no.	k [D]	ϕ	Bulk Density [g/cm^3]	SSA [m^2/cm^3]	
				Estimate	Average
SK1	0.00854	0.464	1.43	1.70	1.91
SK2	0.00544	0.464	1.43	2.13	
RS1	0.00060	0.339	1.76	3.85	3.88
RS2	0.00056	0.364	1.80	4.45	
RS3	0.00052	0.304	1.88	3.47	
RS4	0.00089	0.377	1.66	3.75	

Table 1. The calculated SSA of the core samples using Kozeny's equation before they were ground, and the measured SSA of the ground chalk powders with the BET method.

Using the average SSA calculated from Kozeny's equation for the two types of chalk, we can calculate the ratio between the new surface area and the original surface area for a particle diameter ranging from 63 μm to 160 μm (Figure 2).

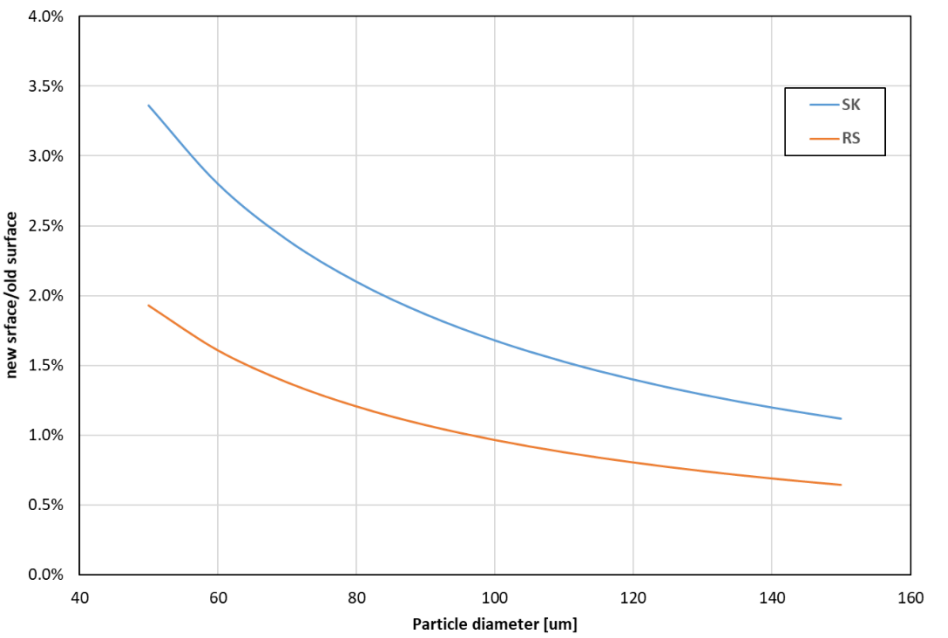

Figure 2. The ratio of a newly exposed surface area to the original surface area for Stevns Klint chalk (SK) and reservoir chalk (RS) powders. The new surface area produced in the grinding process is insignificant compared with the original surface area of the chalks.

It is clear that the newly exposed surface area is insignificant compared with the original internal pore surface. This assures that the experimental observations will be representative of the behavior of natural rock surfaces.

3.2.1.2 Brines

The brines were prepared by dissolving certain salts in deionized water. In this study, we examine the dissolution of calcite in pure water and the exchange process between aqueous Mg^{2+} ions and Ca^{2+} from the solid calcite. An $MgCl_2$ solution was used as a source of Mg^{2+}. The concentration of Mg^{2+} was made to be identical to the North Sea seawater: 0.045 mol/L.

In order to exclude the influence of atmospheric CO_2 on the experimental process, the deionized water and $MgCl_2$ solution were de-gassed in vacuum before the experiments.

3.2.2 Setup

3.2.2.1 Reaction setups

Two types of reaction setups were used in this work. Special attention was paid to remove the effect of the atmospheric carbon dioxide, which might dissolve in the liquid, react with the salt and change the acidity of the solution. The first setup was constructed in a glove box filled with nitrogen. A one-liter sample bottle was used as a reaction cell. The calcite powder and the deionized water/ $MgCl_2$ solution were mixed in the bottle and stirred by a magnetic stirrer in order to make a homogeneous mixture. The bottle was sealed by a cap to prevent evaporation.

Liquid samples from the bulk mixture were taken periodically. Upon taking samples, the cap was removed, and a syringe with a syringe filter (0.2 um pore size) was used to extract samples and to separate the liquid from solid particles. Only 2 ml of the liquid was taken per sample so that the total amount of sampled fluid was insignificant compared with the initial volume. The liquid samples were sealed and stored in the fridge at 4°C for later chemical analysis, no precipitation was observed upon the analysis. The pH of the bulk mixture was measured simultaneously upon extracting samples, by putting a pH probe into the mixture. Since this setup can provide a stable and reliable long-term control of the CO_2, it was used for the experiments that last more than one day.

The second type of setup was designed for short-term experiments (less than one hour), to facilitate the sample extraction procedure at a higher frequency. The powder and liquid were mixed in a one-liter Erlenmeyer flask with a stirring magnet. A nitrogen source was connected to the neck of the flask, with a gentle flow of nitrogen to prevent contact of the mixture with the air. The samples were extracted with the same procedure as in the first setup.

3.2.3 Experimental procedure

3.2.3.1 Dissolution and ion exchange experiments

The prepared powders were weighed with an analytical balance and transferred into the reaction cells. Then one liter of the liquid was added into each cell to start the reaction. All the experiments were performed at room temperature (20°C). The available surface areas for dissolution and ion exchange of each type of the powder were kept identical by adjusting weights of the powders. Since the reservoir sample has the highest SSA, its mass was the smallest. The surface area of 10 grams of the reservoir sample was chosen as a reference value to adjust the weights of other samples so that the calcite surface in contact with the liquid was equal to 26.6 m^2 in each reaction cell. The weights of the calcite and Stevns Klint powder samples were 77.36 and 12.02 grams, correspondingly. Timing started at the moment of mixing. The elapsed time at each sampling point was recorded.

3.2.3.2 Analysis of the samples

The processes studied in this work (calcite dissolution and Ca-Mg exchange) are followed by the measurement of Ca^{2+} and Mg^{2+} concentrations in the mixtures. An accurate chemical analysis of the extracted samples is essential to obtain reliable results. In this work, the Ca^{2+} and Mg^{2+} concentrations in each filtered aqueous sample are obtained by multi-element analysis by ICP-OES (inductively coupled plasma – optical emission spectrometry) on an iCAP 7200 Series ICP-OES spectrometer from ThermoScientific. The metal ions are excited in an argon plasma and the emission spectrum of each element is measured in the spectrometer and the concentration subsequently determined by reference to a

standard multi-elemnent solution. The sample matrix in this case is quite simple and samples did not require sample prepration beyond filtration.

3.3 Experimental Results

3.3.1 Calcite dissolution in pure water

The dissolution of the calcite in pure water was first investigated in setup 1. The first experiment attempt lasted for approximately 4 days, kinetics of dissolution was not captured in this experiment, The first sample was taken approximately 30 minutes after mixing. Calcium concentration was almost constant for each type of material throughout the experimental period, with approximately 6 mg/L for reservoir chalk and 4.5 mg/L for pure calcite and Stevns Klint chalk. pH of the solution also remained constant around 10 during the experimental period.

Since the kinetic process of dissolution was not captured in the first attempt, the experiment was replicated in the second setup with more frequent sampling in the first 15 minutes. The result is shown in Figure 3.

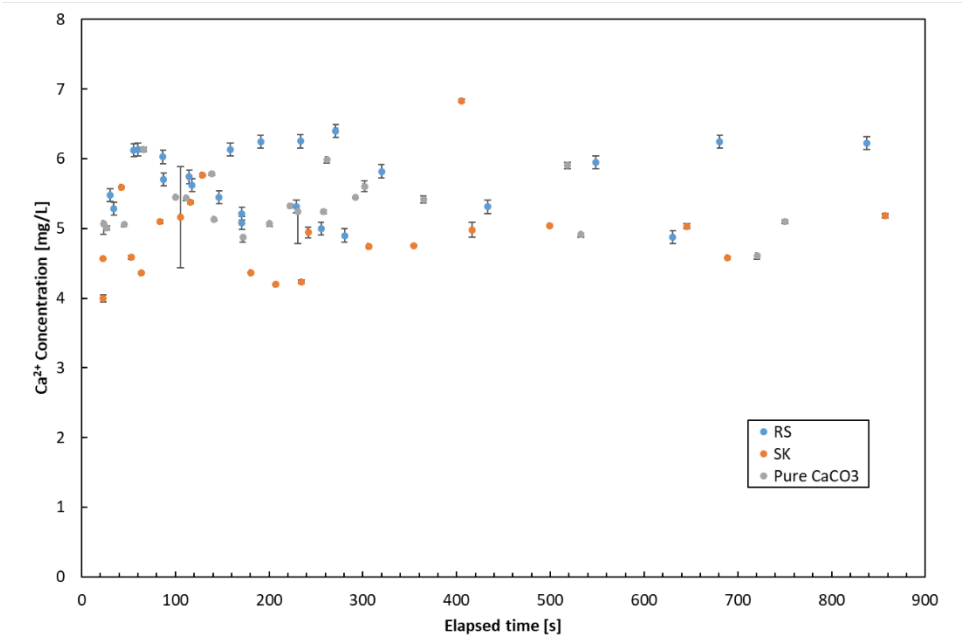

Figure 3. Evolution of the calcium concentration for calcite dissolution in water. The concentrations did not show significant variation, apart from the first few points. The reservoir rock generally produced a slightly higher concentration than the other two materials.

Again, even though the first sample for each type of powder was taken between 22 and 34 seconds after mixing, the kinetic process of the dissolution was not fully captured (apart, probably, from a few initial points). Observations of the equilibrium concentrations were similar to the long-term experiment: the reservoir chalk produced a higher calcium concentration, while pure calcite and Stevns Klint outcrop gave similar and lower concentrations. The equilibrium concentration of Ca^{2+} ion ranged from 4 to 6.5 mg/L, corresponding to 10 to 16 mg/L calcite.

3.3.2 Ion exchange

The study of the reaction between calcite/chalk powders and $MgCl_2$ solution (0.045M) was performed in the first setup. The experiments lasted for a total of 2 weeks with periodical sampling from the bulk mixture. The concentrations of Ca^{2+} and Mg^{2+} in the samples together, with the doubled standard deviation of the measurements, are plotted in Figures 4 and 5.

The reaction between calcium carbonate rocks with the magnesium-containing solution is often described as a ion-exchange process, where the Mg^{2+} ions in the aqueous phase substitute the Ca^{2+} ions from the solid surface. Then the substituted Ca^{2+} ions enters the aqueous phase.

The reaction can be monitored by either increase of calcium concentration or decrease of magnesium concentration in the bulk solution. In our experiments, the concentration of calcium shows a clear and consistent increase during the experimental period, with the most significant increase obtained for the pure calcite powder, and a less significant increase for natural materials. Simultaneously, the magnesium concentration shows a seemingly slight decrease in the first few sampling points. However, given the high initial concentration of magnesium, low consumption in the reaction and uncertainty of the measurement, the Mg^{2+} concentration cannot be determined with sufficient accuracy to describe the reaction.

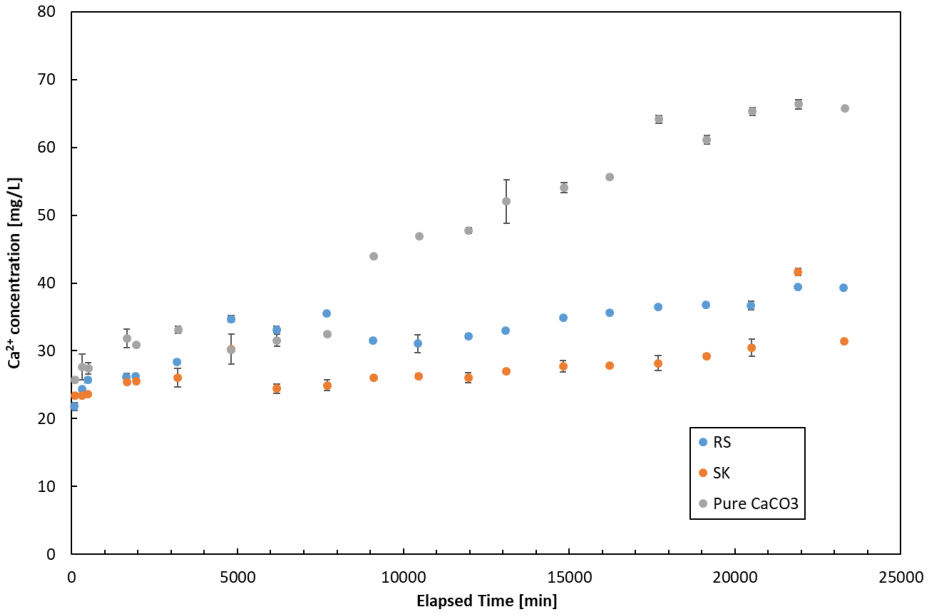

Figure 4. The evolution of the calcium concentration during the ion exchange process between calcite/chalk powders and $MgCl_2$ solution. The process has slow kinetics over the experimental period. The most significant exchange was between pure calcite and $MgCl_2$ solution, while natural rocks had similar behavior and were less active.

It should be noted that, even at early times of the experiment, the calcium concentration was 4 to 5 times higher than that for dissolution in pure water. Afterward, the reaction rate decreased. However, it did not vanish, which indicates that the reaction did not reach equilibrium at the end of the experiment. The first samples were taken between 84-103 minutes from the beginning of the experiments, within which the fast stage of the increase of Ca^{2+} concentration should have reached equilibrium.

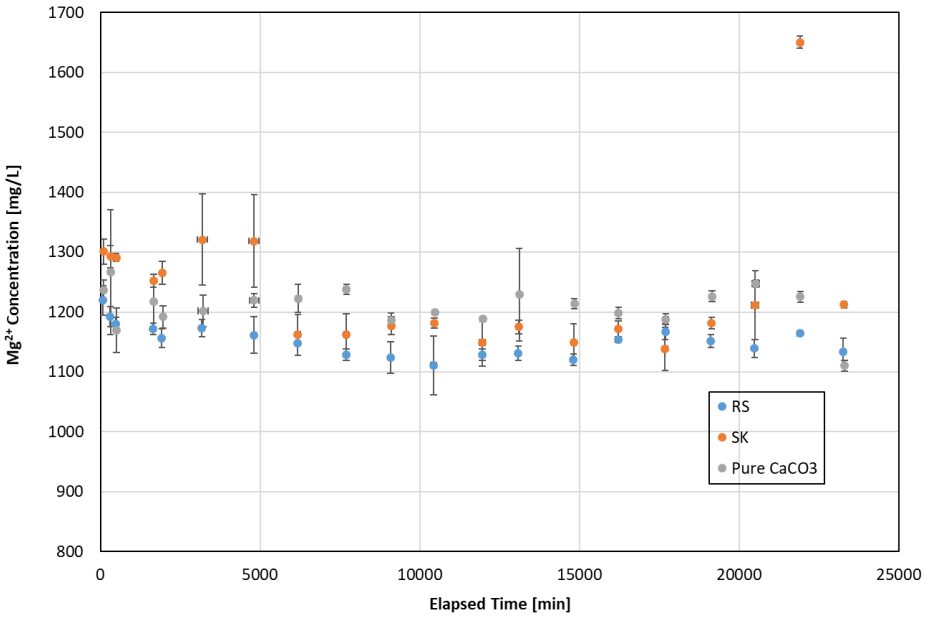

Figure 5. The evolution of magnesium concentration during the ion exchange process between calcite/chalk powders and $MgCl_2$ solution. Due to the high initial concentration and low extent of the exchange process, the Mg^{2+} concentration did not show considerable change.

Similar to the dissolution experiments, the measured pH of the bulk mixture was almost stable throughout the experimental period, with a slightly drop from 9.5 to 9.

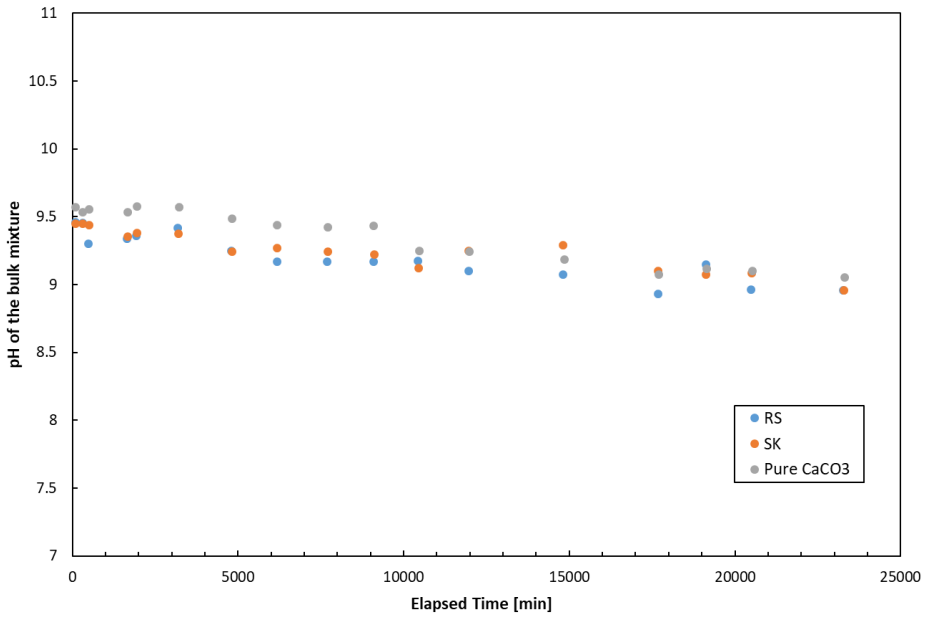

Figure 6. The pH of the mixture during the ion exchange experiments. The measured values are stable throughout the experiments.

3.4 Modeling of experimental data

3.4.1 Modelling of the ion exchange in static experiments

According to the experimental observations, the concentration of Ca^{2+} ions in the Ca-Mg ion exchange experiment can be described as proceeding in the two stages. The first stage is fast. It proceeds rapidly when the calcite surface gets in contact with the $MgCl_2$ solution, resulting in a Ca^{2+} concentration that is 4-5 times higher than for dissolution in pure water. This process reaches equilibrium within 1.5 hours, in this period it dominates the kinetics of the process. It was indicated by the Extended UNIQUAC model (which is implemented in the ScaleCERE software) that the dissolution of calcite can be improved in a $MgCl_2$ solution. This is because in the $MgCl_2$ solution, precipitation of $Mg(OH)_2$ drives the solution to be slightly acidic. The predicted equilibrium concentrations of Ca^{2+} in pure water and in a 0.045M $MgCl_2$ solution are 5.17 and 18.91 mg/L, respectively. These values are consistent with our experimental observation, suggesting the high Ca^{2+} concentration observed in the beginning of the experiment is due to the improved calcite dissolution in $MgCl_2$ solution.

On the other hand, the second stage is slow. After the improved dissolutionreaches equilibrium, it takes over control of the reaction kinetics. A characteristic equilibration time for the second process was found to be above 2 weeks since it was observed that the process did not stop until the end of the experiment. The slow kinetics could be an indication of the ion-exchange process.

Given the above analysis, we propose a conceptual model to describe the equilibration of the two processes. Assume that the calcium ions in calciteare arranged in two layers. The first layer is at the surface of calcite. The ions in this layer are in direct contact with the solution and are readily available for dissolution and exchange with aqueous Mg^{2+}.. The dissolution of this layer is fast, Mg^{2+} also precipitates on this layer as $Mg(OH)_2$ rapidly. The second layer is inside the solid calcite, behind the first layer. In order to release the calcium ions in this layer, the magnesium ions have to get close to the surface and, probably, penetrate through the first layer. There could be more layers in the calcite crystal lattice that can participate in the reaction.In the currenty study, it is sufficient to consider these two layers to represent the two step kinetics..

Apparently, the two layers have different equilibration times. We define the characteristic equilibration times as τ_1 and τ_2 for the first and second layers, respectively. We assume also that the maximum dissolution/exchange capacity, N_{max}, is the same for each layer.

This conceptual representation of the process results in the following mathematical formulation. Let N_i be the total molar quantities of the magnesium ions in the solution ($i = 0$) and in the layers ($i = 1,2$, correspondingly). The conservation law is:

$$\frac{d(N_0 + N_1 + N_2)}{dt} = 0 \tag{4}$$

The ions precipitates on the first layer from the solution, and penetrate the first layer to the second one. The corresponding rates between the layers are v_{01} and v_{12}. Theoretically, there may be ions going in forward and reverse direction. The rates defined here are meant to describe the net effect of the transport processes. The exchange equations are:

$$\frac{dN_0}{dt} = -v_{01}; \tag{5}$$

$$\frac{dN_1}{dt} = v_{01} - v_{12}; \tag{6}$$

$$\frac{dN_2}{dt} = v_{12} \tag{7}$$

Next, we define the exchange rates v_{01} and v_{12}. We apply the simplest model of Langmuir exchange kinetics (Pagonabarraga & Rubí, 1992). The rate v_{01} is proportional to the concentration c_0 of the magnesium ions in the solution, and to the number $N_{max} - N_1$ of the unoccupied sites in the layer:

$$v_{01} = Ac_0(N_{max} - N_1) \tag{8}$$

The value of c_0 is equal to N_0/V. In our system, the amount of magnesium ions is in excess of the available sites, $N_0 \gg N_1, N_2$, so that c_0 does not vary much in the process. Then Ac_0 may be treated as a constant equal to the inverse characteristic time of the exchange between the solution and the first layer:

$$Ac_0 = \frac{1}{\tau_1} \tag{8a}$$

Then equation (15) becomes

$$v_{01} = \frac{1}{\tau_1}(N_{max} - N_1) = \frac{1}{\tau_1}N_{max}(1 - x_1);\ x_1 = \frac{N_1}{N_{max}} \tag{9}$$

The definition of rate v_{12} is more elaborate. Communication of the layers is described as a two-way process so that ions move in both directions between the layers. The net rate v_{12} is

$$v_{12} = v_{1\to2} - v_{2\to1} \tag{10}$$

The rate $v_{1\to2}$ is proportional to the number of the magnesium ions in layer 1 and the fraction of unoccupied sites in layer 2. Similar to the previous derivation,

$$v_{1\to2} = \frac{1}{\tau_2}N_1(1 - x_2);\ x_2 = \frac{N_2}{N_{max}} \tag{11}$$

Similarly,

$$v_{2\to1} = \frac{1}{\tau_2}N_2(1 - x_1) \tag{12}$$

Summing up these equations results in:

$$v_{12} = \frac{1}{\tau_2}N_1(1 - x_2) - \frac{1}{\tau_2}N_2(1 - x_1) = \frac{1}{\tau_2}(N_1 - N_2) \tag{13}$$

This expression may be generalized onto the case where the layers have different capacities. The result is:

$$v_{12} = \frac{1}{\tau_2}N_1(1 - x_2) - \frac{1}{\tau_2}N_2(1 - x_1) = \frac{1}{\tau_2}(N_1 - N_2 + \frac{N_1N_2}{N_{max1}} - \frac{N_1N_2}{N_{max2}}) \tag{14}$$

Equations (4) to (7), with the reaction rates defined by equations (8) to (14) form a system of differential equations. This system was solved by implementing it into Matlab and fitted with experimental data to obtain the essential parameters that characterize the ion exchange process: τ_1, τ_2 and N_{max} (or N_{max1} and N_{max2}). The results are shown in Figure 7.

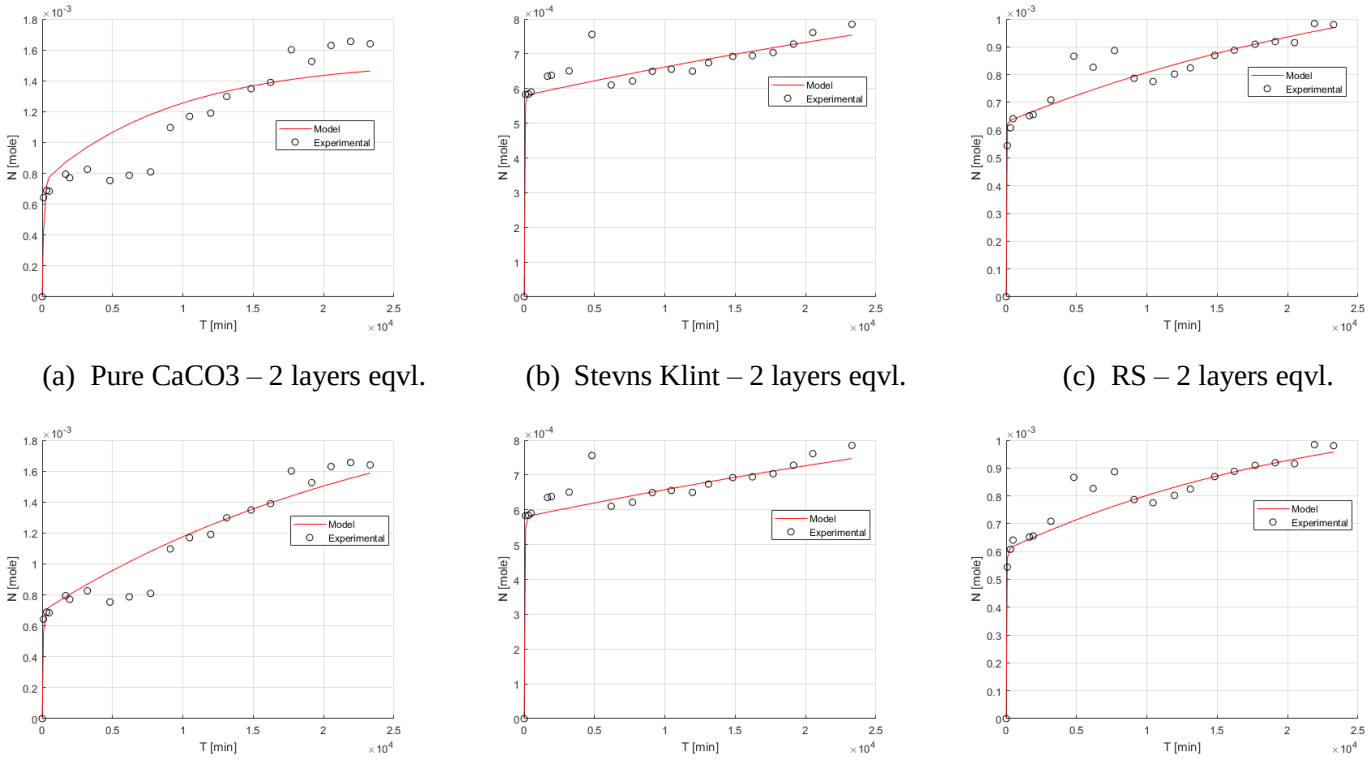

(a) Pure CaCO3 – 2 layers eqvl. (b) Stevns Klint – 2 layers eqvl. (c) RS – 2 layers eqvl.

(d) Pure CaCO3 – 2 layers diff. (e) Stevns Klint – 2 layers diff. (f) RS – 2 layers diff.

Figure 7. Comparison of the proposed 2 layer model and experimental results. Plots (a), (b) and (c) present the results for the model where the two layers have the same capacity. Plots (d), (e) and (f) show the results with the different capacities of the two layers. The two approaches give a similar match with experimental data.

It can be seen that both models match well with experimental data. Given the average standard deviations (STD) of the fitting, the different layer capacities results in a noticeable improvement only for the calcite powder sample. However, fitting with the equal layer capacities is also reasonable, considering the accuracy of the experimental data. For the natural samples, the two fittings behave similarly. The fitted parameters are given in Table 2, the maximum capacities are converted from mol to mol/ m^2 surface area for better comparison.

		τ_1 [min]	τ_2 [$\times 10^4$ min]	N_{max1} [$\times 10^{-5}$ mol/m^2]	N_{max2} [$\times 10^{-5}$ mol/m^2]	Site density [nm^{-1}]	STD of fitting [$\times 10^{-5}$ mol]
Pure CaCO3	2 layers eqvl.	118.4	0.95	2.88	-	17.3	17.4
	2 layers diff.	60.1	1.2	2.63	5.63	15.8	10.6

SK	Eqvl.	30.7	6.5	2.18	-	13.1	3.74
	Diff.	35.0	6.9	2.18	2.33	13.1	3.85
RS	Eqvl.	20.3	3.0	2.37	-	14.3	5.02
	Diff.	28.0	2.5	2.28	2.03	13.8	5.11

Table 2. The fitted parameters from the two modeling approaches that characterize the ion exchange process. Both approaches give similar values for the parameters.

Generally, the two models give similar estimations of the characteristic parameters. The fitted values are consistently in the same order of magnitude. For the cases with the different capacities of the two layers, they are very similar, and the results are close to the layer capacities fitted with an assumption that they are equal. This result, that could not be guessed in advance, confirms the correctness of the two-layer model.

3.4.2 Modelling of the ion exchange in the flooding experiments

In this section, we discuss an impact that the kinetics of ion exchange may have on the results of smart waterflooding. The kinetic model of ion exchange is coupled with transport equations. Then the model is compared with experimental data reported in the literature.

3.4.2.1 Review of single-phase flow-through experiments

Single-phase flooding experiments with the analysis of relevant ion concentrations in the effluent may be used to examine the ion exchange process. The flow should be fast, so that convective flow, rather than diffusion, dominates the process.

The flooding experiments reported by Zhang, Tweheyo, & Austad (2007) and Strand et al. (2008) meet the above-mentioned requirements. They have been used to calibrate surface complexation models (SCM) (Alexeev, 2015; Eftekhari et al., 2017). The flooding experiments by Zhang, Tweheyo, & Austad (2007) were performed with Stevns Klint chalk samples at ambient and at elevated temperatures (130°C). The cores were around 62 mm in length and 35.7 mm in diameter, with a high porosity at 48% and low permeability at 2-5 mDa. The cores were initially saturated with the 0.573 M NaCl solution, then flooded with a solution containing 0.504 M NaCl and equal concentrations of Ca^{2+}, Mg^{2+} and SCN^- at 0.013 M. SCN^- was considered as a tracer. It is inert towards the calcite surface, and the dispersion of its concentration in the effluent reflects the dispersion of the flow. The flooding rate was 0.2 ml/min, corresponding to 9.7 PVI per day. The concentrations of Ca^{2+}, Mg^{2+}, and SCN^- in the produced effluent were analyzed.

It was observed that both at low and high temperature, the production of Mg^{2+} and Ca^{2+} was delayed compared with the tracer. The interplay between the two ions was different. At the low temperature, there was no extra generation of Ca^{2+} since its concentration never exceeded the initial value. On the contrary, at high temperature, a considerable reduction of Mg^{2+} was associated with a significant increase of Ca^{2+} concentration, which indicates the presence of the mass exchange between the aqueous Mg^{2+} and the Ca^{2+} from the rock matrix.

Single-phase flow-through experiments reported by Strand et al. (2008) were performed with a reservoir limestone core. The core was 49.1 mm in length and 37.8 mm in diameter, with a porosity of 24.7% and a permeability of 2.7 mDa. The core was initially saturated by a 0.573 M NaCl solution and subsequently flooded by a brine containing 0.504 M NaCl and equal concentrations of Ca^{2+}, Mg^{2+} and SCN^- at 0.013

M. The same flooding procedure was replicated at 20°C, 70°C, 100°C and 130°C. The injection rate was 0.1 ml/min, equivalent to 10.6 PVI per day.

Unlike the Stevns Klint chalk, the reservoir limestone core did not show an obvious indication of the mass exchange process even at high temperatures. However, with the increase of temperature, the gap between the curves of Mg^{2+} and Ca^{2+} concentration enlarged, which might suggest some interactions between the ions and the rock.

3.4.2.2 The flow-through model

Previously we introduced the mathematical model for the Ca-Mg exchange process. In this section we couple it with the 1D transport equations and match the model to the literature data. The equations are formulated for aqueous species.

The equation for the transport of a neutral tracer is:

$$\varphi \frac{\partial c}{\partial t} + U \frac{\partial c}{\partial x} = 0 \tag{15}$$

Here φ is porosity, U is flow velocity. Similarly, the equations for the transport of Ca^{2+} or Mg^{2+} ions accounting for the exchange reactions are:

$$\varphi \frac{\partial c_i}{\partial t} + U \frac{\partial c_i}{\partial x} = -r_i; \quad i = Ca^{2+}, Mg^{2+} \tag{16}$$

Here r are the reaction rates defined by equations (11) to (14). Since the volume of solutions in the static experiments is 1 liter, the amount N_0 in the rate expressions may be substituted by c. Since it was demonstrated that equal capacities of the layers in the two-layer exchange fit the experimental data equally well, we apply the two-layer model with equal layer capacities. The rates are assumed to be equal (with a different sign) for calcium and magnesium ions:

$$r_{Ca^{2+}} = -r_{Mg^{2+}}$$

Another difference between flow and static experiments is that the characteristic reaction time for the exchange between the solution and the first layer (τ_1) is no longer constant. It may be recalled that, according to Eq. (15a), the value of τ_1 is inversely proportional to c_0. The reason for that is the frequency of the adsorption events (such events where a single ion gets adsorbed) should be proportional to the concentration of the ions. In the static experiments, the variation of the concentration was insignificant, and τ_1 could be considered as constant. However, in the transport process, concentrations of the ions may vary considerably. Then τ_1 becomes dependent on the concentration of the reactant:

$$\tau_1 = \frac{1}{A c_{Mg^{2+}}}$$

The equations are transformed to the dimensionless form with the variables

$$T = \frac{Ut}{\varphi L};\ X = \frac{x}{L};\ C = \frac{c}{c_0} \tag{17}$$

Here L is the length of the core, c_0 is the initial concentration of the solute. The dimensionless equations become:

$$\frac{\partial C}{\partial T} + \frac{\partial C}{\partial X} = 0 \tag{18}$$

$$\frac{\partial C_i}{\partial T} + \frac{\partial C_i}{\partial X} = -R_i; \quad i = Ca^{2+}, Mg^{2+} \tag{19}$$

The rate expressions are also converted into dimensionless form by converting the concentrations and characteristic dimensionless reaction times:

$$\tau_i^* = \frac{U\tau_i}{\varphi L}$$

Equations 18 and 19 were solved numerically by an explicit finite difference method. Similar to Alexeev (2016), the ratio between time step and space step was set to be 1:10, to make numerical dispersion comparable to physical dispersion. The tracer concentration in the effluent calculated by the model were compared with the measured values reported in the literature (Figure 8).

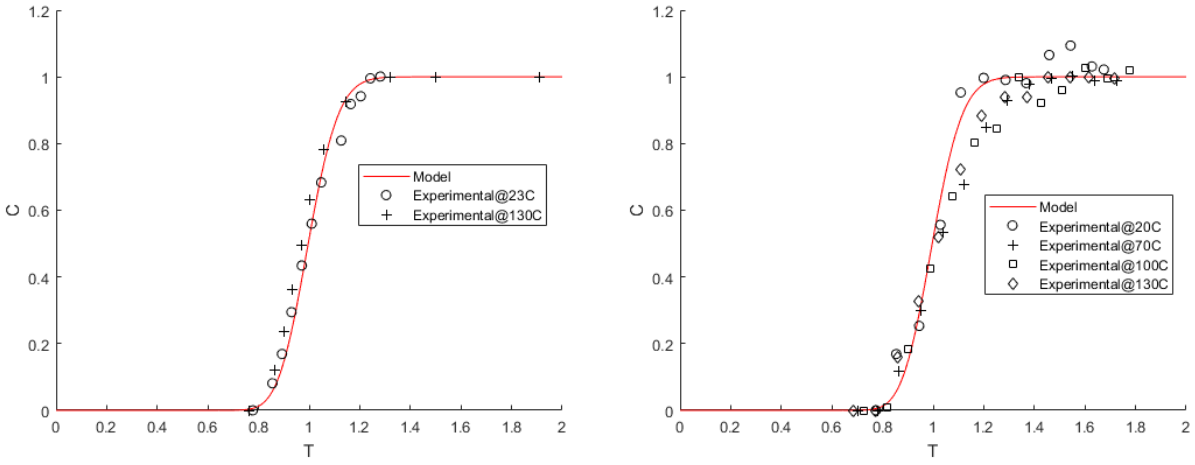

(a) Zhang, Tweheyo, & Austad (2007)

(b) Strand et al., (2008)

Figure 8. The tracer concentration by the model compared to experimental data from (a) Zhang, Tweheyo & Austad, (2007) and (b) Strand et al., (2008). The numerical dispersion is similar to the solute dispersion in porous media.

The model was adjusted to literature data by optimizing A, N_{max} and τ_2, which are the key parameters that characterize the ion exchange process. Adjustment was applied for Mg^{2+} ions, while the concentrations of Ca^{2+} ions were calculated based on the adjusted parameters.

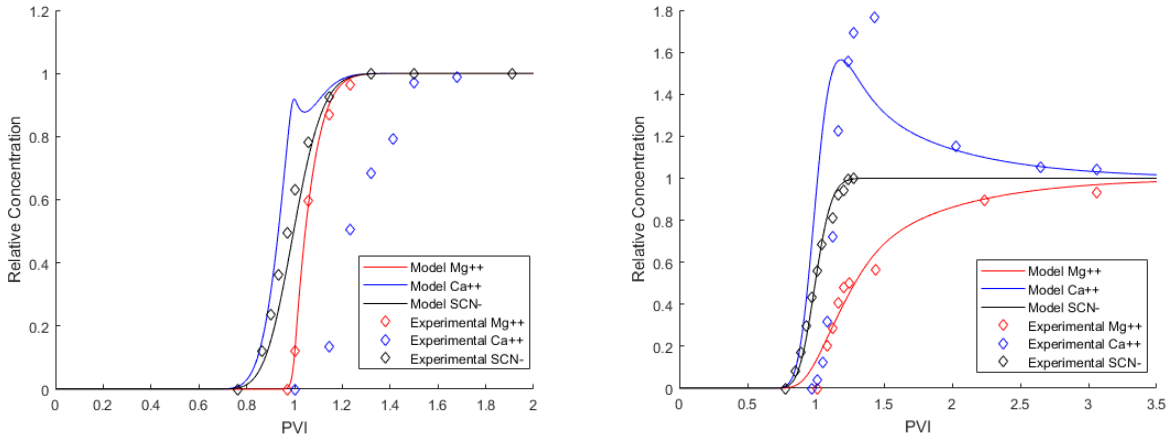

(a) T=20°C (b) T=130°C

Figure 9. Modeling the experimental data by Zhang Tweheyo, & Austad, (2007), accounting for the ion exchange reaction. The model describes better the transport properties of the ions at the high temperature.

For the experiments reported by Zhang, Tweheyo, & Austad (2007), the model was able to reproduce the Mg^{2+} concentration in the effluent, but reproduction of the Ca^{2+} concentration was qualitatively different at low and high temperatures. At low temperature, the model predicted a small peak of Ca^{2+} concentration, which indicates when the ion exchange was most severe.. This was not found in the experimental data. In addition, the front of Ca^{2+} concentration came before that of Mg^{2+}, opposite to experimental data. At high temperature, the model reproduced quite well the behavior of both Mg^{2+} and Ca^{2+} concentrations. This evidences the fluid-rock interactions under the high temperature proceed according to the ion exchange mechanism.

The observations have indicated that the interactions between the chalk surface and the Ca^{2+} and Mg^{2+} ions are fundamentally different at low and high temperatures. Other researchers (Alexeev, 2015; Eftekhari et al., 2017) applied the surface complexation models (SCM) for carbonate surfaces, to approximate the same experimental data. The models account for the competitive adsorption of ions on charged carbonate surface. It was shown that the models could qualitatively reproduce the experimental observations at low temperatures, where our model failed. Apparently, at low temperatures adsorption prevails over the ion exchange, and the balance between deposited magnesium and released calcium ions is destroyed.

At high temperatures, by tuning the equilibrium constants of ion adsorption, the SCM (Alexeev, 2015) qualitatively predicted the behavior of Ca^{2+} and Mg^{2+} concentrations in the effluent. But in this case, our model of ion exchange gave a much better fit with the experimental data. The standard deviation of the fitting is 0.0676 in our approach, while it is 0.240 for the SCM.

The values of the fitted parameters are given in Table 3, the result from the static experiment of Stevns Klint chalk is also listed for comparison.

	Temp. [°C]	A [(min·mol/L)$^{-1}$]	τ_2 [min]	C_{max} [mmol/L]	STD of fitting [non-dimensional]
Fitted with	20	37.16	15761.3	0.78	0.0172

Zhang, Tweheyo, & Austad, 2007.	130	0.14	39.2	3.08	0.0676
Static experiments	20	0.73	65000	0.58	Given in Table 2.

Table 3. The fitted parameters from flow-through experiments of Zhang, Tweeheyo, & Austad, (2007) that characterize the ion exchange process. Results from static experiments are listed for comparison.

It may be speculated that the two different processes take place when flooding chalk cores with magnesium bearing brines: the physical adsorption of ions on the surface and the chemical exchange process between aqueous Mg^{2+} and Ca^{2+} from calcite. These two processes dominate the fluid-rock interaction at different temperatures: at low temperatures, the physical adsorption prevails, while at high temperatures the chemical exchange is stronger and faster.

The fitted values of τ_2 (given in Table 3) support this hypothesis. At high temperature the second layer equilibrates within an hour. Considering that the observed differences in the flooding experiments are between 0.8-1.7 PVI, which corresponds to 2 to 4 hours, equilibration of the second layer within this period means that the production of Ca^{2+} is doubled after both layers have been equilibrated. Meanwhile, at low temperature, exchange with the second layer is just at very early stage. In addition, at high temperature the value of C_{max} increases significantly. This indicates that more sites become accessible for exchange at high temperatures, probably, due to reduction of the energetic barrier or a possibility for ions to faster penetrate to less accessible areas of the natural tortous surface.

It should be mentioned that the static experiments were also performed at ambient temperature, but the physical adsorption was not observed. The reason is that Mg^{2+} ions were in large excess and the measured concentrations of magnesium do not change to such an extent that the changes may be detected. Instead, the Ca^{2+} concentrations were used to model the exchange process, which excluded the impact of physical adsorption.

The fitted values of parameter A show large reduction form low to high temperature, which indicates an increase of the equilibration time of the first layer. This may be associated with the large increase of the maximum exchange capacity at the elevated temperature: more exchange sites become available, which takes a longer time to equilibrate.

Comparing the fitted parameters at 20°C with static experiments, it can be found that both τ_2 and C_{max} are of the same order of magnitude. However, the value of A (related to τ_1) shows large discrepancy. Using the highest concentration in the flooding experiments, which is 0.013 mol/L, the modelled A corresponds to τ_1 equal to 2.07 min. This value is much smaller than in the static experiments (30.7 min). This is probably associated with the sensitivity of the model, as will be further explained in section 4.2.3. Generally, the information distilled from matching the experimental data is that the ion exchange process is largely affected by temperature. The parameters obtained from static experiments can be very different from flooding experiments, they cannot be applied directly to simulate flow through scenarios.

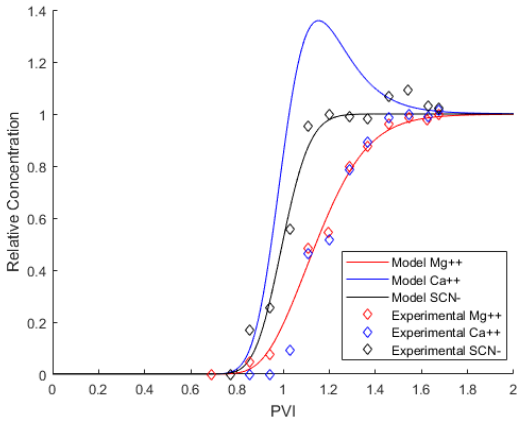

(a) T=20°C

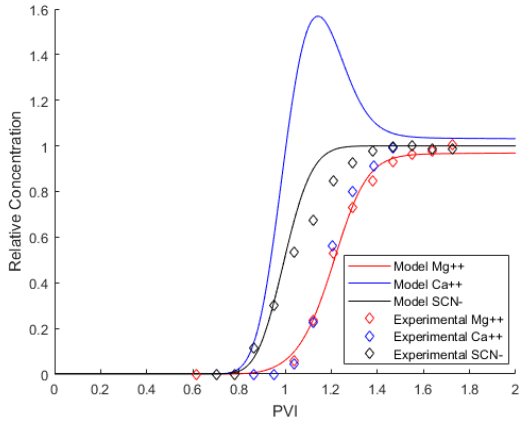

(b) T=70°C

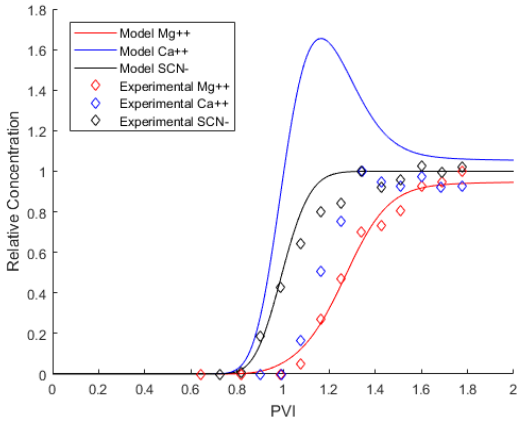

(c) T=100°C

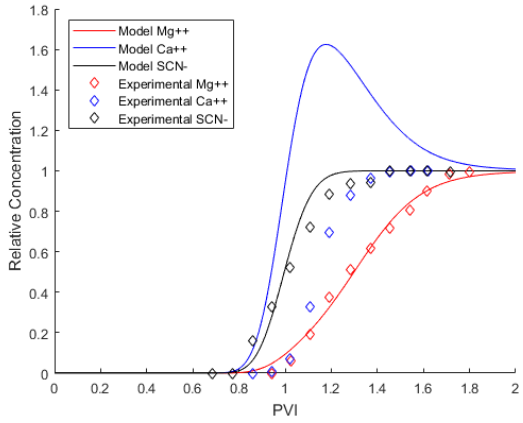

(d) T=130°C

Figure 10. Comparison of the model with experimental data from Strand et al., (2008), accounting for the ion exchange reaction. The model describes concentrations of the tracer and Mg^{2+} but fails to match the data for Ca^2.

Unlike comparison with the data obtained by Zhang, Tweheyo, & Austad, (2007), modeling of the data from Strand et al. (2008) is less successful (Figure 10). The model works well for the Mg^{2+} concentration, but the prediction for the Ca^{2+} concentration is by no means representative. As for the fitted parameters (given in Table 4, converted to dimensional values), only the maximum exchange capacity, C_{max}, shows a consistently increasing trend with the temperature. The fitted values of A remain in the same order of magnitude at different temperatures. There was no clear correlation between τ_2 and temperature.

T [°C]	A [(min·mol/L)$^{-1}$]	τ_2 [min]	C_{max} [mmol/L]	STD of the fitting [non-dimensional]
20	0.35	5109.9	2.08	0.030
70	0.65	185.3	2.65	0.024
100	0.47	130.9	3.40	0.043

130	0.28	5109.6	4.01	0.032

Table 4. The fitted parameters for experimental data of Strand et al., (2008). There is a clear increasing trend of C_{max} along with temperature, but other parameters do not change regularly with the temperature.

A reason for the poor correlation between the predicted Ca^{2+} concentration and experimental data may be the rock mineralogy. The model for ion exchange was derived from a highly pure biogenic chalk, which is composed primarily of calcite with a negligible amount of impurities. While the flow-through experimental data were obtained from a reservoir limestone, whose mineral composition was not clearly indicated. The limestone usually contains varying amounts of clay. The impact of clay on the transport properties of cations has been quantitatively studied (Eftekhari et al., 2017). It was pointed out that even a small amount of clay (1%wt) can dramatically change the surface potential of the carbonate, which could further affect the adsorption of ions on the mineral surface.

3.4.2.3 Sensitivity analysis

Since the model does not always behave consistently with experimental data, it is of interest to inestigate its sensitivity to the parameters. We take the optimized parameters from Table 3 and 4 as initial values, scale each parameter with a factor of 10 and find how the standard deviation (STD) varies. The result for the data from Zhang, Tweheyo, & Austad, (2007) is given in Figure 11.

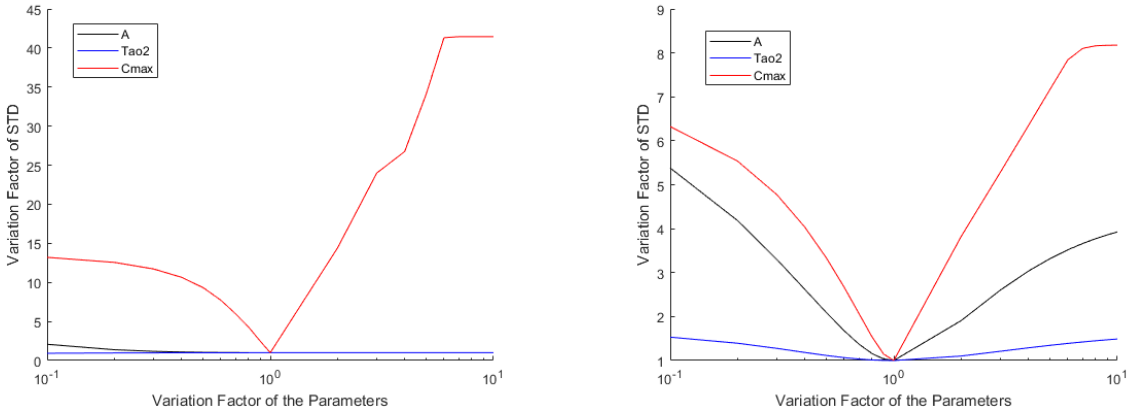

(a) T=20°C (b) T=130°C

Figure 11. Sensitivity analysis for the modelling of experimental data from Zhang, Tweheyo, & Austad, (2007). The model is more sensitive to C_{max} and A, but not τ_2, especially at low temperature.

At high temperature, all the three parameters produced non-monotonic bahaviour of STD with a minimum point at the initial values. However, at low temperature, the quality of fitting does not vary much upon variation of A and τ_2 in the inspected ragne. Further downscale A and τ_2, it can be seen that (Figure 12) τ_2 gives the best fitting at almost 2 orders smaller than the initial value. But the impact of τ_2 on STD is very insignificant after the optimal point. Practically τ_2 should not affect the fitting at any value larger than that. Similar observation is made on A.

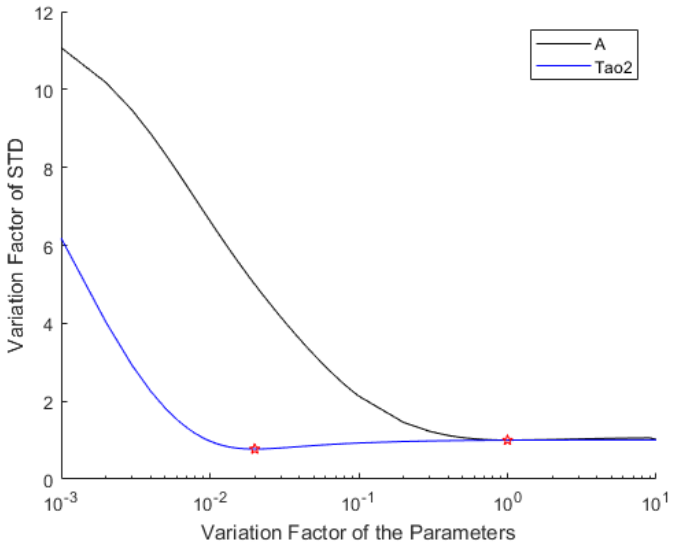

(a) T=20°C

Figure 12. The dependence of STD on A and τ_2 for the modelling of experimental data from Zhang, Tweheyo, & Austad, (2007), Both parameters produced monotonic behavior of STD.

This means the equilibration time of the first layer (inversely propotional to A) can be shorter without much damage to the overall fitting quality. As for τ_2, the experimental data probably could not give a clear indication for it. This is because τ_2 should be longer than 2 weeks at ambient temperature, as demonstrated by the static experiments. Meanwhile, the considered flooding experiments lasted for only a few hours, which means that the second layer was not much involved in the reaction, so that it is difficult to be detected in the experiments.

The analysis for modelling of data from Strand et al., (2008) gives similar observations. As shown in Figure 13, for all the tested temperatures, the model is more sensitive to C_{max} and A than τ_2.

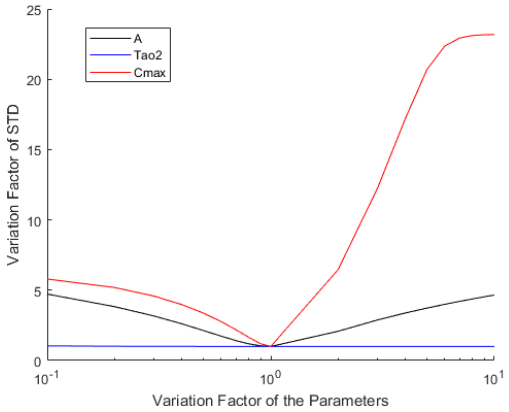

(a) T=20°C

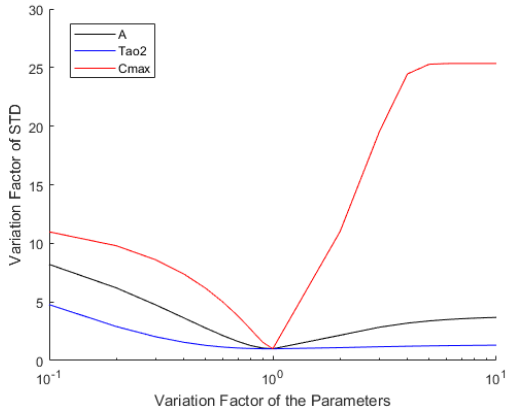

(b) T=70°C

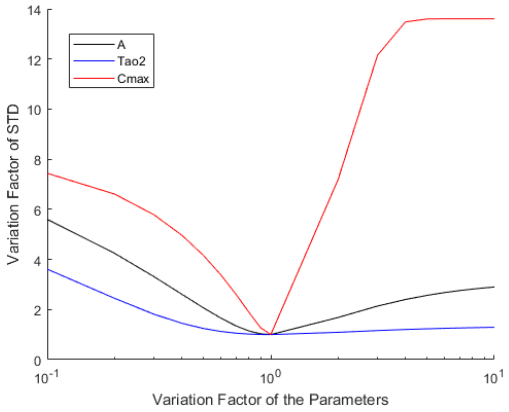

(c) T=100°C

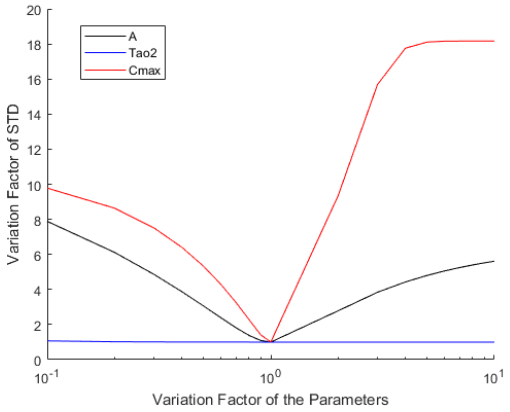

(d) T=130°C

Figure 13. Sensitivity analysis for the modelling of experimental data from Strand et al., (2008). Similar to previous obervations, the model is more sensitive to C_{max} and A, but not τ_2.

A more clear comparison of the impact of τ_2 is given in Figure 14. It can be seen that, further increase τ_2, even with a factor of 10, does not have much influence on the fitting. The reason is, again, the duration of labortary test is too short for the second layer to engage in the reaction. Given this fact, we could practically apply the value of τ_2 obtained from static experiments into the dynamic model. It also means that, core flooding experiments may not provide a full picture of the impact of ion exchange. But at reservoir scale, where the injection lasts for months or even years, the full potential of ion exchange maybe unlocked.

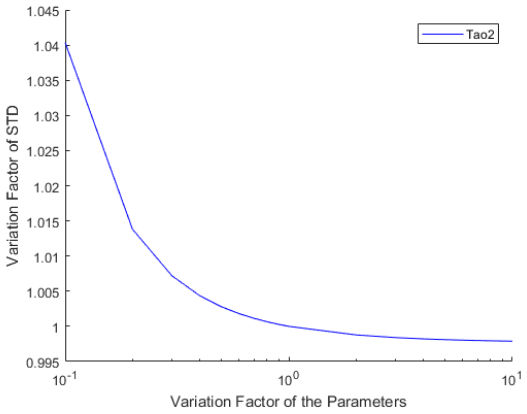

(a) T=20°C

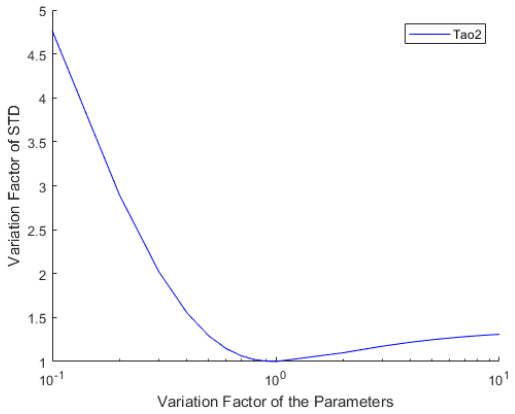

(b) T=70°C

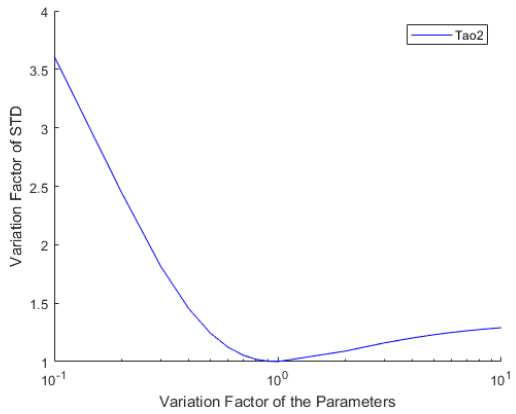

(c) T=100°C

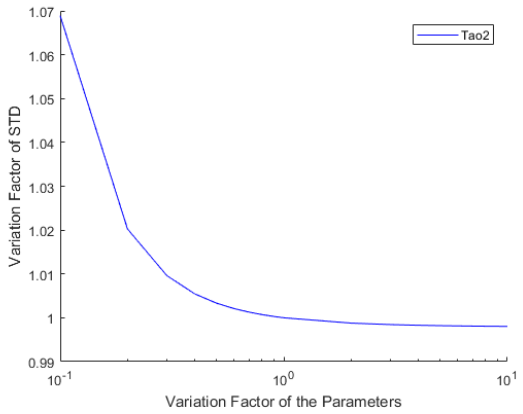

(d) T=130°C

Figure 14. Impact of τ_2 on STD for the modelling of experimental data from Strand et al., (2008). STD behaves monotonicllly upon τ_2 at 20°C and 130°C, but not in the other two temperatures.

3.4.3 Modeling of the dissolution process in static experiments

The results indicate that the saturation of water by calcite was very fast (in the order of seconds). In order to verify the observation, we simulated the process in the PhreeqC software. We adopted the rate expression of calcite dissolution derived by Plummer, Wigley, & Parkhurst (1978):

$$R_{calcite} = r_f A \left(1 - 10^{\frac{2}{3} SI_{calcite}}\right) \left(\frac{\text{mmol}}{\text{s}}\right), \tag{4}$$

where $R_{calcite}$ is the dissolution rate in mmol/cm^2/s; $SI_{calcite}$ is the saturation index of calcite in the solution; r_f is the forward rate constant:

$$r_f = k_1[H^+] + k_2\left[CO_{2(aq)}\right] + k_3[H_2O] \tag{5}$$

Here $[H^+]$, $\left[CO_{2(aq)}\right]$ and $[H_2O]$ are the activities of the corresponding species; k_1, k_2, and k_3 are temperature-dependent constants:

$$k_1 = 10^{0.198 - 444.0/T}; \tag{6}$$

$$k_2 = 10^{2.84 - 2177.0/T}; \tag{7}$$

If T<=25°C,

$$k_3 = 10^{-5.86 - 317.0/T}; \tag{8}$$

If T>25°C,

$$k_3 = 10^{-1.1 - 1737.0/T} \tag{9}$$

Compared to the original expression, the contact surface area $A$was inserted into Eq. (4).

The simulation was performed for 26.61 m^2 calcite surface in one liter of water at 21°C, the initial pH was 7.

The kinetics of the simulated result of calcite dissolution agrees well with the experimental data. The equilibrium was reached around 10 seconds, while our experiments indicate that it is less than 20 seconds. The equilibrium concentration (4.77 mg/L) also agrees well with the experimental results, especially for pure calcite and Stevns Klint chalk. A slightly higher concentration given by reservoir chalk is probably due to the impurities of the material. However, the impact is insignificant considering the low equilibrium concentrations.

A good match between our experimental measurement and PhreeqC simulation confirms the validity and accuracy of the experimental procedure. The final state of the system can be well described by the existing theory.

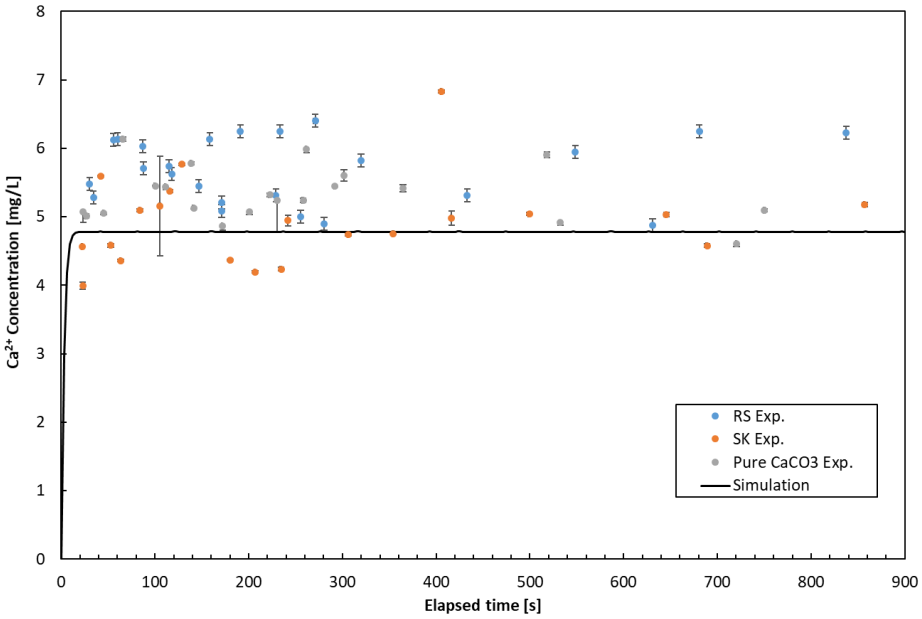

Figure 15. PhreeqC simulated calcium concentration during calcite dissolution in pure water and our experimental data. It can be seen that the model calculation matches well with experimental observations of pure calcite and Stevns Klint chalk, but slightly underestimates the equilibrium concentration for reservoir chalk.

3.4.4 Evaluation of calcite dissolution in flooding experiments

3.4.4.1 Review of experimental data

Two-phase displacement experiments in chalk with the sequential injection of different brines are selected to evaluate the effect of calcite dissolution on oil recovery. In this study, we discuss the flooding experiments reported by Fathi, Austad, & Strand, (2010) and Zahid, Stenby, & Shapiro, (2010). These experiments were carried out with the Stevns Klint chalk samples, similar to the materials in our static experiments.

In the work of Fathi, Austad & Strand (2010), a Stevns Klint outcrop core was flooded twice to test the EOR potential of different brines. In both tests, several brines were injected sequentially, Injection of SW at tertiary stage increased the recovery by 7% and 5%, respectively. Additional oil was produced gradually within 2 PVI (Porous Volume Injected) after switching the injection brine. The flooding was

performed at 120°C and the injection rate was 1 PV/day. The compositions of the brines are given in Table 5.

Ion	FW [mol/L]	SW [mol/L]	dSW10000 [mol/L]	SW0NaCl [mol/L]
HCO_3^-	0.009	0.002	0.001	0.002
Cl^-	1.07	0.525	0.158	0.126
SO_4^{2-}	0	0.024	0.007	0.024
Mg^{2+}	0.008	0.045	0.013	0.045
Ca^{2+}	0.029	0.013	0.004	0.013
Na^+	1.00	0.450	0.135	0.050
K^+	0.005	0.010	0.003	0.010
Ionic strength	1.112	0.657	0.197	0.257
TDS [g/L]	62.80	33.39	10.02	10.01

Table 5. Brine compositions involved in the flooding experiments reported in Fathi, Austad & Strand, (2010).

The work of Zahid, Stenby & Shapiro (2010) involves 15 core flooding experiments with the Stevns Klint chalk cores. Here we select 6 out of 13 experiments that are representative of the different experimental conditions, to avoid repetition. The experimental temperatures were 40°C, 90°C and 110°C. Additional recoveries ranging from 1.16% to 3.38% were observed shortly after injecting the modified seawater. The compositions of the injected brines are given in Table 6.

Ion	SW0S [mol/L]	SW [mol/L]	SW3S [mol/L]
Na^+	0.368	0.358	0.337
K^+	0.010	0.010	0.010
Mg^{2+}	0.045	0.045	0.045
Ca^{2+}	0.013	0.013	0.013
Cl^-	0.492	0.434	0.317
HCO_3^-	0.002	0.002	0.002
SO_4^{2-}	0	0.024	0.072
TDS [g/L]		33.39	

Table 6. Compositions of the brine used in the core flooding experiments reported by Zahid, Stenby & Shapiro (2010).

All the tested conditions are listed in Table 7.

	Brine	T [°C]
Fathi, Austad & Strand, (2010)	FW SW dSW10000 SW0NaCl	120
Zahid, Stenby & Shapiro, (2010)	SW	40 90 110
	SW0S	40 90 110
	SW3S	40 110

Table 7. Summary of the experimental conditions applied to simulate calcite dissolution kinetics using PhreeqC.

3.4.4.2 Calcite dissolution under the reported experimental conditions

It was stated in section 3 that the dissolution of calcite in pure water is a fast process. The equilibration time is in the order of seconds, and the equilibrium concentration is low (between 10 – 16 mg/L $CaCO_3$). The PhreeqC modeling described in section 4.3 gave a reasonably accurate estimation of the dissolution kinetics and of the equilibrium concentration for the pure calcite and the Stevns Klint chalk.

First, we evaluate the dissolution kinetics of calcite under the experimental conditions (temperature and brine composition) involved in the reviewed works.

The Stevns Klint outcrop chalk has a specific surface area of 2 m^2/g. The static dissolution process was simulated with the same experimental configurations as described in the previous section: 26.61 m2 surface area in one-liter of the solution. The result is shown in Figure 16.

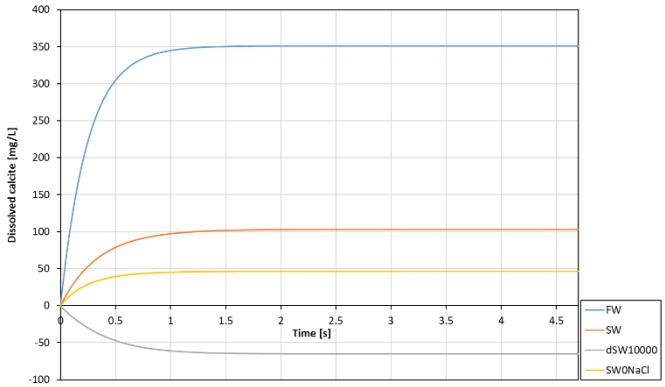

(a) Calcite dissolution under conditions of Fathi, Austad & Strand, 2010.

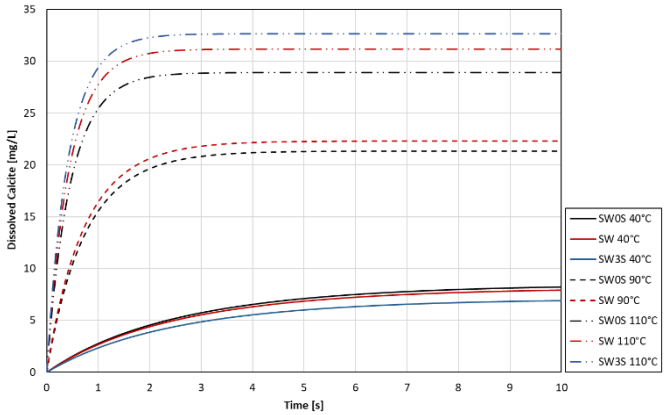

(b) Calcite dissolution under conditions of Zahid, Stenby & Shapiro, 2010.

Figure 16. The simulated calcite dissolution kinetics under the experimental conditions reported in (a) Fathi, Austad & Strand, (2010) and (b) Zahid, Stenby & Shapiro (2010). The temperature has a much more significant impact on the dissolution kinetics than the composition of the brine.

It can be seen that the dissolution of calcite reaches equilibrium very rapidly in both cases. For the experimental conditions in the work of Fathi, Austad, & Strand, (2010), the equilibrium is reached after one second. The different brines correspond to the different equilibrium concentrations rather than equilibration times. The brine termed dSW10000 causes precipitation of calcite instead of dissolution. Simulations based on the conditions from Zahid, Stenby, & Shapiro, (2010), show that the effect of temperature on the dissolution process is more important than the effect of the brine composition. Higher temperatures greatly enhance the dissolution of calcite. Meanwhile, the effect of sulfate concentration on dissolution is rather insignificant.

The simulated pH profiles (Figure 17) correlate with the observations. The dissolution of calcite in the brines is associated with a reduction of pH. The equilibrated solutions usually end up in slightly acidic brines, except for the experiments at 40°C reported by Zahid, Stenby & Shapiro, (2010).

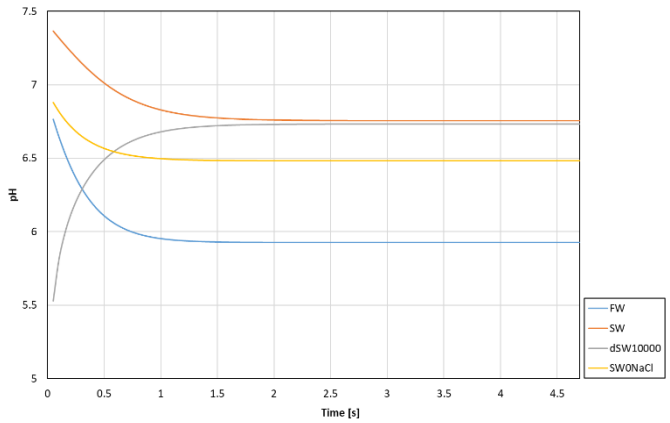

(a) pH profiles under conditions of Fathi, Austad & Strand, 2010.

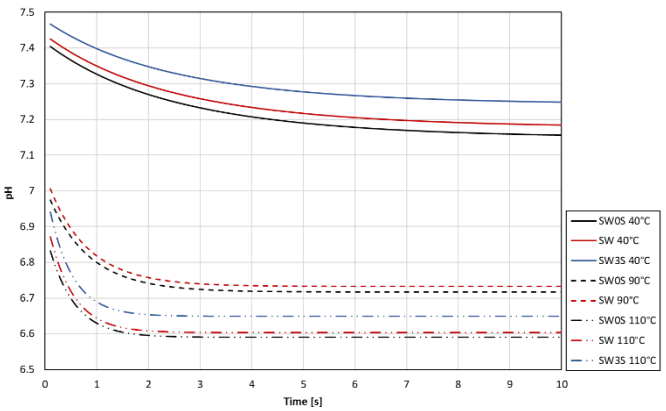

(b) pH profiles under conditions of Zahid, Stenby & Shapiro, 2010.

Figure 17. The simulated pH profiles under the experimental conditions reported in (a) Fathi, Austad & Strand, (2010) and (b) Zahid, Stenby & Shapiro (2010).

The implications of the obtained information (low dissolution times and amounts) on the flooding experiments are two-fold. First, in the flooding experiments, the flow velocity of water is slow. In the reviewed works, the injection rates are 1 and 5 PV/day. On the basis of the given core data, the mobile saturation of water can be calculated using the average irreducible saturations of oil and water, and afterward, the flow velocity of the water can be calculated. The results are given in Table 8.

	L [cm]	D [cm]	PV [ml]	S_{wi} [%]	2nd Rec. [%]	S_{or} [%]	V [mm/s]
S. Fathi et al., 2010	7.0	3.81	35.9	8	57	39.6	0.0015
A. Zahid et al., 2010	7.5	2.54	17.8	0	61.8	38.2	0.0070
		3.81	37.5	0	69.2	30.8	0.0063

Table 8. The calculated flow velocities of the water in the two reviewed works and the parameters used for the calculation. Compared with the very slow flow velocity, the dissolution of calcite should be considered as a fast process.

Comparison of the equilibration time for dissolution (few seconds) and the calculated flow velocity shows that, apparently, the dissolution process will reach equilibrium at the very inlet of the core, while the rest of the core remains unaffected. However, in most cases, additional oil was produced immediately after switching the injection brine or increasing the temperature. Such recoveries should not be attributed to the dissolution occurred at the inlet of the cores.

The equilibrium amount of dissolved calcite is very low. The maximum dissolved amount in the reviewed works is 350 mg/L. For the pore volume of the core, which is usually in the range of 30-40 ml for a typical Stevns Klint core, one liter of injection brine corresponds to 25 to 28.5 PVIs. This injected volume is rarely achieved in the flooding experiments so that the actual amount of dissolved calcite is even lower. Compared with the mass of the core, which can be calculated using the reported core data (given in Table 9), the dissolved mass is negligibly small, the effect is unlikely to be observed visually. However, since the dissolution is fast, long term injection may result in structures like wormholes at the inlets of the cores.

	L [cm]	D [cm]	Porosity [%]	Mass [g]
S. Fathi et al., 2010	7.0	3.81	45	119.0
A. Zahid et al., 2010	7.5	2.54	46.8	54.8
		3.81	43.8	130.1

Table 9. The calculated mass of the cores using reported core information and calcite density of 2.71 g/cm^3.

Advanced mathematical modeling of the dynamic effect of the dissolution on the two-phase displacement is consistent with our observations (Alexeev, Shapiro, & Thomsen, 2015). Fast dissolution affects only

the injection spot, almost without progressing into the rock. In addition, due to the volumetric non-additivity (the volume contribution of the mineral decreases in solution), the dissolution front velocity decreases in the affected section.

On the other hand, Hiorth, Cathles, & Madland (2010) reported a linear correlation between calcite dissolution and oil recovery in the imbibition experiments, assuming uniform dissolution inside the core. However, considering the fast dissolution kinetics, dissolution could have only happened on the surface of the core very soon after it was immersed in the imbibing fluid. When the brine penetrates further into the core, it is already saturated with $CaCO_3$ that was dissolved near the core surface. Additional oil production due to dissolution would thus be insignificant, even though the dissolution may have preferentially occurred at places where oil adsorbs on the calcite, as stated by Stumm, 1992 (p. 162). Probably, there are other surface-chemistry mechanisms of recovery that correlate with the capability of brine to dissolve $CaCO_3$.

While dissolution alone is not likely to lead to a large amount of oil production, it may trigger other, probably, more important effects. Consequences such as pH alteration (Lager et al., 2008), improved pore connectivity (Yousef et al., 2010), modified electric double layer interaction (Karimi et al., 2016) and compaction of chalk (Hao & Shapiro, 2019) were reported in connection with the calcite dissolution. These mechanisms need a separate investigation.

3.5 Conclusions

In this work, we studied experimentally the kinetics of calcite dissolution in pure water and the Ca – Mg ion exchange on the surface of calcite. The experiments were performed with three types of powders: pure calcite, Stevns Klint outcrop chalk, and North Sea reservoir chalk. It was shown that the existing theory of calcite dissolution was able to match the observed kinetics of the tested materials. Another model was proposed to describe the kinetics of calcium-magnesium ion exchange. It was shown that the two-layer exchange model could describe the process of exchange on the two time scales. Significance of the dissolution and ion exchange processes was evaluated for the two-phase flooding experiments and single-phase flow-through experiments reported in the literature. A numerical transport model was developed for the flow-through experiments. The main conclusions are as follows:

- The dissolution of calcite is confirmed to be a fast process and the equilibrium concentration is low. Given the surface area to liquid volume ratio in our experiments, the equilibrium can be reached within a few seconds. Depending on the temperature and brine composition, the equilibrium concentration of calcite can range from a few milligrams to a few hundred milligrams per liter.
- It is not likely that the dissolution of calcite alone is responsible for the observed additional recovery in smart waterflooding experiments. Under the reported experimental conditions, dissolution of calcite should have occurred at the inlets of the cores, while the additional oil production was observed rapidly after the injection water was changed.
- The proposed two-layer model (inner and outer) matches well with the experimental data. It is sufficient to assume that the two layers have equal capacities with regard to the adsorbed amounts of magnisium. The exchange capacity of the surface, as matched by the model, was in the order of 10^{-5} mol/m^2/layer.
- Due to the long equilibration time of the second layer, as described by the two-layer model. The impact of ion exchange may be more profound on reservoir scale than in laboratory tests.
- We have compared the behavior of the ion exchange model proposed in this work with the surface complexation models reported in the literature. Both physical adsorption and chemical

exchange of Ca^{2+} and Mg^{2+} ions take place when flooding chalk cores with Mg^{2+} containing brines. The physical adsorption dominates fluid-rock interaction at low temperatures, while in the model the chemical exchange reaction dominates at high temperatures.

- The different carbonate rocks possess different properties when it comes to the ion exchange process. The mineralogy composition of the rock should be understood in order to analyze the chemical interactions.

Acknowledgment

The authors kindly acknowledge the Danish Hydrocarbon Research and Technology Centre for supporting this project. Ming Li, Duc Thuong Vu, and Annette Eva Jensen are kindly acknowledged for practical assistance in the laboratory.

References

Afekare, D., & Radonjic, M. (2017). From Mineral Surfaces and Coreflood Experiments to Reservoir Implementations: Comprehensive Review of Low-Salinity Water Flooding (LSWF). *Energy and Fuels, 31*(12), 13043-13062.

Alexeev, A. (2015). *Modeling of Salinity Effects on Waterflooding of Petroleum Reservoirs.* Technical University of Denmark, Department of Chemical and Biochemical Engineering.

Alexeev, A., Shapiro, A., & Thomsen, K. (2015). Modeling of Dissolution Effects on Waterflooding. *Transport in Porous Media, 106*(3), 545-562.

Alshakhs, M., & Kovscek, A. (2016). Understanding the role of brine ionic composition on oil recovery by assessment of wettability from colloidal forces. *Advances in Colloid and Interface Science, 233*, 126-138.

Ayirala, S., & Yousef, A. (2016). A critical review of water chemistry alteration technologies to develop novel water treatment schemes for smartwater flooding in carbonate reservoirs. *SPE Symposium on Improved Oil Recovery Conference.* Tulsa, Oklahoma, U.S.A.

Bartels, W., Mahani, H., Berg, S., & Hassanizadeh, S. (2019). Literature review of low salinity waterflooding from a length and time scale perspective. *Fuel, 236*(September 2018), 338-353.

Derkani, M., Fletcher, A., Abdallah, W., Sauerer, B., Anderson, J., & Zhang, Z. (2018). Low Salinity Waterflooding in Carbonate Reservoirs: Review of Interfacial Mechanisms. *Colloids and Interfaces, 2*(2), 20.

Eftekhari, A., Thomsen, K., Stenby, E., & Nick, H. (2017). Thermodynamic Analysis of Chalk-Brine-Oil Interactions. *Energy and Fuels, 31*(11), 11773-11782.

Fathi, S., Austad, T., & Strand, S. (2010). "smart water" as a wettability modifier in chalk: The effect of salinity and ionic composition. *Energy and Fuels, 24*(4), 2514-2519.

Finneran, D., & Morse, J. (2009). Calcite dissolution kinetics in saline waters. *Chemical Geology, 268*(1-2), 137-146.

Gachuz-muro, H., & Sohrabi, M. (2017). Prediction, Control and Validation of Rock Dissolution During Smart Water Injection and Its Impact on Waterflood Performance in Heavy Oil Carbonate Reservoirs. *International Symposium of the Society of Core Analyst*(August), 1-12.

Hamouda, A., & Maevskiy, E. (2014). Oil recovery mechanism(s) by low salinity brines and their interaction with chalk. *Energy and Fuels, 28*(11), 6860-6868.

Hao, J., & Shapiro, A. (2019). Effect of Compaction on Oil Recovery Under Low Salinity Flooding in Homogeneous and Heterogeneous Chalk. *SPE Annual Technical Conference and Exhibition.*

Hao, J., Mohammadkhani, S., Shahverdi, H., Esfahany, M., & Shapiro, A. (2019). Mechanisms of smart waterflooding in carbonate oil reservoirs - A review. *Journal of Petroleum Science and Engineering, 179*(January), 276-291.

Hiorth, A., Cathles, L., & Madland, M. (2010). The Impact of Pore Water Chemistry on Carbonate Surface Charge and Oil Wettability. *Transport in Porous Media, 85*(1), 1-21.

Karimi, M., Al-Maamari, R., Ayatollahi, S., & Mehranbod, N. (2016). Wettability alteration and oil recovery by spontaneous imbibition of low salinity brine into carbonates: Impact of Mg2+, SO42−and cationic surfactant. *Journal of Petroleum Science and Engineering, 147*, 560-569.

Lager, A., Webb, K., Black, C., Singleton, M., & Sorbie, K. (2008). Low Salinity Oil Recovery - An Experimental Investigation. *Petrophysics, 49*(1), 28-35.

Mahani, H., Keya, A., Berg, S., Bartels, W., Nasralla, R., & Rossen, W. (2015). Insights into the mechanism of wettability alteration by low-salinity flooding (LSF) in carbonates. *Energy and Fuels, 29*(3), 1352-1367.

Mortensen, J., Spe, T., Of Denmark, F., Engstrøm, M., Oil, G., & Lind, I. (1998). *The Relation Among Porosity, Permeability, and Specific Surface of Chalk From the Gorm Field, Danish North Sea.*

Pagonabarraga, I., & Rubí, J. (1992). Derivation of the Langmuir adsorption equation from non-equilibrium thermodynamics. *Physica A: Statistical Mechanics and its Applications, 188*(4), 553-567.

Plummer, L., Wigley, T., & Parkhurst, D. (1978). The Kinetics of Calcite Dissolution in CO2-Water Systems at 5° to 60°C and 0.0 to 1.0 atm CO2. *American Journal of Science, 278*, 179-216.

Rashid, S., Mousapour, M., Ayatollahi, S., Vossoughi, M., & Beigy, A. (2015). Wettability alteration in carbonates during "Smart Waterflood": Underling mechanisms and the effect of individual ions. *Colloids and Surfaces A: Physicochemical and Engineering Aspects, 487*, 142-153.

Rezaei Gomari, K., & Hamouda, A. (2006). Effect of fatty acids, water composition and pH on the wettability alteration of calcite surface. *Journal of Petroleum Science and Engineering, 50*(2), 140-150.

Sohal, M., Thyne, G., & Søgaard, E. (2016). Review of Recovery Mechanisms of Ionically Modified Waterflood in Carbonate Reservoirs. *Energy and Fuels, 30*(3), 1904-1914.

Strand, S., Austad, T., Puntervold, T., Høgnesen, E., Olsen, M., & Barstad, S. (2008). "Smart Water" for oil recovery from fractured limestone: A preliminary study. *Energy and Fuels, 22*(5), 3126-3133.

Stumm, W. (1992). *Regulation of Trace Elements by the Solid-Water Interface in Surface Waters.*

Subhas, A., Rollins, N., Berelson, W., Dong, S., Erez, J., & Adkins, J. (2015). A novel determination of calcite dissolution kinetics in seawater. *Geochimica et Cosmochimica Acta, 170*, 51-68.

Sulpis, O., Lix, C., Mucci, A., & Boudreau, B. (2017). Calcite dissolution kinetics at the sediment-water interface in natural seawater. *Marine Chemistry, 195*(June), 70-83.

Yousef, A., Al-Saleh, S., Al-Kaabi, A., & Al-Jawfi, M. (2010). Laboratory Investigation of Novel Oil Recovery Method for Carbonate Reservoirs. *Canadian Unconventional Resources & International Petroleum Conference.* Calgary, Canada.

Zahid, A., Stenby, E., & Shapiro, A. (2010). Improved Oil Recovery in Chalk: Wettability Alteration or Something Else? *SPE EUROPEC/EAGE Annual Conference.* Barcelona, Spain.

Zhang, P., & Austad, T. (2006). Wettability and oil recovery from carbonates: Effects of temperature and potential determining ions. *Colloids and Surfaces A: Physicochemical and Engineering Aspects, 279*(1-3), 179-187.

Zhang, P., Tweheyo, M., & Austad, T. (2006). Wettability alteration and improved oil recovery in chalk: The effect of calcium in the presence of sulfate. *Energy and Fuels, 20*(5), 2056-2062.

Zhang, P., Tweheyo, M., & Austad, T. (2007). Wettability alteration and improved oil recovery by spontaneous imbibition of seawater into chalk: Impact of the potential determining ions Ca2+, Mg2+, and SO4 2-. *Colloids and Surfaces A: Physicochemical and Engineering Aspects, 301*(1-3), 199-208.

Chapter 4. Effect of Flow Diversion on Oil Recovery Under Smart Waterflooding in Homogenous and Heterogeneous Chalk and Sandstone

This chapter has been submitted as a paper manuscript to the *Journal of Petroleum Science and Engineering*

Abstract

This work experimentally evaluates the impact of flow diversion and heterogeneity on enhanced oil recovery (EOR) by smart waterflooding. A systematic experimental study was carried out by comparing the behavior of homogeneous cores with heterogeneous cores, and the sandstone cores with the chalk cores. An advanced mathematical model that includes the mechanism of fines relocation and instant vertical communication in a layered porous media was employed to simulate the experiments. The study is expected to improve the understanding of the important factors for enhanced recovery by smart waterflooding. This study indicates that the generation of a plugging agent by smart waterflooding is possible for both sandstone cores (clay particles) and chalk cores (precipitated salts and emulsification). These plugging agents contribute to oil recovery through the flow diversion mechanism, which increases the sweep efficiency. A higher additional recovery was consistently observed from the heterogeneous cores, which suggests that heterogeneity may amplify the effect of flow diversion. These mechanisms are similar for sandstone and chalk cores.

4.1 Introduction

Smart waterflooding as a method for enhanced oil recovery (EOR) has drawn increasing attention in recent years (Hao et al., 2019). Compared with other chemical EOR methods, smart waterflooding is more cost-effective and environmentally friendly. The first systematic investigation of this approach was carried out for a sandstone rock (Tang & Morrow, 1999). Later on, the research was extended to carbonaceous rocks. Regardless the numerous efforts, there is still no definite conclusion on the working mechanisms (Jackson et al., 2016; Bartels et al., 2019). A lot of focus has been put on explaining the interfacial interactions between rock, oil and brine (Derkani, et al., 2018). Chemical mechanisms, such as ion exchange, double layer expansion, wettability alteration etc. have been proposed to explain the experimental observations (Afekare & Radonjic, 2017; Sohal, Thyne, & Søgaard, 2016). However, dynamic mechanisms, which take place along with the dynamic process of the two-phase displacement, have not been sufficiently studied (Hao et al., 2019).

In sandstone rocks, the presence of clay is considered to be a key factor for low salinity water flooding (LSW) to take effect (Afekare & Radonjic, 2017; Jackson et al., 2016). Tang and Morrow (1999) attributed the additional recovery to potential mobile clay particles in the core. The LSW effect was observed in the cores, which have a certain clay content, but no additional production was observed after the cores have been sintered (which is believed to stabilize the particles). Similar observations was made by Al-Sarihi et al. (2018), where additional oil was always accompanied by the production of fine particles and a reduction of the water permeability. A mechanism that involves migration of fine particles and subsequent straining in narrow pore throats that leads to a pore-scale flow diversion was proposed.

The recordings of an increased pressure drop along with the additional production may be evidence for this mechanism (Tang & Morrow, 1999; Al-Sarihi et al., 2018; Akhmetgareev & Khisamov, 2015; Zhang, Xie, & Morrow, 2007; Halim et al., 2015). The additional production was associated with a pH increase of the effluent (Jackson et al., 2016). It was pointed out that pH could have a significant impact on the surface charge of clay particles (Menon & Wasan, 1986; Gu et al., 2003). Depending on the type of clay, its surface potential may increase or decrease with pH, which may consequently reduce the electrostatic forces between the clay particles and the pore walls. Such an effect destabilizes the adsorption of particles and facilities relocation of the fines (Bedrikovetsky et al., 2012).

For carbonaceous rocks, such dynamic mechanisms are rarely reported in the literature. Nonetheless, a number of studies have indicated potential sources of plugging agents. Zahid, Shapiro, & Skauge (2012) reported potential detachment of fines when flooding unconsolidated carbonate cores. Precipitation of salts by mixing of the existing pore water and injection water may also create free particles in the pore space (Puntervold & Austad, 2008). Emulsions, which may be formed spontaneously on the oil-brine contact or promoted by mixed-wet particles (Mokhtari, Ayatollahi, & Fatemi, 2019; Chakravarty, Fosbøl, & Thomsen, 2015a; Chakravarty, Fosbøl, & Thomsen, 2015b), may be another plugging agent. If the droplets are of a similar size to the pore throats, they can be strained and block the flow paths. In the context of the microbial EOR in carbonate rocks, the mechanism of selective plugging of water paths and diversion of the flux was proposed (Halim et al., 2015). But in the field of smart waterflooding, this mechanism has not been sufficiently studied. A possible reason could be overlooking the heterogeneity of the rocks. Heterogeneity has sometimes been attributed as ‘natural variability’ or ‘geological features’ (Zhang & Sarma, 2012; Romanuka et al., 2012), but, to the best of our knowledge, this factor has not been investigated further. Heterogeneity may enlarge the effect of flow diversion, even on the core scale. The comparison between heterogeneous and homogeneous cores under similar flooding procedure has clearly indicated a greater EOR potential for heterogeneous cores (Mohammadkhani et al., 2019; Halim et al., 2015; Hao & Shapiro, 2019). Mathematical modeling of the flooding process with flow diversion triggered by fines migration suggested improved sweep efficiency in heterogeneous reservoirs (Yuan & Shapiro, 2011; Zeinijahromi, Lemon, & Bedrikovetsky, 2011).

In this work, we aim to identify and evaluate the effect of flow diversion in sandstone and chalk cores. The core flooding experiments were performed with specially selected reservoir cores, with different levels of heterogeneity. The flooding in sandstone and chalk cores, heterogeneous and homogeneous, was compared to extract key factors that contribute to the additional recovery. Advanced modeling was employed to reproduce the experimental results and to obtain important parameters that characterize the recovery process.

The paper is organized as follows: Section 2 presents the experimental part of the work, including experimental materials, methods, and results; Section 3 introduces the mathematical model used in this work, the procedures to match with experimental data and the fitted parameters that characterize the process; Section 4 gives a brief discussion of the main observations from this work; Section 5 contains the derived conclusions.

4.2 Experimental

4.2.1 Materials and Methods

4.2.1.1 Oil

Two kinds of oil were used in this work: crude oil from a North American sandstone reservoir, with density 883 kg/m^3, viscosity 21.11 cP, total acid number 0.26 mg KOH/g; and a light crude oil from a

North Sea chalk reservoir, with density 840 kg/m^3, viscosity 4.45 cP, total acid number 0.504 mg KOH/g. All the properties are measured at room conditions.

4.2.1.2 Brine

Two sets of brines were used for the flooding of sandstone and chalk cores separately. The first set involves the original formation water of the sandstone reservoir (FWS); and a modified version of formation water (MFWS) by replacing Ca^{2+} and Mg^{2+} ions with Na^{2+}, meanwhile keeping the ionic strength constant by adjusting the amount of NaCl. The flooding experiments also involve the MFWS with increased pH (pH range from 11.5 to 12.5), which is prepared by titrating the brine with a saturated NaOH solution. Besides, diluted versions of MFWS (5 and 10 times diluted) were prepared by mixing the brine with deionized water. The recipes of FWS and MFWS are given in Table 1.

	Concentration [mg/L]	
Salt	FWS	MFWS
$CaCl_2$	4.15	0
$MgCl_2 \cdot 6H_2O$	5.61	0
KCl	0.018	0.018
NaCl	39.05	50.32
$SrCl_2 \cdot 6H_2O$	0.0015	0.0015
Na_2SO_4	7.25	7.25
$NaHCO_3$	0.201	0.201
TDS [g]	56.28	57.78

Table 1. The recipes of the brines used for flooding experiments with the North American sandstone cores.

The second set of brines involves the formation water from the North Sea chalk reservoir (FWC) and seawater (SW). The recipes of FWC and SW are given in Table 2.

	Concentration [mg/L]	
Salt	FWC	SW
NaCl	69.013	25.414
KCl	0.475	0.763
$NaHCO_3$	-	0.089
Na_2SO_4	0.429	2.957
$CaCl_2 \cdot 2H_2O$	5.378	1.504
$MgCl_2 \cdot 6H_2O$	4.964	9.151
$SrCl_2 \cdot 6H_2O$	0.426	0.061
$BaCl_2 \cdot 2H_2O$	0.001	-
TDS [g]	80.675	30.939
Ionic strength	1.384	0.675

Table 2. Recipes of the brines used for flooding experiments of the North Sea chalk cores.

4.2.1.3 Cores

Two cores from a North American sandstone (SS) reservoir and two cores from a North Sea chalk (CK) reservoir were used in this work. The porosity and permeability of the cores were measured by nitrogen, the measured permeability was corrected by the 5 point Klinkenberg method. The measured properties of the cores are given in Table 3. The sandstone cores have a certain content of clay (most probably kaolinite). The chalk cores consist of highly pure biogenic calcium carbonate, mostly, skeletons of coccoliths.

Core no.	Length [mm]	Diameter [mm]	Dry weight [g]	Porosity [%]	Permeability [mD]
SS1	53.0	38.2	122.96	22.7	302
SS2	61.1	38.1	142.71	22.5	332
CK1	72.8	37.4	146.3	30.5	0.31
CK2	79.9	37.8	169.1	30.4	0.52

Table 3. The dimensions and petrophysical properties of the cores.

The cores were selected according to their heterogeneity. Similar to our previous work (Hao & Shapiro, 2019), the selection was based on the x-ray computed tomography (CT) images of the dry samples. Each pair of cores consists one heterogeneous and one homogeneous core. Since heterogeneity of the rock is difficult to quantify, in this work “heterogeneous” and “homogeneous” are considered as relative terms. We choose cores that are visibly distinct from each other so that they produce qualitatively different flow characteristics during the two-phase displacement. The CT images of the cores are shown in Figure 2. Both of the sandstone cores have some high density strips along the core. These strips appear as dark lines (see Figure 1), which is most probably the clay (kaolinite) content of the core.

Figure 1. Images showing the visual structure of the heterogeneity (the dark strips on the sandstone core). A preliminary observation of the dark matter suggests that they are most likely to be kaolinite, deposited in the core.

SS1 shows some additional variation close to the surface of the core. Meanwhile, for SS2 the heterogeneity is rather uniform. In terms of the chalk cores, it is evident that CK1 is more heterogeneous than CK2. The dense inclusions and fractures in CK1 are mainly located in the center section of the core. Meanwhile, such characteristics do not show up in CK2.

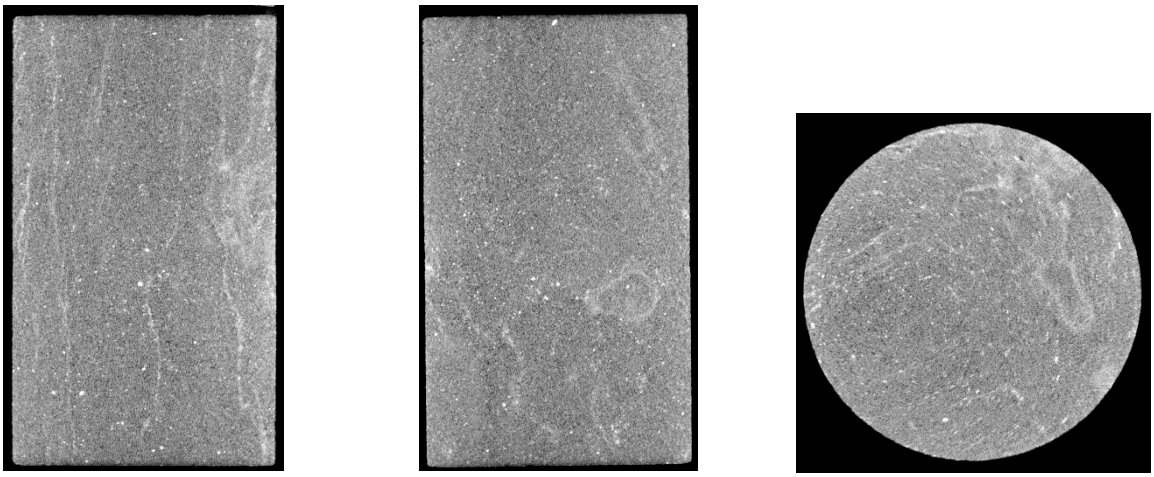

(a) SS1

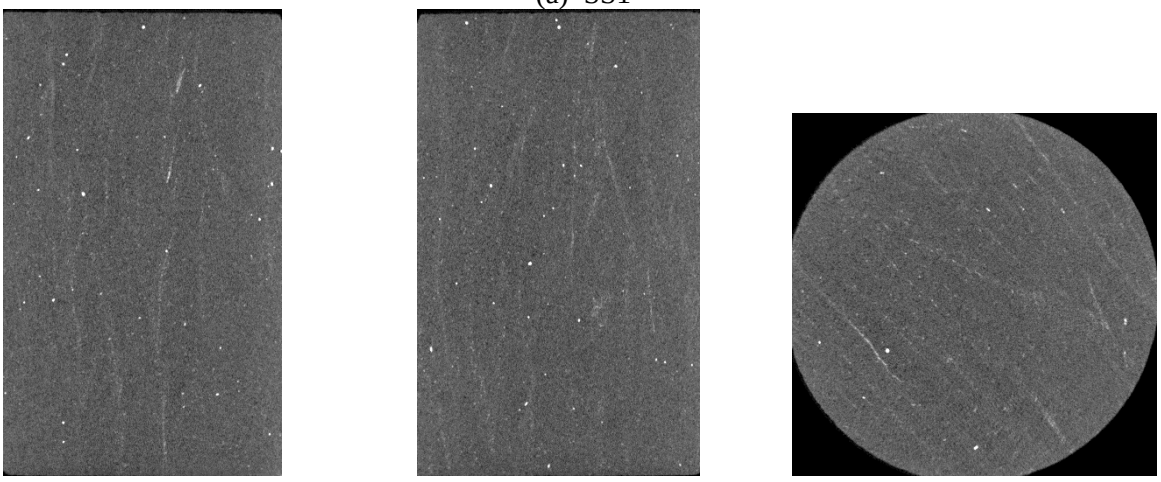

(b) SS2

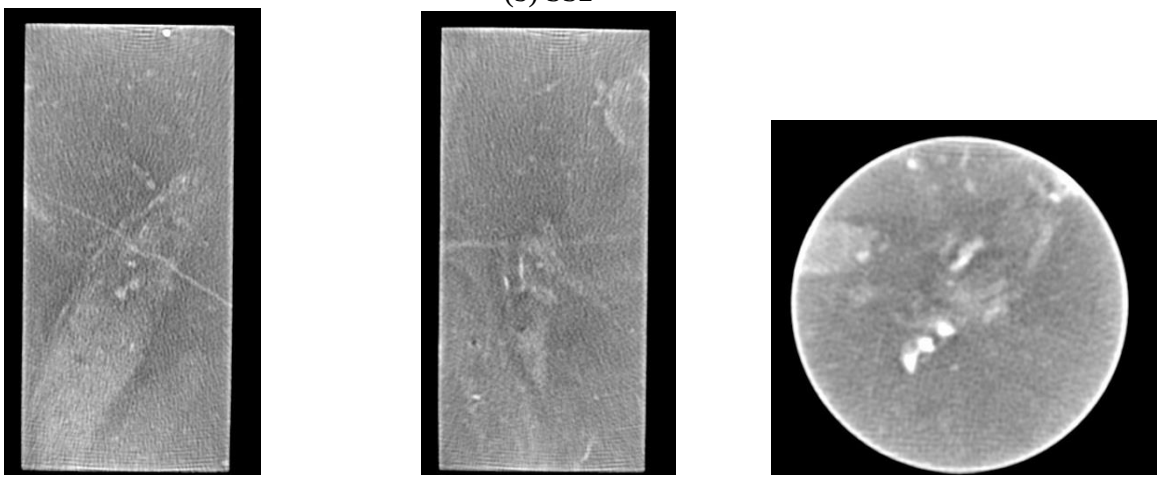

(c) CK1

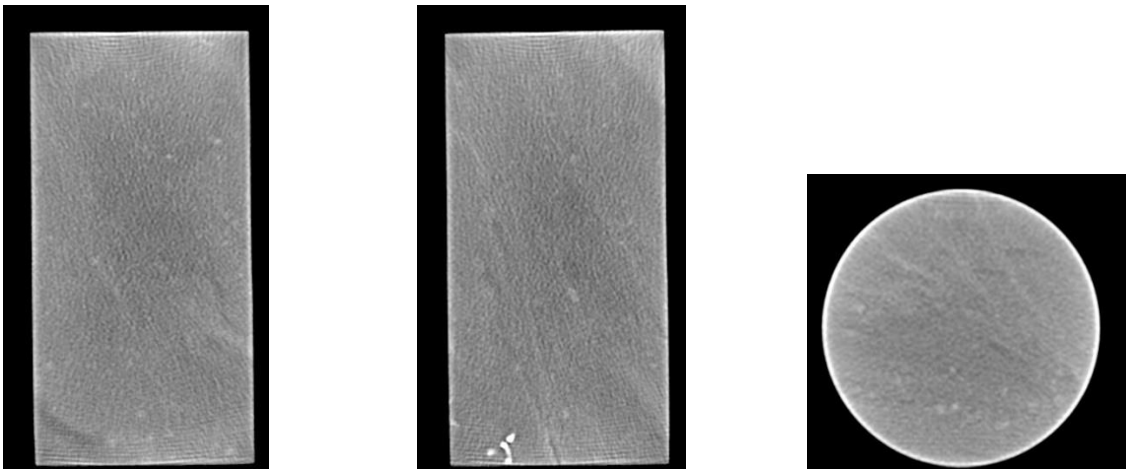

(d) CK2

Figure 2. CT scanning images of the dry cores. SS1 includes more irregular dense inclusions than SS2, close to the surface of the core. Compared with CK2, CK1 shows distinct variations of density together with some fractures in the middle section of the core. These features made CK1 to be considered as a heterogeneous core, while CK2 is homogeneous.

4.2.1.4 Emulsification tests

Spontaneous emulsification of oil when in contact with specific brines was reported in the literature (Mahzari & Sohrabi, 2014; Emadi & Sohrabi, 2013; Mokhtari, Ayatollahi, & Fatemi, 2019). In combination with the heterogeneous character of a core, it was proposed as a potential mechanism for additional recovery in smart waterflooding (Mohammadkhani et al., 2019). In this work, the emulsification tests were performed with the oils and brines to detect the potential interfacial interactions at the oil-brine contacts. 10 ml of brine and oil were added into a 20 ml sample bottle. The fluids were added carefully to avoid mixing. Then the samples were placed in an oven under reservoir temperatures: 40°C and 60°C for the liquids from sandstone and chalk reservoirs, respectively. Two parallel samples were prepared for each pair of oil and brine. Pictures of the oil-water interface were taken every hour.

4.2.1.5 Core flooding procedure

The cores were cleaned by alternative injection of toluene and methanol to remove the residual hydrocarbons and precipitated salts. The cleaned cores were dried in the oven at 60°C until a constant mass was reached. Porosity and permeability of the cleaned dry cores were measured by the nitrogen injection. Then the cores were fully saturated by formation water (FW) under vacuum. The saturation was checked by comparing the porosity calculated by the weight difference of the dry and saturated core, with the porosity measured by nitrogen. Next, the saturated cores were assembled in a Hassler type core holder and connected to the flooding setup. Approximately five porous volumes (PVs) of formation water were injected to remove the air that is possibly trapped in the core. Further, crude oil was injected to establish initial saturations of water and oil. The injection continued until no more water was produced from the core. The injection rate was adjusted according to the petrophysical properties of the cores to ensure the flow velocity of 1 ft/day. Then the core was aged for two weeks. The flooding was performed in a setup similar to the one used in our previous work (Hao & Shapiro, 2019), with the only difference that a heating jacket surrounding the core holder was used instead of the oven.

For the sandstone cores, the experimental temperature was 40°C. The overburden pressure of 20 bar was applied; meanwhile, there was no backpressure, and the outlet of the core was directly in contact with

atmospheric pressure. For the chalk cores, the experiments were performed at 60°C. The backpressure of 190 bar was applied, and the overburden pressure was kept at 30 bar above the inlet pressure.

After aging, several brines were flooded sequentially through the cores to produce the oil. Formation brines, FWS and FWC, were injected for secondary recovery of the sandstone and chalk cores, respectively. Afterward, for the sandstone cores, the modified formation water (MFWS), the MFWS with increased pH, and 5 and 10 times diluted MFWS were sequentially flooded through the cores. Each brine was injected for at least 5 PVs to give sufficient time for the chemical/physio-chemical interactions. For the chalk cores, a NaOH solution of pH 12.9 was injected in tertiary mode.

In order to find the role of clay particles in the recovery process, each of the sandstone cores was flooded twice, with a similar injection scheme. A thorough cleaning procedure was performed between the experiments. First, toluene and methanol were injected to clean up the residual oil and brine from the first experiment, followed by injection of NaOH solution with pH 12.6. The purpose is to trigger the potential physio-chemical processes that could mobilize and remove the clay particles from the core so that the impact of such particles can be reduced/avoided in the subsequent experiment. After that, methanol was injected again to clean up the NaOH solution. Then the cleaned cores were dried and the same saturation and the flooding procedures were repeated.

The flooding effluent was collected in graduated test tubes with fractions of 1/7 to 1/3 PV to obtain an accurate track of the recovery process. The volumes of the produced oil in each tube were measured to calculate the saturation and recovery. For large amounts of oil (more than 0.1 ml), the volumes were read visually from the graduated test tubes. For smaller volumes of oil, which appeared as droplets or a thin film on top of the water, the volumes were measured in two ways. For the effluent from sandstone cores, the weight method was applied. A syringe was used to extract most of the water from the tube, leaving a small volume of water (0.1 – 0.3 ml) with the oil in it. Then the mixture was weighed by an analytical balance. Knowing the densities of water and oil, the volume of oil could be subsequently determined. For the effluent from the chalk cores, the oil was first dissolved in 3 ml of toluene, then the optical density (OD) of the oil-toluene solution measured at the UV wavelength of 750 nm. The measured OD was compared with a standard curve made by the same method with known amounts of oil. The method was described in the literature (Katika, et al., 2016) and applied in our previous work as well (Hao & Shapiro, 2019).

4.2.2 Experimental Results and Analysis

4.2.2.1 Emulsification tests

The compatibility tests with oil and brines for the sandstone cores lasted for 52 hours. The only visible variation on the interface was made with the NaOH titrated MFWS, which has a pH of 12.7. The earliest observation was recorded after two hours of mixing. It can be seen that the oil-brine contact became unstable: fluctuations and separate droplets of oil appeared near the interface. Other brines, including FWS, MFWS and diluted MFWS, did not show any visible changes at the interface. Figure 3 shows the result of the titrated MFWS, for comparison purposes, the result of FWS is also presented in representation of the rest of the brines.

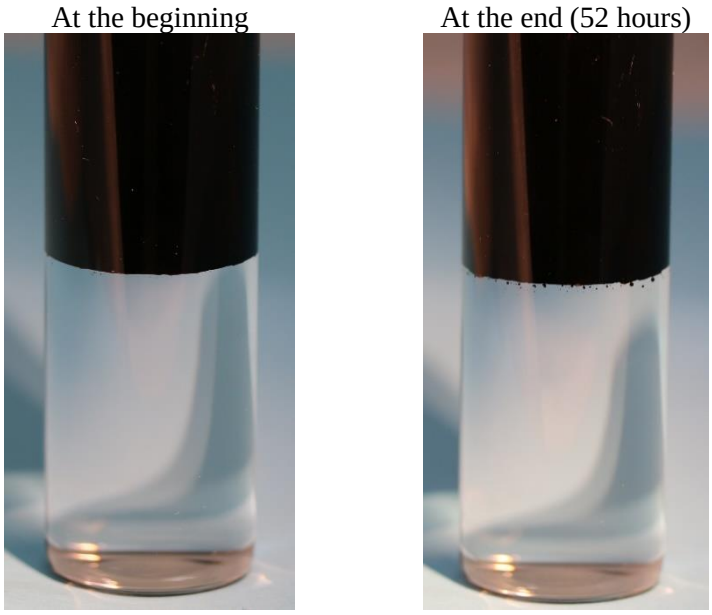

(a) NaOH titrated MFWS

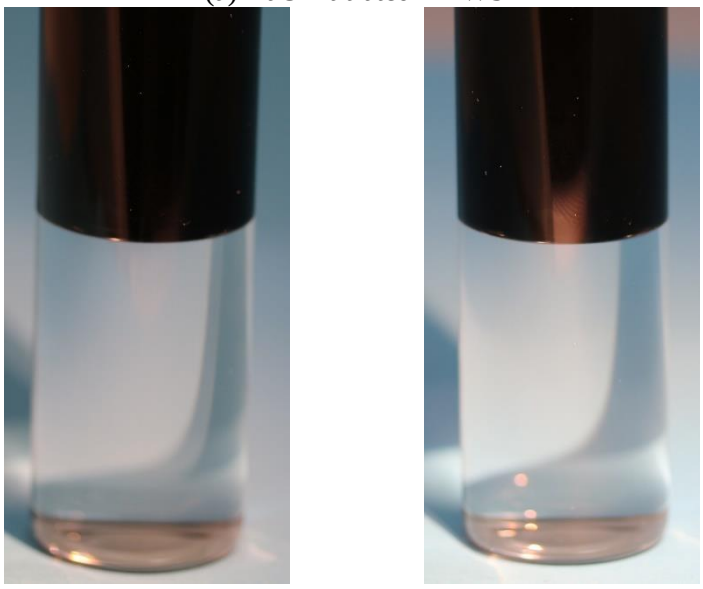

(b) FWS

Figure 3. Results of the emulsification tests for the North American oil and brines. Only the NaOH titrated brine resulted in instability of the oil-brine interface (a), other brines had stable interface with oil throughout the experimental period.

A similar test was performed with the North Sea oil and brines as well. The formation water (FWC), the seawater (SW), the diluted SW (5 times and 20 times diluted, termed as 5DSW and 20DSW), and the deionized water (DW), together with NaOH titrated 20DSW and DW, whose pH is 12.7, were put in contact with oil. Pictures of the interface were taken hourly in the first 4 hours and overnight (16 hours later). Figure 4 presents the images of the interface at the beginning and the end of the experiment.

At the beginning

At the end (16 hours)

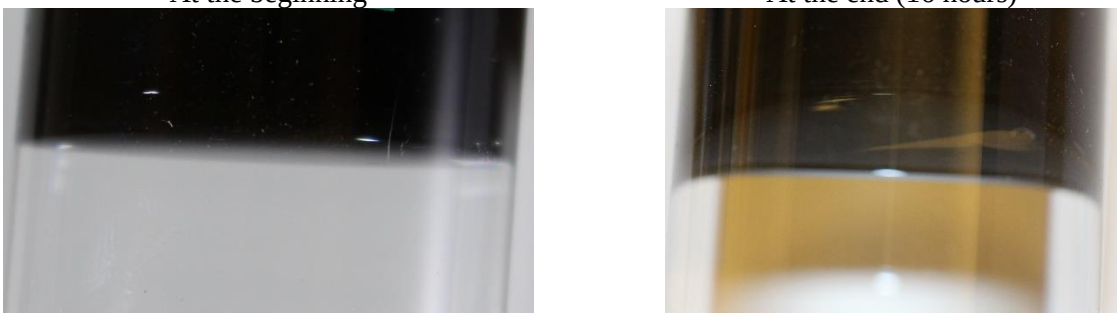

(a) FWC

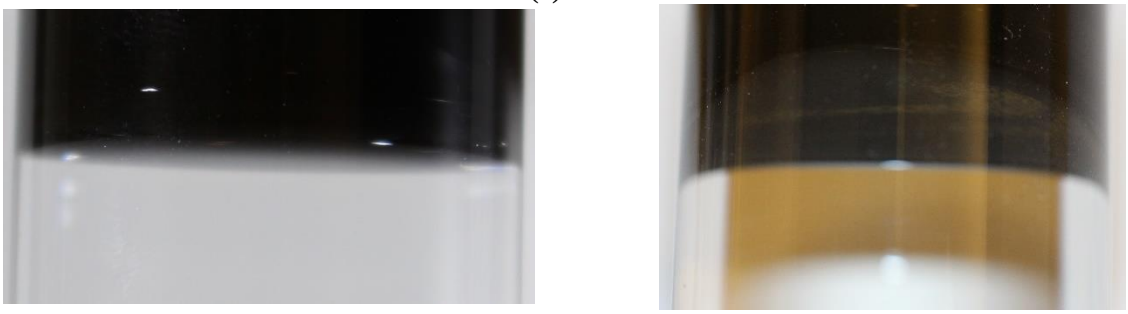

(b) SW

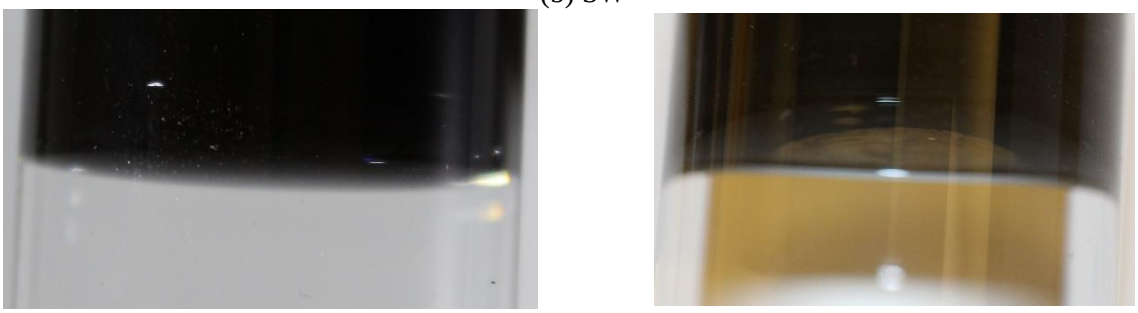

(c) 5DSW

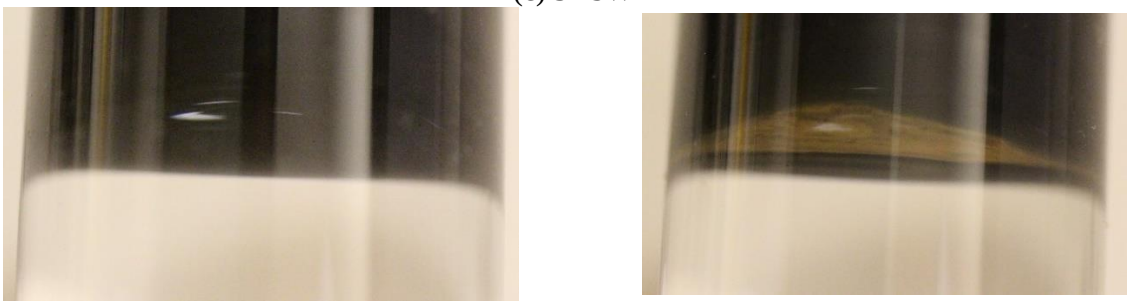

(d) 20DSW

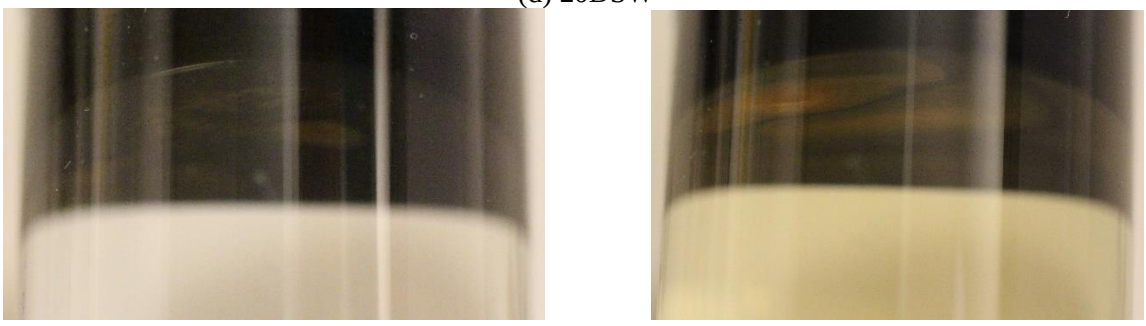

(e) 20DSW at increased pH

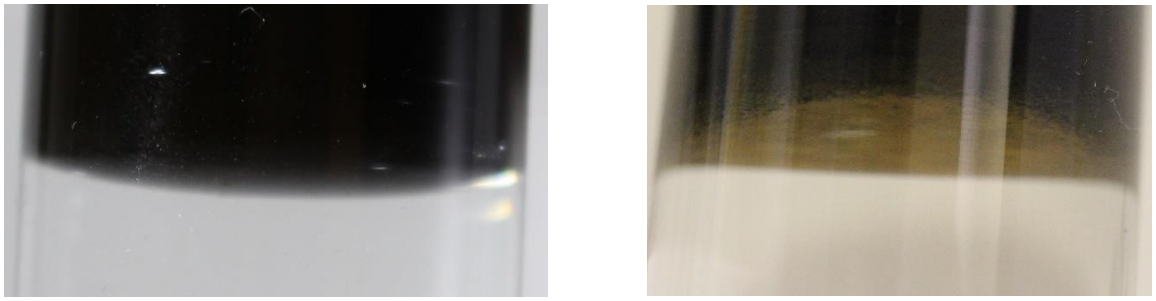

(f) DW

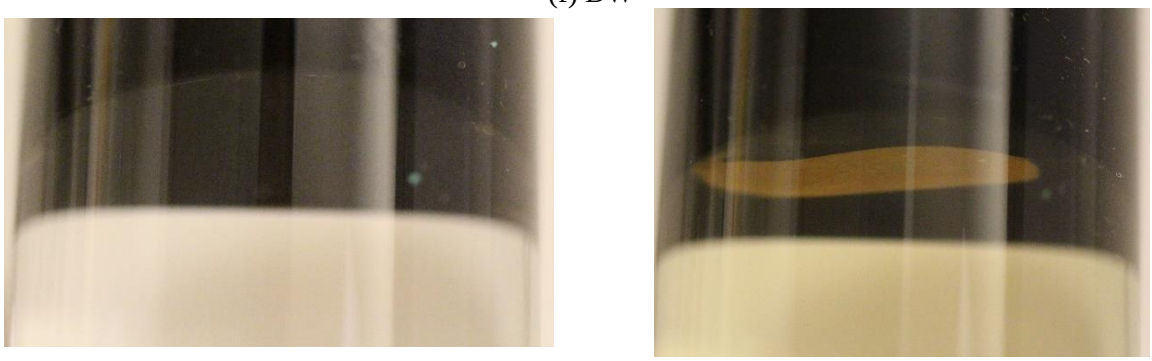

(g) DW at increased pH

Figure 4. Results of the emulsification test with the North Sea oil and brines. Emulsions can be found in all the samples after 16 hours. The least amount of emulsion appears in the samples containing FWC and SW. Emulsification increases with the decrease of the salinity, while pH does not have a significant impact.

It can be seen that after 16 hours the emulsions are formed at the interface for all the tested brines. The least amount of emulsions was found with the FWC and the SW, which have the highest salinity. Combining the results from 5DSW, 20DSW, and DW, it can be qualitatively, but clearly, observed that a decrease in salinity leads to an increase in the formation of emulsions at the oil-brine contact. By comparison of Figure 4(d) with 4(e), and Figure 4(f) with 4(g), it may be found that increasing the pH of the brine does not significantly affect the amount of emulsion formed at the interface. Given this information, the NaOH titrated DW, which is basically a NaOH solution at pH 12.7, was further tested in the core flooding experiment.

The observed spontaneous emulsification at the oil-brine interface is in line with the reported findings in the literature (Mokhtari, Ayatollahi, & Fatemi, 2019; Mohammadkhani et al., 2019; Emadi & Sohrabi, 2013; Mahzari & Sohrabi, 2014). Emulsions can be beneficial in the recovery process. When the sizes of the emulsion droplets are similar to the pore sizes, they may plug the flow paths and divert the flow to other places, so that the displacement efficiency is improved. However, such hypothetical mechanisms need further experimental validation.

4.2.2.2 Core flooding experiments

Sandstone cores

Figure 5(a) (b) shows the result of the first flooding experiment with core SS1. The initial saturations of water and oil are 57.1% and 42.9%, respectively. The high water saturation indicates that the core is probably preferentially water wet. The secondary flooding by FWS resulted in a recovery of only 18.23%. Flooding by the modified formation water (MFWS) and diluted versions of MFWS did not produce

additional oil. However, injection of MFWS with increased pH at 11.55 (by gently titrating saturated NaOH solution) produced 2.38% more oil after 6 PVI, which corresponds to 26 hours of injection.

Figure 5(b) shows the profiles of differential pressure (dP) across the core and the effluent pH throughout the experiment. There is a clear increase in dP between 15 and 17 PVI, before the appearance of the additional recovery. Then the pressure difference dropped down after the oil was produced. The pH profile shows a gradual increase and decrease. This is probably due to the high stagnant water saturation: mixing of connate water and injected brine can result in a more dispersed pH front. It should be mentioned that the increase of differential pressure occurred slightly behind the increase of pH, which indicates that the physical process behind the recovery is not instantaneous, but is time-dependent.

Figures 5(c) (d) shows the result of the second flooding experiment with the core SS1. Overall, the core behaved similarly to the first experiment: an additional recovery of 1.42% was achieved only by MFWS at increased pH, which is less than the first experiment. The behavior of pH and dP in connection with additional production is similar to the first experiment. In the second flooding of SS1, the initial saturations are 49.8% for water and 50.2% for oil. The increase of oil saturation compared to the first experiments is probably suggesting a shift of the wettability state of the core. The secondary recovery by injection of formation brine was also higher than in the first experiment, reaching 21.31%.

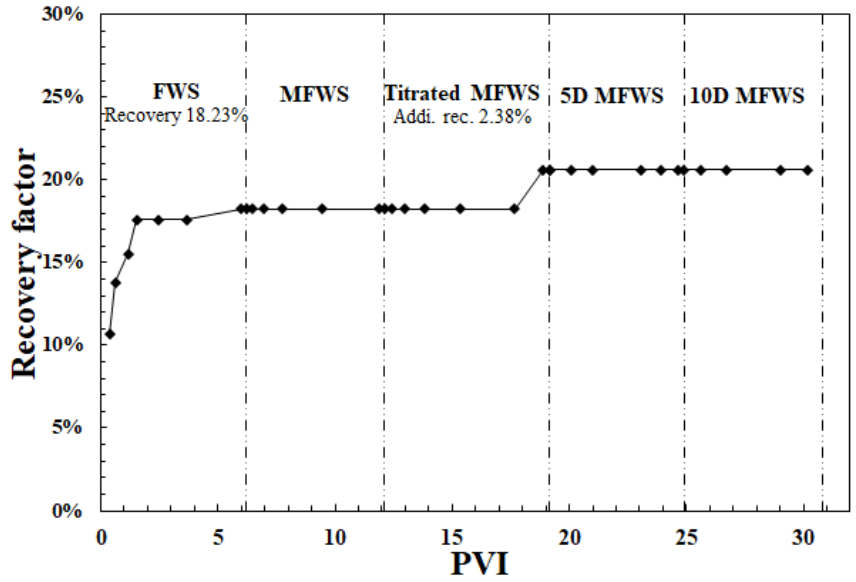

(a) Recovery from the first flooding of SS1

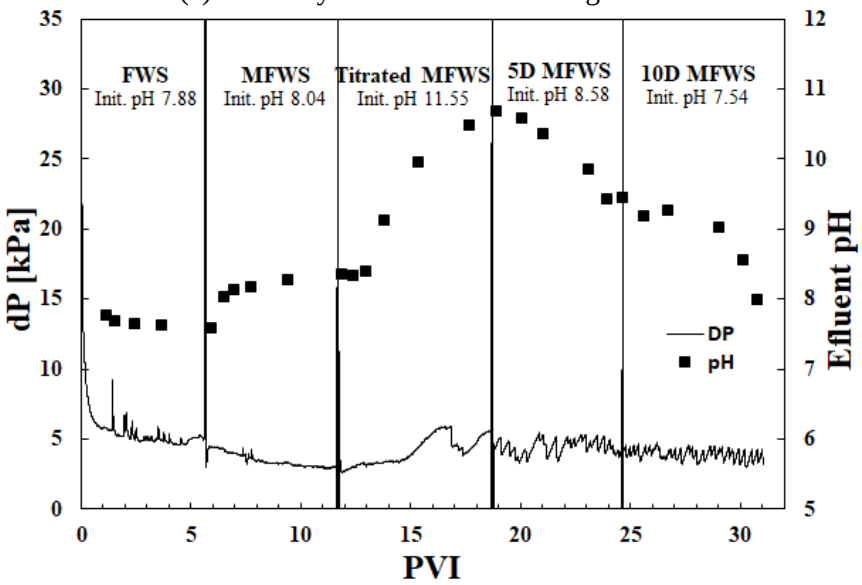

(b) dP and effluent pH of SS1 from the first flooding

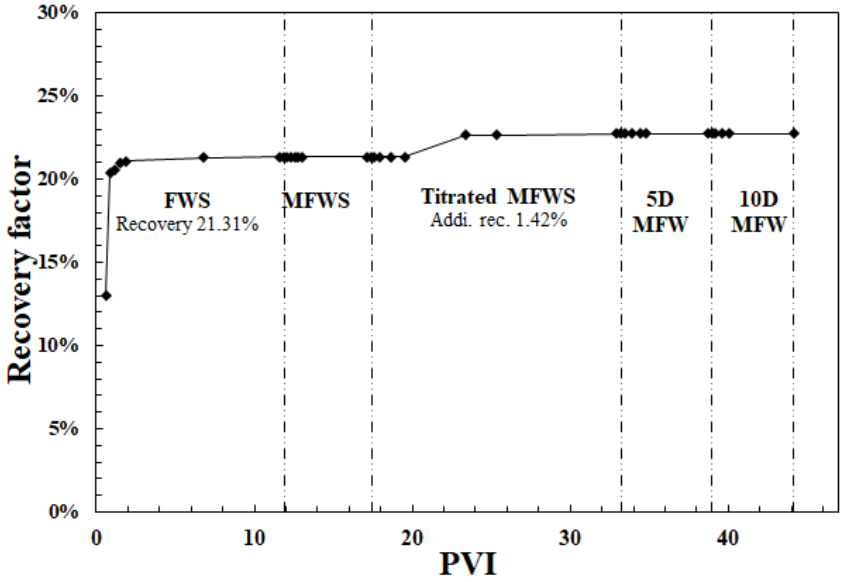

(c) Recovery from the second flooding of SS1

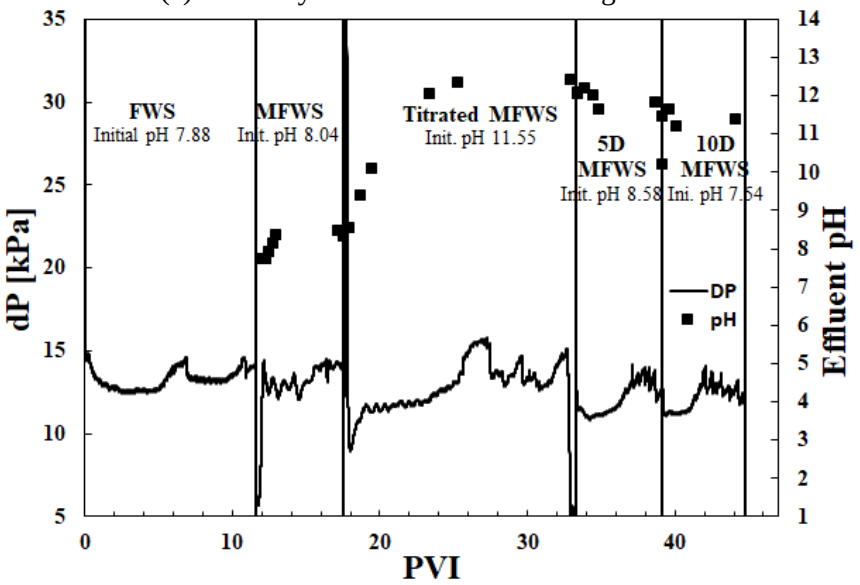

(d) dP and effluent pH of SS1 from the second flooding

Figure 5. The two flooding results of core SS1. (a) (b) and (c) (d) are the recovery plots and pH and dP profiles of the first and second flooding experiment, respectively.

Figures 6(a), (b) show the result of the first flooding experiment with SS2. The initial saturations of water and oil are 39.5% and 60.5%, respectively. 34.55% of oil was produced by injection of formation brine at the secondary recovery stage. Subsequent flooding by the various brines barely increased the recovery factor. Unlike in SS1, the increase of pH did not lead to significant additional production. It should be mentioned that, due to the malfunction of a dP transducer, the measured dP does not reflect the flow condition in the core.

Figures 6(c), (d) show the result of the second flooding experiment with the SS2. The initial saturations were 46.8% for water and 54.2% for oil. The recovery by waterflooding was 42.68%, which is much higher than in the first experiment. The injection of the MFWS with the increased pH was prolonged in this experiment; a total of 10 PVs were injected, corresponding to more than 2 days. Some variations of dP were detected at the later stage of the experiment, which may be an indication of the fluid redistribution in the core. However, there was still no significant oil production during the tertiary stage.

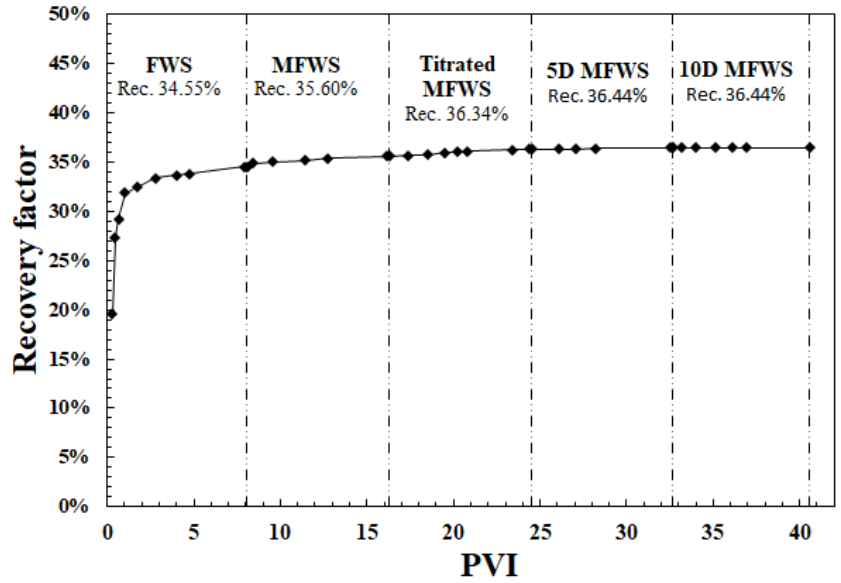

(a) Recovery from the first flooding of SS2

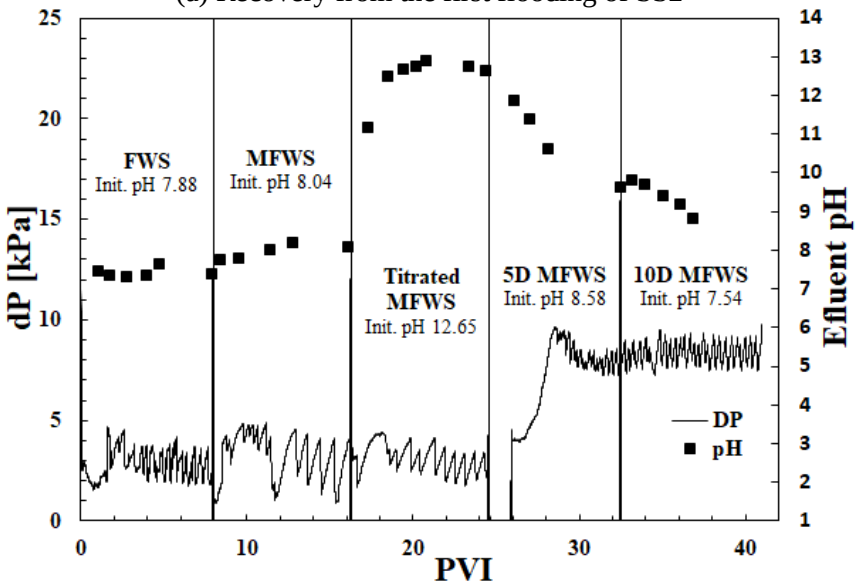

(b) dP and effluent pH of SS2 from the first flooding

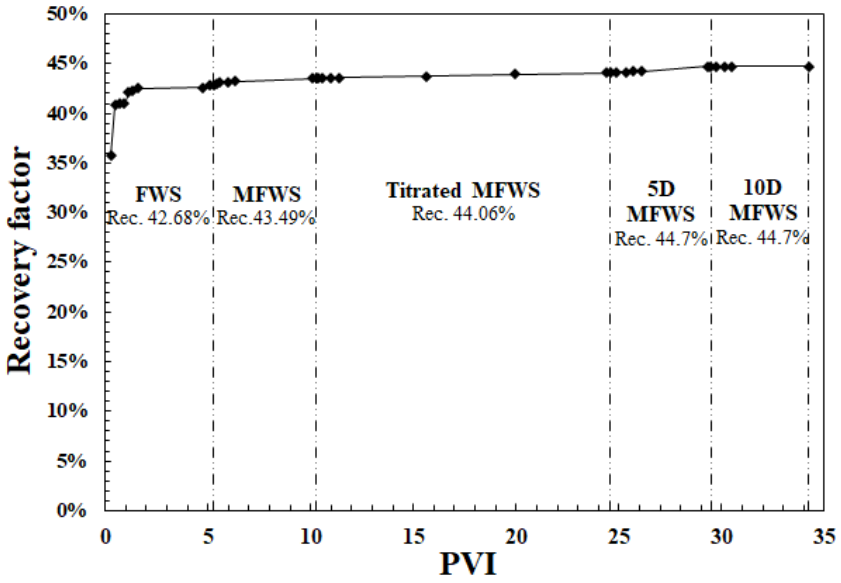

(c) Recovery from the second flooding of SS2

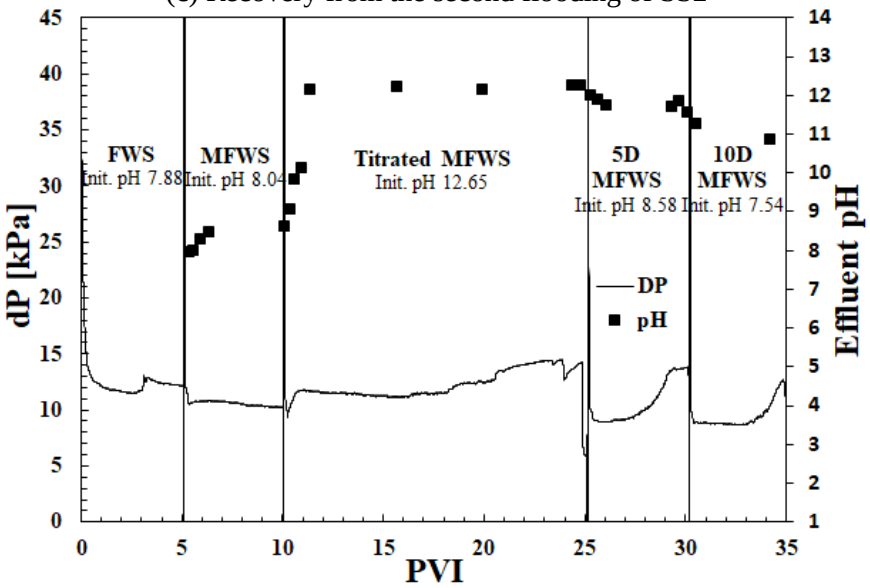

(d) dP and effluent pH of SS2 from the second flooding

Figure 6. The two flooding results of core SS2. (a) (b) and (c) (d) are the recovery plots and pH and dP profiles of the first and second flooding experiment, respectively.

Chalk cores

Figures 7(a), (b) show the flooding results for the heterogeneous core CK1. The initial saturations are 26.3% for water and 73.7% for oil. At the secondary stage, the recovery reached 70.3% by injection of the formation brine. Subsequent injection of NaOH solution with pH 12.95 produced 2.43% of additional oil. The production was delayed by 1.94 PVI after switching the injection water, which indicates that the additional production was not just a continuation of the secondary flooding. Increasing the pH of the injection brine resulted in a consistent increase of dP, with a higher rate at the first 2 PVI, followed by an exponential-like trend. This means that the flow of water experienced additional resistance. The detailed analysis of this observation is given later in this section.

Figures 8(c), (d) show the flooding results for the homogeneous chalk core, CK2. Initial saturations of water and oil are 25.1% and 74.9%, respectively. The secondary recovery is 64.6%, less than that of CK1. The dP profile behaved very similar to CK1. However, only a marginal amount of oil was produced at the tertiary stage (1.2%). Unlike in CK1, the production did not appear as a slug of oil, but as discrete droplets throughout the tertiary flooding.

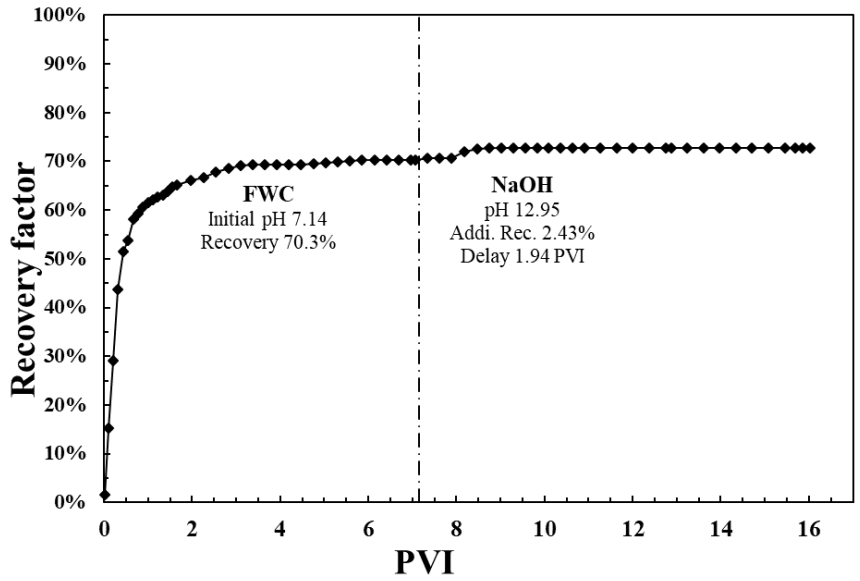

(a) Recovery from CK1

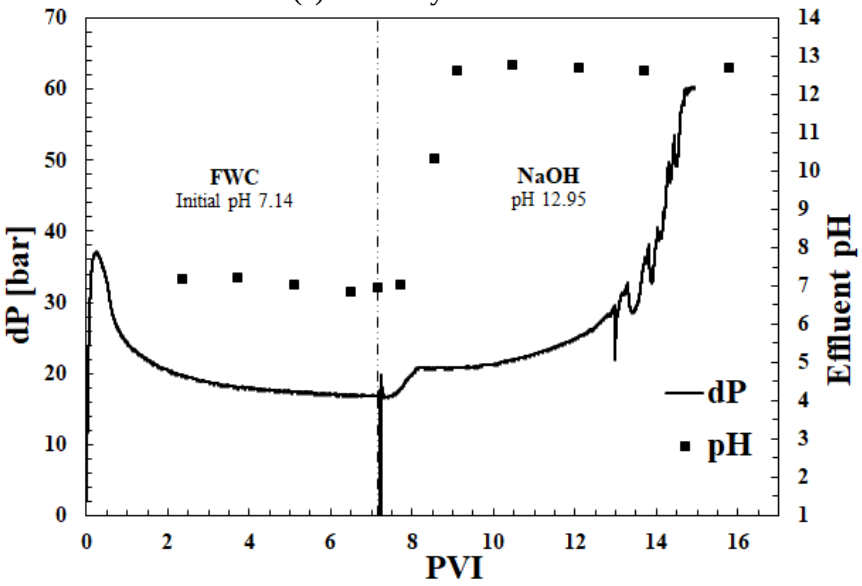

(b) dP and pH profile from CK1

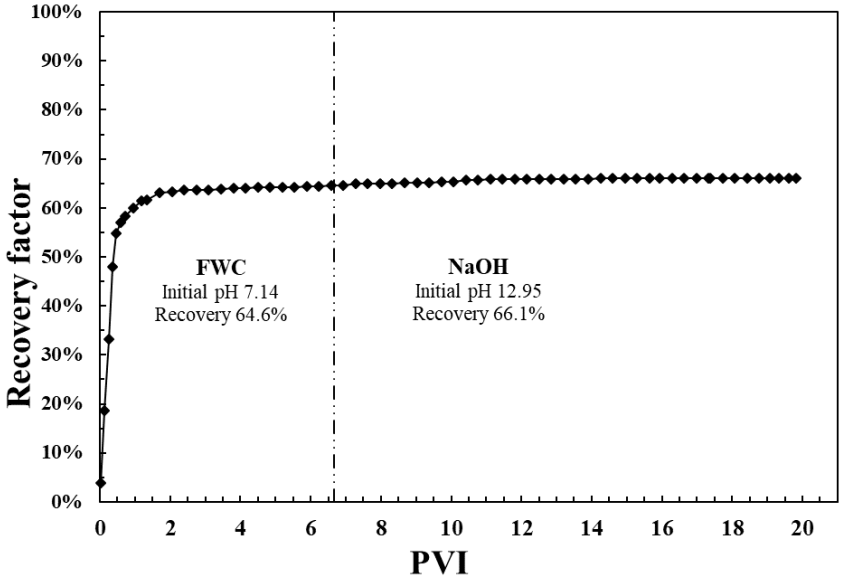

(c) Recovery from CK2

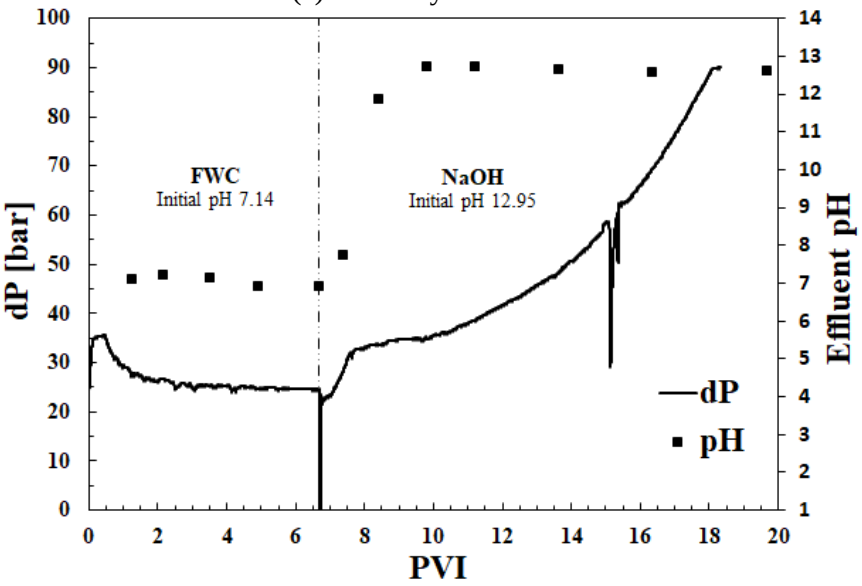

(d) dP and pH profile from CK2

Figure 7. The two flooding results of core CK1 and CK2. (a) (b) and (c) (d) are the recovery plots and pH and dP profiles of CK1 and CK2, respectively.

For both experiments, it was observed that the effluent became cloudy after switching the injection brine. The cloudy effluent came 1.2 and 1.7 PVI for CK1 and CK2 after switching injection brine, respectively. In addition, the additional oil produced from CK1 appeared to be 'dirty' and sluggish, which indicates that the oil was probably contaminated or emulsified. Figure 8 illustrates the above observations. It was also noticed that mixing of formation brine (FWC) with the NaOH solution resulted in precipitation of salts. A PhreeqC simulation by mixing equal volume of the solutions indicates that the precipitation consists of $Ca(OH)_2$ and $Mg(OH)_2$.

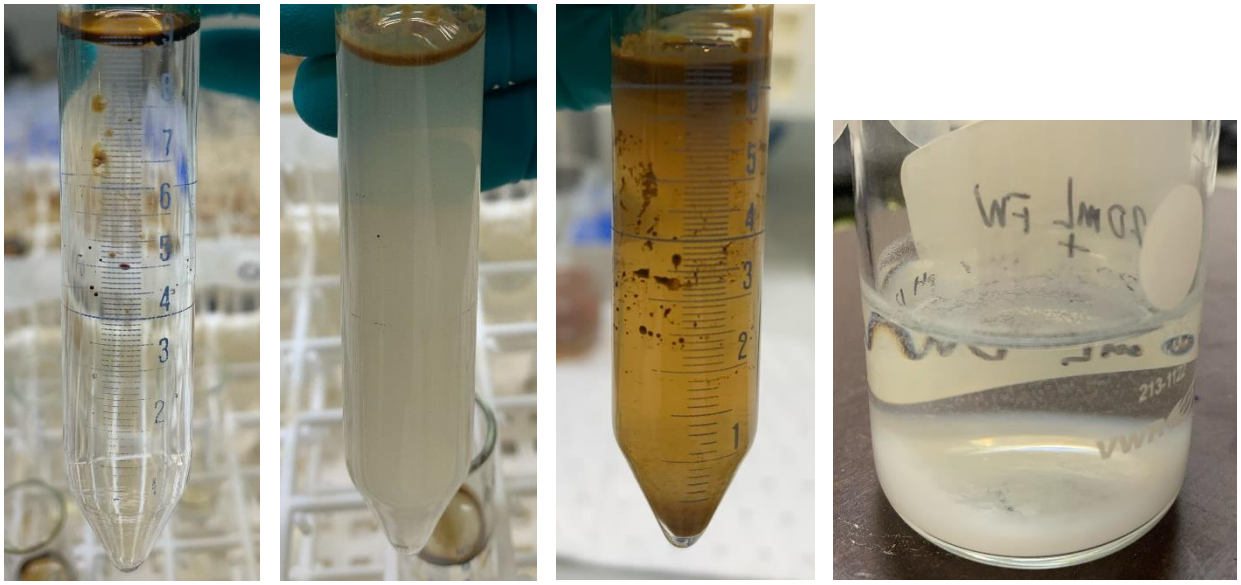

(a) effluent in secondary recovery

(b) effluent in tertiary recovery

(c) additional recovery from CK1: oil on top and water below

(d) precipitation by mixing equal volume of FWC and NaOH solution

Figure 8. The clear water effluent at the secondary stage (a), and the cloudy effluent after switching to high pH brine (b). (c) shows the vial that contains the additional oil along with water produced from CK1. (d) the white precipitation by mixing equal volume of formation brine and the injected NaOH solution.

In order to figure out the substances in the cloudy effluent and sluggish oil, the samples were observed under an optical microscope. Images of the samples were taken by a camera mounted on top of the microscope. The microscope magnifications are 20 and 40 times. The camera also has a built-in magnification of 1.6 times, so the images are 32 or 64 times magnified. Figure 9 shows the images of the samples under the microscope.

Figures 9(a), (b) are the images of the cloudy effluent from tertiary flooding. Water is the continuous phase in these images. It can be seen from Figure 9(a) that there are some oil droplets deposited on the surface of the glass substrate, and some of them have solid particles adsorbed on the surface. Deeper in the bulk liquid (Figure 9(b)), smaller oil drops and solid particles can be observed. Figures 9(c), (d) show the water effluent along with the additionally produced oil. On the glass surface (Figure 9(c)), the deposited oil droplets are larger than the droplets in Figure 9(a). The "dotted" surfaces of the large oil drops indicate adsorption of particles and attachment of the small oil droplets. The particles and the small droplets may also be observed inside the bulk liquid (Figure 9(c)). The sizes of these particles/droplets tend to fall in the range of a few micrometers. This is comparable to the pore sizes in chalk. Figures 9(e), (f) show the additionally produced oil at the two magnifications. Oil is the continuous phase in the images. Large droplets of water can be clearly observed in the oil, along with the adsorbed smaller water

droplets and solid particles on the droplet surfaces. Small droplets of water and particles can also be seen in the bulk oil phase.

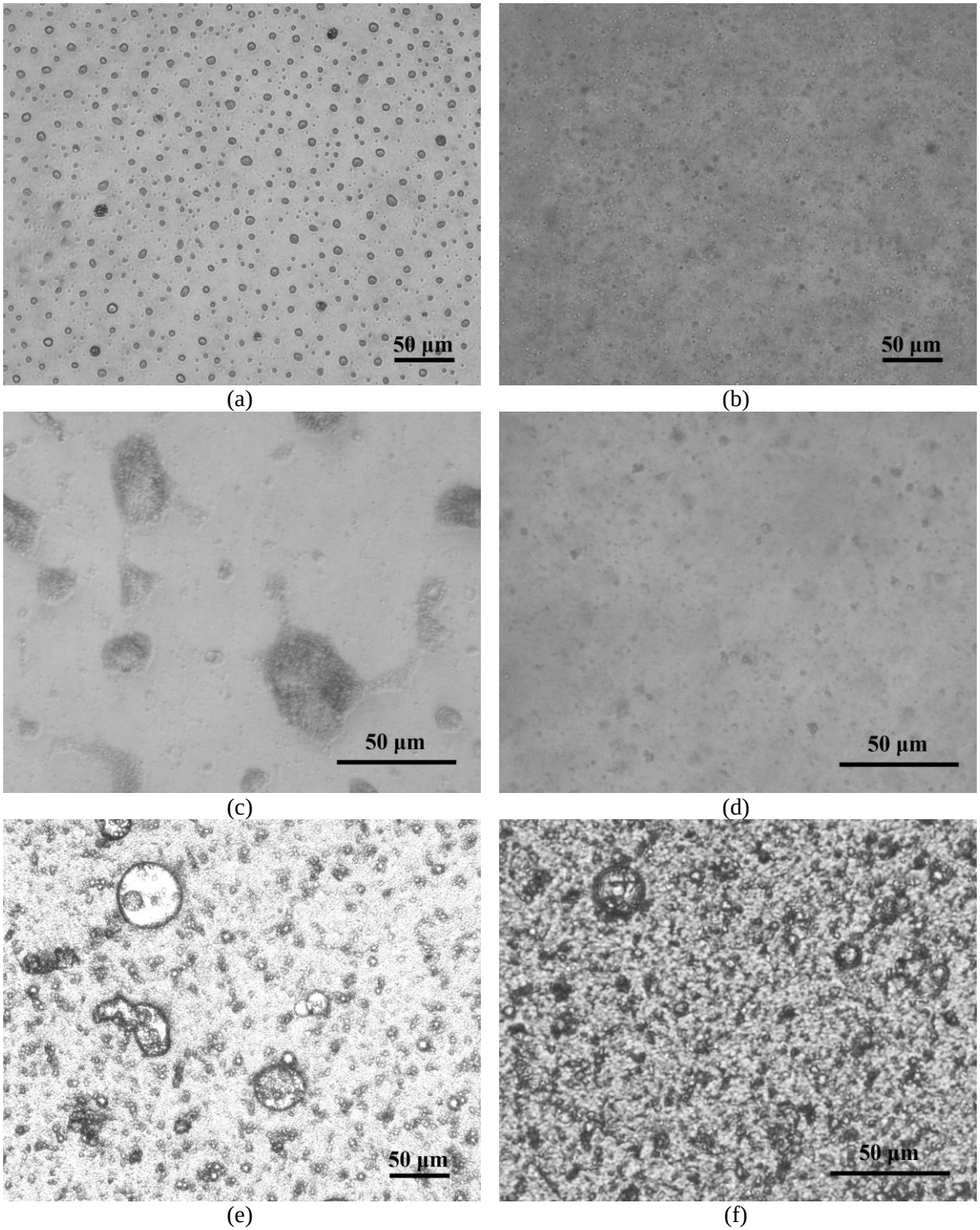

(a) (b) (c) (d) (e) (f)

Figure 9. Microscopic images of (a) deposited droplets/particles on the glass plate from the cloudy water effluent, 32×; (b) further inside the cloudy effluent, 32×; (c) deposited droplets/particles on the glass plate

from the water effluent with additional oil, 64×; (d) inside the water effluent under additional oil, 64×; (e) (f) additionally produced oil, 32× and 64×.

4.2.2.3 Analysis of the flooding experiments

Multiple studies report that mobile clay particles in the sandstone play an important role during smart waterflooding. Depending on the nature of the clay, the particles may be released from rock surfaces due to the weakened electrostatic attraction force by reduced salinity (Bedrikovetsky et al., 2011; Bedrikovetsky et al., 2012); alteration of pH (Menon & Wasan, 1986; Liu et al., 2002; Zhu, Liu, et al., 2011); or surface ion exchange (Doust, Puntervold, & Austad, 2011). These particles may contribute to recovery through the flow diversion mechanism by selectively plugging the water paths (Hussain et al., 2013; Zeinijahromi, Machado, & Bedrikovetsky, 2011; Zeinijahromi et al., 2015). On the other hand, emulsions, as observed in the effluent from chalk cores, could trigger the same mechanism, if the sizes of the droplets are comparable to the pore sizes (Mohammadkhani et al., 2019).

In this work, we observe a systematic difference in the behavior of homogeneous and heterogeneous cores under similar flooding procedures. For both sandstone and chalk, increasing the pH of the injection brine produces more oil from the heterogeneous than homogeneous cores. For the sandstone cores, additional production from the heterogeneous core decreased in the second flooding test. This is consistent with the cyclic flooding tests reported by Tang & Morrow, 1999. A reason may be that the clay content in the cores was reduced due to the previous flooding and cleaning procedures. The pressure variation associated with additional production supports the hypothesis of flow diversion: when partial plugging of a core occurs, the permeability decreases, and higher pressure is needed to displace the oil.

In the experiments with chalk cores, additional oil was produced along with large amounts of emulsions and solid particles. As shown in Figure 8(c) and Figure 9(e)(f), the largest production was obtained with the most significant emulsification. This makes the flow diversion mechanism highly plausible in this case. A rapid increase of the pressure difference in the first 2 PVI after switching the brine correlates with the mixing of formation brine with NaOH solution. Precipitation due to the brine incompatibility may block the pores. It should be mentioned that the additional oil was produced after the initial rapid increase of dP. Although a much higher dP was achieved later on, it did not correspond to additional oil production. Apparently, plugging continued in the waterflooded zones, but the diversion had already happened, and no more oil production potential remained in the core.

4.3 Modeling of experimental results

4.3.1 Formulation of the model

The previous experimental observations suggest a recovery mechanism related to the heterogeneity of the cores and flow diversion by plugging of the water paths. In this section, we employ the model developed by Yuan & Shapiro (2011), which incorporates the concepts of fines relocation (Bedrikovetsky, Siqueira, Furtado, & Souza, 2011) and waterflooding in a vertically communicating stratified porous media (Yortsos, 1995; Zhang, Shapiro, & Stenby, 2011). A major effect of fines relocation is in the reduction of the relative permeability for water; the formation of the emulsions produces a similar effect. The model is used to verify the flow diversion mechanism and its effect on additional production during smart waterflooding.

The model represents two essential ideas. First, the injection of modified brine disturbs the torque balance of electrostatic attraction force (DLVO), gravity and hydrodynamic drag forces exerted on the fine particles that are sitting on the pore wall. This results in the particles being released from the surface and

entering the flow of water. They immediately get re-captured by the pore throats and reduce the mobility of water in their original flow channels. The concentration of detached particles can be determined by the function of critical concentration (Bedrikovetsky et al., 2011). When the critical value is lower than the actual concentration of attached particles, an excessive amount of particles are released. The contribution of released particles on the reduced mobility of water is determined by a dimensionless parameter named the formation damage coefficient (β).

On the other hand, the model considers two-phase flow in a porous media that has a layer-cake structure. The heterogeneity of the porous media is introduced by the different permeabilities and thickness of each layer. The most important assumption of the model is the perfect vertical communication between the layers, i.e. no pressure gradient in the vertical direction (Zhang, Shapiro, & Stenby, 2011). This assumption allows the fluids to communicate freely and instantly between the layers. Once the mobilities of water are different in the neighboring layers, a vertical crossflow can occur. Water is preferentially diverted into the 'easier' layers and displace the oil from there. The combination of these two concepts allows us to evaluate the impact of flow diversion on displacement efficiency.

Evidently, the model reflects only very approximately the realistic geometry and heterogeneity distribution in the core samples. We will show that it is, nevertheless, sufficient for reproduction of the recovery curves.

4.3.2 Fitting procedure

The model was used to determine some key parameters for the recovery process by fitting with experimental data. First, the fitting was performed with secondary production data. The Corey parameters for relative permeabilities were determined by assuming the core is homogeneous i.e. the core has one layer with a single permeability. Afterward, the domain was defined to have two layers with different permeabilities (namely, k_1 and k_2) and thickness (h_1 and h_2). Using the fitted Corey parameters, the permeability contrast (k_1/k_2) and thickness contrast (h_1/h_2) were determined by a new adjustment of the secondary production data. Once the properties of the domain were defined and the simulation was at the end of secondary flooding, the mechanism of fines relocation was included. The fitting continued with the experimental data for tertiary recovery. The formation damage coefficient was determined in this step to evaluate the effect of particle relocation on additional recovery.

4.3.3 Results

Since the two repeated flooding results are similar for the sandstone cores, in order to avoid repetition, only the recovery data for the first flooding experiments of SS1 and SS2 were simulated. The flooding results for both of the chalk cores (CK1 and CK2) were simulated as well.

In the first step, the flow characteristics during the flooding were defined for each core. Figure 10 shows the displacement in the four cores before the breakthrough, to illustrate the flow features.

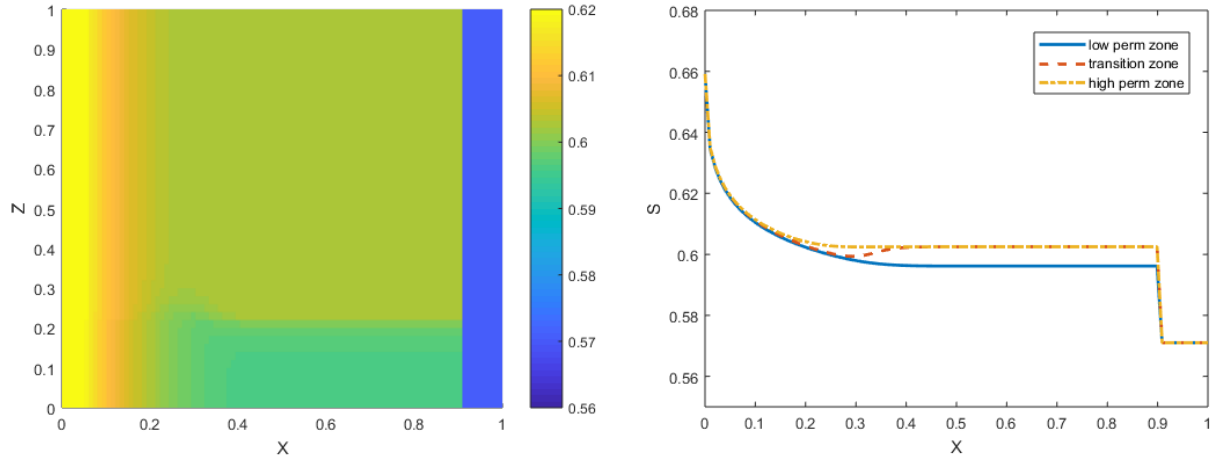

(a) SS1 T=0.03 PVI

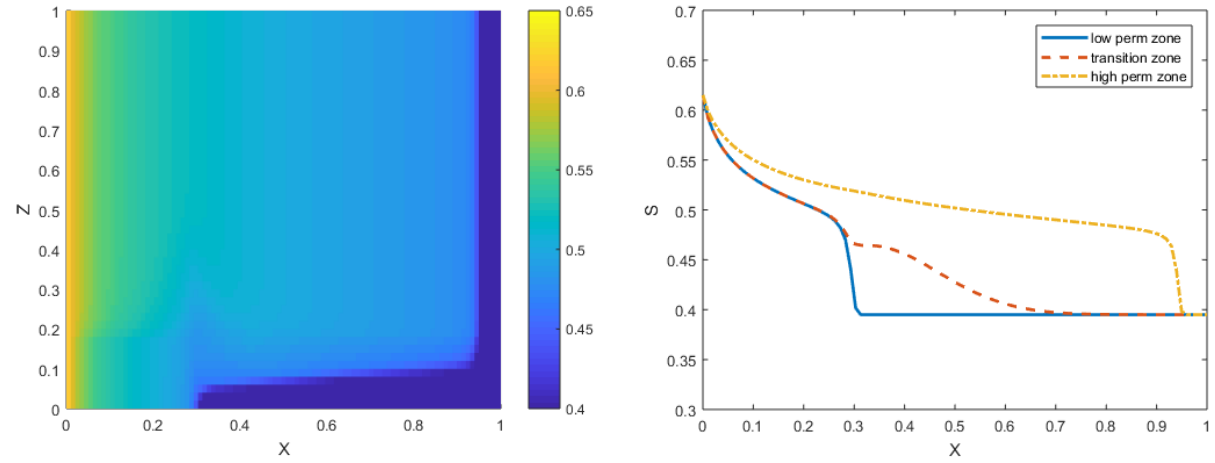

(b) SS2 T=0.1 PVI

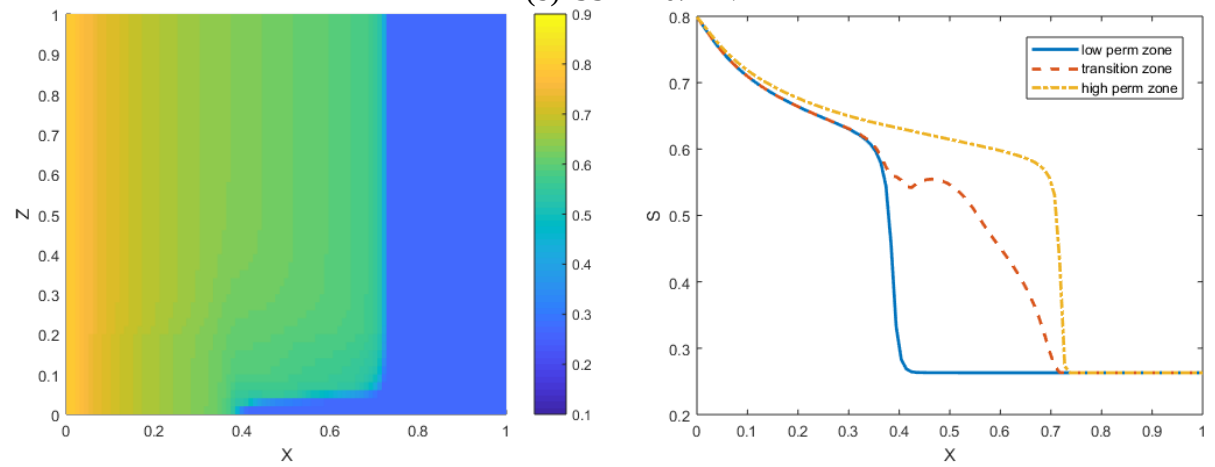

(c) CK1 T=0.4 PVI

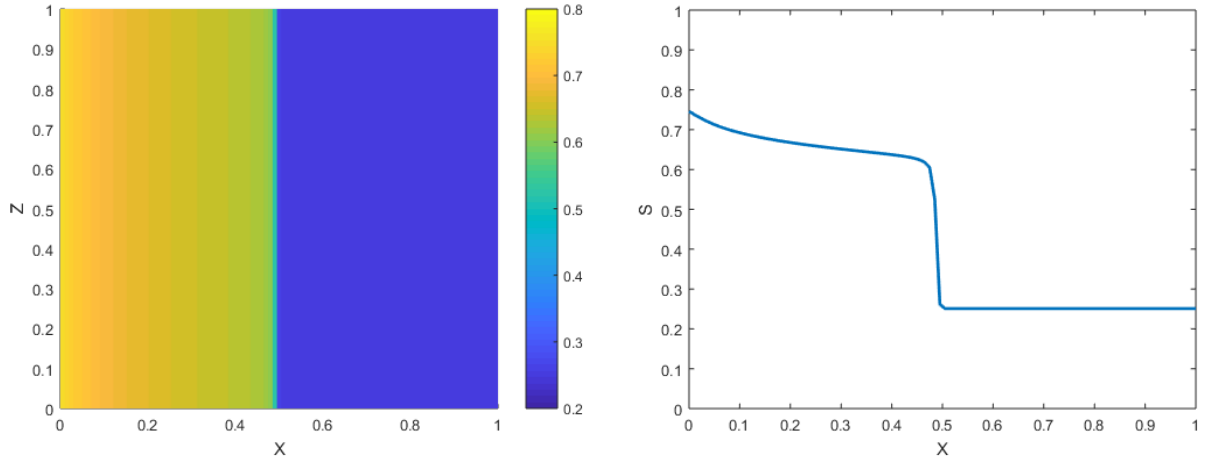

(d) CK2 T=0.2PVI

Figure 10. Flow characteristics in the four cores. The left column shows the saturation in the entire domain. The right column shows the saturation along three typical regions (except for CK2, where the model did not capture the heterogeneity): the high permeability zone, the low permeability zone and the transition zone between them.

From the left column, it can be seen that, for the sandstone cores, SS1 has a thicker low-permeable zone and, thus, is more heterogeneous than SS2. The contrast between homo- and heterogeneity is more distinct for the chalk cores, where there is a thin low-permeable layer in CK1, but the model did not manage to capture any heterogeneity in CK2. The result is consistent with the observations from the CT images. The right column shows the saturation profiles in three typical regions (except for the homogeneous CK2): the high and low permeable zones and the transition zone between them. It can be seen in the case of SS2 and CK1 that the front in the high-permeable layer progresses much faster than in the low-permeable zone. The profile of the transition zone shows a small increase next to the front of the low-permeable zone, which indicates crossflow of the water from the low-permeable to the high permeable zone. This makes a perfect sense according to the concept of flow diversion: water flows from the 'difficult' to the 'easy' channels. Meanwhile, as for SS1, since the range of saturation variation is very narrow (from 0.56 to 0.62), the difference between the two fronts is hardly perceptible, and the difference between the two layers is also not as significant as in other cases.

Next, the recovery curves were simulated. The overall fitting of the recovery data is given in Figure 11, and the magnified details upon additional production from SS1 and CK1 are shown in Figure 12.

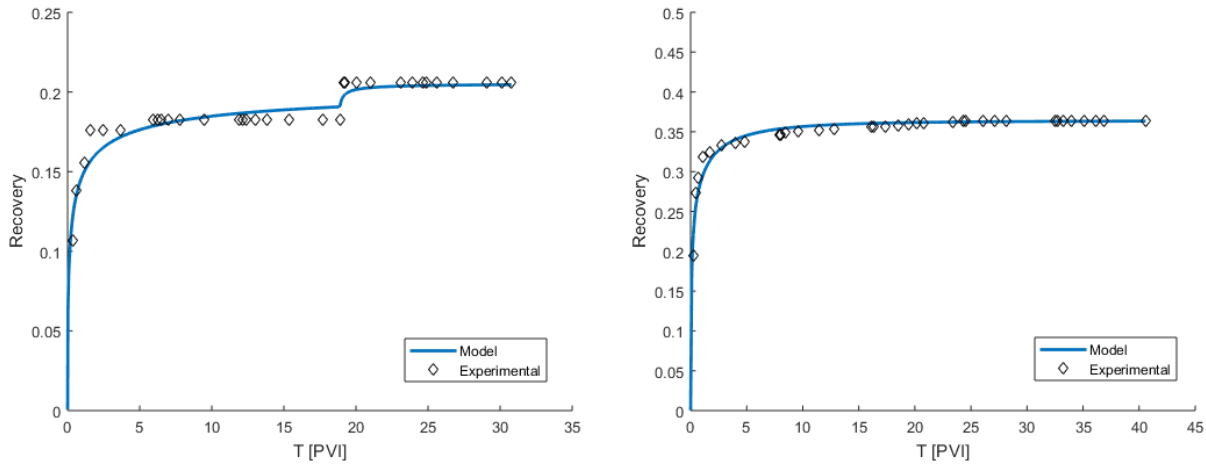

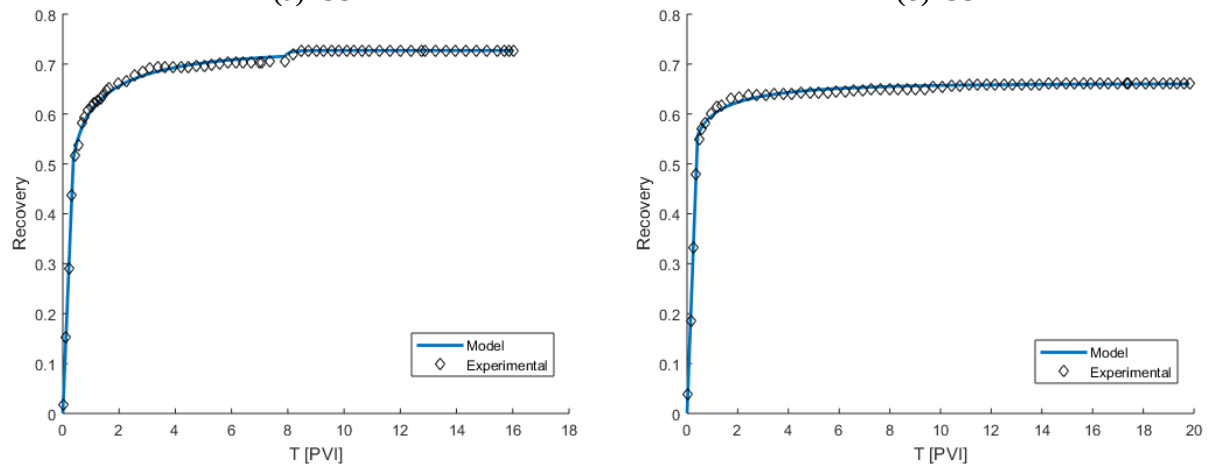

(c) CK1 (d) CK2

Figure 11. The fitted recovery from the four samples. In the cases for both heterogeneous ((a) and (c)) and homogeneous ((b) and (d)) cores, the model was able to reproduce the experimental data accurately.

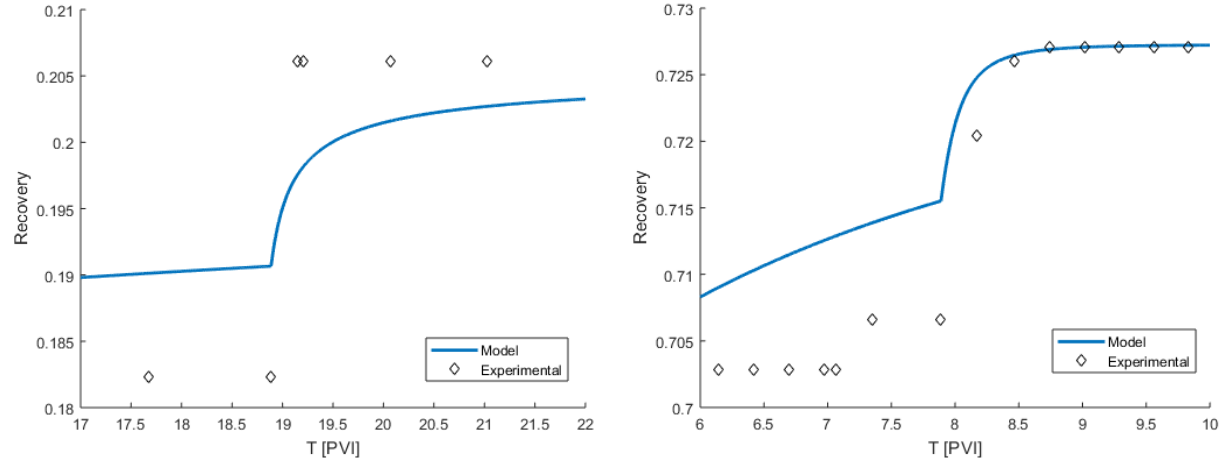

(a) SS1 (b) SS2

Figure 12. The magnified section upon additional recovery in the heterogeneous sandstone (SS1) and chalk (CK1) core. The fitting is reasonably accurate even in the magnified plots.

The model matches the experimental data well. It reproduces the water breakthrough and the production process after it. Thus, even the very simplified model applied here reflects the characteristic features and the flow parameters of the experiment. For the heterogeneous cores, the introduction of the permeability impairment by fines or emulsions results in additional recovery that is closely comparable to the experimental data. This indicates that the reduction of water mobility and flow diversion is a highly plausible mechanism behind the additional recoveries. The fitted parameters are given in Table 4.

Core no.	Corey parameters		Permeability ratio	Thickness ratio	Formation damage coefficient
	a_o	a_w	k_1/k_2	h_1/h_2	β
SS1	2.702	1.459	1.037	3.501	3102
SS2	1.529	2.694	1.378	4.579	-
CK1	1.340	3.695	1.090	4.012	553
CK2	1.311	6.962	-	-	-

Table 4. The fitted parameters that characterize the flooding process.

It can be seen that the permeability ratio for the 'heterogeneous' SS1 is lower than for the 'homogeneous' SS2, but the thickness ratio is the other way around. This means, although the impact of permeability difference is samller in SS1, but it affects a larger area, which makes a more inffluencial overall effect. When comparing the different levels of heterogeneity, both parameters (k_1/k_2 and h_1/h_2) should be considered.

4.4 General Discussion

The flooding experiments were conducted with specially selected sandstone and chalk cores. The additional recoveries were observed in the heterogeneous cores for both types of rocks. The results were reproduced by a model that represents the mechanism of fluid diversion in a vertically communicating stratified porous media. The experimental observations suggest two different mechanisms for the selective plugging of the water pathways. In the sandstones, the additional production was always associated with an increase in pressure drop; most probably, the detachment and re-capture of clay particles in the pore space resulted in plugging of the flow path of water (Akhmetgareev & Khisamov, 2015; Al-Sarihi, et al., 2018; Zhang, Xie, & Morrow, 2007). In line with the reported observations in the literature, the clay content and its migration behavior play an important role in the recovery process of sandstone rocks. In the chalk cores, most probably, the precipitated salts deposited by mixing of the brines and the in-situ generated emulsions acted as the plugging agents. The precipitated particles might also assist emulsification since the particle-assisted (Pickering) emulsions appear to be more stable (Arshad et al., 2018; Arshad et al., 2017).

In both types of rocks, the contribution of heterogeneity is obvious. Under the similar flooding schemes, a distinct oil bank resulting in rapid (although not significant) additional oil production was consistently observed in the more heterogeneous cores. It should be mentioned that additional oil was produced in the tertiary stage from the homogeneous cores as well. However, the production was gradual throughout the flooding process, and the additionally produced oil was less than from the heterogeneous cores. According to the observations in this work, heterogeneity, combined with the fluid diversion mechanism, resulted in a faster and more significant (compared with homogeneous cores) additional oil production.

4.5 Conclusions

This study systematically investigated the effect of flow diversion by comparing heterogeneous and homogeneous cores, sandstone and chalk. Mathematical modeling was used to reproduce experimental data and extract key parameters that characterize the displacement process. The main conclusions are as follows:

1. The mechanism of flow diversion is possible in both sandstone and chalk cores. Re-distribution, generation or deposition of a plugging agent is needed to trigger the mechanism. In this work, the plugging agent was most probably clay particles in sandstone, and emulsions and precipitated salts in chalk.

2. Core scale heterogeneity plays an important role in the production of additional oil. When combined with a flow diversion mechanism, it provides a possibility of producing additional oil.

3. On the macroscopic scale, a simplified layer-cake quasi-1D model is sufficient to simulate the observed peculiarities of the recovery.

Acknowledgment

The authors would like to express many thanks to Danie Subido, Dr. Peng Luo and Tran Thuong Dang for their great assistance in the laboratories. Kelvin D. Knorr is kindly acknowledged for reviewing the manuscript. The Danish Hydrocarbon Research and Technology Centre (DHRTC) is kindly acknowledged for funding the research of Jiasheng Hao. The Saskatchewan Research Cuncil (SRC) is kindly acknowledged for warmly hosting Jiasheng Hao as a research guest. Dr. Hao Yuan is kindly acknowledged for consultations regarding the multilayer model.

References

Afekare, D., & Radonjic, M. (2017). From Mineral Surfaces and Coreflood Experiments to Reservoir Implementations: Comprehensive Review of Low-Salinity Water Flooding (LSWF). *Energy and Fuels, 31*(12), 13043-13062.

Akhmetgareev, V., & Khisamov, R. (2015). 40 years of low-salinity waterflooding in pervomaiskoye field, Russia: Incremental oil. *SPE - European Formation Damage Conference, Proceedings, EFDC, 2015-Janua*, 1-27.

Al-Sarihi, A., Zeinijahromi, A., Genolet, L., Behr, A., Kowollik, P., & Bedrikovetsky, P. (2018). Effects of Fines Migration on Residual Oil during Low-Salinity Waterflooding. *Energy and Fuels, 32*(8), 8296-8309.

Arshad, M., Feilberg, K., Shapiro, A., & Thomsen, K. (2018). Characterization of Emulsion Formation With Nanoparticles for Enhanced Oil Recovery. *SPE Kingdom of Saudi Arabia Annual Technical Symposium and Exhibition.* Dammam, Saudi Arabia.

Arshad, M., Loldrup Fosbøl, P., Shapiro, A., & Thomsen, K. (2017). Water-Oil Emulsions with Fines in Smart Water Enhanced Oil Recovery. *SPE Kuwait Oil & Gas Show and Conference.* Kuwait City, Kuwait.

Bartels, W., Mahani, H., Berg, S., & Hassanizadeh, S. (2019). Literature review of low salinity waterflooding from a length and time scale perspective. *Fuel, 236*(September 2018), 338-353.

Bedrikovetsky, P., Siqueira, F., Furtado, C., & Souza, A. (2011). Modified Particle Detachment Model for Colloidal Transport in Porous Media. *Transport in Porous Media, 86*(2), 353-383.

Bedrikovetsky, P., Zeinijahromi, A., Siqueira, F., Furtado, C., & de Souza, A. (2012). Particle Detachment Under Velocity Alternation During Suspension Transport in Porous Media. *Transport in Porous Media, 91*(1), 173-197.

Chakravarty, K., Fosbøl, P., & Thomsen, K. (2015). Interactions of fines with base fractions of oil and its implication in smart water flooding. *Europec 2015*.

Chakravarty, K., Fosbøl, P., & Thomsen, K. (2015). Significance of fines and their correlation to reported oil recovery. *Society of Petroleum Engineers - Abu Dhabi International Petroleum Exhibition and Conference.* Abu Dhabi, UAE.

Derkani, M., Fletcher, A., Abdallah, W., Sauerer, B., Anderson, J., & Zhang, Z. (2018). Low Salinity Waterflooding in Carbonate Reservoirs: Review of Interfacial Mechanisms. *Colloids and Interfaces, 2*(2), 20.

Doust, A., Puntervold, T., & Austad, T. (2011). Chemical verification of the EOR mechanism by using low saline/smart water in sandstone. *Energy and Fuels, 25*(5), 2151-2162.

Emadi, A., & Sohrabi, M. (2013). Visual Investigation of Oil Recovery by LowSalinity Water Injection: Formation of Water Micro-Dispersions and WettabilityAlteration. *SPE Annual Technical Conference and Exhibition.* New Orleans, Louisiana, USA.

Gu, G., Zhou, Z., Xu, Z., & Masliyah, J. (2003). Role of fine kaolinite clay in toluene-diluted bitumen/water emulsion. *Colloids and Surfaces A: Physicochemical and Engineering Aspects, 215*(1-3), 141-153.

Hao, J., & Shapiro, A. (2019). Effect of Compaction on Oil Recovery Under Low Salinity Flooding in Homogeneous and Heterogeneous Chalk. *SPE Annual Technical Conference and Exhibition.*

Hao, J., Mohammadkhani, S., Shahverdi, H., Esfahany, M., & Shapiro, A. (2019). Mechanisms of smart waterflooding in carbonate oil reservoirs - A review. *Journal of Petroleum Science and Engineering, 179*(April), 276-291.

Hussain, F., Zeinijahromi, A., Bedrikovetsky, P., Badalyan, A., Carageorgos, T., & Cinar, Y. (2013). An experimental study of improved oil recovery through fines-assisted waterflooding. *Journal of Petroleum Science and Engineering, 109*, 187-197.

Jackson, M., Vinogradov, J., Hamon, G., & Chamerois, M. (2016). Evidence, mechanisms and improved understanding of controlled salinity waterflooding part 1: Sandstones. *Fuel, 185*, 772-793.

Katika, K., Ahkami, M., Fosbøl, P., Halim, A., Shapiro, A., Thomsen, K., . . . Fabricius, I. (2016). Comparative analysis of experimental methods for quantification of small amounts of oil in water. *Journal of Petroleum Science and Engineering, 147*, 459-467.

Liu, J., Zhou, Z., Xu, Z., & Masliyah, J. (2002). Bitumen-clay interactions in aqueous media studied by zeta potential distribution measurement. *Journal of Colloid and Interface Science, 252*(2), 409-418.

Mahzari, P., & Sohrabi, M. (2014). Crude Oil/Brine Interactions and Spontaneous Formation of Micro-Dispersions in Low Salinity Water Injection. *SPE Improved Oil Recovery Symposium.* Tulsa, Oklahoma, U.S.A.

Menon, V., & Wasan, D. (1986). Particle-fluid interactions with application to solid-stabilized emulsions part II. The effect of adsorbed water. *Colloids and Surfaces, 19*(1), 107-122.

Mohammadkhani, S., Shahverdi, H., Marie Nielsen, S., Nasr Esfahany, M., & Shapiro, A. (2019). Bicarbonate flooding of homogeneous and heterogeneous cores from a carbonaceous petroleum reservoir. *Journal of Petroleum Science and Engineering, 178*(March), 251-261.

Mokhtari, R., Ayatollahi, S., & Fatemi, M. (2019). Experimental investigation of the influence of fluid-fluid interactions on oil recovery during low salinity water flooding. *Journal of Petroleum Science and Engineering, 182*(June), 106194.

Puntervold, T., & Austad, T. (2008). Injection of seawater and mixtures with produced water into North Sea chalk formation: Impact of fluid-rock interactions on wettability and scale formation. *Journal of Petroleum Science and Engineering, 63*(1-4), 23-33.

Romanuka, J., Hofman, J., Ligthelm, D., Suijkerbuijk, B., Marcelis, F., Oedai, S., . . . Austad, T. (2012). Low Salinity EOR in Carbonates. *SPE Improved Oil Recovery Symposium.* Tulsa, Oklahoma, U.S.A.

Russell, T., Pham, D., Neishaboor, M., Badalyan, A., Behr, A., Genolet, L., . . . Bedrikovetsky, P. (2017). Effects of kaolinite in rocks on fines migration. *Journal of Natural Gas Science and Engineering, 45*, 243-255.

Sohal, M., Thyne, G., & Søgaard, E. (2016). Review of Recovery Mechanisms of Ionically Modified Waterflood in Carbonate Reservoirs. *Energy and Fuels, 30*(3), 1904-1914.

Tang, G.-Q., & Morrow, N. (1999). Influence of brine composition and fines migration on crude oi/brine/rock interactions and oil recovery. *Journal of Petroleum Science and Engineering, 24*(1), 99-111.

Yortsos, Y. (1995). A theoretical analysis of vertical flow equilibrium. *Transport in Porous Media, 18*(2), 107-129.

Yuan, H., & Shapiro, A. (2011). Induced migration of fines during waterflooding in communicating layer-cake reservoirs. *Journal of Petroleum Science and Engineering, 78*(3-4), 618-626.

Yunita Halim, A., Marie Nielsen, S., Eliasson Lantz, A., Sander Suicmez, V., Lindeloff, N., & Shapiro, A. (2015). Investigation of spore forming bacterial flooding for enhanced oil recovery in a North Sea chalk Reservoir. *Journal of Petroleum Science and Engineering, 133*, 444-454.

Zahid, A., Shapiro, A., & Skauge, A. (2012). Experimental Studies of Low Salinity Water Flooding Carbonate: A New Promising Approach. *SPE EOR Conference at Oil and Gas West Asia*.

Zeinijahromi, A., Ahmetgareev, V., Badalyan, A., Khisamov, R., & Bedrikovetsky, P. (2015). Case Study of Low Salinity Water Injection in Zichebashskoe Field. *Journal of Petroleum Science Research, 4*(1), 16-31.

Zeinijahromi, A., Lemon, P., & Bedrikovetsky, P. (2011). Effects of induced fines migration on water cut during waterflooding. *Journal of Petroleum Science and Engineering, 78*(3-4), 609-617.

Zeinijahromi, A., Machado, F., & Bedrikovetsky, P. (2011). Modified Mathematical Model for Fines Migration in Oil Fields. *Brasil Offshore Conference and Exhibition*, (pp. 14-17). Macea, Brazil.

Zhang, X., Shapiro, A., & Stenby, E. (2011). Upscaling of Two-Phase Immiscible Flows in Communicating Stratified Reservoirs. *Transport in Porous Media, 87*(3), 739-764.

Zhang, Y., & Sarma, H. (2012). Improving waterflood recovery efficiency in carbonate reservoirs through salinity variations and ionic exchanges: A promising low-cost "smart-waterflood" approach. *Abu Dhabi International Petroleum Exhibition and Conference 2012 - Sustainable Energy Growth: People, Responsibility, and Innovation, ADIPEC 2012, 3*, 2163-2183.

Zhang, Y., Xie, X., & Morrow, N. (2007). Waterflood performance by injection of brine with different salinity for reservoir cores. *Proceedings - SPE Annual Technical Conference and Exhibition, 2*, 1217-1228.

Zhu, R., Liu, Q., Xu, Z., Masliyah, J., & Khan, A. (2011). Role of dissolving carbon dioxide in densification of oil sands tailings. *Energy and Fuels, 25*(5), 2049-2057.

Chapter 5. Effect of Compaction on Oil Recovery Under Low Salinity Flooding in Homogeneous and Heterogeneous Chalk

This chapter has been presented in the SPE Annual Technical Conference and Exhibition 2019,

Abstract

Compaction of the reservoir chalk (e.g. surface subsidence) may facilitate oil production. However, only few works have linked smart water flooding with chalk compaction and additional oil recovery. In this work, core flooding experiments with sequential injection of low salinity brines were performed to examine the effect of chalk compaction on oil recovery under smart water flooding. X-ray computer tomography scanning was applied to select outcrop and reservoir cores with different level of heterogeneity, which was demonstrated to be an important factor that determines the recovery even on core scale. A linear variable differential transformer (LVDT) device made it possible to detect changes of the core length during the experiments, which served as an indication of the compaction. Overburden pressure was increased stepwise at the final stages of the flooding to achieve higher compaction of the cores.

During secondary flooding, slight gradual compaction of the cores was observed. Subsequent low salinity flooding did not lead to further compaction for all the samples, nor additional oil recovery. Under final compaction, significantly more oil was produced from the heterogeneous cores, especially, from the reservoir core. Some fines production was observed during the core cleaning after the experiments. Fluid diversion due to closing micro-fractures under compaction and/or relocation of the fines is speculated to be a driving mechanism behind additional recovery from heterogeneous cores. Rock compaction appears to be a potential mechanism for enhanced oil recovery, however with a limited efficiency.

5.1 Introduction

Low salinity water (LSW) flooding has been recognized as an effective approach to enhance oil recovery in sandstone (Tang and Morrow, 1999), however, the underlying mechanism is still under debate (Al-Saedi et al., 2019a; 2019b; 2019c). On the other hand, its potential for chalk remains a subject of debate (Ayirala and Yousef, 2016; Sheng, 2014; Sohal et al., 2016). While numerous studies have been focusing on the underlying chemical mechanisms, this work targets at the physical and flow dynamical factors that could potentially determine the effectiveness of LSW in chalk: the compaction of chalk and heterogeneity of the rock material.

Subsidence of seafloor has been detected in the North Sea chalk reservoirs in the 1980s (Boade et al., 1989; Ruddy et al., 1989; Sylte et al., 1999). More than 7.8 meters of subsidence was observed in the Norwegian Ekofisk field since its production form 1971. Initially, it was attributed to the reservoir pressure depletion due to production. However, the subsidence did not stop even the reservoir pressure was stabilized by water injection (Sylte et al., 1999). Field observations triggered several projects to study the water weakening of chalk and reservoir compaction. Experimental results indicated that chalk becomes weaker when water or brine enters the pore space (Newman, 1983). Chemical composition of

the brines also appeared to determine the level of weakening (Høeg et al., 2000; Katika et al., 2015; Nermoen et al., 2018). Several mechanisms, such as dissolution/precipitation of Ca^{2+} containing minerals (Heggheim et al., 2004; Hellmann et al., 2002), activity of pore water (Risnes et al., 2005), and adsorption of SO_4^{2-} and substitution of Ca^{2+} by Mg^{2+} (Austad et al., 2007; Korsnes et al., 2008) were proposed to explain the observed weakening effect. Meanwhile, numerous projects were carried out to study reservoir compaction as a mechanism for oil recovery (Boade et al., 1989; Chin and Thomas, 1999; Ruddy et al., 1989; Sulak et al., 1991). It was concluded that the compaction could add a significant amount of energy to the reservoir system and benefit oil production. Here, the link is obvious, injection of the modified brines result in weakening and compaction of the chalk reservoir; reduction of porosity 'squeezes' the oil out.

To the best of our knowledge, only few works connected the compaction with smart water flooding, where the mechanical properties of oil saturated cores were measured when flooded with brines that contain Mg^{2+} or SO_4^{2-} ions (Katika et al., 2017). A reason may be in the difficulty of detection of the compaction while performing waterflooding experiments. In the present work, we have managed to measure the dynamic compaction of the core plugs during water flooding, and examine its effect on oil recovery.

Heterogeneity of the core samples is another factor that was investigated in this work. Although heterogeneity has been recognized and discussed in the literature (Spildo et al., 2012; Yunita Halim et al., 2015), its impact on smart water flooding has not been sufficiently studied. The impact of heterogeneity on reservoir scale has been well studied and included in the macroscale simulation works (Attar and Muggeridge, 2016; Yuan and Shapiro, 2011; Zeinijahromi et al., 2011b). However, the importance of heterogeneity on core scale is often overlooked. A reason may be that heterogeneity is difficult to quantify and experiments with its involvement are harder to interpret. The dimension and geometry of the pore space could have an impact on the result of core scale experiments (Romanuka et al., 2012). The flow dynamics related to heterogeneity could play a role in core scale recovery mechanisms. As extensively studied for the sandstones, it may contribute to the recovery via mobilization and relocation of reservoir fines by low salinity flooding (Al-Sarihi et al., 2018; Borazjani et al., 2018; Hussain et al., 2013; Yu et al., 2018). However, its effect on smart waterflooding of carbonate rock is rarely reported. In this work, we have selected cores with different levels of heterogeneity based on X-ray computer tomography scanning. Behavior of these cores under waterflooding is studied for similar experimental conditions. The paper is organized as follows: section 2 introduces the materials and experimental procedures involved in this work; section 3 presents the experimental results, such as recovery profiles and compaction measurements; section 4 contains interpretation and discussion of the results; section 5 presents the main conclusions of this work.

5.2 Materials and methods

5.2.1 Oil

The oil applied in this study is a light crude oil from a North Sea chalk reservoir. The oil has a density of 0.840 g/ml, viscosity of 4.45 cP, and a total acid number of 0.504 mg KOH/g. The oil viscosity and density were measured at 60°C and ambient pressure. The oil was first filtered through a filter with 0.2 μm pore size to remove solid particles (mainly, fragments of calcite). The filter surface is neutral to oil, and pore sizes were larger than the molecular sizes, even for the large molecules, so that the oil composition (with a rather insignificant amount of the heavy fraction) remained unchanged under filtration. Then the filtered oil was centrifuged at 3000 rpm for 30 min (no water was separated from the oil).

5.2.2 Brines

Synthetic formation water (FW) and seawater (SW) were used in this study. The brines were prepared by dissolving salts in deionized water. The salts were purchased commercial products with a purity of ≥99.5% . The compositions of the brines are given in Table 1. Different versions of diluted brines were prepared by mixing deionized water with FW or SW at desired ratios.

Compound	Concentration [g/kgw]				
	Seawater	2DSW	10DSW	Formation water	DFW
NaCl	25.414	12.707	2.541	69.013	34.507
KCl	0.763	0.382	0.076	0.475	0.238
$NaHCO_3$	0.089	0.045	0.009	-	-
Na_2SO_4	2.957	1.479	0.256	0.429	0.215
$CaCl_2$, $2H_2O$	1.504	0.752	0.150	5.378	2.689
$MgCl_2$, $6H_2O$	9.151	4.576	0.915	4.954	2.477
$SrCl_2$, $6H_2O$	0.061	0.031	0.006	0.426	0.213
$BaCl_2$, $2H_2O$	-		-	0.001	-
TDS	30.939	15.470	3.094	80.675	40.338
Ionic strength	0.675	0.338	0.066	1.384	0.692

Table 1. Composition of seawater and formation water. FW is almost twice as saline as SW due to its high NaCl concentration. FW also has a higher Ca2+ concentration due to the fact that it is originated from a carbonate reservoir. Whereas SW has higher SO42- and Mg2+concentration than FW.

5.2.3 Rock

Two outcrop chalk cores from Stevns Klint (SK) and two reservoir cores (RS) from a North Sea chalk reservoir were used in this study. Both type of cores are highly pure biogenic chalk, composed primarily by calcite and negligible amounts of silica and other impurities. The porosity and permeability of the samples were measured by nitrogen injection at ambient temperature. Comparison with the weighted difference between the empty and saturated core has shown that the difference is within 3% of the measured value. The measured gas permeability was corrected by the 5-point Klinkenberg method. The dimensions, porosity and permeability of the samples are given in Table 2.

Sample	Length [mm]	Diameter [mm]	Dry mass [g]	Porosity [%]	Permeability [mD]	Swi [%]	Sor [%]
SK1	73.07	37.20	120.10	43.4	5.37	12.6	21.1
SK2	75.38	37.20	122.40	42.8	6.11	12.6	26.3
RS1	73.36	37.60	146.74	33.5	0.56	24.5	19.2

RS2	77.89	37.63	151.51	36.6	1.52	11.0	22.9

Table 2. Properties of the cores before experiments. The two outcrop samples have similar properties. The reservoir samples tend to be tighter, and the homogeneous core (RS 1) has almost only one third of the permeability than the heterogeneous core (RS 2).

Before the experiments, the dry cores were examined by the X-ray computer tomography scanning (CT scan). The obtained images were used as a reference to indicate the heterogeneity of the samples. In this study, we selected one homogeneous and one heterogeneous sample for each type of chalk. The CT images are given in Figure 1. The first two images are along the two orthogonal planes in longitude direction of the plugs with a relative angle of 90°. The third image is along the radial direction at the center of the core.

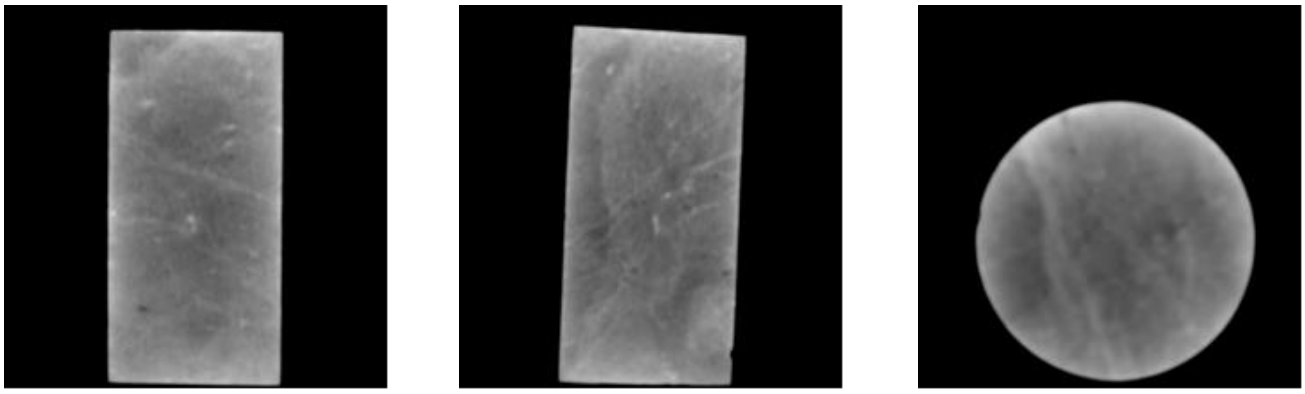

(a) SK1

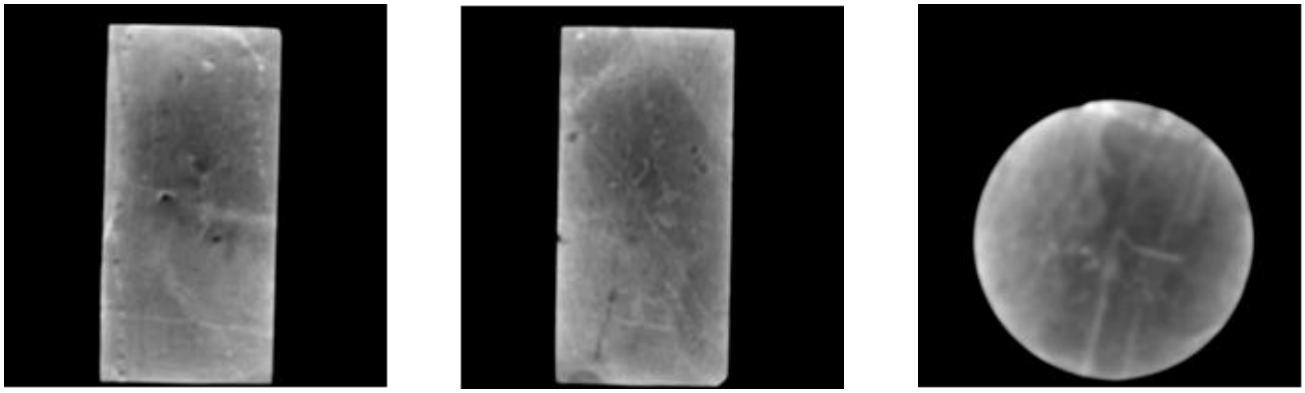

(b) SK2

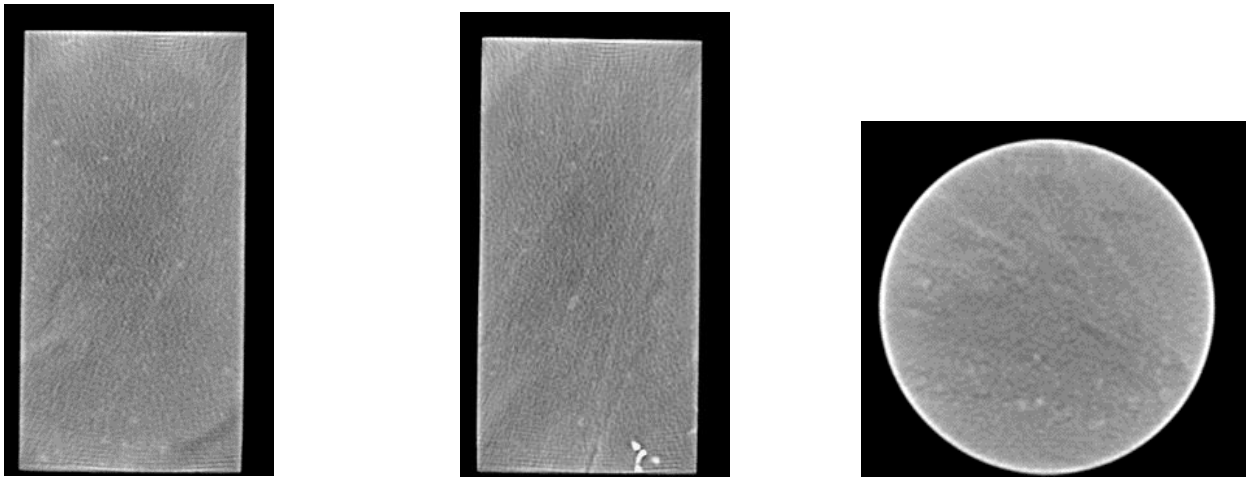

(c) RS1

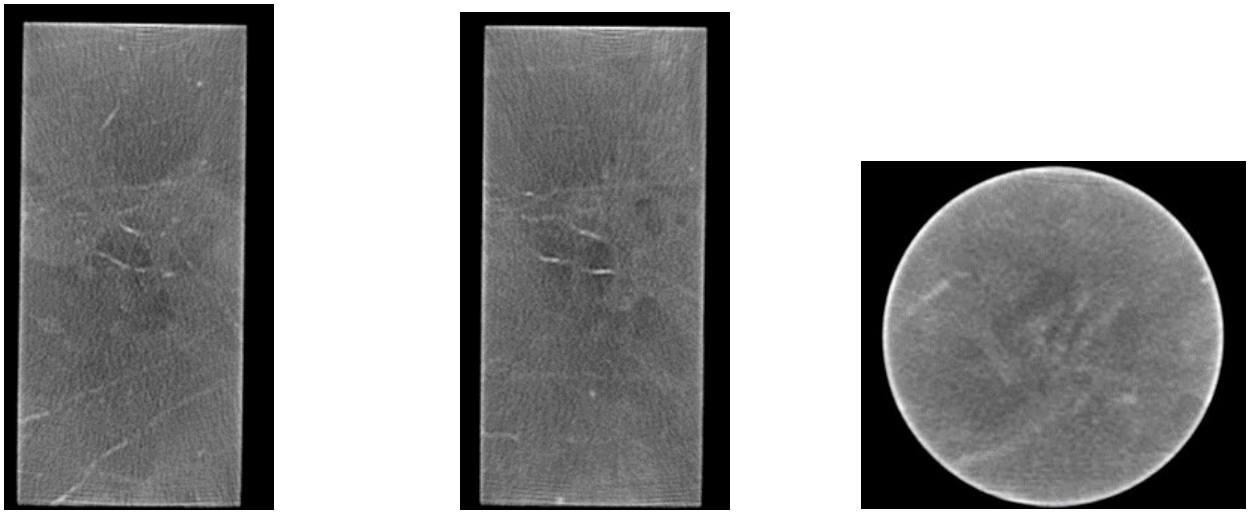

(d) RS2

Figure 1. CT images of the core samples. SK 2 is considered as heterogeneous comparative to SK1, as it has a more distinct variation of density along the longitude direction. RS2 is heterogeneous compared to RS1, the random dense inclusions concentrates at the center of the core, and a few bright white lines lays at the center and end of the core.

Apparently, homogeneity and heterogeneity are relative properties. Neither of the cores are completely homogeneous or totally heterogeneous (whatever that means). In this study, we consider the heterogeneous cores as the ones contain structural elements that are strongly distinct from the other parts of the core. These elements can be an uneven density distribution, or fractures or barriers in the samples, or other distinct elements having a characteristic direction (the density is indicated by the color, more 'white' means higher density while 'black' means lower density; the fractures are usually indicated by the bright white or black curves in the images). Obviously, such a definition of heterogeneity is only qualitative. However, it serves as a fast and reasonably reliable method for selection of the samples. A more precise and quantitative method for determination of the heterogeneity on the core level would require an advanced separate study.

5.3 Flooding setup

The experimental setup was built in-house for core flooding. Figure 2 presents a sketch of the setup. It consists of two pumps, three injection cylinders, a Hassler type core holder, a backpressure regulator (BPR), an oven, multiple valves and pressure transducers, and a data recording system. The main part of the system (except for electronic devices and pumps) was mounted on a rig that was fitted into the oven.

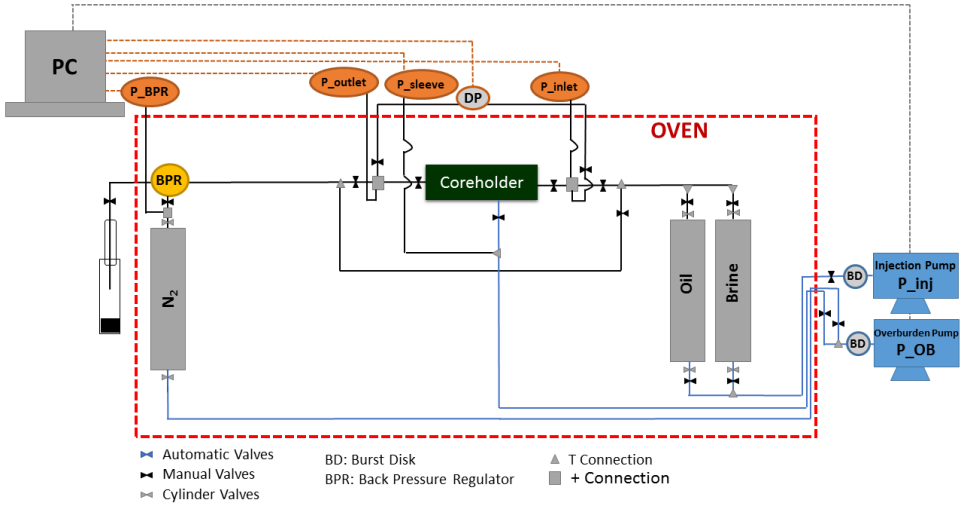

Figure 2. Sketch of the flooding setup. The main components, except for pumps and electronics, are placed in the oven. The data recording system reads the signal from the LVDT device, all the pressure transducers and pumps. The signals were recorded every 30 seconds simultaneously.

Before the experiments, the setup was leak tested by water at 500 bar to guarantee a closed system. The dead volume of the core holder was measured by water. Upon switching an injection fluid, the tubing between the injection cylinder and the inlet of the core holder was saturated by the new fluid to avoid additional dead volume.

The cores were inserted in a core holder. In order to make a more uniform distribution of fluid close to the ends of the cores, two filters made of stainless steel were placed between the pistons of the core holder and the cores. The filters are thin and coarse enough to not add significant dead volume and resistance for the flow. A heat-shrink PTFE sleeve was first covered around the core, the filters and the core holder pistons to align the components. Then a Viton sleeve was covered over the PTFE sleeve to provide extra stability to such a configuration.

5.3.1 Core length measurement

A Linear Variable Differential Transformer (LVDT) device attached at the endcap of the core holder indirectly measures variation of the length of a core. The device was calibrated before mounted to the core holder. The novelty of the core holder in this work is that, the piston and the tubing at the outlet side of the core holder are able to float axially meanwhile maintain a tight contact with the core, so that the compaction of the core can be detected by the displacement of the outlet tubing of the core holder. Such displacement was captured by the LVDT device and recorded by the data acquisition system throughout the experiment. The measurement is interpreted as an indication of the compaction state of the core.

The accuracy of the LVDT device is within the sub-millimeter range, which is sufficient to detect and to quantify the compaction in the laboratory core studies. The measured values of compaction in our study

are of the same orders of magnitude (several per cent of the total length) as compaction observed in petroleum reservoirs.

5.4 Experimental procedures

5.4.1 Core preparation

All the core plugs were cleaned by subsequent alternative flooding of methanol and toluene to remove the precipitated salts and residual hydrocarbon compounds. Complete removal of salts was verified by adding 2-3 drops of 0.03M $AgNO_3$ solution to 3-5 ml methanol effluent. Removal of hydrocarbon compounds was verified by visual observation of a continuous colorless toluene effluent.

The cleaned samples were then placed in an oven at 60°C for at least two days to evaporate the methanol. Afterwards, the samples were subjected to porosity and permeability measurement by the nitrogen injection.

5.4.2 Saturation and aging

The cleaned dry cores were first completely saturated by formation water under vacuum. The degree of saturation was evaluated by the weight difference between dry and saturated core. A saturation within 3% difference with the porosity was accepted. The saturated cores were assembled into the core holder. Overburden (OB) pressure and temperature were built up at this stage. In this study, the experimental temperature was 60°C; the overburden pressure was 42 bar for outcrop cores and 155 bar for reservoir cores, but it varied at the later stages, as described below. Next, two pore volumes (PVs) of FW were injected to refresh the pore water and displace the possibly trapped air bubbles in the core. The initial oil saturation was achieved by injection of crude oil into FW saturated cores until no more water was produced. The obtained initial water saturation is within the range of values in published literature with the same type of rock.

Then the cores were sealed in the core holder for two weeks of aging. This aging time is a common practice for the carbonaceous rocks and oils from the Danish sector of the North Sea. The previous studies with e.g. measurements of electric resistivity (Ahkami et al., 2016) show that the wetting state of a core is likely to be already stabilized after the two weeks. According to the literature, the wettability changes under influence of the acidic, carboxylic or heavy fractions of the oil. However, in this work the oil is light and has a low acid number (0.504 mg KOH/g). We believe 2 weeks of aging would be enough for the adsorption process, a prolonged aging time is not likely to further affect wettability.

5.4.3 Flooding sequence

In order to exclude any LSW effect during secondary recovery, synthetic formation water was injected at this stage. Considering the fact that formation water has a higher ionic strength and different ionic configuration than seawater, switching directly from FW flooding to SW flooding was not desirable, since the low salinity flooding and flooding with brines that contain high concentration of sulfate and magnesium have different potential working mechanisms (Tang and Morrow, 1999; Zhang et al., 2007). It could bring difficulties for interpretation of the flooding results. Therefore, diluted formation water (DFW), which has the same ionic strength as seawater, was injected after the FW flooding. Then seawater, two times and ten times diluted seawater (2DSW, 10DSW), and afterwards, deionized water (DW) were sequentially injected. Each brine was injected for at least 5 PVs to give enough time for the potential mechanisms to take effect. The injection rate was kept at 0.1 ml/min throughout the experiment.

The produced effluent was collected by a fraction collector with fraction sizes between 1/7 to 1/2 porous volumes.

The floating outlet piston of the core holder ensures that the core undergoes a stress condition that is similar to hydrostatic test when overburden pressure is applied. The reported hydrostatic yield pressure for Stevns Klint chalk is about 75 bar (Austad et al., 2007; Heggheim et al., 2004; Korsnes et al., 2008), and 275 bar for North Sea reservoir chalk (Meireles et al., 2018). In order to observe the weakening and compaction of the core plugs during low salinity flooding, a high load on the rock matrix must be created. Therefore, during aging and sequential flooding, overburden pressure was set to be 60% and 56% of the hydrostatic yield pressure of the samples. The OBs are 42 bar for Stevns Klint chalk and 155 bar for North Sea chalk. Meanwhile, back pressure (BP) was not applied (unless otherwise specified). During the injection of deionized water, an enhanced compaction of the cores was introduced by increasing overburden pressure in order to test the potential of compaction on oil recovery. The overburden pressure was increased stepwise and exceeded the hydrostatic yield pressure of the core samples. Each step of the increase was performed linearly within 10 minutes to avoid possible non-uniform loading caused by sudden change of pressure. After testing the effect of enhanced compaction, the back pressure of the homogeneous outcrop core and heterogeneous reservoir core was increased to test the impact of pore pressure on oil recovery.

5.4.4 Quantification of produced oil

The produced fluids were collected by graduated test tubes with different fraction sizes. If the amount of oil in a tube was larger than 0.1 ml, its volume was read visually. For smaller amounts of oil, which appeared as a droplet or a thin film on top of water, the volume was measured by UV-vis spectral adsorption, as described in the literature (Katika et al., 2016). In brief, 3 ml of toluene was added to the test tube to dissolve oil. The toluene-oil solution was then transferred into a cuvette to measure its optical adsorption at an UV wave length of 750 nm. The oil volume was obtained by comparing the measured value with a standard curve, which was produced by the same procedure with known amounts of oil. See Katika et al., (2016) for discussion of the experimental error for this method.

5.5 Results

5.5.1 Outcrop samples

5.5.1.1 Recovery profiles

Figure 3 shows the recovery from the outcrop samples. Secondary recovery by FW injection resulted in 75.61% recovery from the homogeneous core (SK1) and 69.19% from the heterogeneous core (SK2). The high recoveries are consistent with the previously reported data (e.g. Zahid et al, 2012a). Injection of DFW lead to 0.18% and 0.4% additional recovery from the homogenous and heterogeneous core, respectively. Sequential injection of SW, diluted versions of SW and DW did not produce more oil. However, a small amount of oil was produced by increasing the overburden to 210 bar; 0.13% was produced from homogeneous core while a total of 0.32% was produced from the heterogeneous one. Additional production was observed immediately after the compaction. For the homogeneous core, the back pressure was increased to 98 bar to test the impact of pore pressure on oil recovery, which did not show any effect.

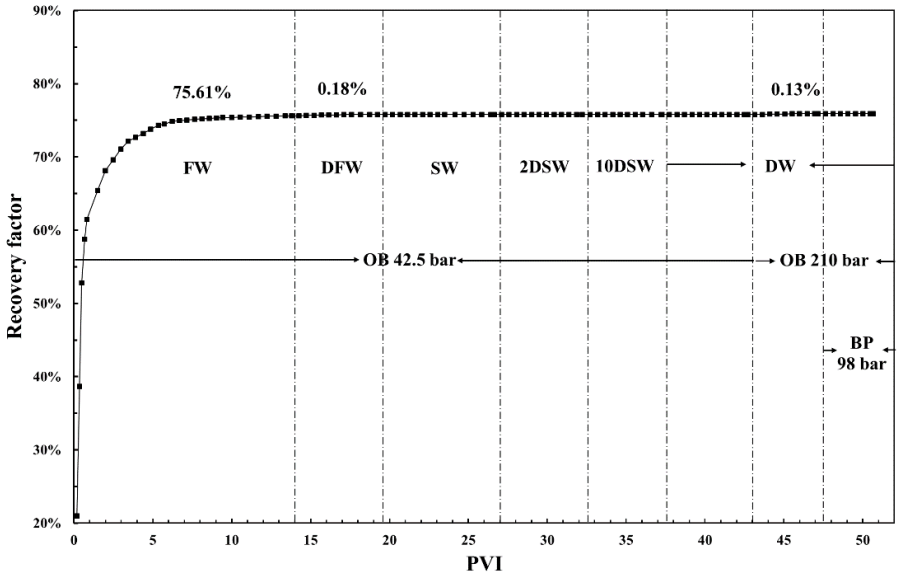

(a) SK1

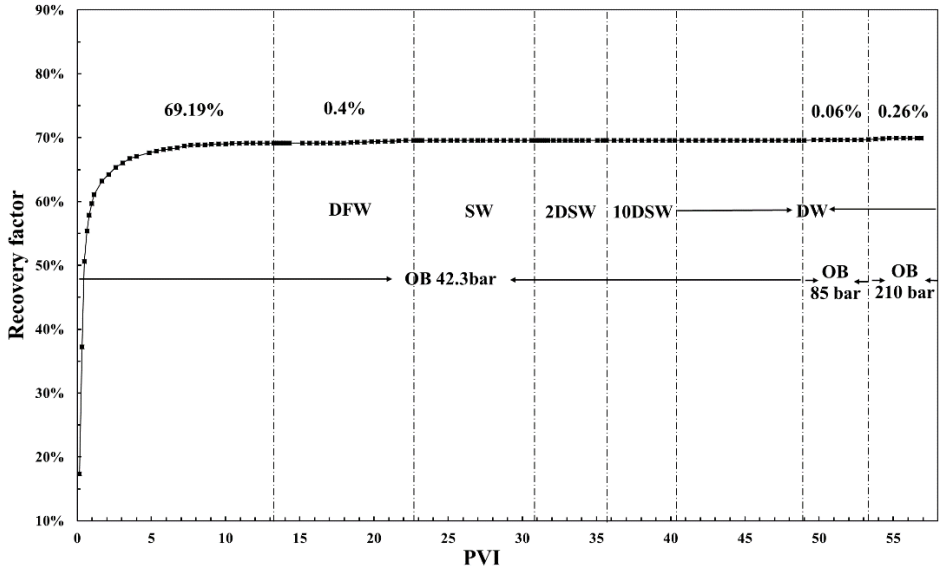

(b) SK2

Figure 3. Recovery profiles of the outcrop cores. More oil was recovered from the homogeneous core (SK 1) in the secondary flooding, this is consistent with the expected behavior of homogeneous and heterogeneous cores. The recovery by DFW flooding appeared to be a continuation of secondary flooding. Additional recovery by the enhanced compaction at the final stages of the experiments was insignificant, but the difference between homogeneous and heterogeneous cores is still considerable.

5.5.1.2 Core compaction

Figure 4 shows the change in core length throughout the experiment. For the homogeneous core, increasing overburden pressure from 42.5 bar to 210 bar resulted in 3.9 mm compaction in length, corresponding to 5.3% of the original core length. Increasing backpressure (BP) to 98 bar did not restore

the strain significantly. For the heterogeneous core, a compaction of 1.01 mm (1.34%) and 3.64 mm (4.83%) was detected when overburden pressure increased to 84 bar and 210 bar, respectively.

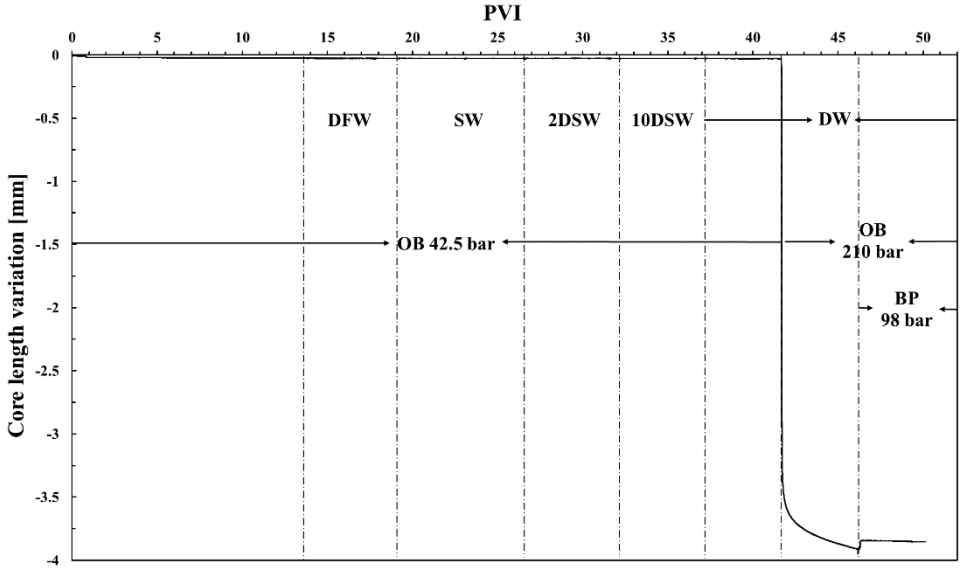

(a) SK1

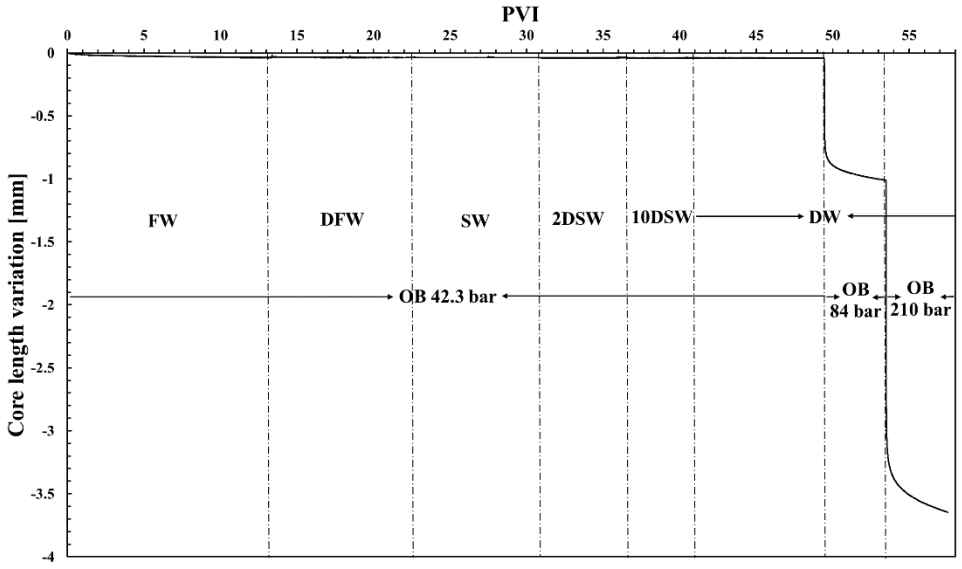

(c) SK2

Figure 4. The variation of core length measured by LVDT throughout the experiments for the outcrop cores. Relaxation of the core length was immediately after the increase of overburden pressure and was not fully stabilized by the end of the experiment. The two cores were compacted similarly at an overburden pressure of 210 bar. Increasing back pressure in SK1 did not significantly restore the compaction.

The core length measurement before increasing overburden pressure is given in Figure 5. Both cores showed a slight gradual compaction during secondary recovery, when majority of the oil was displaced by brine. This observation is consistent with the existing theory of water weakening of chalk: the dry chalk is

stronger than the oil saturated chalk, which, in turn, is stronger than water saturated chalk (Høeg et al., 2000; Madland et al., 2002). Injection of low salinity brines did not compact the cores further.

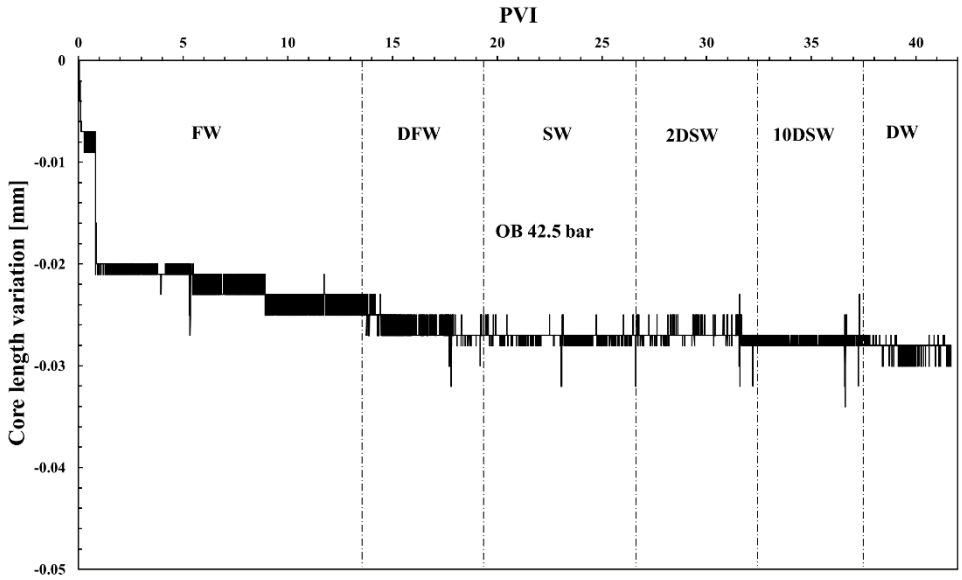

(b) SK1

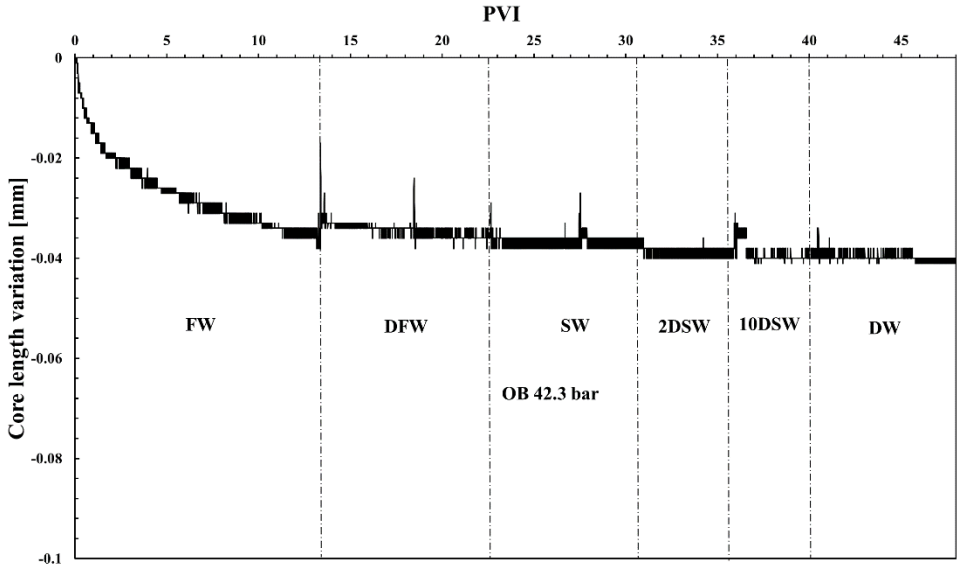

(c) SK2

Figure 5. LVDT measured variation of core length before increasing overburden pressure. A gradual compaction can be observed during secondary flooding for both cores, which is consistent with the existing chalk weakening theory. Injection of low salinity brines did not lead to further compaction.

5.5.1.3 Pressure profiles

Figure 6 shows the pressure difference through the cores during the experiments. For both cores, the pressure drop during FW injection shows typical characteristics of secondary recovery: a sharp increase until breakthrough, followed by a steep decrease, and then gradual stabilization. Sequential flooding of low salinity brines did not cause significant variations of the pressure drop.

Compaction, on the other hand, resulted in a considerable increase of pressure drop. The pressure difference increased from 0.81 bar to 2.85 bar for SK1; and 0.76 bar to 2.81 bar for SK2. This means that the permeability dropped significantly due to compaction, which is verified by permeability measurement after the experiments (shown later in this section). In the case of SK6, after increasing back pressure to 98 bar, the pressure difference dropped to 2.38 bar. This may be linked to the slight restoration of the core due to the reduced effective pressure on the rock matrix.

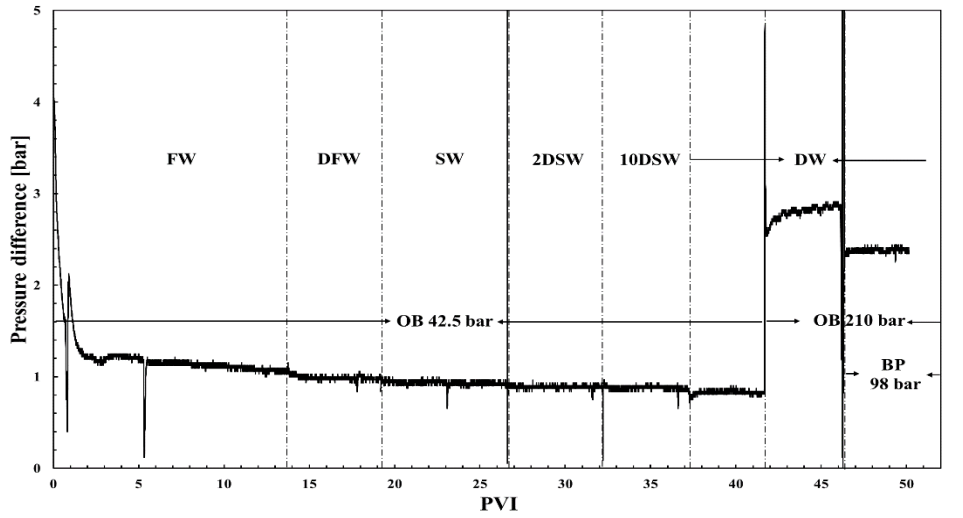

(d) SK 1

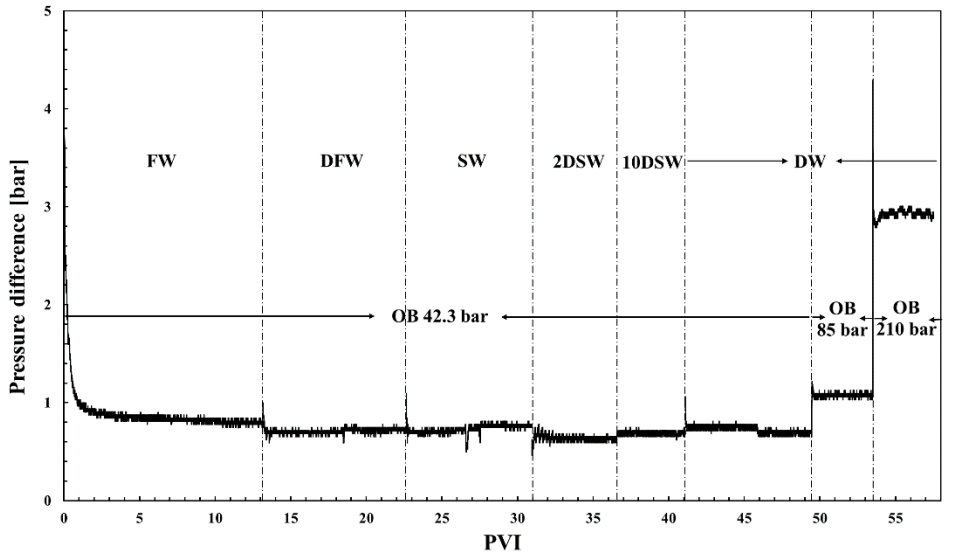

(e) SK 2

Figure 6. Pressure difference across the cores during flooding for outcrop samples. No significant variation was observed by low salinity flooding. The increase of pressure drop by compaction at the final stages of the experiments was corresponding to the permeability reduction (shown later in this section).

5.5.2 Reservoir samples

5.5.2.1 Recovery profiles

Figure 7 shows the recovery profiles from the reservoir samples. The secondary recovery was 74.24% and 72.62% for the homogeneous (RS1) and heterogeneous (RS2) cores, respectively. Further injection of low salinity brines produced insignificant amounts of oil: 0.32% from the homogeneous core by DFW injection, and 0.4% from the heterogeneous core by SW injection. Injection of DW did not produce more oil from either cores. For the homogeneous core, compaction did not result in additional production, even when the overburden pressure increased to 420 bar. On the other hand, a considerable amount of oil (1.1%) was produced from the heterogeneous core when the overburden pressure increased to 350 bar. It should be noted that additional production was observed after 2.4 porous volumes were injected from the moment of the increase of overburden pressure. Finally, increasing back pressure did not have any impact on oil recovery.

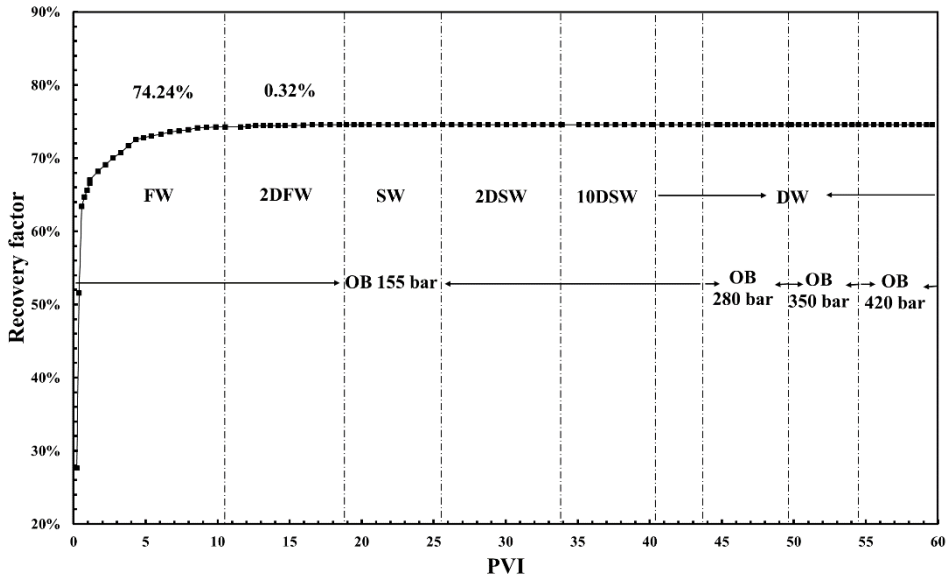

(f) RS1

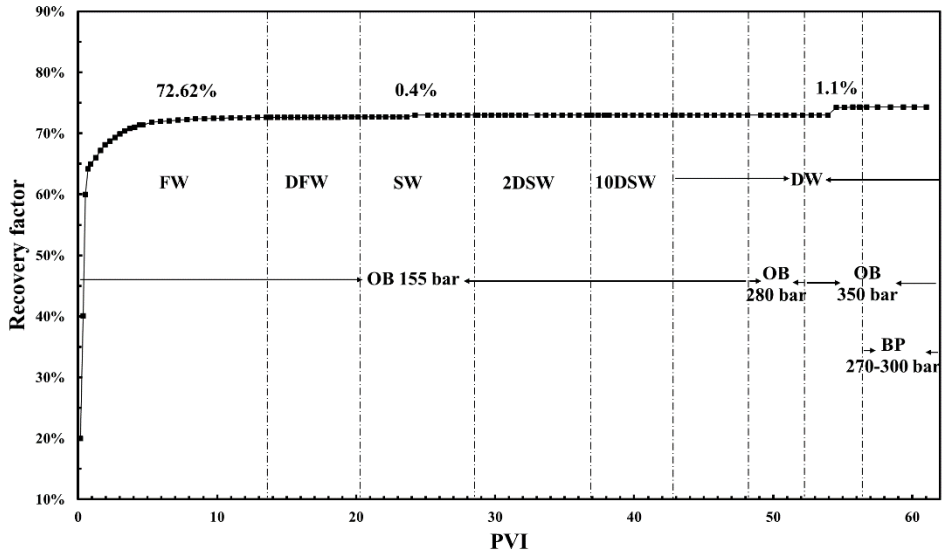

(g) RS2

Figure 7. Recovery profiles of the reservoir cores. Injection of low salinity brines did not produce significant amount of oil from either cores. The compaction by increasing overburden pressure produced 1.1% addition oil form the heterogeneous core (RS2) while no more oil was produced from the homogeneous core (RS1).

5.5.2.2 Core compaction

Figure 8 shows the measurement of core length variation during the experiments. For the homogeneous sample, increasing overburden pressure from 155 bar to 280 bar, 350 bar and 420 bar lead to compactions of 0.28 mm, 0.60 mm and 1.03 mm in length, corresponding to 0.36%, 0.77% and 1.32% of the original core length. For the heterogeneous sample, the compactions are 0.487 mm and 1.198 mm, corresponding to 0.63% and 1.54% of the original core length. Increasing back pressure of the heterogeneous core restored the core length by 0.251 mm. It is obvious for both cores that the strain has not fully reached equilibrium after the increase of overburden pressure.

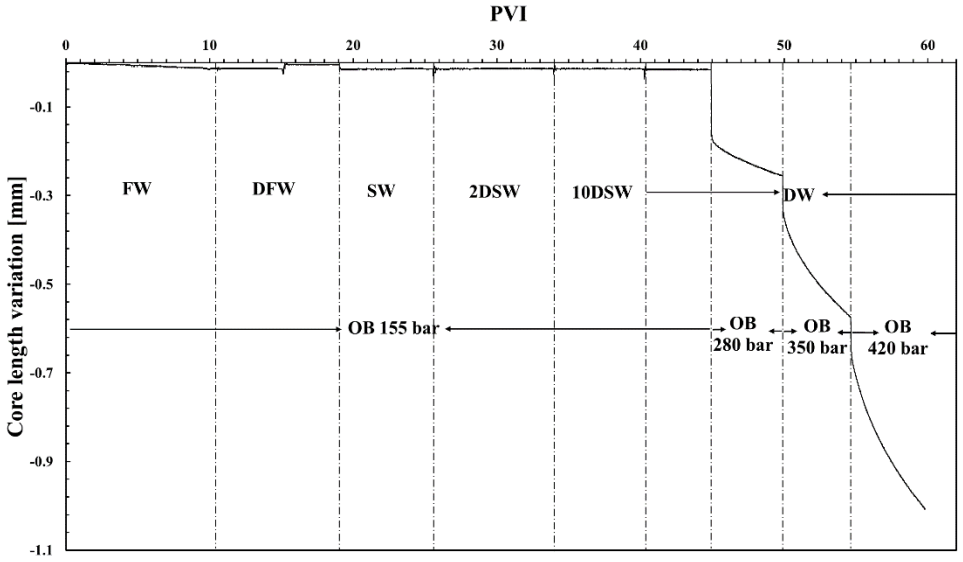

(h) RS1

(i)

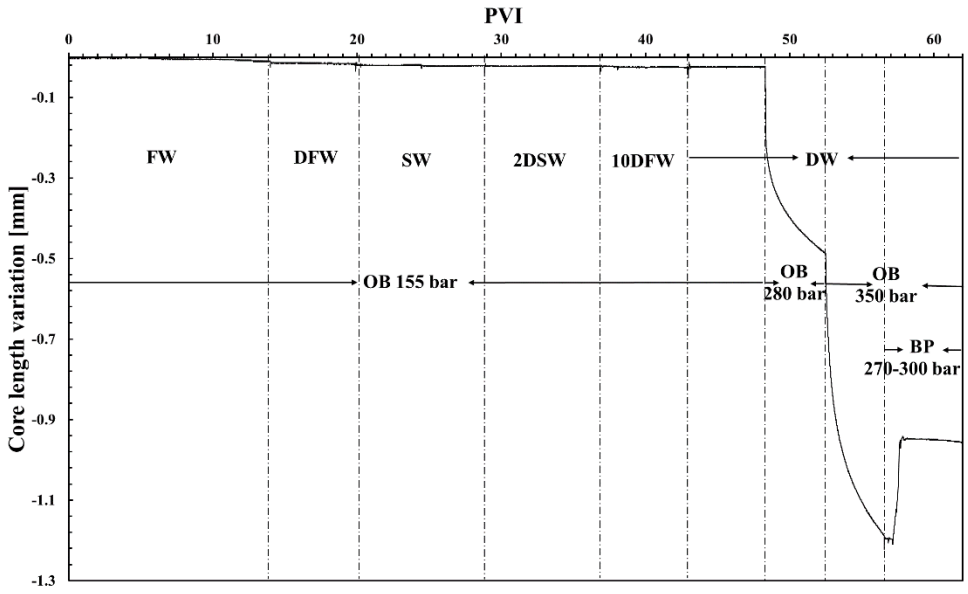

(j) RS2

Figure 8. LVDT measured variation of core length during flooding for the reservoir cores. Increasing overburden pressure stepwise resulted in significant compaction of the cores. The compaction between the steps were not fully relaxed. Increasing back pressure in the heterogeneous (RS2) core stopped the compaction and restored part of the strain.

Figure 9 shows the core length variation before increasing overburden pressure. Like the outcrop samples, there is a slight gradual compaction during secondary recovery in both reservoir samples. Further injection of low salinity brines did not lead to significant compaction. For the heterogeneous core, relaxation of the strain was slower than for the homogeneous core and continued until the SW injection stage.

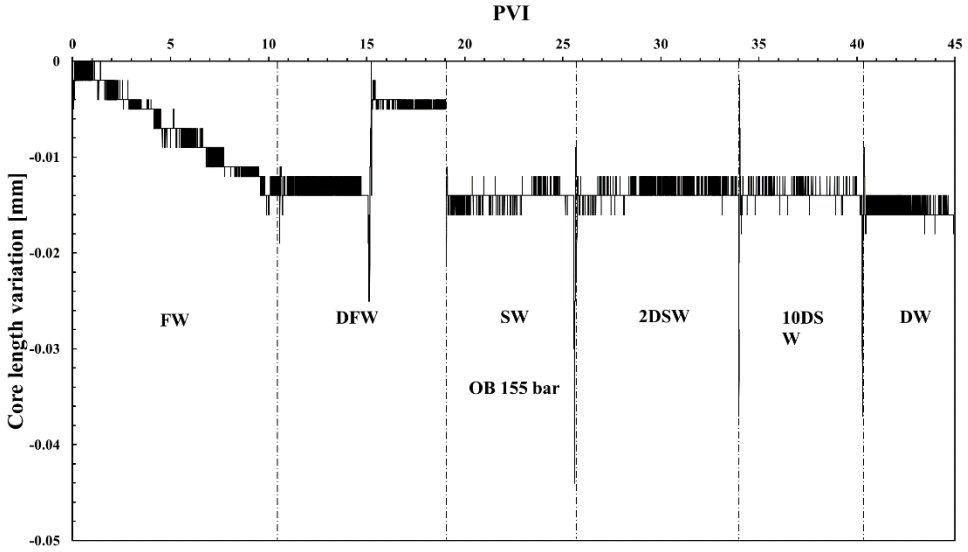

(a) RS1

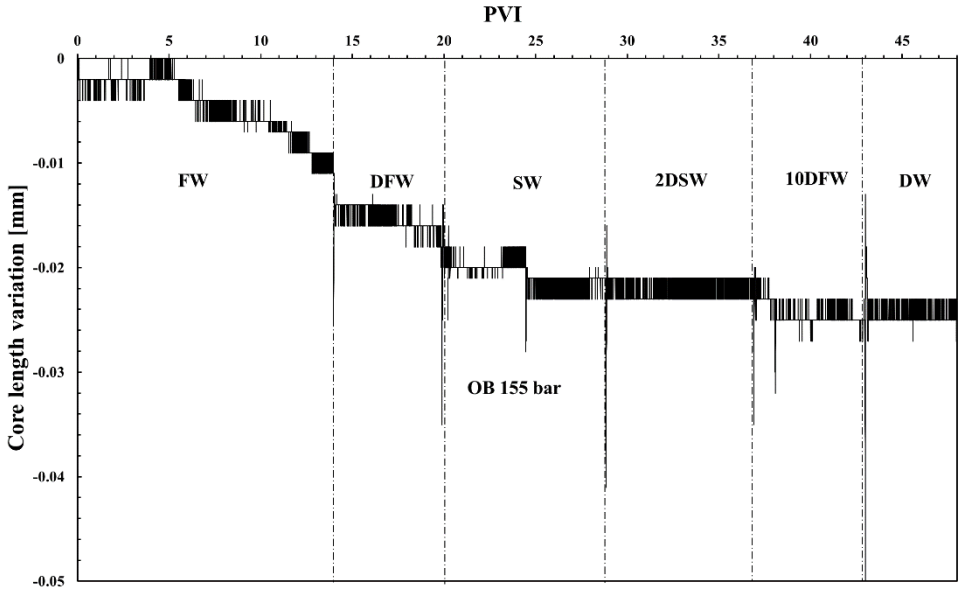

(b) RS2

Figure 9. LVDT measured variation of core length before increasing overburden pressure for the reservoir cores. Similar to the outcrop cores, a gradual compaction can be observed during secondary flooding. For the heterogeneous core (RS2), the compaction continued until SW injection. Following injection of low salinity brines did not lead to further compaction for both cores.

5.5.2.3 Pressure profiles

Figure 10 shows the pressure profiles of the reservoir samples. Similar to the outcrop samples, there was no significant pressure variation during low salinity flooding. However, unlike for the outcrop samples, the increase of pressure difference upon compaction was rather gradual. This might be a result of slow relaxation of the strain.

We failed to observe the behavior of pressure difference with increased back pressure in RS2. A possible reason for the random behavior of the pressure drop could be that the cores transited from the elastic to the plastic regime of compaction (Meireles et al., 2018).

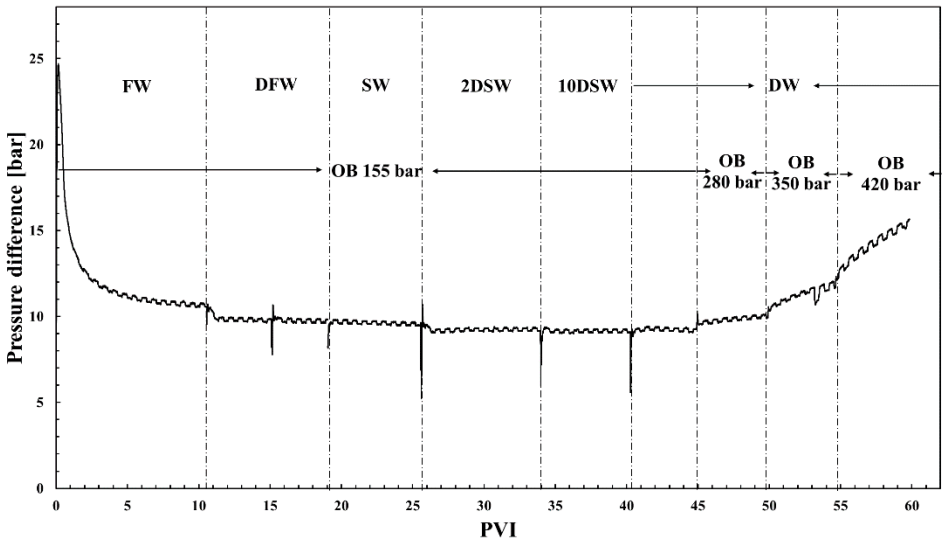

(c) RS1

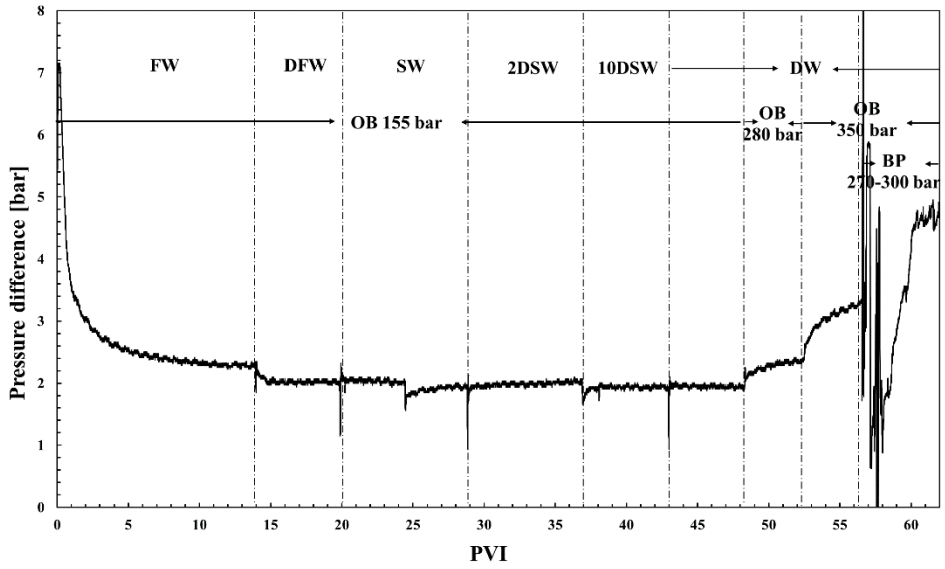

(d) RS2

Figure 10. Pressure difference across the cores during flooding for the reservoir cores. Low salinity flooding did not result in significant variation of pressure drop in both cores. The gradual increase of pressure drop by increasing overburden pressure was attributed to the slow relaxation of the compaction. The random behavior after increasing back pressure of RS2 was most probably due to malfunction of the pressure transducers.

5.5.3 Core handling after experiment

After the experiments, the samples were cleaned by alternative injection of methanol and toluene. Then the cleaned cores were dried in the oven. Production of fine particles was observed in the first round of methanol injection (Figure 11).

Production of fines probably also indicates partial dissolution of the rock under the effect of the injected desalinated water. The effect of dissolution was not strong in our experiments, although some dissolution certainly took place. Strong dissolution would cause strong weakening of the core and much stronger compaction than that detected in our study. A previous study (A. Alexeev et al., 2015) has shown that in the flow through experiments, the effect of dissolution could only affect a small section close to the inlet. This is because the characteristic equilibration time of dissolution is much faster than the convective flow. In our experiments the inlets of the cores did not seem to be affected.

Figure 11. The effluent after first round of methanol injection after the experiments. The brownish slurry-like mixture indicates the production of fine particles.

The porosity and permeability of the cleaned dry cores were measured again by nitrogen injection. The heterogeneous outcrop sample (SK2) was broken in the handling process and therefore not included in the measurements. The results are given in Table 3. The changes a core permeabilities were similar for the homogeneus and heterogeneous cores, which shows that this is not likely to be the main reason for additional production, which was different for these cores.

Sample	Length		Diameter		Dry mass		Porosity		Permeability	
	[mm]	Relative reduction [%]	[mm]	Relative reduction [%]	[g]	Relative reduction [%]	[%]	Relative reduction [%]	[mD]	Relative reduction [%]
SK1	69.65	4.7	35.91	3.5	117.57	2.1	38.5	11.3	1.97	63.4
RS1	72.85	0.76	37.35	0.67	146.41	0.23	32.5	2.9	0.33	42.3
RS2	76.13	2.3	37.42	0.56	146.88	0.31	35.5	3.1	0.99	34.8

Table 3. The measured core properties after experiments. The outcrop sample showed more significant change than the reservoir cores, which is consistent with its soft nature. The reservoir samples showed similar reduction of the measured parameters.

For all the tested samples, the reduction of the measured parameters is not fully reversible. This is an indication that the cores have probably entered plastic regime of compaction. The outcrop sample showed

more significant reduction in all the measured parameters than the reservoir samples. This is consistent with the fact that the outcrop chalk is much softer than the reservoir chalk. Since its reduction of mass is insignificant compared to the dimensions, the porosity reduction was mainly due to compaction of the bulk volume. The reduction in permeability is high for all samples, which should mainly due to a more consolidated arrangement of the grains, the permanently strained fines in the pore throat could also contribute to this.

The measured variation of the parameters for the two reservoir samples are similar. This means the cores have undergone similar compaction processes during the experiments. So, the observed different behavior of oil production can only be attributed to their heterogeneity.

5.6 Discussion

5.6.1 Low salinity flooding in outcrop and reservoir cores

As shown in the previous section, injection of diluted brines and deionized water did not result in significant additional recovery for either Stevns Klint or reservoir chalk cores. Although slight amounts of additional oil were produced, they appeared more like a continuation of the secondary recovery and are far from enough to validate the effect of low salinity flooding.

Production from the Stevns Klint chalk cores was somehow consistent with the literature. Unlike other types of carbonate rocks that are more likely to react on low salinity brine, Stevns Klint chalk is usually reactive to sulfate and magnesium ions in the brine (Romanuka et al., 2012). Numerous experiments with Stevns Klint chalk have shown that an increased concentration of sulfate and/or magnesium could produce more oil (Fathi et al., 2011; Puntervold et al., 2015; Zhang et al., 2007, 2006; Zhang and Austad, 2006). The mechanisms related to surface ion exchange and wettability alteration have also been proposed together with the experimental observations. In our experiments, the increase in sulfate and magnesium was introduced when switching from DFW to SW injection. The sulfate concentration raised up from 1.51 mM/L to 20.8 mM/L; while magnesium from 12.2 mM/L to 45.0 mM/L. However, regardless of the increase, such concentrations are still low and were considered as a base line in many smart water projects (Karoussi and Hamouda, 2007; Puntervold et al., 2015; Zahid et al., 2012a; Zhang and Austad, 2006). Additional recovery was usually reported with several times of spiked sulfate concentration compared to the base value. It is possible that our concentrations are still not high enough to trigger any additional recovery related to the proposed surface ion exchange mechanism. The additional recovery by increased sulfate concentration was often observed in the imbibition tests, which rely upon a different driving force than flooding experiments (capillary force vs. viscous force) and proceed a much longer time. The reported additional recovery in flooding experiments was less significant than that of imbibition tests (Puntervold et al., 2015; Zahid et al., 2012a). A higher temperature, than in our study, was also required for additional recovery (Austad, 2012; Fathi et al., 2011; Strand et al., 2008; Zhang and Austad, 2006).

The reservoir chalk did not react on the low salinity flooding. This is contrary to some previous studies, where reservoir rocks, originated from different carbonate reservoirs, reacted on low salinity flooding (Al-Attar et al., 2013; Al Harrasi et al., 2012; Austad et al., 2015; Romanuka et al., 2012; Yousef et al., 2012, 2010, Zahid et al., 2012b, 2012a). The studies of the Middle East and North Sea reservoir cores suggested potential mechanisms such as fines migration and wettability alteration. Variation of the pressure difference can be an indication of such mechanisms. However, it was not observed in our experiments. The reservoir samples used in this work are well consolidated, they may not contain large amounts of fine particles that can be readily mobilized by low salinity brines. Reduction of dry mass of

the cores may be an evidence of dissolution process, which was reported as a potential recovery mechanism by low salinity flooding. However, in this work it did not appear to facilitate oil recovery.

The properties of oil could be another factor that hindered low salinity effects in this work. The acidic and asphaltenic groups were shown to be necessary for altering the calcite wettability by smart water (Lashkarbolooki et al., 2016; Rezaei Gomari and Hamouda, 2006; Zhang and Austad, 2005). Interaction between the rock surface and crude oil, either by direct adsorption or electrostatic attraction through the thin water film, can be broken or weakened when low salinity brine was injected (Brady and Thyne, 2016; Lashkarbolooki et al., 2016; Zhang et al., 2007, 2006; Zhang and Austad, 2006). However, the oil applied in this work has a low acid number and low amounts of heavy fractions, which did not create conditions for such processes to take place.

5.6.2 Compaction and heterogeneity

Noticeable compaction of the cores was achieved at the last stage of the experiments by increasing overburden pressure. Insignificant, but definite amounts of oil were produced, both from outcrop cores and the heterogeneous reservoir core. For the outcrop, production from the heterogeneous core is 2.5 times higher than the homogeneous core. A more distinct result was observed from reservoir cores: 1.1% additional recovery from the heterogeneous core while no additional oil was produced from the homogeneous core.

In order to further interpret the observations, let us first consider a hypothesis that the compaction results in a uniform reduction of pore volume, then the fluids in the core are uniformly 'squeezed' out of the rock. If the same fraction α of water and oil remained in the rock after compaction, then correspondingly, the same fraction of water and oil was produced. Assume for simplicity that the rock material is isotropic in terms of mechanical properties, so that the relative radial and axial strain is the same. This assumption allows us to estimate the pore volume reduction using the measured core length variation. Then the obtained coefficient α can be used to estimate the oil production. Validity of this hypothesis can be tested by comparing the estimated oil production with the experimental result. Mathematical expression of this hypothesis is given below.

Before compaction:

$$V_{oil} + V_{water} = V_{pore}$$

After compaction:

$$\alpha V_{oil} + \alpha V_{water} = V'_{pore}$$

The produced oil:

$$V^{est}_{additional} = (1 - \alpha)V_{oil}$$

V_{oil} and V_{water} are the volumes of oil and water remained in the core; V_{pore} and V'_{pore} are the pore volumes before and after compaction; $V^{est}_{additional}$ is the estimated volume of additional oil production.

Let us calculate the effective pore volumes before and after compaction. Take SK2 for example: the two steps of compaction reduced core length by 1.01mm and 2.64 mm, respectively. At ambient condition the core length was 75.38mm. If we assume the compaction is linear with regard to overburden pressure, then we can estimate the strains at different overburden pressures. The same strains are used to calculate the diameters. Then, the bulk volumes at different overburden pressures can be calculated, and the effective

pore volumes can be obtained by subtracting the volume differences from the original pore volume. Summary of the results are given in Table 4.

Pressure [bar]	ΔP [bar]	ΔL [mm]	Length [mm]	Strain [%]	Diameter [mm]	Bulk vol. [ml]	Pore vol. [ml]
0	-	-	75.38	-	37.20	81.93	35.37
42.3	42.3	0.99	74.39	1.31	36.71	78.74	32.18
85	42.7	1.01	73.38	2.65	36.21	75.58	29.01
210	125	2.64	70.74	6.16	34.91	67.71	21.15

Table 4. The estimated core dimensions and pore volumes of SK2 at different overburden pressures using the measured compaction data.

Then, α can be calculated by:

$$\alpha = \frac{\mathrm{V'_{pore}}}{\mathrm{V_{pore}}} = \frac{21.15}{32.18} = 0.657$$

The expected oil production (S_{oil} is the residual oil saturation):

$$\mathrm{V^{est}_{additional}} = (1-\alpha)\mathrm{V_{oil}} = (1-\alpha)\mathrm{V_{pore}S_{oil}} = (1-0.675) \times 32.18 \times 26.58\% = 2.93 \text{ ml}$$

Apply the same method for the other cores, the obtained α, estimated additional production $V^{est}_{additional}$, and experimentally measured production $V^{exp}_{additional}$ are given in Table 5.

Core No.	α	$V^{est}_{additional}$ [ml]	$V^{exp}_{additional}$ [ml]
SK1	0.633	2.46	0.036
SK2	0.657	2.93	0.092
RS1	0.882	0.950	-
RS2	0.867	1.06	0.302

Table 5. The estimated additional production using coefficient α, and the experimentally measured additional productions. The values are not even of the same order of magnitude, which means the assumptions of such evaluation are not valid.

It is obvious that the experimental values and the estimated values are not even of the same order of magnitude. Hence, the assumption that the oil is produced uniformly throughout the core is not valid. Increase of the residual oil saturation by reduction of pore volume due to compaction cannot be the primary mechanism for the observed additional recovery. Heterogeneity of the cores must be taken into account to evaluate the working mechanisms.

It has been pointed out in the literature that the core scale heterogeneity is an important factor for different methods of enhanced oil recovery (Spildo et al., 2012). In the context of smart waterflooding in carbonates, it has also been realized by some researchers lately (Romanuka et al., 2012; Zhang and

Sarma, 2012), and often referred as 'natural variability' or 'geological features' of the samples. As observed in this work, heterogeneity can lead to qualitatively different results under similar experimental conditions. Meanwhile, the proposed chemical processes, such as double layer expansion, mineral dissolution, surface ion exchange etc., can hardly explain this difference. If such mechanisms would work alone, they would take effect regardless of the heterogeneity of the rock. The role of flow dynamics related to the heterogeneity has to be carefully evaluated.

As demonstrated before, a uniform production from the whole volume of the core is not possible. Another possibility is that the production occurs from a part of the core. Consider the following scenario: the axial compaction occurs near the outlet end of the core (the 'floating' end piston mentioned in the section 'Experimental procedures'). After compaction, the oil from only the compacted region (and, probably, around it) is produced. In order to verify this hypothesis, assume that the additional oil is produced from a 'slice' of the core of a thickness x. After compaction, residual oil in this slice is completely produced. A more realistic assumption would be that only a part of the residual oil is produced from the slice. However, the oil saturation in the 'slice' after production needs to determined to adopt such assumption, which is impossible under current experimental conditions. Validity of this hypothesis can be tested by comparing the value of x with the measured compaction length. Mathematically,

$$\frac{x}{L}S_{or} = \frac{V_{additional}^{exp}}{V_{pore}S_{or}}$$

Where x is the thickness of the 'slice' of the core, from which the oil is produced; L is the length of the core; S_{or} is residual oil saturation; $V_{additional}^{exp}$ is the experimentally measured volume of additional oil production.

Again, take SK2 for example:

$$x = \frac{V_{additional}^{exp}L}{V_{pore}S_{or}^2} = \frac{0.092 \times 70.74}{32.18 \times 0.266^2} = 2.858\ \text{mm}$$

Apply the method for other cores, the results are given in Table 6, ΔL is the compacted length of the core.

Core No.	x [mm]	ΔL [mm]	Relative difference $[\left\|\frac{x-\Delta L}{\Delta L}\right\| \times 100\%]$
SK1	1.742	3.90	55.3%
SK2	2.858	3.64	21,5%
RS1	0	1.03	100%
RS2	10.15	1.20	745.8%

Table 6. The estimated x values and measured compaction. The values are of the same order of magnitude for the outcrop samples, suggesting a reasonably reliable estimation. The difference is rather large for the reservoir samples, which means some other effects might have taken place and was overlooked in such an estimation.

For the outcrop samples, the estimated value of x is of the same order as the compacted length. The error correlates with the imprecision of the investigated assumption. This gives a qualitatively credible

indication that the additional oil is produced from a small section of the core, whose thickness is of the order of millimeters. Combining the fact that x is comparable to ΔL and the additional production appeared immediately after the compaction, it may be speculated that the additional oil is produced from the compacted section at the outlet end of the core. It should also be noted that the additional recovery from the heterogeneous outcrop core (SK2) is nearly 2.6 times higher than that from the homogeneous core (SK1). This difference may be attributed to the flow diversion process in the heterogeneous core (as discussed later in this section). But since it only took place in a thin section of the core, it was unable to cause large recovery.

The results for reservoir cores showed much larger discrepancies. Additional production from the heterogeneous core was delayed upon compaction, which indicates that the produced oil was not only from the end of the core, but a place deeply inside it. Looking to the CT scanning images, the heterogeneities of RS2 are mainly concentrated at the center of the core, within a section of approximately 2 cm. This is close to the estimated x value, and its location explains the delay in production.

Heterogeneity may contribute to oil recovery by mobilization and relocation of reservoir fines. This effect was extensively studied for the sandstone rocks (Al-Sarihi et al., 2018; Borazjani et al., 2018; Hussain et al., 2013; Yu et al., 2018). The fine particles in the rock may be released due to interaction with low salinity brine. They travel a short distance with the flow of water, and then get captured by narrow pore throats. In this way, the water channel is blocked and water is diverted to the unswept zones. P. Bedrikovetsky and A. Zeinijahromi proposed fines-assisted low salinity waterflooding (LSW) as a version of commonly used EOR-LSW (Marquez et al., 2013; Zeinijahromi et al., 2015, 2011a).

In this work, production of fines was observed in the post-experiment core cleaning process, as shown in the previous section. Most probably, the fines were produced during compaction of the cores. As the overburden pressure increased beyond the hydrostatic yield strength of the cores, some local failures may occur at the grain contacts. Rotation and sliding of the grains could have released some small fragments from the rock matrix. This may explain the non-linear behavior of oil production and compaction in RS2: the additional oil was produced when overburden pressure increased from 280 bar to 350 bar, which exceeded the hydrostatic yield pressure. The porosity of the rock could also become more homogeneous by compaction (Powell and Lovell, 1994). The observed reductions in dry mass of the cores may also be an evidence of fines production.

The above-mentioned fluid diversion by fines relocation probably took place at the center of the heterogeneous reservoir core (RS2). The bypassed oil due to heterogeneity was produced by fines assisted fluid diversion. Another evidence of this inference is that, after compaction, the recovery from the heterogeneous core (74.3%) became very similar to that of the homogeneous core (74.56%). A possible explanation may be that diversion of water makes the displacement more even in the heterogeneous core, which diminishes the difference between the heterogeneous and homogeneous samples.

However, production of fines is not the only possible explanation of the effect of compaction in heterogeneous rock, as discussed below.

5.6.3 Core stability and pore pressure

Regardless of the imposed high stress by compaction (which even exceeded the hydrostatic yield strength), all the core samples were intact after the experiments. Nevertheless, some permanent damage could already occur when the overburden pressure got higher than the yield strength. As the petrophysical measurements after the experiments show, the measured parameters are not fully reversible.

Rearrangement of the grains and micro-fractures could take place during compaction. Although the dimension of the cores only slightly changed, the permeability showed a significant reduction. The compaction could have made the grains more consolidated and the pore throats narrower.

As shown in the case of SK1, the increase of pore pressure resulted in a decreased pressure difference across the core. Probably, the previously closed flow channels by compaction became accessible again by the increased pore pressure; however, more evidence is needed to support this. Another effect of the high pore pressure is that it reduces the effective stress on the rock matrix, so the elastic deformation can be restored. This has been indicated by the slight increase of core length in SK1 and RS2. However, whatever happened by increasing pore pressure, it did not lead to additional oil recovery.

Rearranging of the rock grains and closing the conducting paths (microfractures) may be another explanation of the additional oil production in heterogeneous cores. Water may bypass some oil via high permeable micro-fractures and other conducting paths. When the rock is compacted, these micro-fractures are closed, and the water flow is diverted to displace the bypassed oil. This diversion mechanism is to some extent similar, but still different from the fines mobilization and relocation described in the previous subsection.

5.7 Conclusions

By employing the novel core flooding equipment (LVDT and core holder with a moveable end piston plug), we have explicitly studied the effect of rock compaction on oil recovery under LSW flooding for Stevns Klint chalk and North Sea reservoir chalk. To the best of our knowledge, such kind of work have not been reported in the literature. Sequential injection of low salinity brines did not produce additional oil from either of the rocks. The weakening and compaction of chalk by injection of low salinity brines was insignificant and did not improve oil recovery. However, significant compaction caused by increased overburden resulted in small additional recoveries in both heterogeneous and homogeneous outcrop cores and a considerable (compared to a homogeneous core) additional recovery from the heterogeneous reservoir core.

It is evident that compaction may serve as an additional production mechanism. However, as observed in the outcrop samples, compaction alone cannot be the reason for large additional production, at least, on the laboratory level. A fluid diversion process caused by fines relocation or closing of the micro-fractures was discussed. It appears to be able to explain the observed difference of recoveries between the heterogeneous and homogeneous cores.

The reservoir samples showed more clear correlation with the fluid diversion mechanism. The different results from the homogeneous and heterogeneous reservoir cores indicate that a certain level of heterogeneity is required for fluid diversion to take effect.

This work also demonstrated that heterogeneity is an important factor even at core scale. It could lead to qualitatively different result under similar experimental conditions. In addition to chemical processes, flow dynamics could potentially determine the flooding results related to heterogeneity or other methods of enhanced oil recovery.

Acknowledgements

The Dansih Hydrocarbon Research and Technology Centre is kindly acknowledged for supporting this work. Karen Louise Feilberg is kindly acknowledged for long and productive discussions and useful

advises. Duc Thuong Vu, Jesper Arvedlund Hollensen and Annette Eva Jensen are kindly acknowledged for practical assistance in the laboratory.

References

Ahkami, M., Chakravarty, K.H., Xiarchos, I., Thomsen, K., Fosbøl, P., 2016. Determining Optimum Aging Time Using Novel Core Flooding Equipment. SPE Bergen One Day Seminar. https://doi.org/10.2118/180054-MS

Al-Attar, H.H., Mahmoud, M.Y., Zekri, A.Y., Almehaideb, R., Ghannam, M., 2013. Low-salinity flooding in a selected carbonate reservoir: experimental approach. J. Pet. Explor. Prod. Technol. 3, 139–149. https://doi.org/10.1007/s13202-013-0052-3

Alexeev, A., Shapiro. A.A., Thomsen K., Modeling of dissolution effects on waterflooding, Transp. Porous Media 106 (3), 545-562, https://doi.org/10.1007/s11242-014-0413-5.

Al-Sarihi, A., Zeinijahromi, A., Genolet, L., Behr, A., Kowollik, P., Bedrikovetsky, P., 2018. Effects of Fines Migration on Residual Oil during Low-Salinity Waterflooding. Energy and Fuels 32, 8296–8309. https://doi.org/10.1021/acs.energyfuels.8b01732 Katika et al., 2017

Al Harrasi, A., Al-maamari, R.S., Masalmeh, S.K., 2012. Laboratory Investigation of Low Salinity Waterflooding for Carbonate Reservoirs. Abu Dhabi Int. Pet. Conf. Exhib. https://doi.org/10.2118/161468-MS

Al-Saedi, Hasan, N., Flori, R. E., & Brady, P. V. (2019a). Effect of divalent cations in formation water on wettability alteration during low salinity water flooding in sandstone reservoirs: Oil recovery analyses, surface reactivity tests, contact angle, and spontaneous imbibition experiments. Journal of Molecular Liquids, 275, 163-172. https://doi.org/10.1016/j.molliq.2018.11.093

Al-Saedi, Hasan, N., Brady, P. V., Flori, R. E., & Heidari, P. (2019b). Insights into the role of clays in low salinity water flooding in sand columns. Journal of Petroleum Science and Engineering, 174, 291-305. https://doi.org/10.1016/j.petrol.2018.11.031

Al-Saedi, Hasan, N., & Flori, R. E. (2019c). Effect of divalent cations in low salinity water flooding in sandstone reservoirs. Journal of Molecular Liquids. https://doi.org/10.1016/j.molliq.2019.03.112

Attar, A., Muggeridge, a H., 2016. Evaluation of Mixing in Low Salinity Waterflooding, in: SPE EOR Conference at Oil and Gas West Asia. Muscat, Oman. https://doi.org/10.2118/179803-MS

Austad, T., 2012. Water-Based EOR in Carbonates and Sandstones: New Chemical Understanding of the EOR Potential Using "Smart Water," in: James Sheng (Ed.), Enhanced Oil Recovery Field Case Studies. Elsevier Ltd. https://doi.org/10.1016/B978-0-12-386545-8.00013-0

Austad, T., Shariatpanahi, S.F., Strand, S., Aksulu, H., Puntervold, T., 2015. Low Salinity EOR Effects in Limestone Reservoir Cores Containing Anhydrite: A Discussion of the Chemical Mechanism. Energy and Fuels 29, 6903–6911. https://doi.org/10.1021/acs.energyfuels.5b01099

Austad, T., Strand, S., Madland, M. V., Puntervold, T., Korsnes, R.I., 2007. Seawater in Chalk: An EOR and Compaction Fluid, in: International Petroleum Technology Conference. Dubai, UAE. https://doi.org/10.2118/118431-PA

Ayirala, S.C., Yousef, A.A., 2016. A critical review of water chemistry alteration technologies to develop novel water treatment schemes for smartwater flooding in carbonate reservoirs, in: SPE Symposium on Improved Oil Recovery Conference. Tulsa, Oklahoma, U.S.A. https://doi.org/https://doi.org/10.2118/179564-MS

Boade, R.R., Chin, L.Y., Siemers, W.T., 1989. Forecasting of Ekofisk Reservoir Compaction and Subsidence by Numerical Simulation. J. Pet. Technol. 41. https://doi.org/10.2118/17855-pa

Borazjani, S., Behr, A., Genolet, L.C., Kowollik, P., 2018. Fines-Migration-Assisted Waterflooding to Improve Sweep Efficiency Analytical Model, in: SPE International Conference and Exhibition on Formation Damage Control. Lafayette, Louisiana, USA.

Brady, P. V., Thyne, G., 2016. Functional Wettability in Carbonate Reservoirs. Energy and Fuels 30, 9217–9225. https://doi.org/10.1021/acs.energyfuels.6b01895

Chin, L.Y., Thomas, L.K., 1999. Fully Coupled Analysis of Improved Oil Recovery by Reservoir Compaction, in: SPE Annual Technical Conference and Exhibition. Houston, Texas, USA. https://doi.org/10.2118/56753-ms

Fathi, S.J., Austad, T., Strand, S., 2011. Water-based enhanced oil recovery (EOR) by "smart water": Optimal ionic composition for EOR in carbonates. Energy and Fuels 25, 5173–5179. https://doi.org/10.1021/ef201019k

Heggheim, T., Madland, M. V., Risnes, R., Austad, T., 2004. A chemical induced enhanced weakening of chalk by seawater. J. Pet. Sci. Eng. 46, 171–184. https://doi.org/10.1016/j.petrol.2004.12.001

Hellmann, R., Renders, P.J.N., Gratier, J.-P., Guiguet, R., 2002. Experimental Pressure Solution Compaction of Chalk in Aqueous Solutions: Part 1. Deformation Behavior and Chemistry, in: Hellmann, R.S.A.W. (Ed.), Water-Rock Interactions, Ore Deposits, and Environmental Geochemistry: A Tribute to David A. Crerar. The Geochemical Society, pp. 129–152.

Høeg, K., Gutierrez, M., Øino, L.E., 2000. The Effect of Fluid Content on the Mechanical Behaviour of Fractures in Chalk. Rock Mech. Rock Eng. 33, 93–117. https://doi.org/10.1007/s006030050037

Hussain, F., Zeinijahromi, A., Bedrikovetsky, P., Badalyan, A., Carageorgos, T., Cinar, Y., 2013. An experimental study of improved oil recovery through fines-assisted waterflooding. J. Pet. Sci. Eng. 109, 187–197. https://doi.org/10.1016/j.petrol.2013.08.031

Karoussi, O., Hamouda, A.A., 2007. Imbibition of sulfate and magnesium ions into carbonate rocks at elevated temperatures and their influence on wettability alteration and oil recovery. Energy and Fuels 21, 2138–2146. https://doi.org/10.1021/ef0605246

Katika, K., Addassi, M., Alam, M.M., Fabricius, I.L., 2015. The effect of divalent ions on the elasticity and pore collapse of chalk evaluated from compressional wave velocity and low-field Nuclear Magnetic Resonance (NMR). J. Pet. Sci. Eng. 136, 88–99. https://doi.org/10.1016/j.petrol.2015.10.036

Katika, K., Ahkami, M., Fosbøl, P.L., Halim, A.Y., Shapiro, A., Thomsen, K., Xiarchos, I., Fabricius, I.L., 2016. Comparative analysis of experimental methods for quantification of small amounts of oil in water. J. Pet. Sci. Eng. 147, 459–467. https://doi.org/10.1016/j.petrol.2016.09.009

Katika, K., Alam, M.M., Alexeev, A., Chakravarty, K.H., Fosbøl, P.L., Revil, A., Stenby, E., Xiarchos, I., Yousefi, A., Fabricius, I.L., 2017. Elasticity and electrical resistivity of chalk and greensand during water flooding with selective ions. J. Pet. Sci. Eng. 161, 204–218. https://doi.org/10.1016/j.petrol.2017.11.045

Korsnes, R.I., Madland, M. V., Austad, T., Haver, S., Røsland, G., 2008. The effects of temperature on the water weakening of chalk by seawater. J. Pet. Sci. Eng. 60, 183–193. https://doi.org/10.1016/j.petrol.2007.06.001

Lashkarbolooki, M., Riazi, M., Hajibagheri, F., Ayatollahi, S., 2016. Low salinity injection into asphaltenic-carbonate oil reservoir, mechanistical study. J. Mol. Liq. 216, 377–386. https://doi.org/10.1016/j.molliq.2016.01.051

Madland, M.V., Korsnes, R.I., Risnes, R., 2002. Temperature effects in Brazilian , uniaxial and triaxial compressive tests with high porosity chalk, in: SPE Annual Technical Conference and Exhibition. San Antonio, TX, USA. https://doi.org/10.2118/77761-MS

Marquez, M., Williams, W., Knobles, M., Bedrikovetsky, P., You, Z., 2013. Fines Migration in Fractured Wells:Integrating Modeling, Field and Laboratory Data. SPE Eur. Form. Damage Conf. Exhib. 5–7. https://doi.org/10.2118/165108-MS

Meireles, L.T.P., Storebø, E.M., Welch, M.J., Fabricius, I.L., 2018. Investigation of controlling parameters on geomechanical properties of the Southern Danish Central Graben chalk, in: Engineering in Chalk: Proceedings of the Chalk 2018 Conference. London, UK.

Nermoen, A., Korsnes, R.I., Storm, E.V., Stødle, T., Madland, M.V., Fabricius, I.L., 2018. Incorporating electrostatic effects into the effective stress relation - Insights from chalk experiments. Geophysics 83.

https://doi.org/10.1190/geo2016-0607.1

Newman, G., 1983. The Effect of Water Chemistry on the Laboratory Compression and Permeability Characteristics of Some North Sea Chalks. J. Pet. Technol. 35, 976–980. https://doi.org/10.2118/10203-PA

Powell, B.N., Lovell, G.L., 1994. Mechanisms of chalk compaction, in: SPE/ISRM Rock Mechanics in Petroleum Engineering Conference. Delft, The Netherlands. https://doi.org/10.2118/28132-MS

Puntervold, T., Strand, S., Ellouz, R., Austad, T., 2015. Modified seawater as a smart EOR fluid in chalk. J. Pet. Sci. Eng. 133, 440–443. https://doi.org/10.1016/j.petrol.2015.06.034

Rezaei Gomari, K.A., Hamouda, A.A., 2006. Effect of fatty acids, water composition and pH on the wettability alteration of calcite surface. J. Pet. Sci. Eng. 50, 140–150. https://doi.org/10.1016/j.petrol.2005.10.007

Risnes, R., Madland, M. V., Hole, M., Kwabiah, N.K., 2005. Water weakening of chalk - Mechanical effects of water-glycol mixtures. J. Pet. Sci. Eng. 48, 21–36. https://doi.org/10.1016/j.petrol.2005.04.004

Romanuka, J., Hofman, J., Ligthelm, D.J., Suijkerbuijk, B., Marcelis, F., Oedai, S., Brussee, N., van der Linde, H., Aksulu, H., Austad, T., 2012. Low Salinity EOR in Carbonates, in: SPE Improved Oil Recovery Symposium. Tulsa, Oklahoma, U.S.A. https://doi.org/10.2118/153869-MS

Ruddy, I., Andersen, M.A., Pattillo, P.D., Bishlawi, M., Foged, N., 1989. Rock Compressibility, Compaction, and Subsidence in a High-Porosity Chalk Reservoir: A Case Study of Valhall Field. J. Pet. Technol. 41, 741–746. https://doi.org/10.2118/18278-PA

Sheng, J.J., 2014. Critical review of low-salinity waterflooding. J. Pet. Sci. Eng. 120, 216–224. https://doi.org/10.1016/j.petrol.2014.05.026

Sohal, M.A., Thyne, G., Søgaard, E.G., 2016. Review of Recovery Mechanisms of Ionically Modified Waterflood in Carbonate Reservoirs. Energy and Fuels 30, 1904–1914. https://doi.org/10.1021/acs.energyfuels.5b02749

Spildo, K., Johannessen, A., Skauge, A., 2012. Low Salinity Waterflood at Reduced Capillarity, in: Eighteenth SPE Improved Oil Recovery Symposium. Tulsa, Oklahoma, U.S.A., pp. 1–13. https://doi.org/10.2118/154236-MS

Strand, S., Austad, T., Puntervold, T., Høgnesen, E.J., Olsen, M., Barstad, S.M.F., 2008. “Smart Water” for oil recovery from fractured limestone: A preliminary study. Energy and Fuels 22, 3126–3133. https://doi.org/10.1021/ef800062n

Sulak, R.M., Thomas, L.K., Boade, R.R., 1991. 3D Reservoir Simulation of Ekofisk Compaction Drive (includes associated papers 24317 and 24400). J. Pet. Technol. 43, 1272–1278. https://doi.org/10.2118/19802-PA

Sylte, J.E., Thomas, L.K., Rhett, D.W., Bruning, D.D., Nagel, N.B., 1999. Water Induced Compaction in the Ekofisk Field, in: SPE Annual Technical Conference and Exhibition. Houston, Texas, USA. https://doi.org/10.2118/56426-MS

Tang, G.-Q., Morrow, N.R., 1999. Influence of brine composition and fines migration on crude oi/brine/rock interactions and oil recovery. J. Pet. Sci. Eng. 24, 99–111. https://doi.org/10.1016/S0920-4105(99)00034-0

Yousef, A.A., Al-Saleh, S., Al-Jawfi, M.S., 2012. Improved/Enhanced Oil Recovery from Carbonate Reservoirs by Tuning Injection Water Salinity and Ionic Content, in: SPE Improved Oil Recovery Symposium. Tulsa, Oklahoma, U.S.A. https://doi.org/10.2118/154076-MS

Yousef, A.A., Al-Saleh, S., Al-Kaabi, A., Al-Jawfi, M., 2010. Laboratory Investigation of Novel Oil Recovery Method for Carbonate Reservoirs, in: Canadian Unconventional Resources & International Petroleum Conference. Calgary, Canada.

Yu, M., Hussain, F., Arns, J.Y., Bedrikovetsky, P., Genolet, L., Behr, A., Kowollik, P., Arns, C.H., 2018. Imaging analysis of fines migration during water flow with salinity alteration. Adv. Water Resour. 121, 150–161. https://doi.org/10.1016/j.advwatres.2018.08.006

Yuan, H., Shapiro, A.A., 2011. Induced migration of fines during waterflooding in communicating layer-cake

reservoirs. J. Pet. Sci. Eng. 78, 618–626. https://doi.org/10.1016/j.petrol.2011.08.003

Yunita Halim, A., Marie Nielsen, S., Eliasson Lantz, A., Sander Suicmez, V., Lindeloff, N., Shapiro, A., 2015. Investigation of spore forming bacterial flooding for enhanced oil recovery in a North Sea chalk Reservoir. J. Pet. Sci. Eng. 133, 444–454. https://doi.org/10.1016/j.petrol.2015.06.011

Zahid, A., Shapiro, A., Stenby, E.H., Yan, W., 2012a. Managing injected water composition to improve oil recovery: A case study of north sea chalk reservoirs. Energy and Fuels 26, 3407–3415. https://doi.org/10.1021/ef2008979

Zahid, A., Shapiro, A.A., Skauge, A., 2012b. Experimental Studies of Low Salinity Water Flooding Carbonate: A New Promising Approach. SPE EOR Conf. Oil Gas West Asia. https://doi.org/10.2118/155625-MS

Zeinijahromi, A., Al-Jassasi, H., Begg, S., Bedrikovetski, P., 2015. Improving sweep efficiency of edge-water drive reservoirs using induced formation damage. J. Pet. Sci. Eng. 130, 123–129. https://doi.org/10.1016/j.petrol.2015.04.008

Zeinijahromi, A., Lemon, P., Bedrikovetsky, P., 2011a. Effects of induced fines migration on water cut during waterflooding. J. Pet. Sci. Eng. 78, 609–617. https://doi.org/10.1016/j.petrol.2011.08.005

Zeinijahromi, A., Machado, F.A., Bedrikovetsky, P.G., 2011b. Modified Mathematical Model for Fines Migration in Oil Fields, in: Brasil Offshore Conference and Exhibition. Macea, Brazil, pp. 14–17. https://doi.org/10.2118/143742-MS

Zhang, P., Austad, T., 2006. Wettability and oil recovery from carbonates: Effects of temperature and potential determining ions. Colloids Surfaces A Physicochem. Eng. Asp. 279, 179–187. https://doi.org/10.1016/j.colsurfa.2006.01.009

Zhang, P., Austad, T., 2005. The Relative Effects of Acid Number and Temperature on Chalk Wettability. SPE Int. Symp. Oilf. Chem. 3–9. https://doi.org/10.2118/92999-MS

Zhang, P., Tweheyo, M.T., Austad, T., 2007. Wettability alteration and improved oil recovery by spontaneous imbibition of seawater into chalk: Impact of the potential determining ions Ca2+, Mg2+, and SO42-. Colloids Surfaces A Physicochem. Eng. Asp. 301, 199–208. https://doi.org/10.1016/j.colsurfa.2006.12.058

Zhang, P., Tweheyo, M.T., Austad, T., 2006. Wettability alteration and improved oil recovery in chalk: The effect of calcium in the presence of sulfate. Energy and Fuels 20, 2056–2062. https://doi.org/10.1021/ef0600816

Zhang, Y., Sarma, H., 2012. Improving waterflood recovery efficiency in carbonate reservoirs through salinity variations and ionic exchanges: A promising low-cost “smart-waterflood” approach. Abu Dhabi Int. Pet. Exhib. Conf. 2012 - Sustain. Energy Growth People, Responsib. Innov. ADIPEC 2012 3, 2163–2183. https://doi.org/10.2118/161631-MS

Chapter 6. General Conclusions and Suggestions for Future Work

6.1 General conclusions

This Ph.D. study investigated possible recovery mechanisms by smart waterflooding from three aspects: the kinetics of calcite/chalk dissolution and Ca-Mg ion exchange, as well as their impacts on flow-through experiments; the effect of flow diversion in sandstone and chalk cores with different levels of heterogeneity; and the impact of chalk compaction on oil recovery during low salinity flooding. The overall goal has been to establish relative importance of static and dynamic mechanisms governing additional recovery in the course of smart waterflooding. To achieve this goal, comparative studies of recovery from homogeneous and heterogeneous rock samples have been carried out.

First, the static dissolution and ion exchange experiments were carried out with calcite and chalk powders. The evolution of Ca^{2+} and Mg^{2+} concentrations were measured to obtain the kinetics of the studied processes. The PhreeqC software was used to model the dissolution of calcite and chalk, and a two-layer model was proposed to describe the Ca-Mg ion exchange process. It was found that the dissolution of calcite is a fast process (equilibrates within seconds) with low equilibrium concentration (in the order of milligrams per liter). These findings indicate that, in the flow-through scenarios, dissolution is limited to the first few millimeters close to the injection spot, it is unlikely to cause significant additional production.

Meanwhile, the Ca-Mg ion exchange on the calcite surface exhibits slow kinetics. The exchange did not stop after the two weeks of experimental time. The modeled exchange capacity was in the order of 10^{-5} $mol/m^2/layer$. Such slow kinetics is also unlikely to have a large impact within the time frame of flooding experiments, but it may be more profound on the reservoir scale.

Next, core flooding experiments were performed on sandstone and chalk cores. Based on the CT scanning images, the cores were selected to be homogeneous and heterogeneous. Additional recovery was consistently observed from the heterogeneous samples for both types of rocks. The experiments were accompanied by mathematical simulation using a simplified multi-layer transport model. The study demonstrated that, core scale heterogeneity is an important factor in flooding experiments. Heterogeneity can contribute to recovery through a flow diversion mechanism, which can be triggered by the production of pore-plugging agents. This mechanism can take place in both sandstone and chalk cores.

In the last part, the flooding experiments with homogeneous and heterogeneous chalk were carried out. The experiments were accompanied by simultaneous measurement of the core length, which served as an indication of the compaction. It was found that compaction alone was not able to produce large amounts of additional oil. But compaction combined with heterogeneity could lead to more significant production (compared to homogeneous cores). The flow diversion mechanism was discussed in consideration of the compaction process. It appeared to be the most plausible explanation for the observed recoveries.

Overall, the study shows that, the time scale, or the kinetics, of the chemical processes, is important to evaluate their significance under smart waterflooding. Meanwhile, dynamic mechanisms, which take place along with the flow, can play an important role in smart waterflooding. Recovery from heterogeneous rock samples was consistenly higher than from the homogeneous cores. This shows that

production of the plugging agents (fines, emulsions, closing the microfractures) and subsequent flow diversion cause a large part of improved oil recovery under smart waterflooding.

6.2 Suggestions for future work

Future studies on the chemical processes should focus more on the kinetics of the reactions. The research may start with simple systems to reveal the nature of the reactions. Then, more complex conditions similar to oil reservoirs can be included. The core flooding experiment is still an essential method to investigate the EOR potential of the processes. When performing flow-through experiments, heterogeneity of the core samples should be carefully evaluated. Additional studies are required for classification and quantification of the relevant heterogeneity patterns. The flow dynamics during two-phase displacement plays an important role in the EOR processes. More dedicated research involving flooding with computer X-ray tomography to obtain in-situ fluid distribution is highly recommended to study the processes of enhanced and improved oil recovery.